

DEVELOPMENT OF GIS BASED TRAJECTORY STATISTICAL ANALYSIS
METHOD TO IDENTIFY POTENTIAL SOURCES OF REGIONAL AIR
POLLUTION

A THESIS SUBMITTED TO
THE GRADUATE SCHOOL OF NATURAL AND APPLIED SCIENCES
OF
MIDDLE EAST TECHNICAL UNIVERSITY

BY

RIZA FİKRET YIKMAZ

IN PARTIAL FULFILLMENT OF THE REQUIREMENTS
FOR
THE DEGREE OF MASTER OF SCIENCE
IN
GEODETIC AND GEOGRAPHIC INFORMATION TECHNOLOGIES

MAY 2010

Approval of the thesis:

**DEVELOPMENT OF GIS BASED TRAJECTORY STATISTICAL
ANALYSIS METHOD TO IDENTIFY POTENTIAL SOURCES OF
REGIONAL AIR POLLUTION**

submitted by **RIZA FİKRET YIKMAZ** in partial fulfillment of the requirements
for the degree of **Master of Science in Geodetic and Geographic Information
Technologies Department, Middle East Technical University** by,

Prof. Dr. Canan Özgen
Dean, Graduate School of **Natural and Applied Sciences**

Assoc. Prof. Dr. Mahmut Onur Karslıoğlu
Head of Department, **Geodetic and Geographic Inf. Tech.**

Prof. Dr. Gürdal Tuncel
Supervisor, **Environmental Engineering Dept., METU**

Assoc. Prof. Dr. Zuhal Akyürek
Co-Supervisor, **Civil Engineering Dept., METU**

Examining Committee Members:

Assoc. Prof. Dr. Ayşegül Aksoy
Environmental Engineering Dept., METU

Prof. Dr. Gürdal Tuncel
Environmental Engineering Dept., METU

Assoc. Prof. Dr. Zuhal Akyürek
Civil Engineering Dept., METU

Assoc. Prof. Dr. İsmail Yücel
Civil Engineering Dept., METU

Tuncay Küçükpehlivan
General Manager, Başarsoft

Date: 05/05/2010

I hereby declare that all information in this document has been obtained and presented in accordance with academic rules and ethical conduct. I also declare that, as required by these rules and conduct, I have fully cited and referenced all material and results that are not original to this work.

Name, Last Name: Rıza Fikret YIKMAZ

Signature :

ABSTRACT

DEVELOPMENT OF GIS BASED TRAJECTORY STATISTICAL ANALYSIS METHOD TO IDENTIFY POTENTIAL SOURCES OF REGIONAL AIR POLLUTION

Yıkmaz, Rıza Fikret

M.Sc., Department of Geodetic and Geographic Information Technologies

Supervisor: Prof. Dr. Gürdal Tuncel

Co-supervisor: Assoc. Prof. Dr. Zuhâl Akyürek

May 2010, 186 pages

Apportionment of source regions affecting a certain receptor in the regional scale is necessary information for air quality management and development of national policy for exchange of air pollutants with other countries. Source region apportionment can be studied either through numerical modeling or by using trajectory statistics that is a hybrid methodology of modeling and measurements. Each of these approaches has their advantages and disadvantages.

In this study treatment of back-trajectory segments in Potential Source Contribution Function (PSCF), which is one of the tools used in trajectory statistics will be investigated, to increase the reliability of the apportionment process. In the current method run in GIS, especially two parameters gains importance. One is that the vertical locations of trajectory segments are not taken into account at present. In this study, how the evaluation of the segments in 3-D instead of 2-D could improve the results will be assessed. The other parameter that is rainfall at each segment will be included in the PSCF calculations and its effects on the spatial distribution of PSCF

values will be evaluated. A user interface in Geographical Information System (GIS) will be developed for effective use of improved methodology.

Keywords: Trajectory Statistics, Geographical Information System, Potential Source Contribution Function, Regions of Influence.

ÖZ

BÖLGESEL HAVA KİRLİLİĞİ KAYNAKLARININ TESPİTİ İÇİN CBS TABANLI YÖRÜNGE İSTATİSTİKSEL ANALİZ METODUNUN GELİŞTİRİLMESİ

Yıkma, Rıza Fikret

Y. Lisans, Jeodezi ve Coğrafi Bilgi Teknolojileri Bölümü,

Tez Yöneticisi: Prof. Dr. Gürdal Tuncel

Ortak Tez Yöneticisi: Doç. Dr. Zuhal Akyürek

Mayıs 2010, 186 sayfa

Bölgesel düzeyde herhangi bir reseptör bölgesindeki aerosollerin kimyasal kompozisyonlarını etkileyen kaynak bölgelerinin bilinmesi hem hava kalitesi yönetimi açısından hem de ülkelerin hava kirliliğinin diğer ülkeler arasında takas edilmesine ilişkin uluslararası platformda savunabilecekleri ulusal politikaların geliştirilmesi için gerekli bir bilgidir. Bu tür bilgiler ya sayısal modelleme yaklaşımıyla ya da geri yörünge istatistiği olarak bilinen, modelleme ile ölçümlerin birlikte kullanıldığı hibrit bir yaklaşım ile elde edilebilir. Her iki tekniğin de kendine özgü avantaj ve dezavantajları bulunmaktadır.

Bu çalışmada, kaynak bölgelerinin belirlenmesi sürecinde güvenilirliğini artırmak için, geri yörünge segmentlerinin yörünge istatistiğinde kullanılan yöntemlerden birisi olan “Potansiyel Kaynak Katkı Fonksiyonu (PKKF)” yönteminde kullanılma şekli incelenmesi amaçlanmaktadır. Mevcut süreçte, özellikle iki parametre önem kazanmaktadır. Bunlardan birisi, geri yörünge segmentlerinin değerlendirilmesinde segmentlerin yükseklik boyutu hiç göz önüne alınmamaktadır. Bu çalışmada,

segmentlerin deęerlendirilmesinin iki yerine üç boyutlu yapılmasının sonuçları ne kadar geliştirileceęi deęerlendirilecektir. Deęerlendirilecek dięer bir parametre de geri yörünge segmentlerindeki yağışın PKKF hesaplarına dâhil edilmesi ve bunun PKKF deęerlerinin mekânsal dağılımını nasıl bir etkileyeceęi olacaktır. Geliştirilen metodun etkin bir şekilde kullanılabilmesi için Coęrafi Bilgi Sistemi (CBS) içinde bir kullanıcı arayüzü geliştirilecektir.

Anahtar Sözcükler: Yörünge İstatistięi, Coęrafi Bilgi Sistemi, Potansiyel Kaynak Katkı Fonksiyonu, Etki Bölgeleri.

To My Family...

ACKNOWLEDGEMENTS

I would like to express my sincere thanks and gratitude to my supervisor Prof. Dr. Gürdal Tuncel for his invaluable guidance, encouragement and insight throughout the research. I would like to show gratitude to my co-supervisor Assoc. Prof. Dr. Zuhâl Akyürek for her guidance, comments and support. The comments and contributions of examining committee members are greatly appreciated.

I would like to thank to anybody who contributed this study and to show my exclusive appreciations to Assist. Prof. Dr. Fatma Öztürk, Ahmet Dabanlı, D. Deniz (Genç) Gerçel, Hakan Moral and Dr. Mihriban (Yılmaz) Civan for their contributions and supports throughout the study.

I want to thank to my friends and colleagues from State Planning Institution especially Dr. Sema Bayazıt, İzzet Arı, S. Ersin Esen and Selin Dilekli for their indispensable encouragement and supports.

I acknowledge Middle East Technical University, Environmental Engineering Department and Ministry of Health, Refik Saydam Hygiene Center for the aerosol measurements, Co-operative Programme for Monitoring and Evaluation of the Long-range Transmission of Air Pollutants in Europe (EMEP) for the emission inventory, the NOAA Air Resources Laboratory for the provision of the HYSPLIT transport and dispersion model and READY website (<http://www.arl.noaa.gov/ready.php>) and the European Centre for Medium-Range Weather Forecasts (ECMWF) for the use of ECMWF backtrajectory data.

Finally, I would like to express my heartfelt thanks to my family for their everlasting support, understanding and patience throughout this study and my life.

TABLE OF CONTENTS

ABSTRACT	iv
ÖZ	vi
ACKNOWLEDGEMENTS	ix
TABLE OF CONTENTS	x
LIST OF TABLES	xii
LIST OF FIGURES	xiii
LIST OF ABBREVIATIONS	xvi
CHAPTERS	
1. INTRODUCTION	1
1.1. Purpose and Scope	7
1.2. Plan of the Thesis	8
2. LITERATURE REVIEW	9
2.1. Trajectories	9
2.2. Trajectory Statistics	14
2.2.1. Flow Climatology	14
2.2.2. Cluster Analysis	15
2.2.3. Potential Source Contribution Function Analysis (PSCF).....	16
2.2.4. Concentration Weighted Trajectory (CWT)	20
2.3. GIS Usage in Atmospheric Studies	23
3. MATERIALS AND METHODS.....	28
3.1. Study Area	28
3.2. Data Description and Preparation	33
3.3. Methodology	53
3.3.1. Residence Time Analysis.....	53
3.3.2. Potential Source Contribution Function	56
3.3.3. Regions of Influence Analysis (RoI).....	62
4. RESULTS AND DISCUSSIONS.....	67

4.1. Comparison of Two Different Trajectory Models	68
4.1.1. Visual Comparison of the Trajectories	70
4.1.2. Comparison of the Residence Times	75
4.1.3. Comparison of PSCF Results	85
4.2. Assigning Potential Source Areas Based on Emission Inventories and Transport Patterns (Regions of Influence-RoI)	92
4.2.1. Calculation of Potential Source Areas and Comparison with PSCF Distribution in the Study Domain	94
4.2.2. Effect of Trajectory Starting Altitude on RoI Distribution.....	97
4.2.3. Variation of Regions of Influence with Time	99
4.2.4. Comparison of the Potential Source Areas Affecting Eastern and Western Mediterranean Basins	101
4.3. Inclusion of Segment Height and Rain Amount in PSCF Calculations	107
4.3.1. The Effect of Precipitation on PSCF Calculations	108
4.3.2. The Effect Trajectory Segment Altitude on Calculated PSCF Values ...	115
4.4. GIS Used and Developed in the Study	127
5. CONCLUSION AND RECOMMENDATIONS	130
5.1. Conclusion	130
5.2. Recommendations for the Future Studies.....	132
REFERENCES	133
APPENDICES	
A. SAMPLE RAW DATA OF A HYSPLIT BACKTRAJECTORY	149
B. SOURCE CODE OF HYSPLIT TRAJECTORY DATA IMPORT TOOL	156
C. SAMPLE RAW DATA OF A ECMWF BACKTRAJECTORY	158
D. SOURCE CODE OF ECMWF TRAJECTORY DATA IMPORT TOOL	167
E. SOURCE CODE OF CREATE LINE TOOL.....	170
F. SOURCE CODE OF PSCF TOOL.....	175
G. SOURCE CODE OF TOOL FOR RAIN & HEIGHT INTEGRATION TO PSCF CALCULATIONS	178

LIST OF TABLES

TABLES

Table 3.1 Data file format of SO ₄ ²⁻ measurements.....	34
Table 3.2 Settings applied Web-dab application in EMEP website (CEIP, 2009)...	35
Table 3.3 Data format of gridded SOx emissions.....	36
Table 3.4 HYSPLIT model parameters.....	44
Table 3.5 HYSPLIT trajectory data file format (ARL, 2010d).....	45
Table 3.6 ECMWF model parameters	49
Table 3.7 ECMWF trajectory data file format	49
Table 4.1 Fraction of grids (with data) in the domain indicating difference.....	83
Table 4.2 Weightings used in the inclusion of segment altitudes into PSCF calculations	116

LIST OF FIGURES

FIGURES

Figure 2.1 An example for cluster analysis results presented in Salvador et al. (2008).....	15
Figure 2.2 An example plot of PSCF analysis for summer nighttime propylene based on data from Clinton site in Houston, Texas (Xie and Berkowitz, 2007).	19
Figure 2.3 An example plot of CWT analysis for Nova Gorica, Slovenia in Žabkar et al. (2008).....	22
Figure 2.4 A screenshot of Trajstat (Wang et al., 2009) user interface	26
Figure 3.1 Study area and locations of sampling stations.	29
Figure 3.2 $1^{\circ} \times 1^{\circ}$ gridded domain	32
Figure 3.3 Wind rose used in study	33
Figure 3.4 $1^{\circ} \times 1^{\circ}$ and $0.5^{\circ} \times 0.5^{\circ}$ emission grids	38
Figure 3.5 HYSPLIT trajectories of having 3 different starting altitudes.....	43
Figure 3.6 Flowchart of trajectory data preparation process in GIS.....	52
Figure 3.7 Flowchart of Residence Time Analysis (RTA) methodology in GIS	55
Figure 3.8 Flowchart of PSCF methodology in GIS	61
Figure 3.9 Flowchart of Regions of Influence methodology in GIS	66
Figure 4.1 Visual comparisons of the HYSPLIT and ECMWF trajectories	70
Figure 4.2 Visual comparisons of the HYSPLIT and ECMWF trajectories of different starting height	73
Figure 4.3 Percentage of time air masses spent at each wind sector, calculated using trajectories computed by ECMWF and HYSPLIT trajectory models at different starting altitudes (%).....	76
Figure 4.4 Grid-based residence times calculated using ECMWF and HYSPLIT trajectories	79
Figure 4.5 Grid-by-grid differences in air mass residence times calculated using ECMWF and HYSPLIT trajectories.....	82

Figure 4.6 Comparison of potential source areas affecting SO_4^{2-} concentrations measured at Çubuk station, with PSCF using trajectories calculated with ECMWF and HYSPLIT trajectory models (Trajectories from all starting altitudes are combined)	86
Figure 4.7 Distribution of percent difference, between the PSCF values for SO_4^{2-} obtained from ECMWF and HYSPLIT trajectories (Trajectories from all starting altitudes are combined)	88
Figure 4.8 Distribution of PSCF values in the study domain at different trajectory starting altitudes	89
Figure 4.9 Distribution of percent difference, between the PSCF values for SO_4^{2-} obtained from ECMWF and HYSPLIT trajectories	90
Figure 4.10 Comparison of PSCF and RoI results calculated using combined trajectories for the years 2004, 2005 and 2006 at Çubuk station	95
Figure 4.11 Regions of Influence calculated for Antalya station for each trajectory starting altitudes	98
Figure 4.12 Variation in the distribution of regions of influence calculated for Antalya station between 1990 and 2000	100
Figure 4.13 Variation in the distribution of regions of influence between different stations in the year 1990.....	102
Figure 4.14 Variation in the distribution of regions of influence between different stations in the year 1995.....	105
Figure 4.15 Variation in the distribution of regions of influence between different stations in the year 2000.....	106
Figure 4.16 Distribution of PSCF values for %40 highest SO_4^{2-} calculated for Çubuk Station for the years 2004-2006 (Rain threshold is 1 mm)	111
Figure 4.17 Distribution of PSCF values for %40 highest SO_4^{2-} calculated for Çubuk Station for the years 2004-2006 (Rain threshold is 0.8 mm)	111
Figure 4.18 Distribution of PSCF values for 40% highest SO_4^{2-} calculated for Çubuk Station for the years 2004-2006 (Rain threshold is 0.5 mm)	112
Figure 4.19 Distribution of PSCF values for %40 highest SO_4^{2-} calculated for Çubuk Station for the years 2004-2006 (Rain threshold is 0.3 mm)	112

Figure 4.20 Distribution of PSCF values for %40 highest SO_4^{2-} calculated for Çubuk Station for the years 2004-2006 (Rain threshold is 0.2 mm)	113
Figure 4.21 Distribution of PSCF values for %40 highest SO_4^{2-} calculated for Çubuk Station for the years 2004-2006 (Rain threshold is 0.1 mm)	113
Figure 4.22 Distribution of PSCF values for %40 highest SO_4^{2-} calculated for Çubuk Station for the years 2004-2006 using only segments having height <1000 m in PSCF calculations	117
Figure 4.23 Distribution of PSCF values for %40 highest SO_4^{2-} calculated for Çubuk Station for the years 2004-2006, using the following weights: 0-500m → $m_{ij}^* 1$, >500 m → $m_{ij}^* 0.5$	118
Figure 4.24 Distribution of PSCF values for %40 highest SO_4^{2-} calculated for Çubuk Station for the years 2004-2006 using the following weights 0-500m → $m_{ij}^* 1$, 500-1000 m → $m_{ij}^* 0.8$, >1000 m → $m_{ij}^* 0.5$	119
Figure 4.25 Distribution of PSCF values for %40 highest SO_4^{2-} calculated for Çubuk Station for the years 2004-2006 using the following weights 0-500m → $m_{ij}^* 1$, 500-1000 m → $m_{ij}^* 1$, >1000 m → $m_{ij}^* 0.5$	120
Figure 4.26 Distribution of PSCF values for %40 highest SO_4^{2-} calculated for Çubuk Station for the years 2004-2006 using the following weights 0-500m → $m_{ij}^* 1$, 500-1500 m → $m_{ij}^* 0.8$, >1500 m → $m_{ij}^* 0.5$	121
Figure 4.27 Distribution of PSCF values for %40 highest SO_4^{2-} calculated for Çubuk Station for the years 2004-2006 using the following weightings 0-500m → $m_{ij}^* 1$, 500-1000m → $m_{ij}^* 0.9$, 1000-1500m → $m_{ij}^* 0.8$, >1500m → $m_{ij}^* 0.5$	122
Figure 4.28 Distribution of PSCF values for %40 highest SO_4^{2-} calculated for Çubuk Station for the years 2004-2006 (All height weightings).....	125
Figure 4.29 Distributions of PSCF after weighting for both rain and segment altitude.....	126

LIST OF ABBREVIATIONS

AGL	Above Ground Level
AMSL	Above Mean Sea Level
ARL	Air Resources Laboratory, United States
BADC	British Atmospheric Data Centre, UK
CEIP	Centre on Emission Inventories and Projections, Austria
CLRTAP	Convention on Long-Range Transboundary Air Pollution
COHA	Causes of Haze Assessment
CSU	Colorado State University, United States.
CWT	Concentration Weighted Trajectory
ECMWF	European Centre for Medium-Range Weather Forecasts, UK
EMEP	Co-operative Programme for Monitoring and Evaluation of the Long-range Transmission of Air Pollutants in Europe
GIS	Geographical Information Systems
GUI	Graphical User Interface
HYSPLIT	HYbrid Single Particle Lagrangian Integrated Trajectory Model
IMS	Irish Meteorological Service, Ireland
MARS	Meteorological Archival and Retrieval System
METEX	METeorological data EXplorer
METU	Middle East Technical University, Turkey
MoEF	Ministry of Environment and Forestry, Turkey
MSC-E	Meteorological Synthesizing Centre-East, Russia
MSC-W	Meteorological Synthesizing Centre-West, Norway
NCAR	National Center for Atmospheric Research, United States
NCEP	National Centers for Environmental Protection, United States
NILU	Norwegian Institute for Air Research (Norsk Institutt for Luftforskning)
NOAA	National Oceanic and Atmospheric Administration, United States
NOx	Nitrogen Oxides

NWP	Numerical Weather Prediction
PM	Particulate Matters
POPs	Persistent Organic Pollutants
PSCF	Potential Source Contribution Function
READY	Real-time Environmental Applications and Display sYstem
RTA	Residence Time Analysis
RoI	Regions of Influence
SOx	Sulfur Oxides
SPO	State Planning Organization, Turkey
UK	United Kingdom
UN	United Nations
UNECE	United Nations Economic Commission for Europe
VOCs	Volatile Organic Matters

CHAPTER 1

INTRODUCTION

Environment is the place where human beings and nature composed of air, water, land resources and flora and fauna interact with each other. It is an indispensable component of life. Human and environment interact such a way that environment provide the place and resources to be utilized by human beings. While human utilize natural resources as inputs for the economical activities, wastes that are generally pollutants for the environment are generated. If no precautions taken, these pollutants cause pollution and deterioration of environment. Looked at the result-chain, pollution of environment will cause damage on natural resources vital for human life and economical development, risk food security and widespread diseases and hunger, etc. Pollution means the loss of the quality of life and even an inevitable end of life for some living species.

Air, water and soil pollutions are the main types of environmental pollution according to the receiving media. All types of pollution have adverse impact on the sustainability of the natural resources and life. Moreover, global environmental problems such as climate change, reduction of ozone layer and desertification are affecting the common future of the world. Among those, climate change and thinning of ozone layer are closely related with air pollution. Air pollution, in other words atmospheric pollution, is specifically interested nowadays as an adverse effect of industrialization because it includes complex physical and chemical interactions, has multi-scalar i.e. local and regional extents, affecting human life seriously (respiratory diseases, acid rains, climate change and etc.). The main environmental problems associated with air pollution are harm to human health, acidification and eutrophication of water and soils, and damage to natural

ecosystems, agricultural crops, cultural heritage and material in general (De Leeuw, 2002).

Air pollution and pollutants formally defined as “the introduction by man, directly or indirectly, of substances or energy into the air resulting in deleterious effects of such a nature as to endanger human health, harm living resources and ecosystems and material property and impair or interfere with amenities and other legitimate uses of the environment and “air pollutants” shall be construed accordingly” (UNECE, 1979). Examples of air pollutants could be given as nitrogen oxides (NO_x), sulfur oxides (SO_x), carbon monoxide (CO), hydrocarbons, volatile organic compounds (VOCs), particulate matter (PM), smoke and haze. Air pollutants could be in gaseous (i.e. carbon monoxide, SO_x, NO_x and hydrocarbons) or in the form of particulate (i.e. smoke and dust) and can be classified as either primary or secondary. Primary air pollutants are the pollutants such as carbon monoxide, sulfur dioxide and total suspended particles that retains in the same form as they emitted from the sources. On the contrary to primary pollutants, secondary pollutants are formed in the atmosphere as a result of reactions such as hydrolysis and oxidation. An example of a secondary pollutant is ozone, which causes photochemical smog, formed by photo-induced chemical reaction of hydrocarbons (or VOCs) and NO_x. Source control of primary pollutants is the most important strategy for effective air pollution control. This is also crucial for source control of secondary pollutants as they are formed by the reactions of primary pollutants. (Liu and Lipták, 2000)

When the pollution sources considered, these could be divided into two types: anthropogenic (manmade) sources (i.e. power plants, motor vehicles, incineration plants and industrial processes, etc.) and natural sources (pollens of plants, dusts blown by winds, lightning generated forest fires, volcanic eruptions, etc.) (Liu and Lipták, 2000). Anthropogenic sources are generally located in urban and industrial areas while natural sources hard to locate because any place that natural particulates formed on could be a source location.

In general these sources affect most the air quality of the places near to these sources. But, under appropriate conditions, pollutant particles can be transported long distances even across continents by air flow. Pollution at a location could be affected by many source locations and it is important to look at the air pollution problem rather regionally and even globally. The history of the actions for the long-range transport of pollutants can be traced back to the 1960s, when scientists showed the connections between sulfur emissions in Europe and the acidification of Scandinavian lakes. In 1972, the United Nations (UN) Conference on the Human Environment held in Stockholm indicated the start of active international cooperation to combat acidification. Between 1972 and 1977 several studies confirmed that air pollutants could travel several thousands of kilometers before deposition and damage occurred. This also implied that cooperation at the international level was necessary to solve problems such as acidification. This issue turned out to an international action in 1979 and 32 members of UN Economic Commission for Europe (UNECE) set on the table to sign Convention on Long-range Transboundary Air Pollution (CLRTAP) to address this threat to human health and well-being. The Convention aims to limit, gradually reduce and prevent air pollution including long-range transboundary air pollution among parties. The convention entered into force in 1983 and extended by eight protocols. These are the protocols to abate acidification, eutrophication and ground-level ozone (1999); on persistent organic pollutants (POPs) (1998); on heavy metals (1998); on further reduction of sulfur emissions (1994); concerning the control of emissions of volatile organic compounds or their transboundary fluxes (1991), concerning the control of nitrogen oxides or their transboundary fluxes (1988); on the reduction of sulfur emissions or their transboundary fluxes (1985); on long-term financing of the Cooperative Programme for Monitoring and Evaluation of the Long-range Transmission of Air Pollutants in Europe (EMEP) (1984). Currently 51 countries ratified the CLRTAP. Turkey signed the CLRTAP in 1979 and ratified the Convention in 1983. She also signed EMEP Protocol in 1984 and ratified it after one year (UNECE, 2004).

EMEP is an international monitoring programme that is aiming to regularly provide Parties of the CLRTAP with scientific information to support the development and evaluation of the protocols on emission reductions under the CRLTAP. EMEP programme includes three main missions: (1) collection of SO₂, NO_x, VOCs and other air pollutant emissions data, (2) measurement of air quality and precipitation and (3) modeling of atmospheric transport and dispersion (EMEP, 2010a). By January 2009, there are approximately 302 monitoring stations in 37 European countries, which constitute the monitoring network of EMEP (NILU, 2010a).

In addition to CRLTAP and its protocols, some other international agreements related to protection of atmosphere such as Barcelona Convention for Protection of Mediterranean Region Against Pollution (1976) which was amended in 1995, Vienna Convention for the Protection of the Ozone Layer (1985) and Bucharest Convention on the Protection of the Black Sea Against Pollution (1992) are adopted. Turkey ratified Barcelona Convention in 1981 and its amendment in 2002, Vienna convention and Bucharest Convention in 1994 (SPO, 2007).

In Turkey, air pollution has been an important environmental problem as an undesirable result of high rate of population increase, increasing energy use as a result of urbanization and industrialization, increasing number of transportation vehicles (SPO, 2007). The reasons of air pollution originated from heating in winter seasons were identified as the usage of poor quality fuels without recovery process, appliance of wrong incineration techniques and inadequate maintenance of furnaces. However with the utilization of natural gas and other high grade fuel in heating, some improvement has been seen in the air pollution in the big cities of Turkey compared to the 1990s. The inappropriate site selection of the industrial facilities also contributes to the air pollution caused by the thermal power stations that are generally burning coal. The SO₂ emissions originating from high sulfur content of domestic lignite constitute another risk. Exhaust gases emitted from motor vehicles are also an important problem for which necessary precautions must be taken for air pollution in cities (MoEF, 2006). As of 2009, the air quality in the country is currently monitored by using the 119 monitoring stations in 81 provinces

of Turkey by Ministry of Environment and Forestry. In all of these stations, SO₂ and PM parameters have been measured automatically and in addition to these parameters NO_x, CO and O₃ have been assessed in some of the stations (MoEF 2010). Air pollution causes many severe environmental and health problems as explained before. It directly affects the people especially children and elder living in the cities or the residential areas near industrial areas.

Effective management of air pollution requires good inventory of the pollution sources, estimating the emissions, modeling of atmospheric dispersion and transport and efficient monitoring of air quality levels (Hsu et al., 2003). Identification of the pollution sources is the initial step. Local sources are easy to be identified because they are more visible (i.e. if there is an industrial plant that emits plumes near city then it is probable that this plant would be a pollution source). In addition to the pollution caused by local sources, pollutants emitted from sources outside of the borders contribute the degradation of the air quality at a receptor area. For this reason, knowledge of long range transport in addition to the information at local level has great importance in understanding the air pollution problem at a location. Besides, without proper source inventories and known source locations, dispersion models cannot be used to estimate impacts on ambient air concentrations for air quality management (Hsu et al., 2003).

Apportionment of source regions in other words determination of sources contributions on observed levels of pollution in the regional scale is necessary information for air quality management and development of national policy for exchange of air pollutants with other countries. If the source location is not known but there is information on concentrations then trajectories providing geographical and meteorological information could facilitate finding possible locations of pollution sources. Source region apportionment can be studied either through numerical modeling or by using trajectory statistics that is a hybrid methodology of modeling and measurements. To identify potential pollution sources, several trajectory statistics techniques were developed. Flow Climatology, Potential Source Contribution Function (PSCF) (Ashbaugh et al., 1985) and Concentration Weighted

Trajectory (CWT) (Seibert et al., 1994) are some examples of these techniques. Among all, PSCF was primarily concerned in this study. Although PSCF was a widely used methodology in source identification, it has some deficiencies such as rain and height information are not being considered in the current studies. There is a need for improving the PSCF methodology to decrease these uncertainties. In addition, these types of methodologies require expensive long term measurements. Therefore simple approaches should be developed to identify potential source areas using very few and simple input data, so that they can be used to gather preliminary information where expertise on running sophisticated numerical transport and chemical models is not available.

Geographical Information Systems (GIS) have been widely used in air pollution and quality studies (Lin and Lin, 2002; Jin and Fu, 2005; Briggs et al., 1997; Borrego et al., 2003; Elbir, 2004; Elbir et al., 2010; Canepa et al., 2007; Lee et al., 2004; Shad et al., 2009; Vienneau et al., 2009; Woodfine et al., 2002; Shadbolt et al., 2006; Wang et al., 2009). It has many advantages such as effective management of extensive data, integration of different models, efficient visualization, etc. In the source apportionment studies done in Environmental Engineering Department of Middle East Technical University (METU), GIS were mainly used for visualization and thematic mapping of the analysis results. But, significant parts of the analyses such as data processing and calculations have been done in different platforms although they could also be applied in an integrated approach in GIS. GIS have prominent capacity and their use in source apportionment studies, where use of spatial information is required, is significant and crucial. In addition, implementation of the source apportionment methodologies in a comprehensive and integrated way could provide better management of the large amount of data, faster analyses and easier interpretation of the results.

1.1. Purpose and Scope

The need for improvement of the current methodologies and implementation of the source identification methods effectively within GIS that explained the previous part constituted the rationale for this study. Therefore this study aims comparison of two widely-used trajectory calculation schemas, developing an air pollution source identification methodology, improving existing tools of trajectory statistics and enhancing the GIS use in air pollution studies in environmental engineering. In order to fulfill these aims, the following scopes are covered in this study:

- The backtrajectories obtained from 2 types of models, namely Hybrid Single Particle Lagrangian Integrated Trajectory Model (HYSPLIT) (Draxler and Hess, 1998) and a trajectory model developed by Irish Meteorological Service (IMS) (McGrath, 1989) running at European Centre for Medium-Range Weather Forecasts (ECMWF) are compared in different aspects,
- Regions of Influence (RoI) methodology is developed,
- Potential Source Contribution Function (PSCF) methodology is improved,
- Processes in these methods are integrated and automated using GIS techniques,
- Potential source regions affecting pollutant concentrations are assessed for 4 locations in the Mediterranean region (Amasra, Ankara and Antalya in Turkey and Corsica in France) in order to find potential pollution sources in regional scale.

Since this study was focused mainly in methodology, the data production was not under primary concern. The pollution and trajectory data used in the analyses were not produced in the context of the study; instead, pollution information was obtained from previous studies and an online registry of EMEP emissions while trajectory data was acquired from the ECMWF and Air Resources Laboratory websites. Therefore the data production steps were not explained in detail.

1.2. Plan of the Thesis

Chapter 1 introduces the problem and presents the aim, scope and the context of the thesis study.

In Chapter 2, literature review for the subject was provided. Some background information on trajectories and trajectory models were given. Trajectory statistics with some examples of widely used methods was explained. GIS usage in the air pollution studies were discussed with some different example studies.

In Chapter 3 of the thesis, the study area and the data used in the thesis study were described. Data sources were explained and data gathering and processing steps were described. The methodology and its application within GIS were described.

In Chapter 4, two trajectory models namely HYSPLIT and ECMWF were compared based on visual perception, residence times and PSCF values. How the inclusion of rain and height in PSCF calculations achieved was discussed. In addition, “Regions of Influence” methodology developed in the context of this study was described and the validation of the results of this method was explained.

Chapter 5 concludes the study and the recommendations for future studies were presented in this chapter.

CHAPTER 2

LITERATURE REVIEW

Identification of pollutant sources is an important component of air pollution management. Without information on source locations and their contributions to pollution, efficient policies and actions could not be identified. There are various techniques for identification of source areas. Trajectories, paths of air parcels, could be used for the analyzing air flow pattern. HYSPLIT and ECMWF models have been widely used for the calculation of trajectories. When combined with the pollution information, trajectory information will give significant insights on identification of potential sources. Backtrajectory statistics are used to show the direction and sources of air pollution at a receptor site. Trajectory statistics such as clustering (Harris and Kahl, 1990), potential source contribution function (PSCF) (Ashbaugh et al., 1985) and concentration weighted trajectory (CWT) (Seibert et al., 1994) are popular techniques used in this field.

In this section, concepts of trajectories with some generally used trajectory statistics are explained. The use of GIS in air pollution studies are told with some examples.

2.1. Trajectories

A trajectory defined as the path of an air parcel, more scientifically, the time integration of the position of an air parcel as it is transported by the wind. Trajectory models have been used to study dynamical processes in the atmosphere. They are applied in investigating air mass flow around mountains (Steinacker, 1984), in identifying pathways of water vapor transport (D'Abreton and Tyson,

1996) and desert dust (Chiapello et al., 1997) and in establishing source-receptor relationships of air pollutants (Stohl, 1996).

There are two approaches to understand air motions. Eulerian approach focuses on points fixed in space through which the air flows. Whereas, Lagrangian approach takes individual air parcels as they move through time and space. (Byers, 1974; Dutton, 1986; Stohl, 2002)

Assuming that there is a specific infinitesimally small air parcel, then its trajectory is defined by the differential trajectory equation;

$$\frac{dX}{dt} = \dot{X} [X(t)] \quad (2.1)$$

where t : time, X : position vector and \dot{X} : wind velocity vector. If the initial position X_0 of the parcel at time t_0 is known, then its path could be determined through Eq. (2.1). It can be written:

$$X(t) = X(X_0, t) \quad (2.2)$$

Inverse transformation of it could be written as,

$$X_0(t=t_0) = X_0(X, t) \quad (2.3)$$

Eq. (2.3) gives the initial coordinates of the parcel which is at position X at time t . Consequently, air parcels may be tracked either forward in time to produce forward trajectories or backward in time to obtain backtrajectories. The spatial coordinates X_0 at time t_0 provide a means of identifying each air parcel for all time. These initial coordinates are called Lagrangian coordinates (Dutton, 1986).

Eq. (2.1) can be solved by finite difference approximation for meteorological applications (Walmsley and Mailhot, 1983). Expanding $X(t)$ in a Taylor series about $t=t_0$ and evaluating at $t=t_0+\Delta t$, it can be obtained:

$$X(t_1) = X(t_0) + (\Delta t) \left. \frac{dX}{dt} \right|_{t_0} + \frac{1}{2} (\Delta t)^2 \left. \frac{d^2 X}{dt^2} \right|_{t_0} + \dots \quad (2.4)$$

The first approximation of the Eq. (2.4) yields:

$$X(t_1) \approx X(t_0) + (\Delta t) \dot{X}(t_0) \quad (2.5)$$

Eq. (2.5) could be solved by iteration and then the solution becomes:

$$X^i(t_1) \approx X(t_0) + \frac{1}{2} (\Delta t) [\dot{X}(t_0) + \dot{X}^{i-1}(t_1)] \quad (2.6)$$

where the superscript (i) indicates the number of iteration, and $\dot{X}^i(t_1)$ is the wind velocity vector taken at position $X^i(t_1)$. This called kinematic solution because only the wind information is used in solution. Danielsen (1961) developed a methodology to build trajectories by labeling air parcels with (quasi-) conservative quantities such as potential temperature. Danielsen's (1961) method called dynamic due to the velocity and mass field information and dynamic equations linking the two (Merrill et al., 1986) were used in.

Dynamic methods were popular (Merrill et al., 1986; Steinacker, 1984) because they allowed using long intervals between the wind fields. However, it is showed in Stohl and Seibert (1997) that dynamic trajectories calculated with dynamic method (Steinacker, 1984) can perform unrealistic oscillations at travel times longer than 24 to 48 h. Kinematic trajectories are found to be more accurate than dynamic trajectories because accurate wind fields with high space and time resolution are available nowadays (Stohl and Seibert, 1997).

Trajectories can be confused with streamlines, which are the directions of flow at a fixed instant of time. Streamlines are tangent to the velocity vectors. At a certain instant of time, each particle in the flow is moving along its trajectory and so the streamlines are parallel to the trajectories, but as time passes, the streamlines must adjust to the flow and trajectories and streamlines are no longer parallel. Only during stationary conditions, the trajectories and the streamlines are the same (Stohl, 2002).

Trajectories can be calculated by interpolating between the locations of wind observations. But, trajectory calculations are typically based on the gridded output of numerical models in practice. Wind data at discrete locations in space and time are accessible either as irregularly spaced observations or as the gridded output of meteorological models. In both cases, the wind speed should be estimated at the trajectory position by the trajectory model. This interpolation causes errors that affect the trajectory's accuracy substantially. Temporal and spatial resolutions of the trajectories are the main triggers for the trajectory errors. They must be in balance to limit the trajectory errors. An increase in spatial resolution alone does result in just marginally more accurate trajectories when the temporal resolution is low. As oppose to, increasing the temporal resolution alone is also not very effective when the spatial resolution is low (Stohl, 2002).

In most of the trajectory models, horizontal components of trajectories are calculated by using observed or analyzed winds, while, vertical components are computed based on one of the following assumptions (Doğan, 2005):

- Isobaric: trajectory is assumed to follow a constant pressure,
- Isentropic: trajectory is assumed to follow a constant potential temperature,
- Kinematic: trajectory is assumed to move with the vertical velocity wind fields generated by diagnostic or prognostic model.

Trajectory errors are also related to different assumptions regarding the vertical wind component. In contrast to the horizontal wind, there are no routine observations of vertical winds. Fields of vertical wind are a sole product of meteorological models, and hence they are less accurate than the fields of the horizontal wind. Even the vertical winds are less accurate, kinematic assumption results more accurate results than others because it includes vertical wind information (Stohl, 2002).

Wind field errors and errors in starting positions of trajectories are the other errors occurred in calculations that affect the accuracy of trajectories. According to the type of wind fields used, wind field errors can occur as analysis errors or forecast errors. Trajectory errors caused by erroneous forecasts are relatively simple to evaluate by comparing forecast with analysis trajectories. Uncertainties in starting positions of the trajectories on the other hand are often significant to be considered such as in the estimations of the effective source height of accidentally released material (Stohl 2002).

Differences between the model topography and the real topography create another uncertainty which makes the selection of a trajectory starting height difficult. The initial trajectory position errors could be rather small but they could strongly increase in divergent (forward trajectories) or convergent (backtrajectories) flow (Stohl, 2002).

Forward and backtrajectories are useful in describing the atmospheric dynamics of various weather systems. Backtrajectories have been used as a standard tool in air quality studies. They have been using to describe source-receptor relationship, analyze meteorological mechanisms related with pollutant observations, and set up time scales for various chemical reactions (Fast and Berkowitz, 1997). When constructing backtrajectories an air parcel is followed backward from the receptor in hourly steps for a specified length of time. While, in forward trajectories, particles are released from the source and their trajectories are tracked forwardly in time.

2.2. Trajectory Statistics

Trajectories have been used to interpret individual flow situations for a long time, but statistical analysis methods for large sets of trajectories have been developed more recently (Stohl, 2002). In the recent methods, trajectory information is used together with pollutant concentrations to identify pollution sources. In these methods, measured pollutants concentrations are combined with air backtrajectories from receptor area to obtain information on the source regions. Some widely used methods of trajectory statistics are described in this part.

Trajectories accepted as an oversimplification of the atmosphere where atmospheric dispersion was not taken into account (CSU, 2010). Some other assumptions that often have to be made in utilizing trajectory statistics methods are as follows: pollutant measurements are correct and representative for the study area; atmospheric transport processes are explained properly with the air trajectories; and the pollutants are not subject to decay processes such as chemical reactions, deposition and radioactive decay with time-scales shorter than that of transport (Wotawa and Kröger, 1999). These assumptions cause uncertainties in trajectory analyses.

2.2.1. Flow Climatology

Flow climatology is the earliest trajectory statistics method for the identification of the pollution sources. It is often used to determine the pollution input from distant sources to a selected region and also allows understanding of airflow patterns. In flow climatology method, backtrajectories were calculated for several years and then they classified according to their travel speeds and transport directions using some criteria (Stohl, 2002; Doğan 2005).

Miller and Harris (1985) developed flow climatology for a 7-year period to Bermuda to understand transport of pollutants off the North American continent. Similarly, Katsoulis (1999) used flow climatology to improve the understanding of

atmospheric transport pathways to Greece and to evaluate the polluting potential of distant source regions outside the country.

Munzur (2008) applied this method at İzmir-Çandarlı Turkey to determine potential source regions for pollutants. She found out the frequency of air flows from Russia and Western Europe are higher implying that emissions from these industrial regions affecting the chemical composition of particulate matter. Also she identified that contributions from central and eastern European countries are significantly high because of frequent air mass transport.

2.2.2. Cluster Analysis

A multivariate statistical technique, cluster analysis divides a data set into a number of groups. Cluster analysis is rather subjective classification methodology since the selection of the clustering algorithm, the distance measure and the numbers of clusters are subjective (Stohl, 2002). It resembles to flow climatology in terms of both method includes classification, but cluster analysis thought to be more objective than flow climatology since it accounts for variations in transport speed and direction simultaneously (Moody and Samson, 1989; Harris and Kahl, 1990).

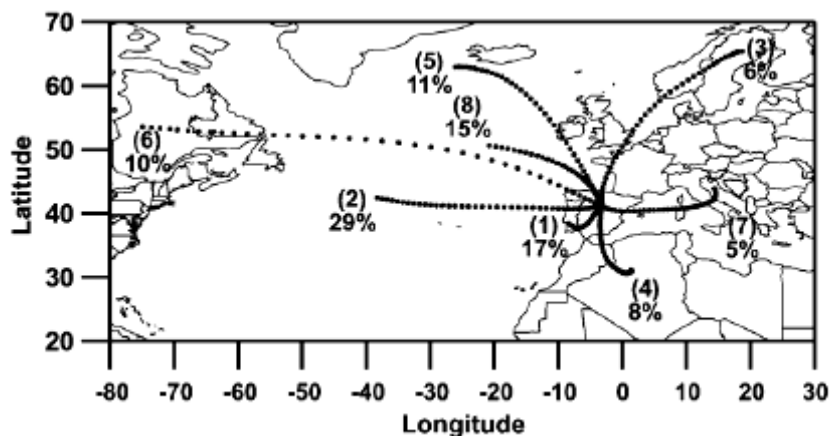


Figure 2.1 An example for cluster analysis results presented in Salvador et al. (2008)

Figure 2.1 shows eight clusters of the analysis done depending on their direction and speed by Salvador et al. (2008). The percentages of trajectories occurring in each cluster are shown next to the cluster number. Each cluster represented a characteristic meteorological scenario, i.e.: cluster 1 represents low while, cluster 2 gathers westerly trajectories moderately moving from the mid Atlantic Ocean. In this study, they applied cluster and residence time analysis to a set of 7 years of back-trajectories to describe the main flow patterns over central Spain.

Rozwadowska et al. (2010) used cluster analysis to classify backward air trajectories into groups of similar history, i.e. similar direction of advection and velocity of air movement in order to research the impact of air back-trajectories on aerosol optical properties at Hornsund, Poland.

Baker (2010) applied cluster analysis of four-day backtrajectories for the years 1998 to 2001 in order for a better understanding of the pollution meteorology influencing Birmingham, UK.

In another study, Park et al. (2007) used trajectory cluster analysis for exposure assessment in order to evaluate the relation between health effects and exposure to air pollution. They examined whether the association of measured air pollutants with heart problems differed by cluster.

2.2.3. Potential Source Contribution Function Analysis (PSCF)

In flow climatology and cluster analysis methods, trajectories are classified without including air pollution data. As compared with the previous methods, potential source contribution function (PSCF) analysis fills this gap. Developed by Ashbaugh et al. (1985), PSCF was defined as the conditional probability that an air parcel with a level of pollutant concentration above a criterion value arrives at a receptor site after having passed through a specific geographical area. By using the chemical concentrations and air parcel trajectories, the PSCF model combines chemical data

with meteorological data to provide an indication of the locations where pollutants are emitted.

In the literature, PSCF has been used in a number of prior studies to identify possible locations of sources (Zeng and Hopke, 1989; Gao et al., 1993, 1996; Plaisance et al., 1997; Hsu et al., 2003; Liu et al., 2003; Güllü et al., 2005; Hwang and Hopke, 2007; Doğan, 2005; Işıkdemir, 2006; Doğan et al., 2008; Munzur, 2008).

The procedure of calculation of PSCF was described in Plaisance et al. (1997) as follows:

An i by j array of grid is superimposed over the whole geographic region covered by the trajectories, so that PSCF will be a function of grid cell addresses (i, j). Size of the grid cells depends on the geographical scale of the problem. If pollutant specie emitted within the grid cell (i, j) and trajectory of an air parcel passes over this cell at the time of emission, it is assumed that air parcel collects the pollutant emitted in the cell and transported it along the trajectory to the receptor site.

Taking N as the total number of trajectory end points during the study period, t . If n_{ij} endpoints fall into ij^{th} cell, the probability of event, A_{ij} is given as (Eq. 2.7):

$$P[A_{ij}] = \frac{n_{ij}}{N} \quad (2.7)$$

$P[A_{ij}]$ is the probability of a random selected air parcel is present in the ij^{th} cell relative to time period, t . In the same cell, if there are a subset of m_{ij} endpoints of trajectories that are considered to be ending at receptor area at a time when pollutant concentration above a selected criterion. Then the probability of this event (Eq. 2.8) is defined as:

$$P[B_{ij}] = \frac{m_{ij}}{N} \quad (2.8)$$

$P[B_{ij}]$ is the probability of a random contaminated air parcel is present in the ij^{th} cell relative to same time period, T. Then the potential source contribution function (PSCF_{ij}) is then defined as a conditional probability (Eq. 2.9):

$$PSCF_{ij} = \frac{P[B_{ij}]}{P[A_{ij}]} = \frac{m_{ij}}{n_{ij}} \quad (2.9)$$

PSCF_{ij} is the conditional probability that an air mass with specified pollutant concentration arrived at the receptor site after having resided in the ij^{th} cell. PSCF takes the value between 0 and 1. Any grid cell having PSCF of 0 is unlikely to be the source region, while the value of 1 has high probability of being source region. Cells containing pollution sources should have higher PSCF values, if there are trajectories passing this cell that can transport pollution to the receptor.

An example plot from the study by Xie and Berkowitz (2007), in which potential source contribution function was used to identify source regions and advection pathways of hydrocarbon emissions in Houston, Texas, is given in Figure 2.2.

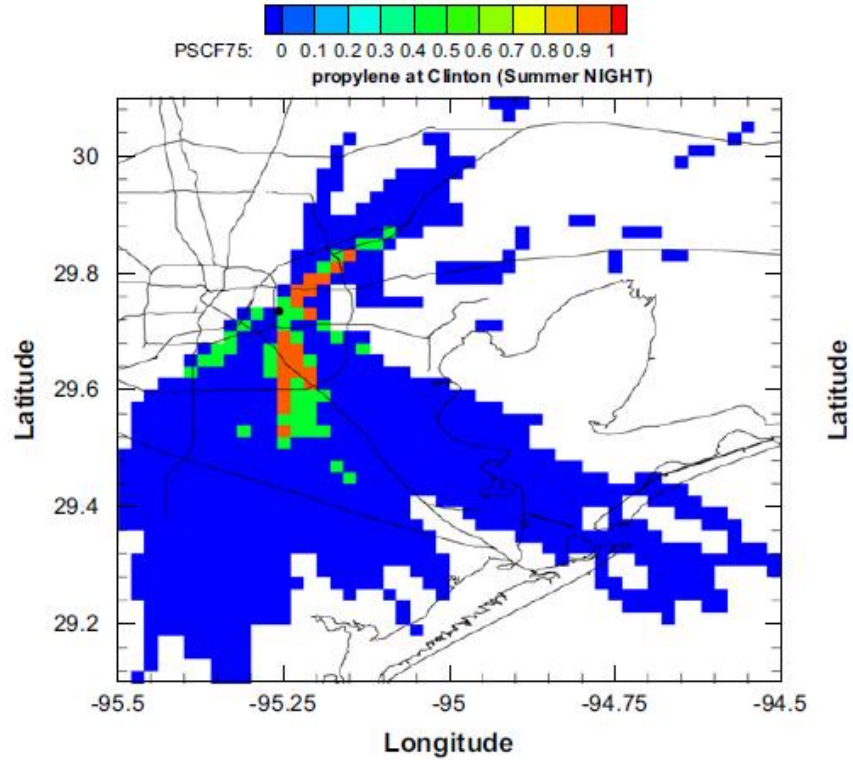


Figure 2.2 An example plot of PSCF analysis for summer nighttime propylene based on data from Clinton site in Houston, Texas (Xie and Berkowitz, 2007).

For large values of n_{ij} , the results are statistically stable. If only one segment end point exists in a cell (i,j) and this end point is related to the pollution event then PSCF value of cell becomes 1 but the confidence of this situation is low. Therefore it is necessary to reduce the effect of small values of n_{ij} by developing a weight function. Using arbitrary weighting based on the average value of n_{ij} (Eq. 2.10) for the small values of n_{ij} can be utilized for this purpose (Hopke et al. 1995; Polissar et al. 2001; Zhao and Hopke, 2006; Xu and Akhtar, 2009).

$$w(n_{ij}) = \left\{ \begin{array}{ll} 1.0 & n_{ij} > 2 \cdot n_{avg} \\ 0.75 & n_{avg} < n_{ij} \leq 2 \cdot n_{avg} \\ 0.5 & n_{avg} / 2 < n_{ij} \leq n_{avg} \\ 0.15 & n_{ij} \leq n_{avg} / 2 \end{array} \right\} \quad (2.10)$$

Another way of the weighting the PSCF results, the bootstrapping could be used to provide better estimates of the probability values and their uncertainties (Wehrens et al., 2000). This method assumes that the concentration values are independent and identically distributed. From the original concentration data set, $C = \{c_1, c_2, \dots, c_N\}$, B random subsamples of size equal to the length of the data set, $C^* = \{c_{1*}, c_{2*}, \dots, c_{N*}\}$, are drawn with replacement. For each bootstrapped sample k , the corresponding PSCF spatial distribution, $P^*_{k;ij}$, is calculated. These values are ordered as $P^*_{(1);ij} < \dots < P^*_{(B);ij}$, where $k = 1, \dots, B$, and α is the chosen significance level. If

$$P_{ij} \geq P^*_{((B+1)(1-\frac{\alpha}{2});ij)} \quad (2.11)$$

then, null hypothesis that there is no association between concentrations and trajectories is rejected at $(1 - \alpha)$ 100% confidence level. Then, only the PSCF values satisfying the above relation are retained in analysis (Lupu and Maenhaut, 2002; Güllü et al., 2005; Doğan et al., 2008).

Although PSCF is a relatively easy, the assumptions such as emissions are swept by air parcel, concentrations atmospheric removal and chemistry are not considered as an air parcel transports to the receptor site (Cheng et al., 1993; Plaisance et al., 1997; Lupu and Maenhaut, 2002). Combined with the uncertainties in trajectory calculation (Zhou et al., 2004; Stohl, 1998; 2002), those assumptions form the main weaknesses in PSCF methodology.

2.2.4. Concentration Weighted Trajectory (CWT)

A limitation of the PSCF method is that grid cells can have the same PSCF value when sample concentrations are either only slightly higher or much higher than the criterion. As a result, it can be difficult to distinguish moderate sources from strong ones. Seibert et al. (1994) computed concentration fields to identify source areas of pollutants. A grid domain was used as in the PSCF method. For each grid cell, the logarithmic mean concentration of a pollutant species was calculated as follows:

$$\ln(\overline{C}_{ij}) = \frac{1}{\sum_{k=1}^N \tau_{ijk}} \sum_{k=1}^N \ln(c_k) \tau_{ijk} \quad (2.12)$$

where i and j are the indices of grid, k the index of trajectory, N the total number of trajectories used in analysis, c_k the pollutant concentration measured upon arrival of trajectory k , and τ_{ijk} the residence time of trajectory k in grid cell (i, j) . A high value of \overline{C}_{ij} means that, air parcels passing over cell (i, j) would, on average, cause high concentrations at the receptor site (Stohl, 1996).

In the Concentration Weighted Trajectory (CWT) analysis, the concentration values at the receptor site are assigned to the corresponding backward trajectories. The mean or logarithmic mean concentration is computed and used as a weight for the residence time of each grid cell (Zhou et al., 2004).

CWT method was improved by Stohl (1996) into residence-time weighted concentrations (RTWC) method by redistributing the concentration fields in an iterative process.

CWT method used in various studies. For example, Žabkar et al. (2008) analyzed summertime ozone pollution in Slovenia. They used CWT to gather information about possible emission source regions. The CWT method distributes the ozone concentration along the trajectories evenly and is able to distinguish major sources from moderate ones by calculating concentration gradients. A plot of CWT analysis in that study was given as an example in Figure 2.3. In this plot, text box denotes the cluster number and the percentage of trajectories involved in cluster. Path widths measure average above ground level (AGL) of cluster trajectories. Topography (resolution 9.5 km) above 500 m above mean sea level (AMSL), with the contour intervals 500 m are shown in the background.

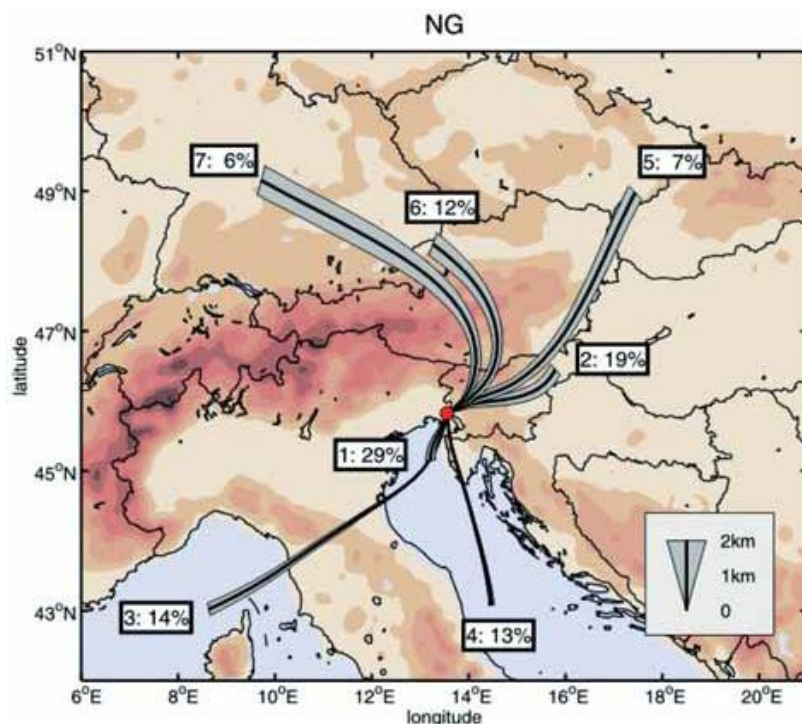


Figure 2.3 An example plot of CWT analysis for Nova Gorica, Slovenia in Žabkar et al. (2008)

Lupu and Maenhaut (2002) compared PSCF and CWT methods, and found the two methods provided similar results and correctly identified known emission sources. They saw both methods as complementing each other. The PSCF method works with probabilities, the CWT method with concentrations. CWT seems being more readily understanding and easily interpreted. But, when analyzing common sources for multiple sites, PSCF method is advantageous in that working with probabilities provides the same comparison base for all sites. Another advantage of the PSCF method is that it allows one to examine the smearing of a real source by means of an ideal source test.

2.3. GIS Usage in Atmospheric Studies

A Geographical Information System (GIS) is a computer based system for capturing, storing, integrating, manipulating, analyzing and displaying the geographic (spatial) data to help making decisions on interested subjects. A popular definition was done by Aronoff (1989) as “a computer-based system that provides the following four sets of capabilities to handle geo-referenced data: 1) input; 2) data management (data storage and retrieval); 3) manipulation and analysis; and 4) output”. GIS integrate database operations such as query and statistical analysis with the visualization and geographical analysis benefits offered by maps. These abilities distinguish GIS from other information systems and make them valuable to a wide range of applications in science and technology (Sharma et al. 2010).

In air pollution/quality studies, GIS are used extensively to prepare geographical input data, analyze receptor-source relationship and to process, analyze and visualize modeling results. Air dispersion modeling is a well-established discipline that can produce results in a spatial context. The integration of dispersion modeling with GIS would empower the predictive capacity of modeling with the data management, analysis, and display capabilities of GIS (Dent et al., 2000). GIS are also essential tools used in identifying possible source areas of atmospheric pollutants by receptor models or air mass trajectory statistics. For example in trajectory statistics, GIS provide the way to analyze air mass residence times in each cell of a geographical grid covering the area of interest, make the essential numerical operations and to visualize potential source areas properly (Dvorská, 2008).

Some examples on the use of GIS in atmospheric studies, such as air quality and pollution mapping, local and regional modeling and decision support systems were given in the following parts.

Lin and Lin (2002) utilized GIS to estimate the emissions and spatial distribution of traffic pollutants in Taichung, Taiwan, China by integrating a vehicle emission model, pollutant dispersion model, backward trajectory model and related databases. Jin and Fu (2005) combined dispersion models with GIS to forecast and evaluate the status of environment pollution in urban traffic by simulating the dispersion of vehicle emissions on urban roads. A similar study was done by Briggs et al. (1997) in which a regression-based methodology for mapping traffic-related air pollution like NO₂ was developed within a GIS environment. They expressed the benefits of using digital data on urban road networks, which provides a valuable data source for pollution modeling and using the spatial analysis and overlay techniques available in GIS providing powerful tools for pollution mapping of NO₂. Moreover, they denoted GIS-based regression mapping as a powerful tool in small area studies, where monitored data are scarce and there is a need for high resolution maps.

An integrated modeling system was developed and applied in Lisbon, Portugal by Borrego et al. (2003) to predict air quality in urban areas. GIS were used to facilitate the processing of spatial data and to improve conversion of the resulting emission data to the format required by air quality models. Elbir (2004) developed a GIS based decision support system to support local authorities in air quality management in large cities of Turkey. The system is based on a dispersion model, digital maps and related databases to estimate the ambient air pollution levels at high temporal and spatial resolutions and to enable mapping of emissions and air quality levels. Related to this study, Elbir et al. (2010) developed a GIS-based decision support system for urban air quality management in the city of Istanbul.

A GIS-based decision support tool for the concentration assessment of radioactive pollutants after an accidental release was developed by Canepa et al. (2007). The developed software integrated GIS with a numerical model which simulates transport, diffusion, and deposition of airborne gaseous pollutants and particulate matter in the low atmosphere at both local and regional scale. The GIS allowed a direct interaction with the territory elements in which the simulation takes place and

provide the opportunity to relate concentrations with population distribution and other geo-referenced maps.

Lee et al. (2004) used the measured ^7Be radioactivity information with GIS to construct regional ^7Be intensity fields for different altitude levels. Then they compared the time taken for the air masses from the ^7Be source to Hong Kong with the experimentally determined residence times. Finally, the experimentally determined residence times and the back-trajectories were used together to locate the ^7Be sources.

Shad et al. (2009) used fuzzy genetic linear membership kriging in GIS for predicting air pollution. Vienneau et al. (2009) developed a GIS-based moving window approach to generate high resolution air pollution maps over large geographic areas. They used moving window technique to derive a distance-weighted model of relationships between area-level emissions and monitored concentrations at a set of training sites, and then applied this technique to estimate concentrations at un-sampled locations across the European Union.

Woodfine et al. (2002) developed a national scale contaminant fate model for Canada. The ecological regions were linked with flows of air and water to provide a broad description of contaminant fate over the entire country, including long-range transport between regions. The model made use of GIS in parameterization of environmental characteristics, interpretation of emissions data, and presentation of model results.

Shadbolt et al. (2006) used airflow trajectories to create 40-year air mass climatology for the lower peninsula of Michigan, United States of America. GIS were used to manage and display the extensive amount of trajectories. In addition, a residence time analysis done by using GIS.

Wang et al. (2009) developed a GIS based software namely TrajStat, which enable users to view, query, and cluster the trajectories and compute the potential source contribution function (PSCF) and concentration weighted trajectory (CWT) analyses. It includes a geographic information system technique built from an open-source GIS component for spatial data management, visualization and analyses. The system uses HYSPLIT model to calculate trajectories as an external process. A screenshot of TrajStat software was shown in Figure 2.4:

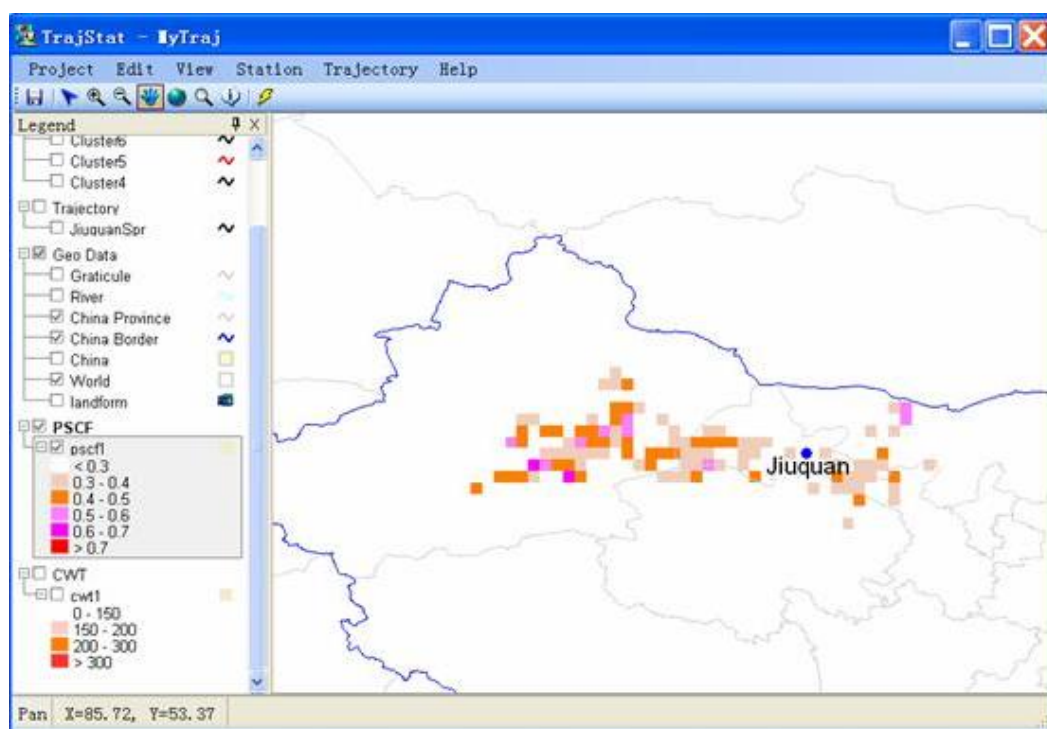


Figure 2.4 A screenshot of Trajstat (Wang et al., 2009) user interface

Related to the air quality studies, integration of dispersion modeling in GIS found a usage area in health studies. The utilization of air emission data and air dispersion modeling with GIS enable public health professionals to identify and define the potentially exposed population, estimate the health risk burden of that population, and determine correlations between point-based health outcome results with

estimated health risk (Dent et.al, 2000). Jensen (1998) developed a model for population exposure to traffic air pollution in order to improve assessment of health impacts and in support of risk management. The model combined the air pollution data with population data from existing administrative databases within GIS.

CHAPTER 3

MATERIALS AND METHODS

In this chapter, information on the study area and the stations where the analyses based on were given. And then the data used in the thesis study and how they were acquired and processed were explained. After that, methodology was explained with the detailed procedures in GIS.

Throughout of the study, MapInfo 7.5 (MapInfo Corp., 2003) with Vertical Mapper 3.0 (Northwood Technologies Inc. and Marconi Mobile Limited, 2001) was used extensively. Data manipulation, editing, analysis, querying and visualization, etc. were done on the GIS software, only a few parts in the data analysis and graphing, where it is best suited to do in spreadsheet software, were done with Excel (Microsoft Corp., 2007). All works on development of GIS tools was done on MapBasic 5.5 (MapInfo Corp., 1999).

3.1. Study Area

Considering air flows to Turkey and the geographical entities like trajectories and stations, the study area (Figure 3.1) was selected as starting from west of the UK and extending to east of the Caspian Sea in east-west direction (20°W and 60°E longitude) and from the middle of the Siberia to almost to the equator in north-south direction (75°N and 15°N latitudes). Therefore, the analyses were done in an aerial extend that covers whole Europe, west parts of Asia, Middle East, and northern Africa. Because the long range air pollution was under concern, the study area was selected large enough to cover the trajectories and pollution source areas.

Four sampling stations were selected as representatives for the region under concern: Antalya (Eastern Mediterranean), Amasra (Black Sea), Çubuk (Central Anatolia) and Corsica (Western Mediterranean). These four locations were selected because, large data present in those sites and concentrations of various pollutants were found to be significantly different from each other at these receptor points (for Corsica: Migon et al., 2008; Garcia-Orellana et al., 2006; Pérez et al., 2008; Ridame et al., 1999; Sandroni and Migon, 1997 - for Antalya: Doğan et al., 2010; Erduran and Tuncel, 2001; Kuloğlu and Tuncel, 2005; Tuncel et al., 2008; - for Amasra: Anwari et al., 1992; Hacısalihoğlu et al., 1991a; 1991b; 1992; Alagha et al., 2001; Alagha and Tuncel, 2003; Karakaş et al., 2004, and for Çubuk: Gaga et al., 2009; Kaya and Tuncel, 1997; Tuncer et al., 2001) The locations of stations were shown on Figure 3.1 within the study area below.

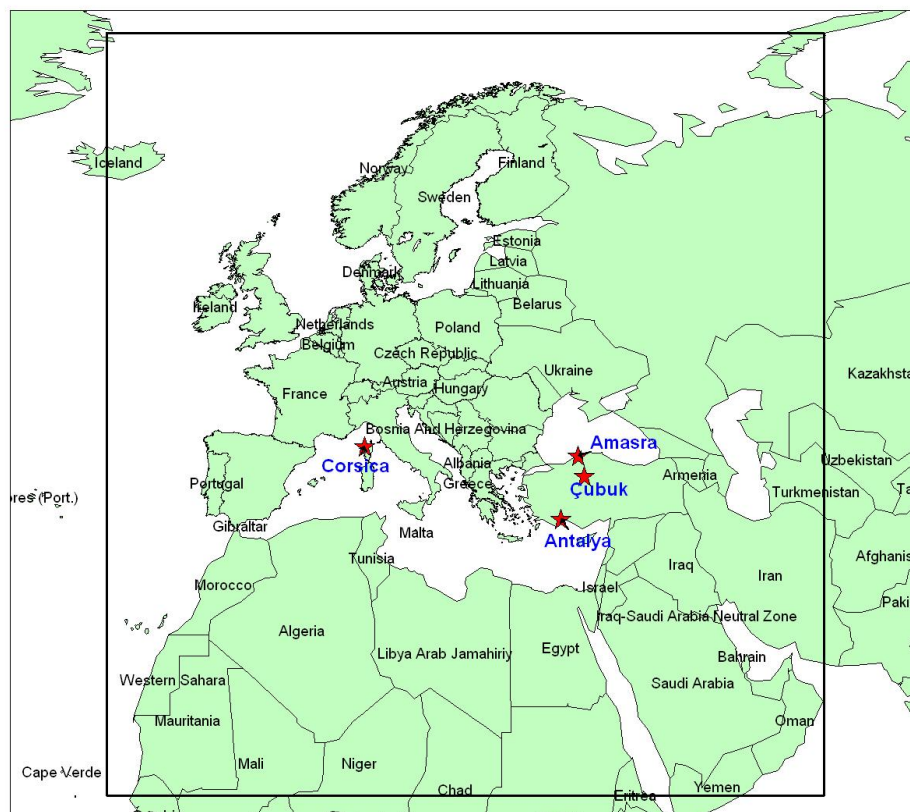


Figure 3.1 Study area and locations of sampling stations.

Locations of the sampling stations concerned have great importance in long-range transport studies. The sampling site should not be under the influence of any local point or area sources to be able to detect low levels of pollutants that are being carried from upper atmosphere. Site selection criteria are fairly well established and include factors such as minimum distance from settlement areas, from industrial point sources, from major and secondary roads. Brief information on the sampling stations selected in this study was given below (Doğan, 2005):

a. Eastern Mediterranean Station (Antalya)

The Eastern Mediterranean station is located at the coast approximately 20 km to the east of Antalya (31.0°E, 36.8°N). The station is at a height of 20 meters AMSL. Because there was extensive tourism developed in Mediterranean region of Turkey, some difficulties were faced in site selection. A recreational area owned by the Ministry of Environment and Forestry was selected for the station to be located. The area was under the protection and electricity supplied throughout the year. The nearest populated area was the city of Antalya, which was approximately 20 km away from the sampling station.

b. Black Sea Station (Amasra)

The Black Sea station (32.3°E, 41.5°N) was situated on a storage area under the responsibility of Ministry of Environment and Forestry. The storage area is located 20 km to the east of the town of Amasra. The station is approximately 3 km away from Black Sea coast. The altitude of the station is approximately 150 m AMSL. The Black Sea station consists of a platform and a field laboratory.

c. Central Anatolia Station (Çubuk, Ankara)

Central Anatolia Station (33.10°E, 40.10°N) is located at Çubuk, which is approximately 50 km away from the city of Ankara and having altitude of 1169 m AMSL. Çubuk station consists of a rectangular cabin (field station) with a surface area of 12 m², which hosts automated measurement devices and a platform. A high volume sampler, a precipitation meter, a meteorological mast and a stack filter unit are installed on this platform.

Çubuk station is the only EMEP station situated in Turkey. The site selection, sampling and analytical procedures were based on the EMEP protocols, that were applied commonly in all EMEP stations in Europe. The station has been operated by the Ministry of Health, Refik Saydam Hygiene Institute since 1993. Daily aerosol and precipitation samples have been collected and the parameters of SO₂, SO₄, NO₂, HNO₃+NO₃ and NH₃+NH₄ have been measured in air samples while SO₄, NO₃, NH₄, Na, Mg, Ca, K, Cl, pH and conductivity parameters and precipitation amounts have been assessed using the precipitation samples at Çubuk station (NILU, 2010b). The collected data have been delivered to the EMEP secretariat. In EMEP, data from sampling stations are used for continent wide comparisons and model calibrations.

d. Western Mediterranean Station (Corsica, France)

Corsica is an island located in the remote western Mediterranean Sea, south of the Gulf of Genoa, 80 km from the Italian coast and approximately 160 km from the French Riviera. The station located (42.53°N, 8.72°E) on the western coast of Cavli with a sea level altitude.

A 1° × 1° gridded domain covering the whole study area was used (Figure 3.2). The gridded domain was created by using Grid Maker version 1.3 which is an integrated tool of MapInfo. The boundary coordinates were entered using the aerial extents of study area. And then grid cell size was selected as 1° × 1° and object type was selected as closed polygon (total of 4800 grid cells).

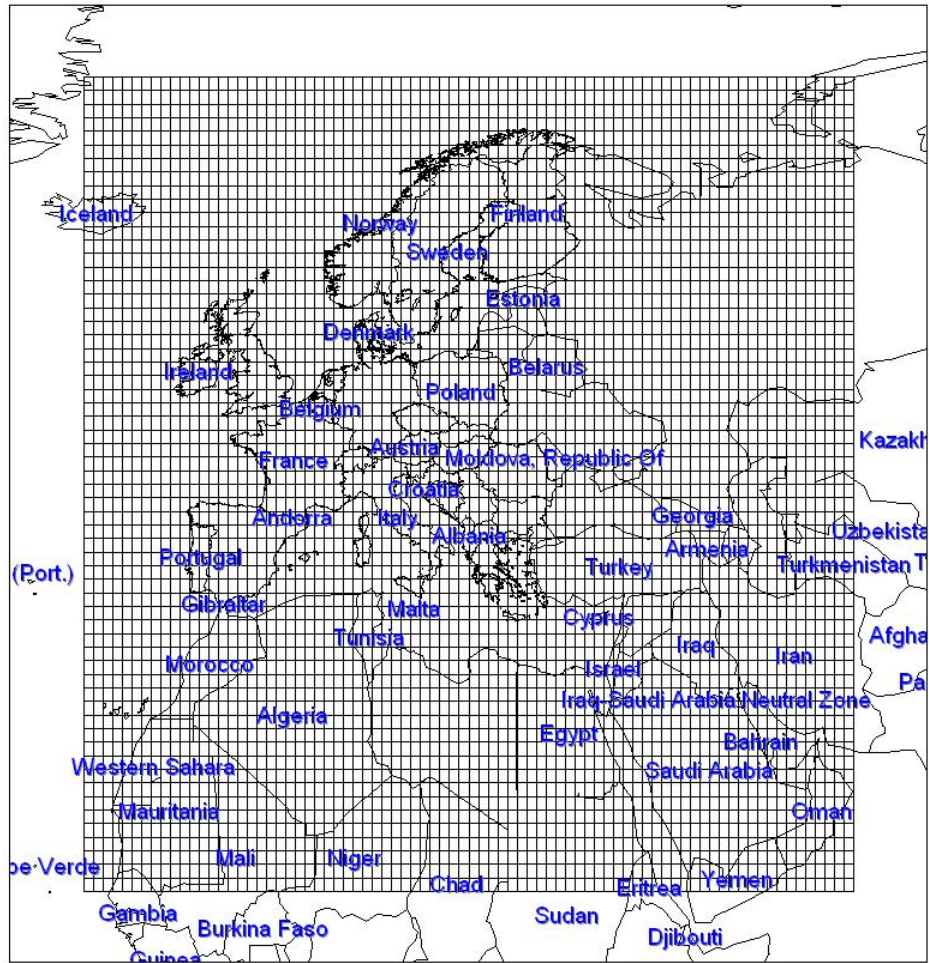


Figure 3.2 $1^{\circ} \times 1^{\circ}$ gridded domain

In section 4.1.2 of this study, a different domain was also used. A wind rose centered on at 33.10°E , 40.10°N (the coordinates of Çubuk station) was drawn on the MapInfo (Figure 3.3). The extents of wind rose were set large enough to cover many of the trajectories from the data set and it also covers the great proportion of 1 degree gridded domain. Wind rose described here formed as a polygon uniformly divided into 16 pies which show the wind sectors. It was drawn using Create Line by Length (Version 3) tool of MapInfo. The pies were initially composed polyline objects, and then they were converted to regions (polygon) to use it in the analyses.

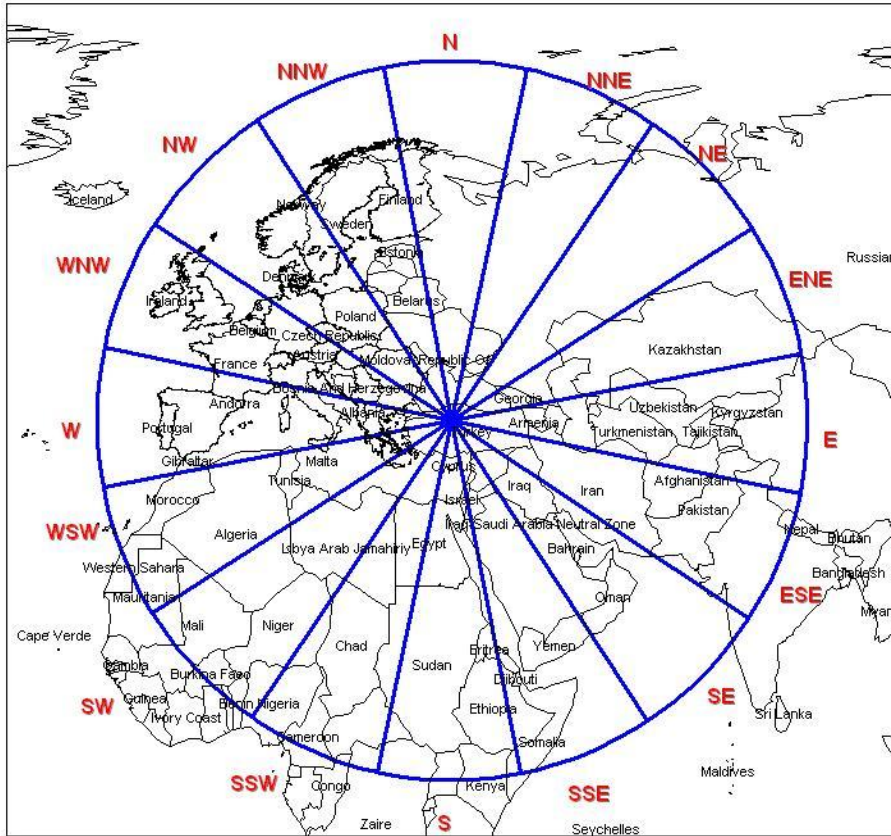


Figure 3.3 Wind rose used in study

3.2. Data Description and Preparation

Data used in this study could be split into 2 groups: pollution data and trajectory data.

a. Pollution data

Data to characterize the pollution includes SO_4^{2-} concentrations measured at central Anatolia station (Çubuk) and SO_4^{2-} emissions of the EMEP region that monitoring has been carried out.

SO₄²⁻, which is derived from gas to particle conversion processes of SO₂ oxidation, was selected because it is a primary pollutant causing acid rains and it can be transported long distances. SO₄²⁻ measurements of aerosol samples taken from Çubuk station were used. The station became operational in 1992 and air and precipitation samples are being collected since 1993. In this study, samples collected for the years 1995, 2000, 2004, 2005 and 2006 were used. In this period, 1477 daily aerosol samples had been collected and analyzed in the laboratories of Ministry of Health, Refik Saydam Hygiene Center. The results were originally archived in Excel file format (173 kilobyte-KB). Data were imported into MapInfo GIS from Excel spreadsheet and saved as table file. All concentrations were in ug/m³. The excel data format of SO₄²⁻ measurements is shown in Table 2.1.

Table 3.1 Data file format of SO₄²⁻ measurements

id	year	month	day	Jday	SO ₄
881	1995	5	31	151	0,96
882	1995	6	1	152	1,11
883	1995	6	2	153	1,5
884	1995	6	3	154	1,26
885	1995	6	4	155	1,65
886	1995	6	5	156	2,46

“id”: number of the day from the beginning of measurements

“year”, “month” and “day”: forms the date of measurement

“jday”: order of the measurement day in specified year

“SO₄”: concentration measured in ug/m³

SO₄²⁻ concentrations were used in PSCF calculations. In addition to the concentration measurements, emissions of sulfur oxides (SO_x) mainly composed of SO₂ (the precursor of SO₄²⁻) were obtained from EMEP. SO_x emissions of years “1990, 1995, 2000, 2004” (Vestreng et al., 2006), 2005 (Vestreng et al., 2007a) and 2006 (CEIP, 2008) were obtained for the whole EMEP region. Emission data were mainly used in the regions of influence analysis. Emissions were provided as the

national totals (in units of Mg $\cdot 10^6$ grams) and data were used in EMEP/MSC-W (Meteorological Synthesizing Centre-West) reports, and by EMEP/MSC-E (Meteorological Synthesizing Centre-East). Emission data were based on officially reported emissions, but some of the officially reported data have been corrected and/or gap-filled.

Six years' emission data were downloaded in text file format (total 14.2 megabyte-MB) by using Web-dab (web application developed by EMEP) (CEIP, 2009). The settings applied in Web-dab are shown in (Table 3.2):

Table 3.2 Settings applied Web-dab application in EMEP website (CEIP, 2009)

PARAMETER	VALUE
Countries / Areas:	All (all countries reporting to the United Nations-Economic Commission for Europe (UN-ECE) and other areas where emission values are only expert estimates, i.e. ship emissions, natural marine emissions, North Africa and remaining Asian areas)
Years:	1990, 1995, 2000, 2004, 2005, 2006
Pollutants:	SO _x from the list of main pollutants
Sectors:	National Totals (without other sources and sinks)
Type and Format:	Grid (0.5° × 0.5°), Semi-column separated

The data provide gridded emissions. At EMEP, a grid system having a cell-size of (50km × 50km) and based on a polar-stereographic projection with real area at latitude 60° N have been using to produce gridded emissions. Grid domain includes 132 × 159 points (with x varying from 1 to 132 and y varying from 1 to 159) (EMEP, 2010b). But the data in 50km × 50km grid format have also been provided as interpolated to 0.5° × 0.5° cell sized grid format. This interpolated EMEP grid extends between 29.75°W and 60.25°E longitude in east–west direction and between 75.25°N and 30.25°N latitudes in north–south direction. Thus, the emission data were downloaded from EMEP website in such grid format (0.5° × 0.5° cell size)

having latitude/longitude coordinate system. Sample gridded emission data with its format were shown below (Table 3.3).

Table 3.3 Data format of gridded SO_x emissions

ISO2	YEAR	SECTOR	POLLUTANT	LONGITUDE	LATITUDE	UNIT	NUMBER/ FLAG
IS	1995	SNAP NATIONAL	SO _x	-14	64.5	Mg	2.4766
IS	1995	SNAP NATIONAL	SO _x	-14	65	Mg	83.6832
IS	1995	SNAP NATIONAL	SO _x	-14	65.5	Mg	21.415
IS	1995	SNAP NATIONAL	SO _x	-14	66	Mg	1.5873
IS	1995	SNAP NATIONAL	SO _x	-14	66.5	Mg	0.2656

ISO2: country code

YEAR: year of emission calculated

SECTOR: sector name

POLLUTANT: name of pollutant

LONGITUDE: longitude of center point of grid cell

LATITUDE: latitude of center point of grid cell

UNIT: unit of pollutant emissions

NUMBER/FLAG: numerical value of pollutant emission in specified units

This yearly data were imported into MapInfo GIS table files where unnecessary columns (ISO2, Sector, unit and pollutant) were deleted. Using the coordinates at each row, point objects describing the centers of 0.5° × 0.5° grid cells were created by selecting “create points” option in MapInfo.

Emissions in EMEP are given per country, which means that country border cells are listed several times, once for each country sharing the borders. Therefore there were multiple emission values for each cell in gridded data. To get the total emission the values of all locations for these cells should be added up. To do this, point objects having the same coordinates were aggregated by using Vertical Mapper 3.0 (point aggregation with statistics). Averaging technique was selected as

summing the emission values of coincident points. Therefore, 22588 points were aggregated into 14683 points, resulting in data size reduction from 1.9 MB to 0.95 MB.

As these points are the centers of $0.5^{\circ} \times 0.5^{\circ}$ cell sized emission grid (extending 29.75°W and 60.25°E longitude in east – west direction and between 75.25°N and 30.25°N latitudes in north – south direction), this grid was formed by using Grid maker (version 1.3) tool of MapInfo. In this way, point objects containing aerial data were converted to polygon based objects (grid) to be used in future analyses. This $0.5^{\circ} \times 0.5^{\circ}$ grid then overlaid with the previously aggregated points to convey the emission information to the grid. This achieved by updating the emission column in the grid file with spatially joining the grid cells with center points. After these steps, a $0.5^{\circ} \times 0.5^{\circ}$ cell sized grid file containing yearly emission information have been obtained.

However, in this study, a $1^{\circ} \times 1^{\circ}$ grid as explained in section 3.1 had been selected for the analyses. In order to use the EMEP data in the analyses, emission grid having $0.5^{\circ} \times 0.5^{\circ}$ cell size was aggregated into the $1^{\circ} \times 1^{\circ}$ cell size grid. This was achieved by overlaying 0.5° cell sized grid with 1° sized grid, summing emission values of 0.5° sized grids proportionally to the area under 1° sized grid in MapInfo GIS. Because the edges of 0.5 degree grid do not covered by 1 degree grid, the uncovered parts are omitted in this analysis. The emission grids are presented in Figure 3.4.

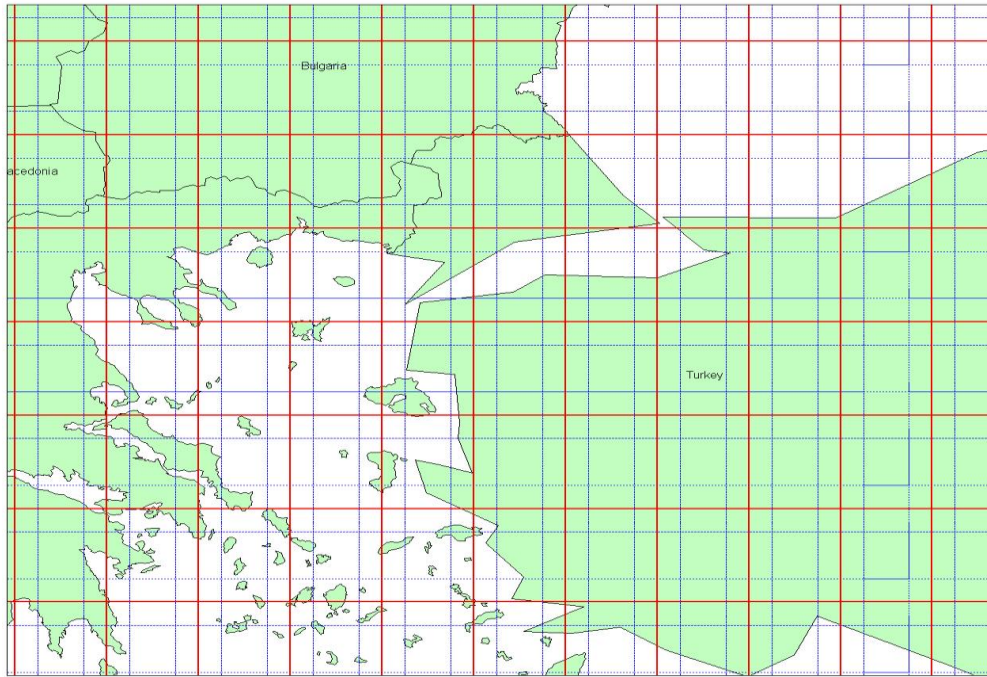


Figure 3.4 $1^{\circ} \times 1^{\circ}$ and $0.5^{\circ} \times 0.5^{\circ}$ emission grids

Data preparation steps of emission and concentrations that explained in this part summarized as a flowchart in Figure 3.5.

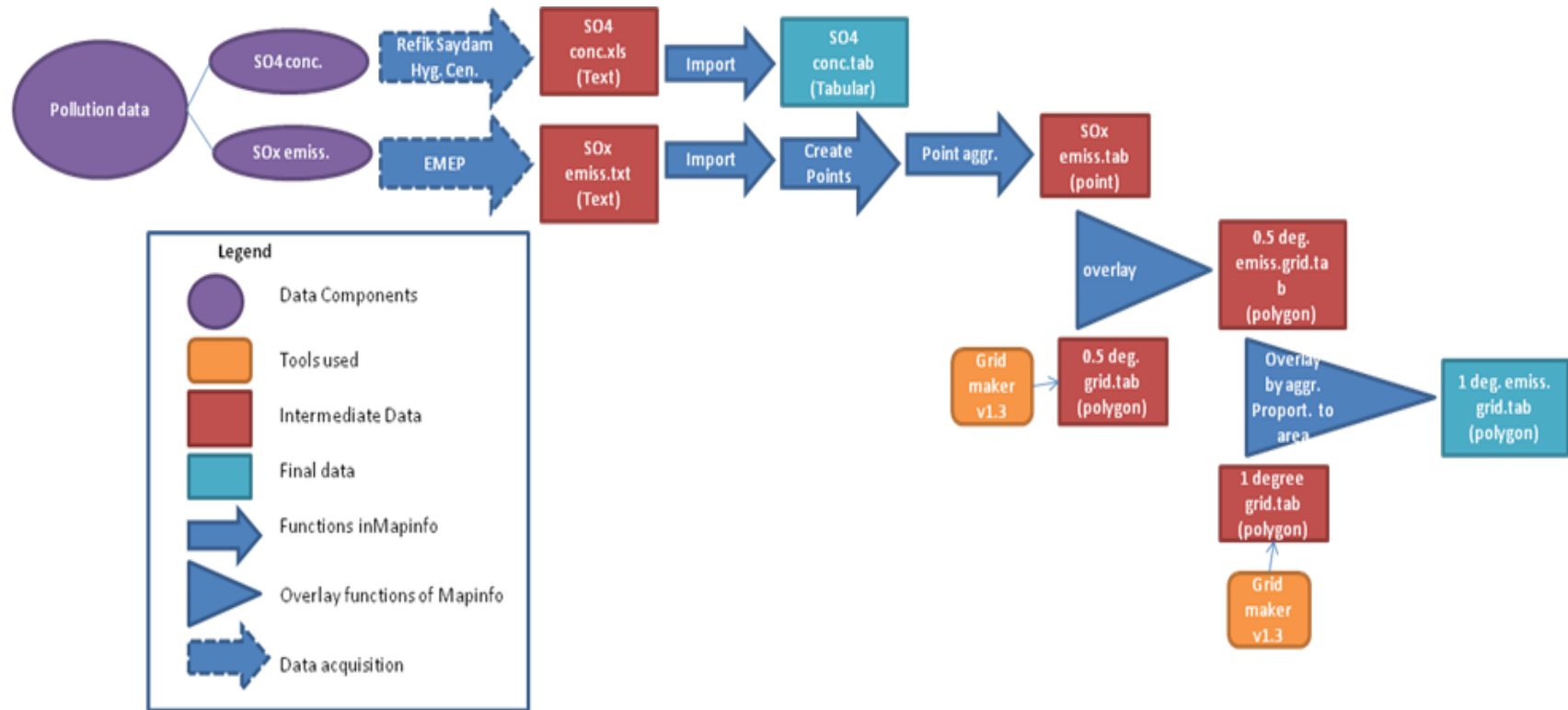


Figure 3.5 Pollution data preparation flowchart

b. Backtrajectory data

Two commonly used types of backtrajectory data was used in this study: HYSPLIT and ECMWF backtrajectories. These data were explained with the model descriptions in detail below:

HYbrid Single-Particle Lagrangian Integrated Trajectory (HYSPLIT) model and trajectory data

Hybrid-Single Particle Lagrangian Integrated Trajectory (HYSPLIT) model (Draxler and Hess, 1998) developed by the National Oceanic and Atmospheric Administration's (NOAA) Air Resources Laboratory (ARL). The HYSPLIT model is used to support a wide range of applications related to the atmospheric transport, dispersion and deposition of pollutants and hazardous materials on the Earth's surface. Some of its applications include tracking and forecasting the release of radioactive material, volcanic ash, wildfire smoke, and pollutants from stationary and mobile emission sources. Operationally, the model is used by NOAA's National Weather Service through the National Centers for Environmental Prediction and at local Weather Forecast Offices (ARL, 2010a).

The HYSPLIT model can output trajectories and air concentrations. The model calculation method is a hybrid methodology between the Lagrangian approach (using a moving frame of reference as the air parcels move from their initial location) and the Eulerian approach (using a fixed three-dimensional grid as a reference frame). In the model, advection and diffusion calculations are made on a Lagrangian framework to describe the transport of the air parcel and trajectories, while a fixed grid is used to calculate pollutant concentrations (ARL, 2010a).

Using Lagrangian model, dispersion is computed following the particle or puff. Therefore, the advection of a particle is computed independently of the dispersion calculation in HYSPLIT model. Time integrated advection term of a particle taken as the trajectory computed using basic horizontal (U, V) and vertical (ω) wind

components of meteorological data. The calculations of trajectories were told in Draxler and Hess, 1997 and 1998 as follows:

After the wind components of meteorological data processed and integrated into the model's internal grid, the advection of a particle or puff is computed from the average of the three-dimensional velocity vectors for the initial-position $P(t)$ and the first-guess position $P'(t+\Delta t)$. Then the velocity vectors, V are linearly interpolated in both space and time. The first guess position is calculated according to Eq. (3.1) as:

$$P'(t + \Delta t) = P(t) + V(P, t)\Delta t \quad (3.1)$$

And the final position becomes:

$$P(t + \Delta t) = P(t) + 0.5 [V(P, t)\Delta t + V(P', t + \Delta t)] \Delta t \quad (3.2)$$

The integration time step (Δt) can vary during the simulation and computed from the requirement that the advection distance per time-step should be less than the 0.75 of the meteorological grid spacing. Trajectory computation terminates once the trajectories exceed the model top defined in the model setup, but the trajectories stay on the surface and advection continues if the trajectories intersect the ground. Higher order integration methods were considered by Draxler and Hess (1998) but they were rejected because they will not yield higher precision due to the data observations are linearly interpolated from the grid to the integration point.

The model uses previously gridded meteorological data on one of three conformal map projections (Polar, Lambert and Mercator). The meteorological data used by HYSPLIT is gridded four-dimensional (x, y, z, t) meteorological fields outputted as analysis or forecast wind fields from the NOAA National Centers for Environmental Protection (NCEP) weather prediction models. Model output field resolution varies according to the model, anywhere from standard pressure levels (1000, 925, 850 hPa) to every 25 hPa intervals for the regional models. (ARL, 2010b) For example, NCEP/NCAR (National Center for Atmospheric Research)

Reanalysis data set (NCAR, 2010) has a resolution of T62 (209 km) with 28 vertical sigma levels. Results are available at 6 hour intervals. Using a single analysis system, historical meteorological data beginning from 1948 has been reanalyzed within the NCEP/NCAR Reanalysis Project. Analyses are available every six hours per day and daily or monthly values from that date to present exist. There are over 80 different variables, (including geopotential height, temperature, relative humidity, U and V wind components, etc.) in several different coordinate systems, such as 17 pressure level stack on 2.5×2.5 degree grids, 28 sigma level stack on 192×94 Gaussian grids, and 11 isentropic level stack on 2.5×2.5 degree grid. They are organized as different subgroups in the archive. In addition to analyses, diagnostic terms (for example: radiative heating, convective heating) and accumulative variables (like precipitation rate) are present.

HYSPLIT can be run interactively on ARL's READY (Real-time Environmental Applications and Display sYstem) web site (ARL, 2009), or it can be installed on a PC and run using a graphical user interface (Draxler and Rolph, 2003; Rolph, 2003). The web version has been configured with some limitations. The HYSPLIT model and meteorological data could be installed on a computer and run locally. Registered versions can work with no restrictions but users must obtain their own meteorological data files. But unregistered versions cannot utilize forecast meteorological data in calculation of plume concentrations. The trajectory-only model has no restrictions and forecast or archive trajectories may be computed with either version (ARL, 2010c).

HYSPLIT backtrajectories from multiple heights are often run to capture the effects of vertical variation of horizontal winds within the mixed layer depth (COHA, 2010). Sample backward trajectories of Antalya station with multiple start height obtained from HYSPLIT-READY system are shown in Figure 3.5.

NOAA HYSPLIT MODEL
 Backward trajectories ending at 1400 UTC 01 Aug 90
 CDC1 Meteorological Data

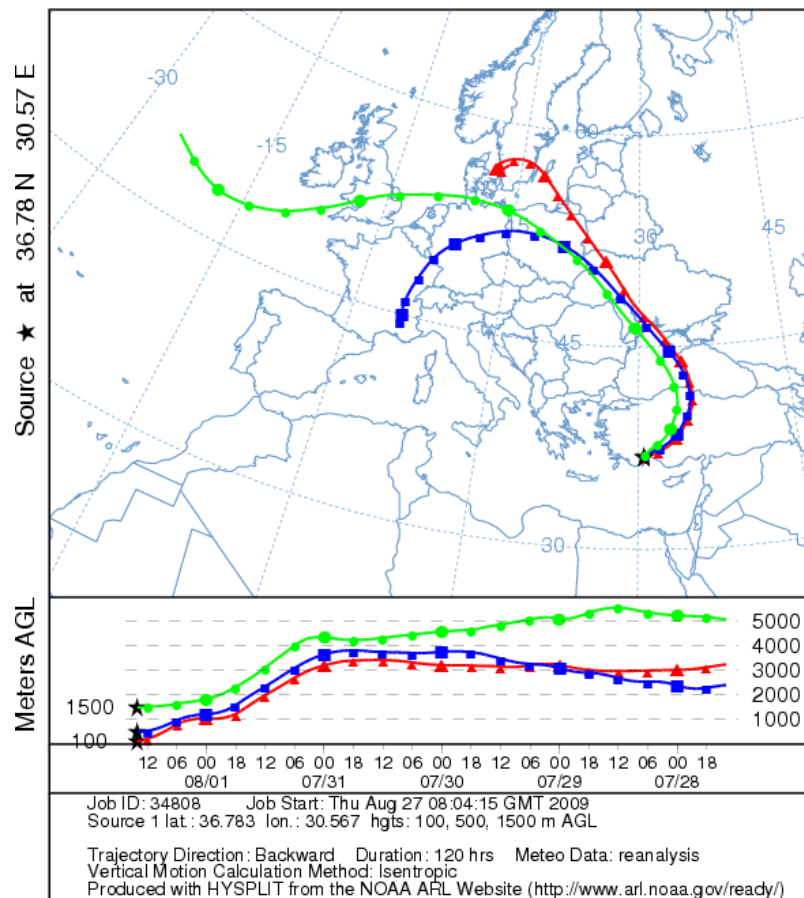


Figure 3.5 HYSPLIT trajectories of having 3 different starting altitudes

HYSPLIT trajectories were also used in many scientific studies (Crawford et al., 2007; 2009; Shan et al., 2009; Challa et al., 2008; McGowan and Clark, 2008; Escudero et al., 2006; Wain et al., 2006; Draxler and Rolph, 2003; Rolph 2003). For example: McGowan and Clark (2008) used HYSPLIT trajectories to identify dust transport pathways from Lake Eyre, Australia. Escudero et al. (2006) used HYSPLIT model to quantify the proportions of mineral dust originated from specific geographical areas in northern Africa to PM₁₀ concentrations over the central Iberian Peninsula.

HYSPLIT trajectories used in the study

In this study, HYSPLIT trajectories were obtained by using ARL's READY web application (Draxler and Rolph, 2003; Rolph, 2003; ARL, 2009). NCEP/NCAR global re-analysis meteorological dataset (1948-present) was used as input data for trajectory calculation. Using HYSPLIT model, backtrajectories starting at 4 stations were calculated for each day of the years 1990, 1995, 2000, 2004, 2005 and 2006. Vertical motion was modeled as isentropic, where trajectories were assumed to follow constant temperature potentials. Trajectories started at 14 pm in every day and calculated 120 hours backwardly (5 day). Up to 3 simultaneous trajectories can be calculated at multiple levels by READY application therefore 3 starting heights (100, 500, 1500 meters) were selected. Rainfall information in mm/hour at each segment of trajectory was also requested. Model parameters were summarized in the Table 3.4.

Table 3.4 HYSPLIT model parameters

PARAMETER	VALUE
Duration	120 hours (5 day) backward in time
Vertical Motion	Isentropic
Meteorological fields	NCEP/NCAR Re-analysis
Trajectory end time	14:00
Trajectory end heights	100, 500 and 1500 meters

After configuring READY application according to the settings, the model was run and trajectory files were obtained for each day of the study period. One trajectory file contains summary of model settings, 3-D segment endpoint coordinates of 3 trajectories having different starting heights and the information on the wind speeds and rain.

At each READY run of HYSPLIT model, only one day's trajectories could be calculated. Therefore it took relatively long time to acquire trajectory data. Totally 2191 days trajectories in 3 different starting heights for 4 stations (total 26,292 trajectories) were acquired.

The data downloaded as text files for each day (3 trajectories of different starting height in each file consumes 40 KB memory on hard disk, totally 342 MB). HYSPLIT output text file format is shown in Table 3.5 and a sample trajectory file is in Appendix A.

Table 3.5 HYSPLIT trajectory data file format (ARL, 2010d)

No. of lines		Description													
1		Number of meteorological grids used in calculation													
3 (number of grids)		Meteorological Model identification and Data file starting Year, Month, Day, Hour, Forecast Hour													
1		Number of different trajectories in file, direction of trajectory calculation (FORWARD/BACKWARD) and vertical motion calculation method (OMEGA, THETA...)													
3 (number of trajectories)		Starting year, month, day, hour Starting latitude, longitude Starting level above ground (meters)													
1		Number of diagnostic output variables Label identification of each variable (PRESSURE, THETA...)													
N		Trajectory segment end points													
Col 1	Col 2	Col 3	Col 4	Col 5	Col 6	Col 7	Col 8	Col 9	Col 10	Col 11	Col 12	Col 13	Col 14	Col 15	
Trajectory number	Meteorological grid number	Time year	Time month	Time day	Time hour	Time min.	Forecast hour at point	Age of trajectory (hours)	Position- Latitude	Position-Longitude	Position height in meters above ground	N diagnostic output variables (1st output is always pressure)	N diagnostic output variables (1st output is always pressure)	Rainfall	

Every row in the HYSPLIT output file after header rows stores the data of trajectory segment end points. Because of the header rows in text files, large number of text files and 3 trajectory data in one file, HYSPLIT output trajectories cannot be opened in MapInfo using manual methods. A MapBasic application (Dabanlı, 2009) that previously developed in METU for custom converting HYSPLIT text files into MapInfo table file, was used with some modifications and bug fixed. Source code was provided in Appendix B. This tool reads all trajectory files from 10th row of each text file in a directory specified and then aggregates the trajectories into 3 files according to the starting heights (100, 500, 1500 m). The convert tool adds a column showing the date as a number compose of “day+month+last 2 digit of year” (i.e. 1 January 1995 converted into 010195). This provides the seamless trajectory segments to differentiate the trajectories of different days. As a result for each station, 3 trajectory file (one for each starting height of 100, 500, 1500m) were obtained for each station. And, each trajectory file consists approximately 264,000 trajectory segments and consumes 36.3 megabyte memory. Data preparation ended with creating point objects for each segment endpoint of trajectories in MapInfo.

ECMWF model and trajectory data

A trajectory model (McGrath, 1989) developed by Irish Meteorological Service (IMS) to calculate the trajectories using global wind fields of European Centre for Medium-Range Weather Forecasts (ECMWF). This model was designed to run on the CRAY computer in ECMWF using analyzed or forecast wind fields stored in two online databases containing data on forecast model levels and the other on standard pressure levels. U, V, ω components of wind speed and the logarithm of surface pressures for model level data available as spectral fields in GRIB codes of ECMWF. Both database was updated daily and hold the latest 15 day analysis and 100 days of forecast at 6h-12 h intervals. Older wind fields' data of ECMWF are obtained from the Meteorological Archival and Retrieval System (MARS), which is the main repository of meteorological data at ECMWF. MARS contains terabytes of operational and research data as well as data from special projects, which is freely

available to registered users in the Member States and Co-operating States of ECMWF (ECMWF, 2010).

Using IMS model (McGrath, 1989), trajectories could be calculated forward or backward in time with pressure level or model level data in 2-D or 3-D if vertical velocity component, ω is used. During the calculation of ECMWF trajectories, GRIB coded spectral fields were read and according to the selected spectral truncation, the wind values are synthesized at each point along the trajectory path. This minimizes the number of spectral to grid-point transformations required and reduces the execution time in computer. Denoting $X(t)$ as the horizontal position and $P(X, t)$ as the pressure of the trajectory at time, t and $\underline{U}(X, t)$ is the corresponding 2 dimensional wind field then, following iterative method is used to calculate the positions of trajectory at time $t+\Delta t$:

$$\begin{aligned}
 X_1(t+\Delta t) &= X(t) + \underline{U}(X, t) \cdot \Delta t \\
 P_1(t+\Delta t) &= P(t) + \omega(X, t) \cdot \Delta t \\
 &\vdots \\
 X_n(t+\Delta t) &= X(t) + 0.5 [\underline{U}(X, t) + \underline{U}(X_{n-1}, t+\Delta t)] \cdot \Delta t \\
 P_n(t+\Delta t) &= P(t) + 0.5 [\omega(X, t) + \omega(X_{n-1}, t+\Delta t)] \cdot \Delta t
 \end{aligned} \tag{3.3}$$

Where the \underline{U} and ω velocities were derived by linear interpolation in time and in vertical by linear interpolation in $\log(P)$. If the 2-D trajectories required pressure is kept constant. The model iteration is stopped at $n=2$ because it gives acceptable accuracy for $\Delta t < 1$ hour (McGrath, 1989).

The model was originally written in 1989, but updated over the years to reflect changes in computer architecture at ECMWF and changes to the ECMWF model resolutions. Now, the model can use either reanalysis (ERA-15, ERA-40 or ERA-Interim) or operational Numerical Weather Prediction (NWP) model (analysis or forecast) data. IMS model can be run after secure logging in “ecgate”, a server of ECMWF (ECMWF, 2009) using command line or using a script file.

ECMWF trajectories were used in various studies (Khosrawi et al., 2010; Lee et al., 2010; Thomas and Bracegirdle, 2009; Froude, 2009; Morcrette et al., 2009; Bashir et al., 2008; Delcloo and De Backer, 2008) while IMS model was used in some studies (Bigg et al., 1996; Birch et al., 2009; Eneroth et al., 2003; Fink and Knippertz, 2003; Heintzenberg and Leck 1994; Knippertz et al., 2003; Norman et al., 2003; Paatero et al., 2003).

ECMWF trajectories used in the study

Trajectory model of McGrath (1989) was used to calculate 5-day ECMWF back-trajectories of Çubuk station for the years 1990, 1995 and 2000. For the trajectory calculations, wind fields data of operational Numerical Weather Prediction (NWP) model (T213 L31) of the European Centre for Medium-Range Weather Forecasts (ECMWF) were used. The T213 L31 ECMWF model produce wind field data at T213 (approximately 60 km) horizontal resolution on 31 levels (approximately 10 levels below 2800 m) on a 1° resolution grid (Stohl and Koffi, 1998).

ECMWF trajectories were downloaded for comparison with the HYSPLIT model. To make the trajectories comparable, model parameters equivalent to HYSPLIT were selected as similar as possible (Table 3.6). Vertical positions are represented as pressures in ECMWF trajectories, so, equivalent starting heights were selected as pressure levels (1000 Pa for 100m, 955 HPa for 1000m and 850 HPa for 1500m). There was no isentropic option available in IMS model therefore this could not be considered in ECMWF trajectories. But, vertical positions (pressures) were calculated in IMS model by using the vertical wind information in spectral data file. And also the trajectories downloaded for 134 hours back in time, but the excess trajectory segments were dropped out as explained in the coming parts.

Table 3.6 ECMWF model parameters

Parameter	Value
Duration	134 hours (5.6 day)
Meteorological fields	Operational NWP model of ECMWF
Receptor end time	14:00 EST
Receptor Heights (surface pressure)	1000, 955, 850 HPa

ECMWF trajectories were requested by using ecgate from internet with a script file. The site does not publicly open, requires password to request trajectories. Then the requests were queued to be processed. After the trajectories calculated, they sent as attached to e-mails. Approximately, 30 days of trajectories could be obtained in one day. The resultant trajectory files were in text format. The ECMWF trajectory files have the following general file format shown in Table 3.7. A sample ECMWF trajectory file was presented in Appendix C.

Table 3.7 ECMWF trajectory data file format

# of lines	Description								
3	Empty								
9	Trajectory header, date, time, number information								
1	Variable name line (hr, latitude, longitude, level u, v, and w- winds, ps) 8 variables								
1	Empty								
135	trajectory data values for Trajectory 1 (135 trajectory end point)								
3	Empty								
135	trajectory data values for Trajectory 1 (135 trajectory end point)								
3	Empty								
135	trajectory data values for Trajectory 1 (135 trajectory end point)								
2	Empty								
12	Notes, containing the text NOTES:								
Col 1	Col 2	Col 3	Col 4	Col 5	Col 6	Col 7	Col 8	Col 9	Col 10
HOURS	LAT	N/S ident.	LON	E/W ident.	LEVEL	U-WIND	V-WIND	W-WIND	PS

LAT: Latitude value,
N/S ident.: North/south identifier
LON: Longitude value,
E/W ident.: East/west identifier
U-WIND: u-component of wind (meters per second)
V-WIND: v-component of wind (meters per second)
W-WIND: vertical wind component (Pascal per second)
PS: surface pressure (HPa)

The first 9 row gives information about trajectory (trajectory start and end time, starting pressure level and coordinates). Latitudes and longitudes are given in degrees. Pressure levels are in hectopascals (hPa).

ECMWF trajectories including 3 trajectories starting from 3 different pressure level (1000, 955, 850 HPa) downloaded as text files for each day (each file uses 26.3 KB totally 22.4 MB). After the data downloaded, they were converted into MapInfo table file using a newly developed MapBasic application that is based on the HYSPLIT convert tool (source code given in Appendix D). Because the data format is different from HYSPLIT, different procedure was applied in separating trajectories in a text file. ECMWF conversion tool reads the text files and selects the trajectories according to their starting pressure levels. This tool retains only the first 120 hours of backtrajectories for comparison with HYSPLIT. It adds date information as a separate column in order to differentiate the trajectory segments. Date information is added similarly as a number compose of day+month+last 2 digit of year (i.e. 010195). The application automatically adds (-) sign before the coordinates of south latitudes and west longitudes and then create points for each trajectory endpoint. After that it saves all trajectories into 4 files; 3 table file for each pressure level (10.7 MB each) and 1 for the combination of all trajectories (30.4). Totally 874 day trajectory file consisting of approximately 314000 trajectory segments were processed. Then, point objects were created for the trajectory end points.

Comparing HYSPLIT file format, trajectories having different starting height were grouped under headings (trajectory number 1, etc) while they are not grouped but designated by numbers at first columns. The other difference is that direction of coordinates of trajectory end points were denoted by “N” (for North) “E” (for East), in ECMWF, whereas south and west directions are affiliated by (-) sign before coordinates in HYSPLIT.

A separate data set for the comparison of the two trajectory models was prepared for the Çubuk station. ECMWF data was obtained for the last 5 months of 1990 and whole years of 1995 and 2000. Therefore HYSPLIT trajectories for the same time period were extracted from the large data set. As explained before, these trajectories have calculated using similar configurations. Trajectories started at 14:00 afternoon at three different altitudes (100 m, 500 m, and 1500 m in HYSPLIT equivalently 1000, 955, 850 hPa in ECMWF). Main differences between the trajectory data are the meteorological data used for calculation which significantly affect the accuracy, assumptions for vertical motion and the trajectory models used. Since the number of days and number of segments should be identical for both models in this comparison, data were first checked for consistency and completeness. Because some days or some hours may be missing in one of the two trajectory sets, these data were eliminated from both trajectory sets to make them identical. Several queries were applied in MapInfo to find these inconsistent trajectories. After this manipulation, a data set compose of total 308550 hourly segments of 850 daily trajectories from each model was prepared.

For visualization of trajectories, a tool that draws trajectory lines using segment end point was developed in MapBasic. Some parts of this tool were previously developed (Dabanlı, 2009). The tool can draw the trajectories of ECMWF and HYSPLIT separately for the selected date or for all dates. It can also draws the ECMWF and HYSPLIT trajectories for randomly selected 30 days. The source codes were presented in Appendix E.

The operations in the trajectory data preparation are summarized in Figure 3.6.

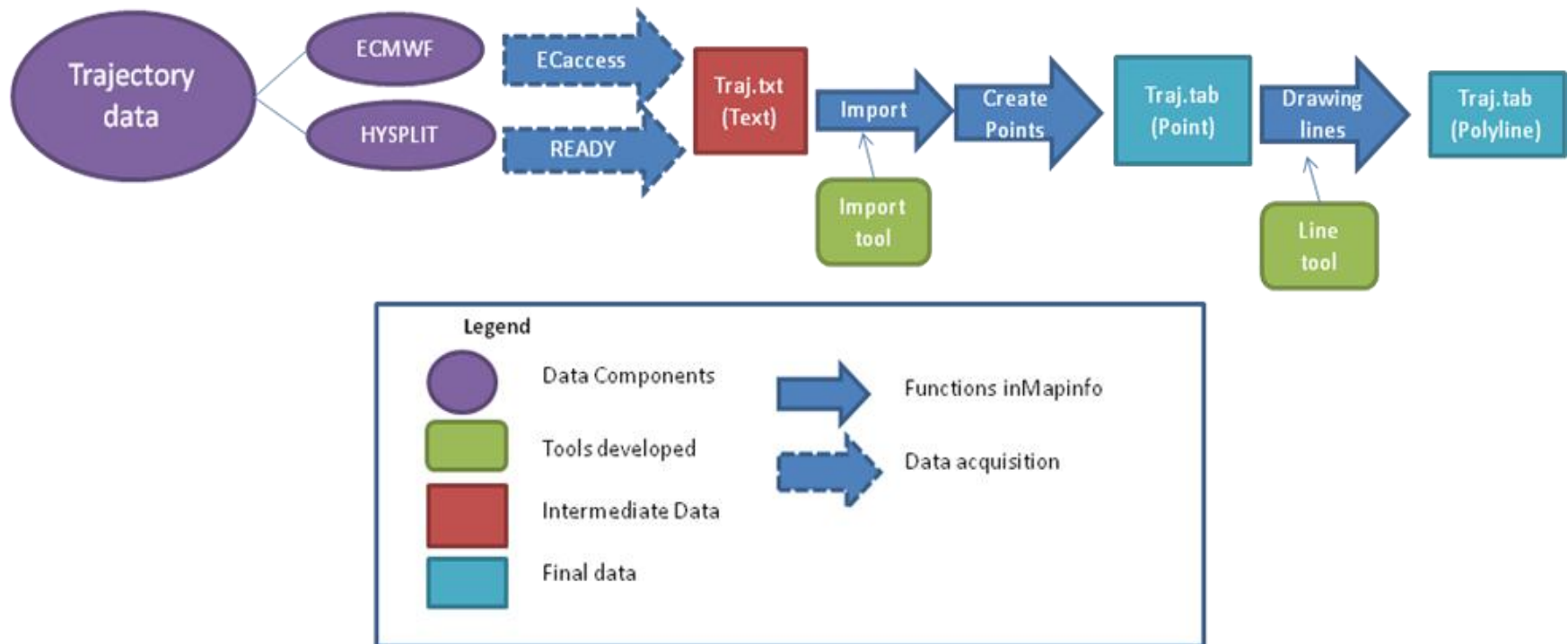


Figure 3.6 Flowchart of trajectory data preparation process in GIS

3.3. Methodology

Based on the background information given in Chapter 2, the methodologies used in this study such as Residence Time, Potential Source Contribution Function and Regions of Influence analyses are described. GIS analyses accomplished in the study are explained in detail.

3.3.1. Residence Time Analysis

Residence Time Analysis (RTA) is a receptor model developed by Ashbaugh et.al, (1985) to identify the source regions of pollutants. It is defined as the probability of a randomly selected air parcel to be present in the ij^{th} cell on a gridded domain relative to time period, t . Taking N as the total number of trajectory segment endpoints during the study period, t , if n_{ij} endpoints fall into ij^{th} cell, the probability of this event, A_{ij} (Eq. 3.4) is given as:

$$P[A_{ij}] = \frac{n_{ij}}{N} \quad (3.4)$$

RTA methodology then formed a basis for PSCF analysis where residence time of air parcels having higher concentrations are incorporated jointly with this analysis.

Total number of trajectories in each grid or sector indicates total number of hours air masses spent at each grid or sector, which is by definition the residence time. Analysis of residence times are suggested to be an effective way of tracing trajectories on an annual basis, thus minimizing the uncertainties of individual trajectories (Shadbolt et al., 2006). As the number of segments increases the air parcel stays more in the region that increases the contact time of air parcel with the pollution sources.

In this study residence times of the air parcels in each grid/sector cell were calculated in GIS by using $1^{\circ} \times 1^{\circ}$ grid and wind rose described in section 3.1. To calculate it, first the number of the trajectory segment end points under each cell were counted using spatial join of grid/wind rose table with trajectory tables. Then dividing these numbers by the total number of trajectory segment endpoints inside of the whole grid using “calculate statistics” function of MapInfo and taking percentage, the residence time values were calculated. Finally thematic maps were created for the visualization of the results. In the sector based analysis, where the wind rose used, the results were presented using radar graphs produced in Excel.

The implementation of RTA is given in Figure 3.7

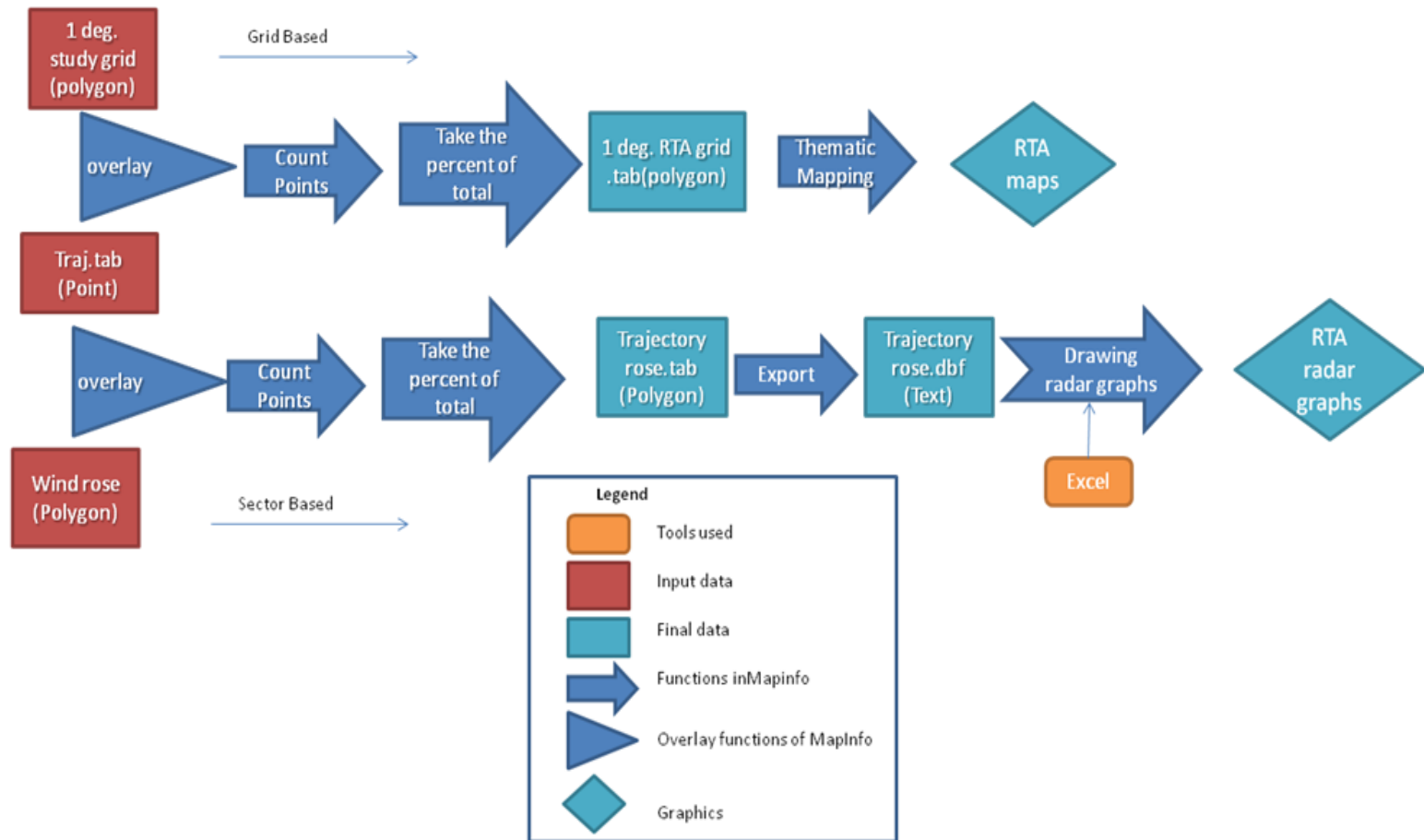


Figure 3.7 Flowchart of Residence Time Analysis (RTA) methodology in GIS

3.3.2. Potential Source Contribution Function

Using the background information given in Chapter 2, the methodology described in Plaisance et al. (1997) was mainly followed in this thesis.

The PSCF of an element X in ij^{th} cell of a grid is calculated by using Eq. (3.5):

$$PSCF_{ij} = \frac{m_{ij}}{n_{ij}} \quad (3.5)$$

where n_{ij} is the total number of trajectory segments in the ij^{th} cell and m_{ij} is the total number of polluted trajectory segments in the same ij^{th} cell during the study period. It is important to notify that grid cell size must be sufficiently large for the assimilation of reasonable trajectory segment endpoints. Thus, the grid described in section 3.1 having cell size of $1^\circ \times 1^\circ$ degree was used in the PSCF analysis.

To calculate the PSCF values, first the n_{ij} values for each grid cell were calculated as counting the total trajectory segments falling in these cells with a spatial joining grid file and trajectories in MapInfo. In order to calculate m_{ij} values, first daily SO_4 measurements for these years were ordered high to low. Then from this ordered values, highest 40% of the concentration values was taken as pollution above the selected criterion and the backtrajectories started in the days when these high measurements occur were selected as polluted trajectories. A column added into the trajectory table indicating the polluted or unpolluted trajectories. Then the m_{ij} values were added into grid file by selecting the polluted trajectories by querying and counting the number of the segments of polluted trajectories falling into the grid cells.

Then the PSCF values calculated for each grid cell by dividing m_{ij} values by n_{ij} values and stored in grid file as separate column. PSCF values takes value between 0 and 1. Cells with high PSCF value approaching to 1 have high potential to be the source of pollution while cells having a PSCF value of 0 are unlikely to be source

regions. However, if the total number of segments in a grid cell, n_{ij} is small, it results in a high PSCF value with a high uncertainty. To minimize the effect of small values of n_{ij} , an arbitrary weighting method as described in various studies (Hopke et al., 1995; Polissar et al., 2001; Zhao and Hopke, 2006; Xu and Akhtar, 2009) was used in this study. Then, the PSCF values were weighted according to the rule described in Zhao and Hopke (2006) using the average number of segments in grid cells, as shown in Eq. (3.6):

$$w(n_{ij}) = \begin{cases} 1.0 & n_{ij} > 2 \cdot n_{avg} \\ 0.75 & n_{avg} < n_{ij} \leq 2 \cdot n_{avg} \\ 0.5 & n_{avg} / 2 < n_{ij} \leq n_{avg} \\ 0.15 & n_{ij} \leq n_{avg} / 2 \end{cases} \quad (3.6)$$

Although PSCF is a relatively easily applicable methodology, the assumptions such as emissions are swept by air parcel without considering trajectory height and transported to the receptor site without concentration decrease by atmospheric removal and chemistry adds some uncertainty into the calculations (Plaisance et al., 1997; Cheng et al., 1993; Lupu and Maenhaut, 2002). In addition to the errors and uncertainties in trajectory calculation (Stohl, 1998; 2002; Zhou et al., 2004), those assumptions form the main weaknesses in PSCF methodology. In real situations, air parcel does not collect pollutant particles at the same amount at different heights and an occasional rain on the air parcel's trajectory washing out the pollutant carried by the air parcel will contribute inaccuracy of the PSCF results. To overcome these deficiencies, trajectory segment precipitation and height information was tried to be incorporated into the PSCF analyses.

Precipitation would have significant effects on the results of PSCF analysis. Assuming that backtrajectory information is included in the each segment endpoint of the backtrajectory, if the amount of precipitation in some part of the trajectory is high to washout the pollutant, the assumption of transport of the pollutants without loss does not hold anymore and the probability of the locations before that point on the trajectory being a potential pollution source vanishes. The probability of being a pollution source before that point is low due to the occurrence of rain. Therefore it

is logical to remove the trajectory segments before the point where rain above a defined amount is first seen on the backtrajectory. This will increase the statistical confidence of the results.

As the air parcels moves along its trajectory, they collect pollutants when they pass over the emission sources. But the collection of pollutants greatly depends on the segment height at the source. An air parcel at higher altitudes is not affected by the emission source as high as the air parcel at lower altitudes. The effects of trajectory height on the PSCF results were previously discussed by Doğan (2005). Generally, trajectories, far from the receptor site, are in high altitudes and if just segments below lower altitudes are to be used in the studies, then the effect of source regions away from the receptor will be underestimated. On the other hand, in real situation air parcels at different heights passing through a pollution source do not collect pollutant particles at the same amount i.e. plumes do not rise above mixing height therefore the air parcels above this height do not collect pollutant. Therefore, use of appropriate weights for trajectory segments according to different altitudes would improve PSCF and enable more accurate assessment of source regions. It is also expressed by Doğan (2005) as a recommendation for future studies.

A MapBasic application, where the pseudo-code of that application is given in Appendix F, was developed for the PSCF analysis. This application opens the excel file of concentration measurements in MapInfo and adds a column for date information similar to the trajectory files. And then it automatically orders the concentration values and select 40% of the highest concentration values. After that it selects the trajectories having the same dates of highest concentration occurrences by querying and adds “1” for polluted and “0” for unpolluted trajectories to the column in trajectory file. Then it calculates m_{ij} , n_{ij} and PSCF values using update column function with spatial joining of grid table and trajectory table. To minimize the uncertainty, tool then applies the arbitrary weighting on PSCF values, by multiplying the original PSCF values with the weights presented above according to the n_{ij} values of grid cells.

Inclusion of rain was implemented in MapInfo as follows. Rain information at each segment endpoint had been requested within the HYSPLIT backtrajectory data. Several rain filters were applied between 0.1 to 1 mm/hr. For each polluted trajectory, precipitation values were checked backwardly on time. From the first existence of the selected amount of precipitation, trajectory segments previous to this point were deleted from data set. Then m_{ij} , n_{ij} and PSCF values were calculated using new data set. Then, PSCF values were weighted to reduce the effect of small n_{ij} values.

Inclusion of segment height was achieved by applying a weighting in GIS as follows. First arbitrary weights were defined for different height intervals. If a trajectory defined as polluted trajectory, air parcel assumed to collect pollutants to the receptor area different amounts at different heights. In PSCF analysis, all segments of the polluted trajectories have the same contribution to the PSCF values of the grids. But when weighted according to segment heights, the PSCF analysis represents the real situations more. The arbitrary weights were applied only to the polluted trajectories, resulting in an adjustment of the m_{ij} values therefore of the PSCF values. Normally a polluted segment counted as one in the calculation of m_{ij} , but after weighting its contribution is decreased. The polluted trajectory segments were selected by querying, and their weighted contributions calculated in a separate column in the trajectory file. Then m_{ij} values of grid cells were calculated using these weighted contributions. The n_{ij} values were not affected from this weighting. After calculating m_{ij} and n_{ij} values, regular procedure for arbitrary weighting for small number of n_{ij} was applied. A MapBasic application was developed to make necessary calculations for inclusion of segment height and rain information into the PSCF. The source code is provided in Appendix G.

The effects of the weighing on segment height and precipitation were quantified by taking percent change on the original results. In this analysis, differences between rain or height weighted PSCF values and original PSCF values were calculated as the percentage change of the original PSCF values. All different weighting results compared with the original grid only.

The results of PSCF analyses were visualized by creating thematic maps using grid files in MapInfo GIS. Because a PSCF value varies between 0 and 1, ten equal intervals were selected in thematic maps. The thematic maps of PSCF were drawn by using the grid cells only covering the land areas. This information was added to the grid cells by spatially joining the grid with globe map. Globe map used in the visualization was obtained from the sample data of MapInfo.

The methodology applied in GIS was summarized in Figure 3.8.

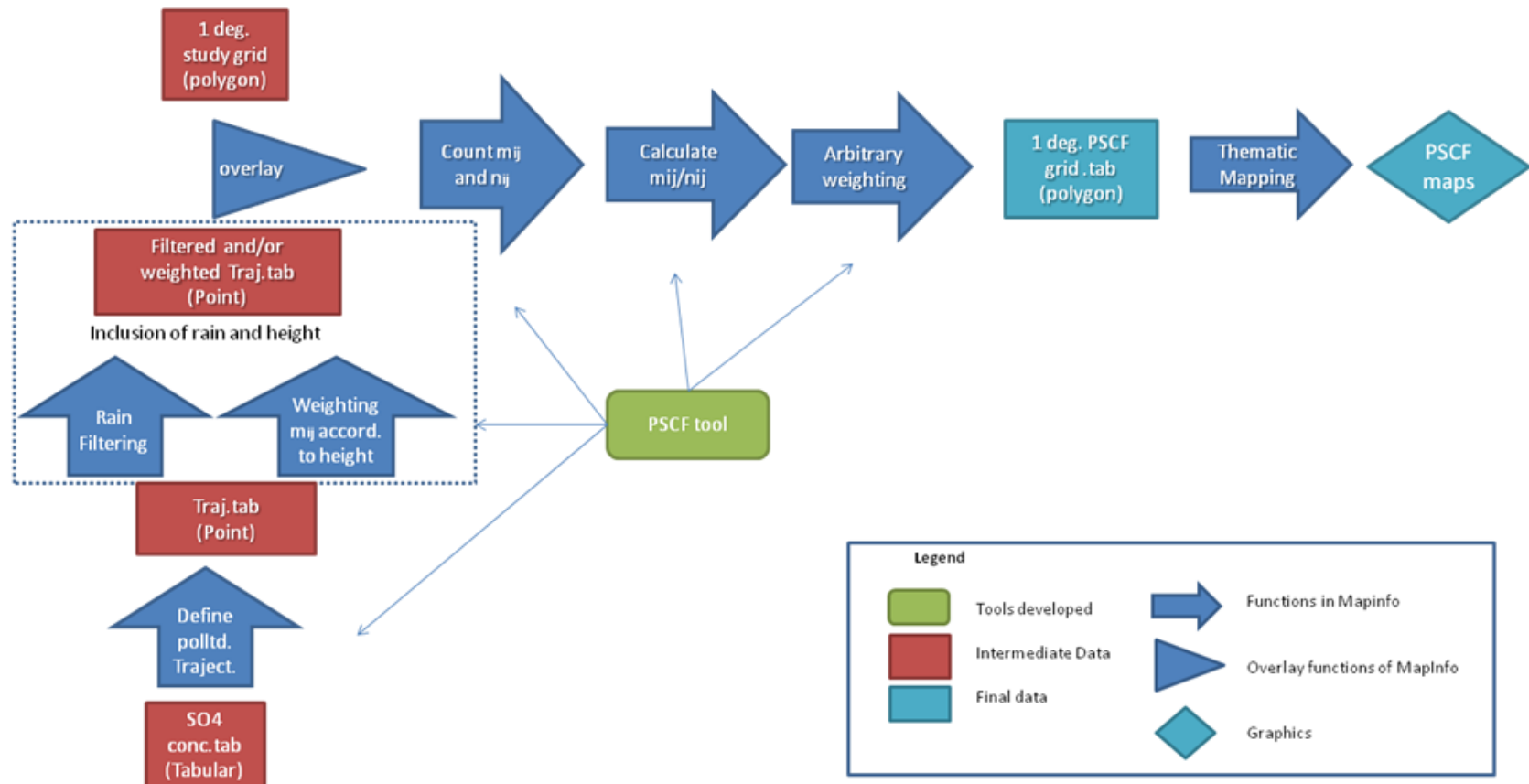


Figure 3.8 Flowchart of PSCF methodology in GIS

3.3.3. Regions of Influence Analysis (RoI)

There are two different approaches to determine source regions affecting pollutant concentrations at a given receptor (source region apportionment). These are classified as “source oriented” and “receptor oriented” approaches. Source oriented approaches, bases on source information, such as emissions, source characteristics to calculate pollutant concentrations at the receptor. This general class includes numerous different numerical models, which start with source and meteorological data, simulates transport of pollutants in the atmosphere and finally calculates concentrations at the receptor.

The second category, namely “receptor oriented approach”, starts with concentration data generated at the receptor through an extensive measurement program. To this data statistical tools, with various degree of sophistication, are applied and sources or source regions responsible from measured concentrations are revealed. This approach, where measured concentrations of pollutants at the receptor are used to determine types of sources responsible for those pollutant concentrations, is called “receptor modeling” (although it has nothing to do with numerical modeling). Discussion on receptor modeling is not in the scope of this study.

Trajectory statistics that previously explained in section 2.2 is a category in receptor oriented approaches. It again starts with pollutant data generated at the receptor, but instead of relating these concentrations to source types, it determines the source regions from where these pollutants are emitted to atmosphere. Such an assessment naturally requires combing information on concentrations of pollutants with geographical information. The geographical information is provided by backtrajectory analysis. Then both of these information is fed to a statistical tool to generate information on potential source regions of pollutants.

Both of these approaches have their own advantages and disadvantages. Numerical models are generally cheaper and easier to operate, because they base on existing data on emissions and meteorology and do not require a measurement program. However, they have high uncertainties as they try to simulate atmospheric processes which are not well known. The uncertainty of numerical models increase with increasing distance scale, and models that simulate long range, transboundary transport of pollutants becomes too sophisticated to be routinely used in every laboratory. Generally two models, one to simulate meteorology and the other one to simulate chemistry is used.

Trajectory statistics, on the other bases on measurement data, which have small uncertainty, but relies on accuracy of backtrajectory computations, which has higher uncertainty than measurements. Its dependence on measurement results is also a disadvantage, because long term measurements are expensive and such data is not always available.

This method is a hybrid source-receptor model developed to identify the source regions which affects the pollution at a receptor area. It represents the contribution of a source region ij^{th} cell to the pollution at the receptor area in terms of emission loads.

Suppose N represents the total number of trajectory segment endpoints during the whole study period, t and n_{ij} represent endpoints fall into the ij^{th} cell. Then the residence time of the trajectories as percentages in the cell (i,j) given in Eq. (3.7) :

$$RT_{ij} = \frac{n_{ij}}{N} \times 100 \quad (3.7)$$

Residence times means how long the trajectories stay in the grid cell (i,j) that reveals some information on how much these grid cells affect the receptor area. But this is solely in terms of how often the trajectories pass or reside in grid cells. Pollution information is needed to be incorporated with trajectory information to

identify the pollution sources. Then the residence time value multiplied with the total emissions at the grid cell (i,j) to find RoI values of cell (Eq. 3.8):

$$RoI_{ij} = RT_{ij} \times E_{ij} \quad (3.8)$$

Where E_{ij} is the total emissions of the pollutant under concern of the grid cell (i,j) over study period, t . The resultant value has mass unit (ton or kg).

This method has some similarities with PSCF which uses trajectory data and chemical data. The main difference is that instead of using pollutant concentrations, emission values are used to identify source regions. Therefore, RoI could be called a source oriented method. In this method, the known sources contributed most to the pollution at the receptor is under concern, while in PSCF the possible locations is tried to be determined. But at the end both method determine probable source locations for the pollution at the interested area.

Similar to PSCF model, the possible source region covered by trajectories is divided into a gridded i by j array. If a trajectory endpoint lies in the ij^{th} cell, it is assumed that trajectory collects material emitted in the cell and the material is assumed to be transported along the trajectory to the receptor site. In addition to these, the same assumptions as in PSCF are hold that atmospheric removal and chemistry are not considered as an air parcel transports to the receptor site.

The procedure (Figure 3.9) includes the calculation of residence times and then multiplying with emission values in GIS. EMEP emissions discussed in section 3.2 were used. The residence times were calculated for 4 stations using HYSPLIT trajectories of having different start heights by following the procedure described in section 3.3.2. Then RoI values calculated by multiplying the emission values with the residence time values of grid cells. RoI values for trajectories having different start height with yearly values were calculated at each station to analyze source-receptor relationship in these areas.

In order to validate this methodology, the results were compared with the PSCF results. PSCF values for Çubuk station for the period of 2004-2006 and RoI values for the same time interval with the same trajectory data were calculated using the procedures explained before. Then the results were compared with each other to validate the use of RoI methodology. PSCF is used as a reference method because it is widely used in many studies (Zeng and Hopke, 1989; Gao et al., 1993, 1996; Plaisance et al., 1997; Hsu et al., 2003; Liu et al., 2003; Güllü et al., 2005; Hwang and Hopke, 2007; Doğan, 2005; Işıkdemir, 2006; Doğan et al., 2008; Munzur, 2008) and therefore a scientifically validated methodology. Both methods have similarities as mentioned before (the same assumptions on transport, used similar logic, combines chemical information with the meteorological information, etc.)

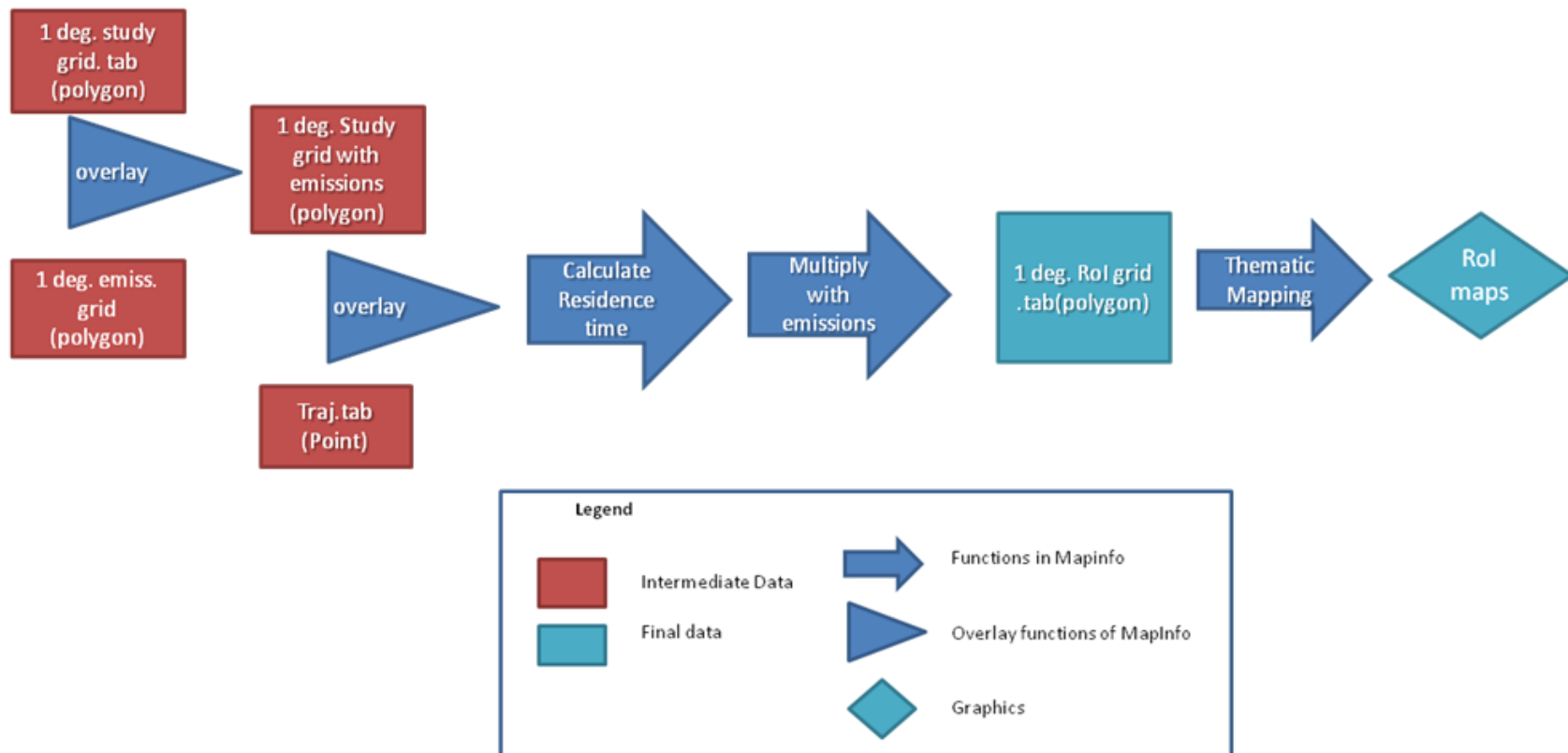


Figure 3.9 Flowchart of Regions of Influence methodology in GIS

CHAPTER 4

RESULTS AND DISCUSSIONS

In this section various aspects in trajectory statistics are discussed. Discussions cover a wide range of sophistication, starting from simple visual inspection of backtrajectories and goes all the way to inclusion some new parameters to methods used in trajectory statistics. There are four main objectives of this study.

The first objective is to find the magnitude of differences in the trajectories computed with two well documented backtrajectory models, namely, ECMWF and HYSPLIT 3D trajectory models. Both of these models are widely used in literature and both are claimed to generate reliable backtrajectories. This comparison was performed at one selected receptor.

The second objective is to compare different locations in Mediterranean area for their receptor characteristics. This was accomplished by finding potential source areas that can affect pollutant levels at well-documented receptor locations in the western Mediterranean, Eastern Mediterranean, Black Sea and Central Anatolia. The specific locations selected as receptor coordinates included Amasra for the Black Sea, Çubuk for the central Anatolia, Antalya for the Eastern Mediterranean and Corsica for the Western Mediterranean. These four locations were selected because, fairly large data sets are available in those sites and concentrations of various pollutants reported for these receptor points are significantly different from each other (Pérez et al., 2008; Migon et al., 2008; Garcia-Orellana et al., 2006; Ridame et al., 1999; Sandroni and Migon, 1997, for Corsica, Tuncel et al., 2008; Erduran and Tuncel, 2001; Doğan et al., 2008; 2010; Kuloglu and Tuncel, 2005, for Antalya, Hacısalıhoğlu et al., 1991a; 1991b; 1992; Anwari et al., 1992; Alagha et

al., 2001; 2003; Karakaş et al., 2004, for Black Sea and Gaga et al., 2009; Kaya and Tuncel, 1997; Tuncer et al., 2001 for Çubuk)

The third objective of the study is to develop a new trajectory based approach, which would allow identification of potential source locations for selected receptors without the need of generating expensive data sets or running sophisticated models. Details of this method development exercise are given in coming sections. This exercise is also performed for the same set of four locations.

The fourth objective of the study is to improve existing methods in the field of trajectory statistics by weighting segments depending on their altitude and rainfall amount. This exercise was performed in one of the four stations and not repeated in the others.

4.1. Comparison of Two Different Trajectory Models

Backtrajectories are very useful to incorporate geographical information to measurement results. Because of this, backtrajectory computations are very widely used to relate measured concentrations of atmospheric constituents to sources and source areas. A variety of backtrajectory models are available. Some examples include TRAIET (Reap, 1972), LACYTRAJ (Clain et al., 2010), METeorological data EXplorer (METEX) (Akata et al., 2009), British Atmospheric Data Centre (BADC) (Russell et al., 2008), APTRA (Delcloo and De Backer 2008) and FLEXTRA (Stohl et al., 2001). However, two of these models found much wider scale use than the others. These two models among them, namely HYSPLIT (Draxler and Hess, 1998), which is developed by NOAA, USA and ECMWF model (McGrath, 1989), which was developed for the use at European Center for Medium Range Weather Forecast (ECMWF, Redding, UK) find wide application in literature (HYSPLIT (Draxler and Hess, 1998) model: Crawford et al., 2007; 2009; Shan et al., 2009; Challa et al., 2008; McGowan and Clark, 2008; Escudero et al., 2006; Wain et al., 2006; Draxler and Rolph, 2003; Rolph, 2003; ECMWF (McGrath, 1989) model: (Bigg et al., 1996; Birch et al., 2009; Eneroth et al., 2003;

Fink and Knippertz, 2003; Heintzenberg and Leck, 1994; Knippertz et al., 2003; Norman et al., 2003; Paatero et al., 2003). These models have also been used in the Environmental Engineering Department of Middle East Technical University (METU) since early 90's. Hence, these two models were used throughout this study.

No matter how frequently they are used, uncertainty in backtrajectory modeling had always been a serious concern (Riddle et al., 2006; Stohl, 1996; Stohl et al., 2001; 2002; 2005). A rule of thumb approximation in uncertainty is approximately ± 150 km horizontal displacement (deviation from calculated centerline) at 3rd day of computations (Stohl et al., 2001). In this study we compared outputs of the two trajectory model, namely HYSPLIT and ECMWF to assess differences of not only trajectories computed by the two model but also to understand the extent of difference they generate in the results of trajectory statistics.

The comparison was performed in three levels. In the first level trajectories generated by the two models for the same time interval were visually compared. In the second step, residence times of air masses computed by the two models were compared on an annual basis. In the third step, Potential Source Contribution Function (PSCF), which is a statistical tool in trajectory statistics, were performed using trajectories calculated by the two models and results of the PSCF calculations were compared.

The comparison of the two trajectory model was done for the Çubuk station. Backtrajectories extending 5 days (120 hours) backward in time were calculated using both ECMWF and HYSPLIT models. Trajectories started at 14:00 afternoon at three different altitudes (100 m, 500 m, and 1500 m). Computations with both models were performed for every day in last 5 months of 1990 and whole year in 1995 and 2000. Since the number of days and number of segments should be identical for both models in this comparison, data were first checked for consistency and completeness. Because some days or some hours may be missing in one of the two trajectory sets, these data were eliminated from both trajectory sets to make

them identical. After this manipulation, a total of 308550 hourly segments generated by 850 daily trajectories were used in computations.

4.1.1. Visual Comparison of the Trajectories

In this part backtrajectories of 30 days of were randomly selected from the HYSPLIT and ECMWF trajectory data sets. Then the backtrajectories of two models were compared pair wise for the same days. To save the space, only four of backtrajectories from this set were shown and compared in Figure 4.1. Backtrajectories starting from 100m, 500m and 1500 m (equivalently 1000, 955 and 850 hPa in ECMWF) were drawn on the map in different colors and styles. HYSPLIT and ECMWF backtrajectories were drawn in blue and red color respectively.

a. 15 September 1990

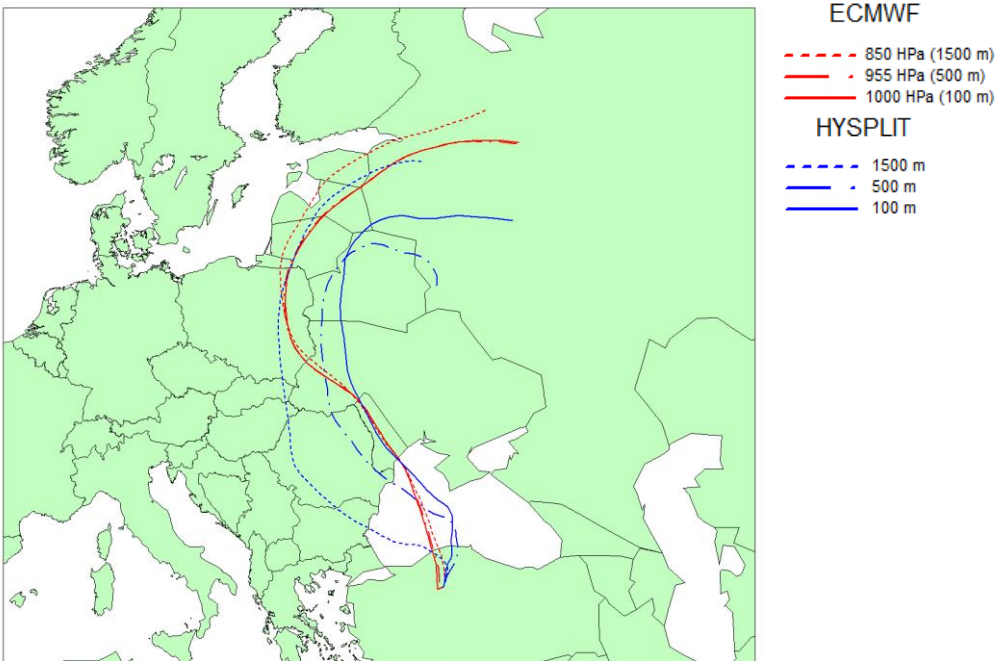
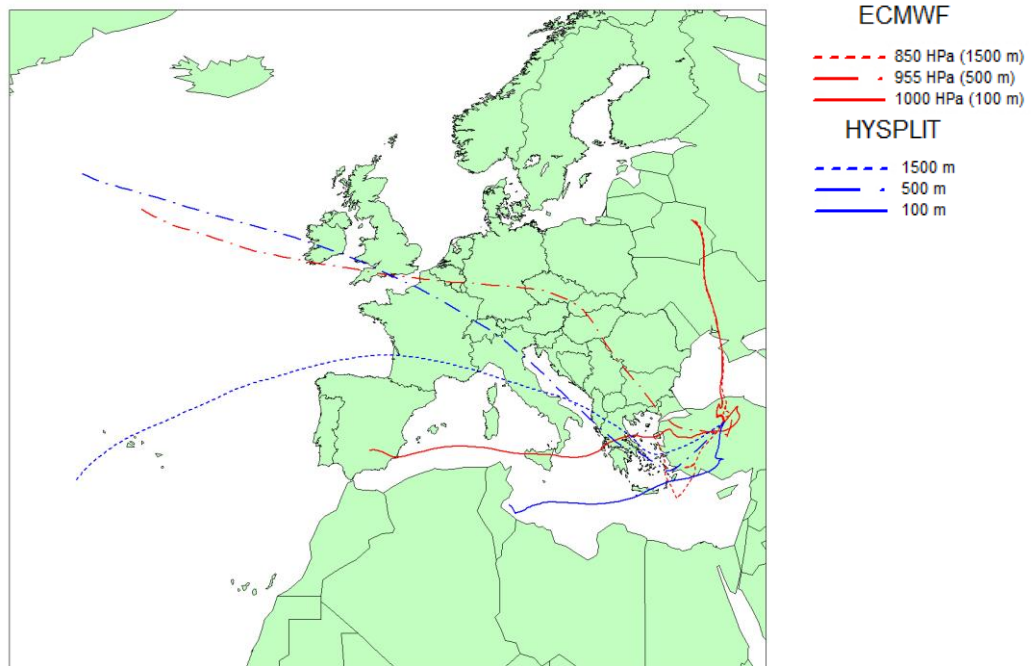


Figure 4.1 Visual comparisons of the HYSPLIT and ECMWF trajectories

b. 27 January 1995



c. 11 February 2000

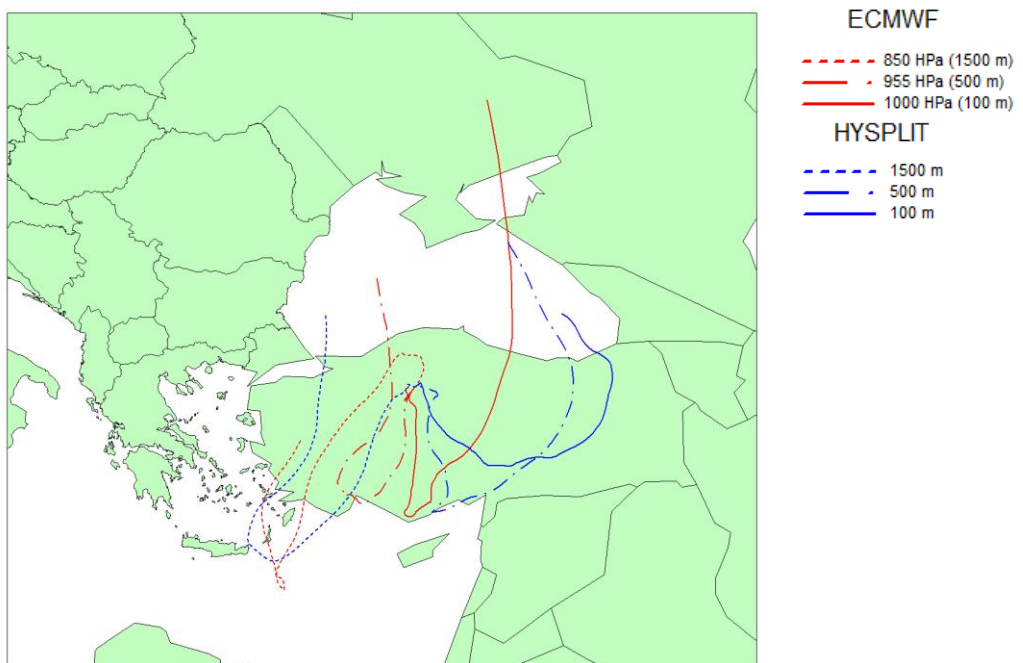


Figure 4.1 Visual comparisons of the HYSPLIT and ECMWF trajectories, (cont'd)

d. 15 October 2000

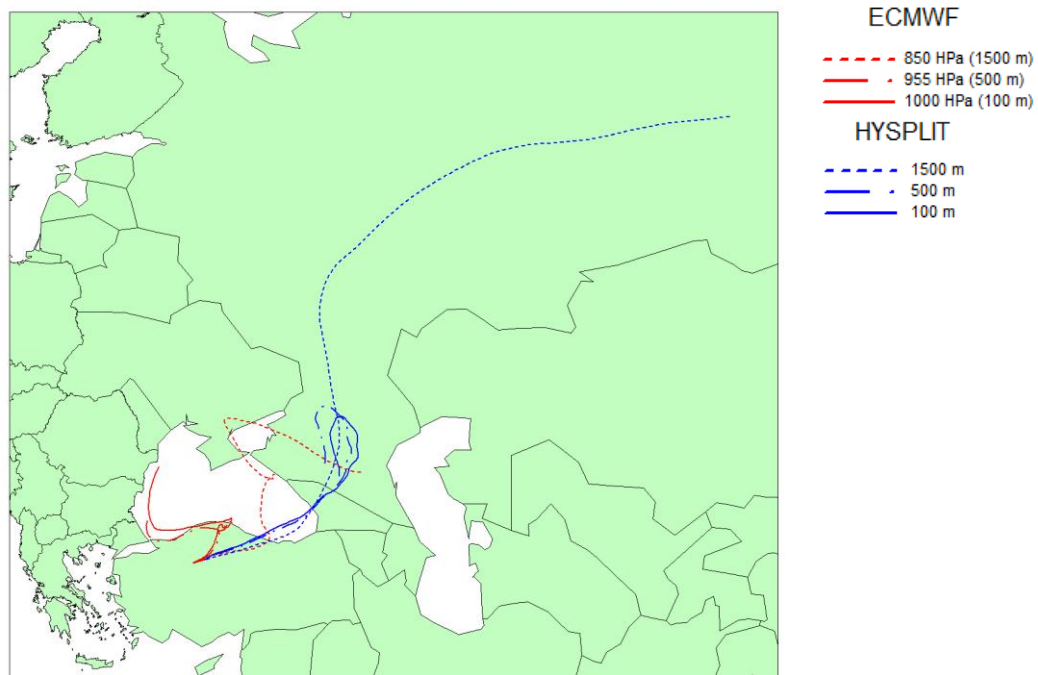
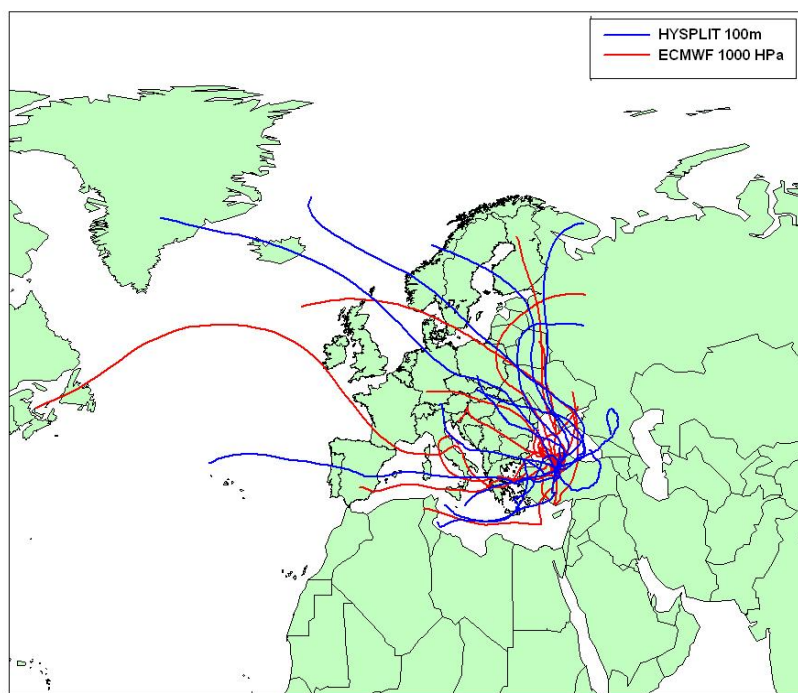


Figure 4.1 Visual comparisons of the HYSPLIT and ECMWF trajectories, (cont'd)

When Figure 4.1 is analyzed, it could be drawn that the trajectories of HYSPLIT and ECMWF moderately differ from each other in terms of direction, shape and length. In some days, the directions of trajectories, where air masses come from, look similar but in general both models produce different results. For example in Figure 4.1-a, good similarity is perceived but when turned to Figure 4.1-d it is easy to see that two model produced different results. In Figure 4.1-b, similar pattern is seen at 500 m, whereas in Figure 4.1-c the same path is seen at only 1500m but interestingly all trajectories points to North. The directions of trajectory ensembles somehow seem similar but the length and the pathways not the same at all. The same observations could also be drawn for the remaining 26 days. To see how different results produced by two models in different starting heights more comprehensively, 15 days were selected from previously selected 30 days and drawn on the maps, grouped by starting heights (Figure 4.2).

a. 100 m



b. 500 m

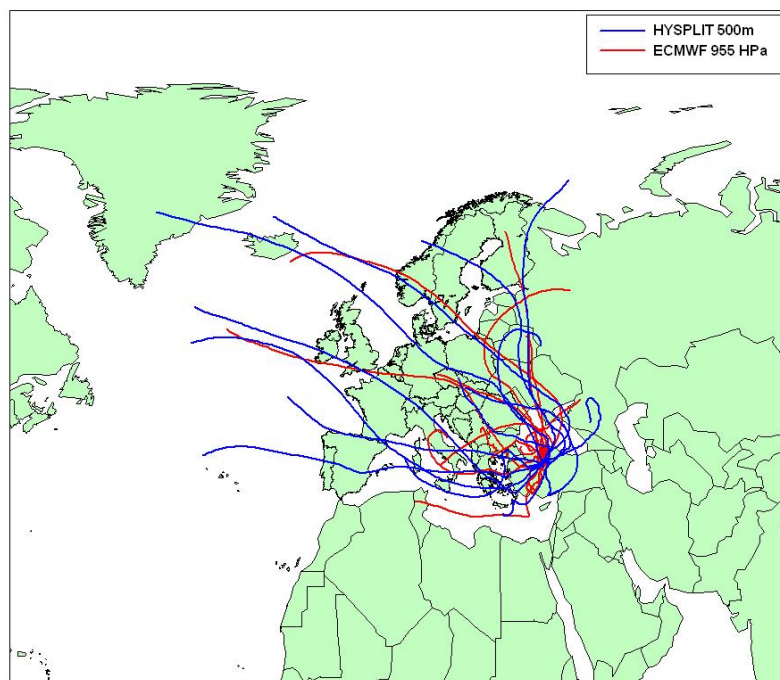


Figure 4.2 Visual comparisons of the HYSPLIT and ECMWF trajectories of different starting height

c. 1500 m

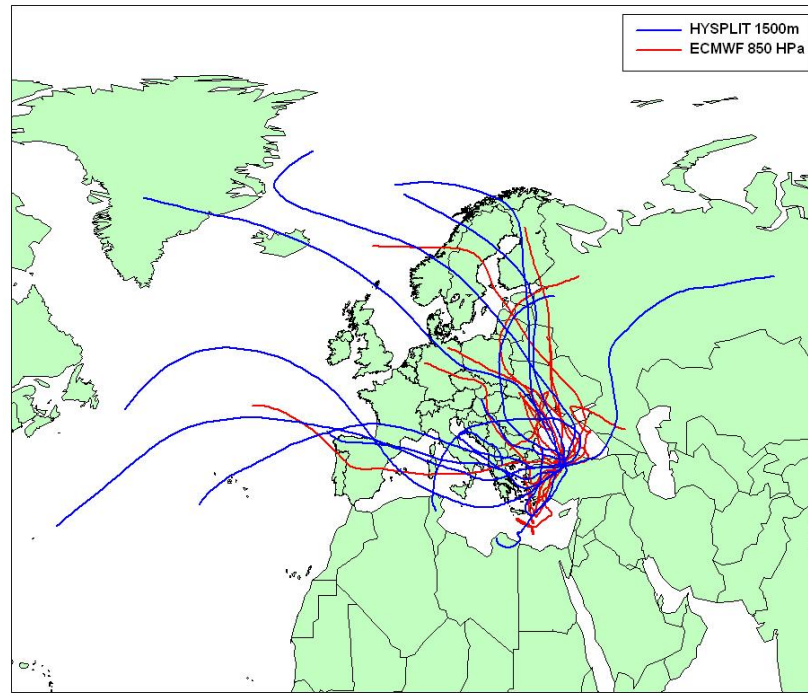


Figure 4.2 Visual comparisons of the HYSPLIT and ECMWF trajectories of different starting height, (cont'd)

Grouping the trajectories of 15 days in one map according to starting height would provide a general perception to the differences between the patterns of ECMWF and HYSPLIT trajectories. Analyzing the backtrajectories according to their starting height (Figure 4.2) reveals some findings. One is that HYSPLIT trajectories travel from more distant places. For example, at 1500m starting height (Figure 4.2-c), 7 HYSPLIT trajectories out of 15 are travelling out of the border of Europe, whereas only 2 ECMWF trajectories could extend out of Europe. This difference gets decreased in lower starting altitudes. Another finding from this visual analysis is that the backtrajectories having higher starting heights travels from larger distances.

Being a qualitative analysis, visual comparisons could only provide information on the similarities between these trajectories in shape or direction and little perception on the frequency of flow over an area. There is not a good agreement seen between

HYSPLIT and ECMWF trajectory models when compared visually by trajectory ensembles of the same days. But this is strongly related to the number of trajectories used for visual comparison. In this part a limited number of trajectories were compared but in order to generalize the model differences, statistical methods should be utilized with larger number of samples. For instance, using daily trajectories of 1 year or more time period could provide information on the transport paths of pollutants. Trajectory statistics could more explicitly define the similarities between 2 models which would not be identified by visual comparison.

4.1.2. Comparison of the Residence Times

Visual inspection of an ensemble of trajectories calculated by both methods provides qualitative information on similarities of the results generated by the two codes, but cannot provide quantitative information. To be more quantitative, in the second step, trajectory segments are compared. A trajectory segment is the location of the air parcel at every hour. A 120 hr long (5 days) backtrajectory consisted of 120 segments. Both models were used to compute backtrajectories which give the coordinates of trajectory segments. Coordinate of each segment end point gives the location where air parcel resided for one hour. The residence time analysis (RTA) was performed first by calculating the residence times in wind sectors and then by counting the segments in grid cells of our grid system, which was described in section 3.1 in the manuscript.

a. Comparison Based on Sectors

In sector based comparison, number of segments in each wind sector was counted using the wind rose described in Chapter 3.1. Trajectory segments were distributed into 16 wind sectors of wind rose, which is centered at Çubuk station. The wind rose, or in this case trajectory rose, was constructed by counting the number of segments in each sector. The outer boundaries of the sectors were the limits of our study domain, which is described previously in the manuscript. Two trajectory rose were constructed at each starting altitude using trajectories calculated by HYSPLIT

and ECMWF trajectory models. Then, residence times of air masses in each sector calculated by the two models are presented in Figure 4.3.

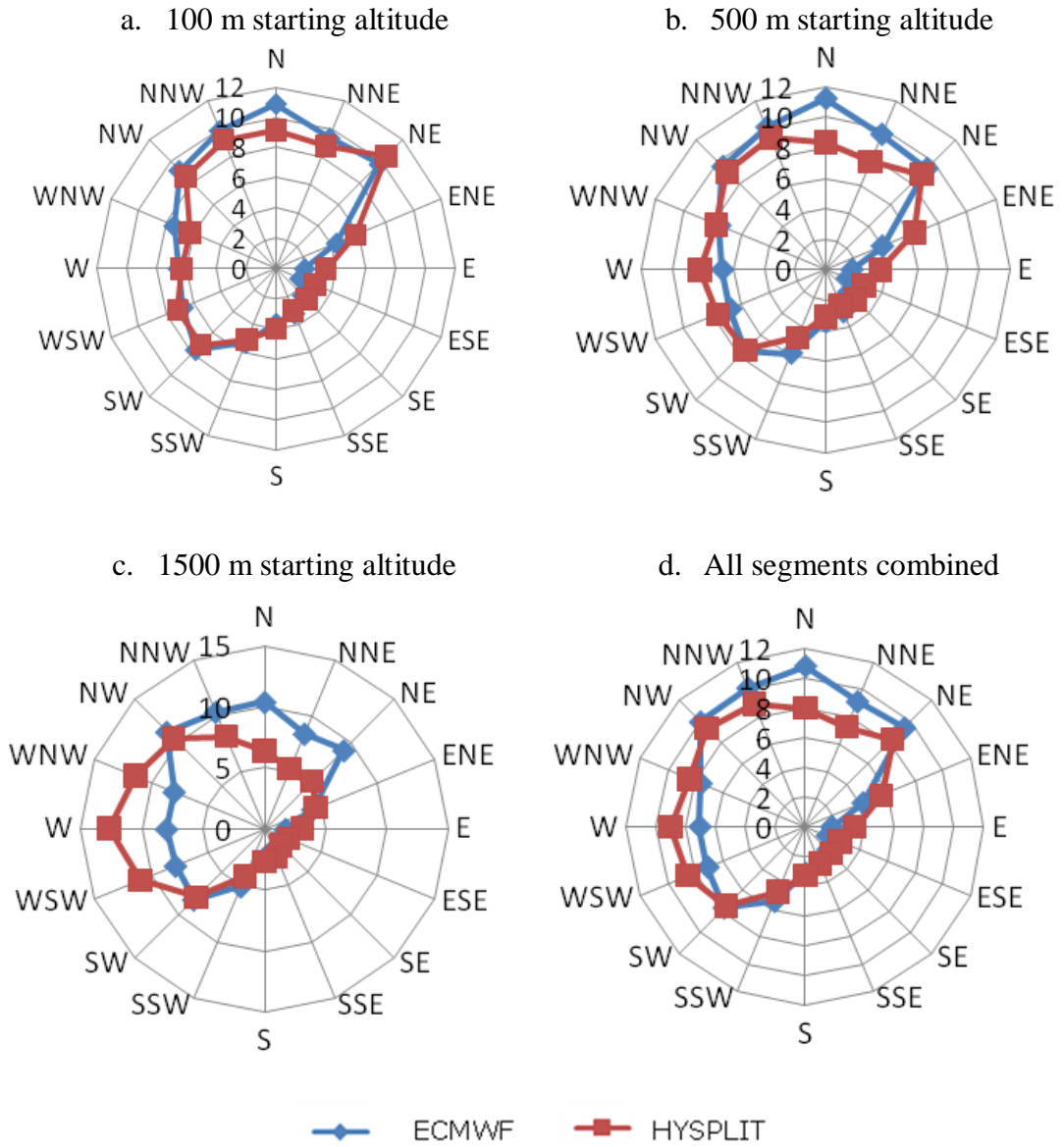


Figure 4.3 Percentage of time air masses spent at each wind sector, calculated using trajectories computed by ECMWF and HYSPLIT trajectory models at different starting altitudes (%)

There are two important points that should be highlighted. The first important point to note is that general features of the air mass residence time distribution between sectors obtained from both models are similar but not identical. In both models, the longest residence times of air masses occur between west and NNE sectors and this is more or less true in all starting altitudes.

The second point worth noting is that the difference between air mass residence times computed for each sector using trajectories generated by HYSPLIT and ECMWF models differs with increasing starting altitude. Differences between trajectories generated by the two models are negligibly small at 100 m starting altitude (Figure 4.3-a), also small in 500 m starting altitude (Figure 4.3-b) and somewhat larger at 1500 m starting altitude (Figure 4.3-c). For example the largest difference between the air mass residence times at 100 m starting altitude is not more than 2% in any of the factors, in 500 m starting altitude the difference is approximately 3% in North sector. However, the difference is 5% and more in WSW, W and N sectors. In this case ECMWF trajectories predicted longer residence times of air masses (compared to HYSPLIT trajectories) at N, NNE and NE sectors and lower residence times of air masses (relative to HYSPLIT trajectories) at WSW, W and WNW sectors. This means that, higher contribution of pollution sources located at NNW, N, NNE and NE sectors, which includes countries like Ukraine and Russia, can be predicted when HYSPLIT trajectories starting at 1500 m are used in trajectory statistics and higher contribution of sources located at Western Europe can be predicted when trajectories calculated with ECMWF model.

This observation suggests that the trajectory model used is not the limiting factor on uncertainties of source apportionment if starting altitudes < 1000 m are used. However, differences between predictions of source regions using trajectory statistics can have larger uncertainties if trajectory starting points are high. One reason for higher uncertainties associated with trajectories, which have higher starting altitudes, can be the longer nature of the high-starting trajectories as the length of backtrajectories often increases with starting altitude. Nevertheless, this

discussion suggests that trajectories with low starting altitudes should be used whenever possible. To compare trajectory models based on wind sectors, each 1-hour segment of backtrajectories was assigned to a wind sector and the total number of segments in each of the 16 wind sectors was counted and then residence times were calculated. Comparison was done using the trajectories starting different altitudes separately and combined. The detailed description of the methodology of residence time analysis was given in section 3.3.1.

b. Comparison Based on Grids

The sector-based comparison, which was discussed in the previous section provides information on the similarities and differences in the trajectories calculated with two different backtrajectory models. However, one disadvantage of the system is that it treats each sector as one single unit and does not provide information whether differences between models has anything to do with the distance from the receptor. For example, the conclusion in previous section was that both models generate similar information in low-starting trajectories. However, distributions of segments in trajectories with starting altitude of 1500 m are not so similar. One reason can be the longer nature of the trajectories. Usually the length of backtrajectories increase with starting altitude, because their interaction with surface decreases with starting altitude. This reasoning for observed increase in the difference between trajectories generated by different models at higher starting altitudes is a speculation based on our experience.

In this part of the work, it was attempted to calculate the differences between trajectory segments calculated in $1^\circ \times 1^\circ$ grids (approximately $110 \text{ km} \times 80 \text{ km}$ in this part of the world, but changes with latitude) in the study domain. Firstly, the residence times of trajectories generated by each trajectory model in each grid were counted as explained in section 3.3.1, and then the percent differences were calculated using the following relation (Dutton et al., 2009):

$$\% \text{Diff} = \frac{|x_1 - x_2|}{(x_1 + x_2) / 2} \times 100 \tag{4.1}$$

In Eq. (4.1), x_1 is the residence time in the grid cell calculated by the trajectory model 1 (ECMWF in our case), x_2 is the residence time in the same grid cell calculated by the trajectory model 2 (HYSPLIT in our case). The percent differences were calculated only for grid cells having segments from both models. Residence times of air masses calculated by using trajectories computed by ECMWF and HYSPLIT trajectory models are given in Figure 4.4.

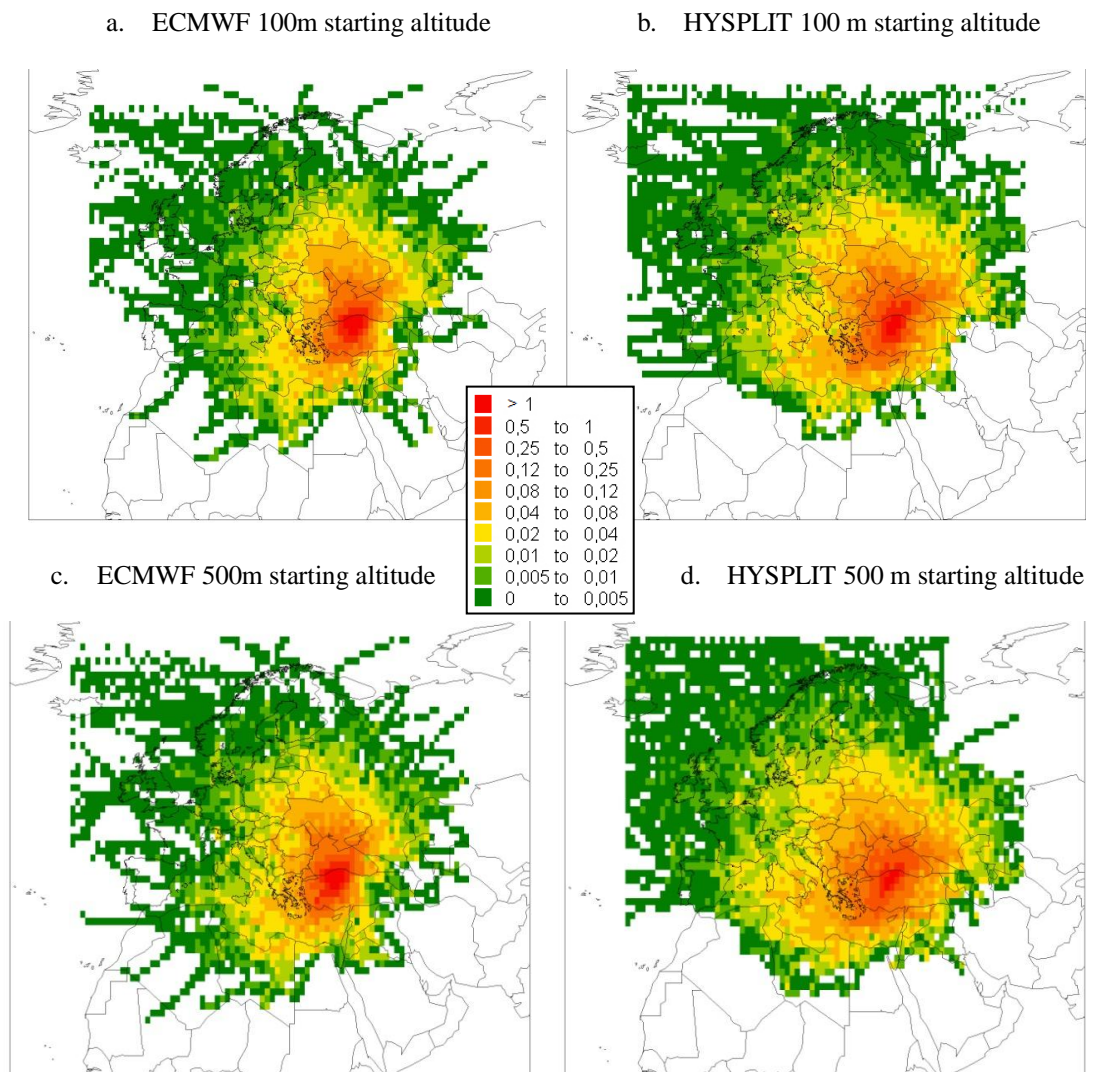


Figure 4.4 Grid-based residence times calculated using ECMWF and HYSPLIT trajectories

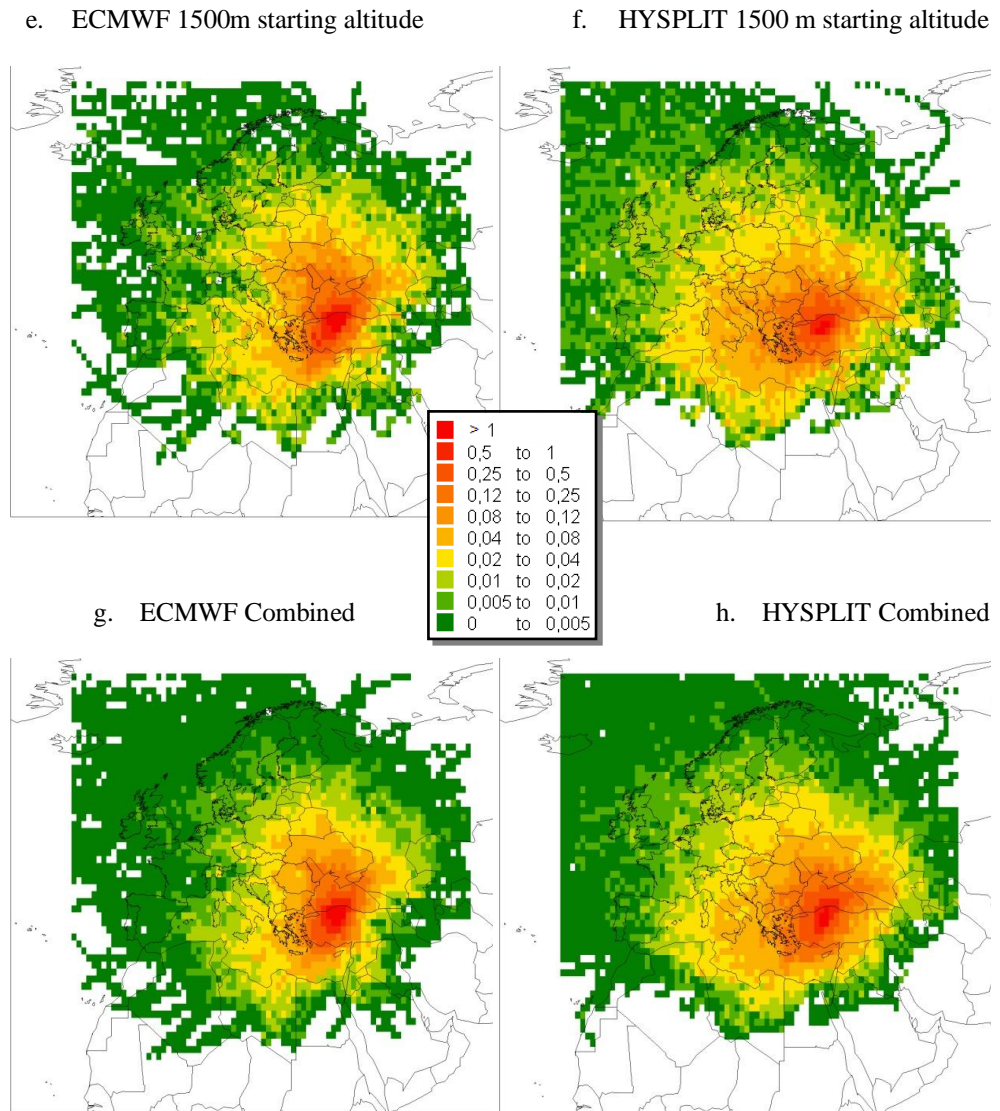


Figure 4.4 Grid-based residence times calculated using ECMWF and HYSPLIT trajectories, (cont'd)

The longest residence times of air masses are in the grids that are close to receptor (Çubuk station). This should be expected because, all trajectories without any exception converges to the grid in which the receptor is located. In other words, all trajectories, whatever the trajectory model is, have to pass through that particular grid and grids in the immediate vicinity of the station. Trajectories, with 100 m starting altitude, calculated using ECMWF and HYSPLIT models produce qualitatively very similar distributions of air mass residence time (Figure 4.4-a,b).

For trajectories with 500 m and 1500 m starting altitudes trajectories calculated by HYSPLIT trajectory model generated more uniform distribution of air mass residence time in the sector between SW and N, compared to distribution of air mass residence times calculated by using trajectories computed by ECMWF model (Figure 4.4-c, d, e, f). ECMWF model, on the other hand, generated more elongated air mass residence times on the SSW – NNE axes. This discussion on grid based air mass residence time is qualitative and also does not give hints on the dependence of differences between models on the distance from the receptor. More quantitative information can be obtained by calculating grid-by-grid differences in residence times found by using different models. The grid based differences were calculated using Eq. (4.1) and results are presented in Figure 4.5.

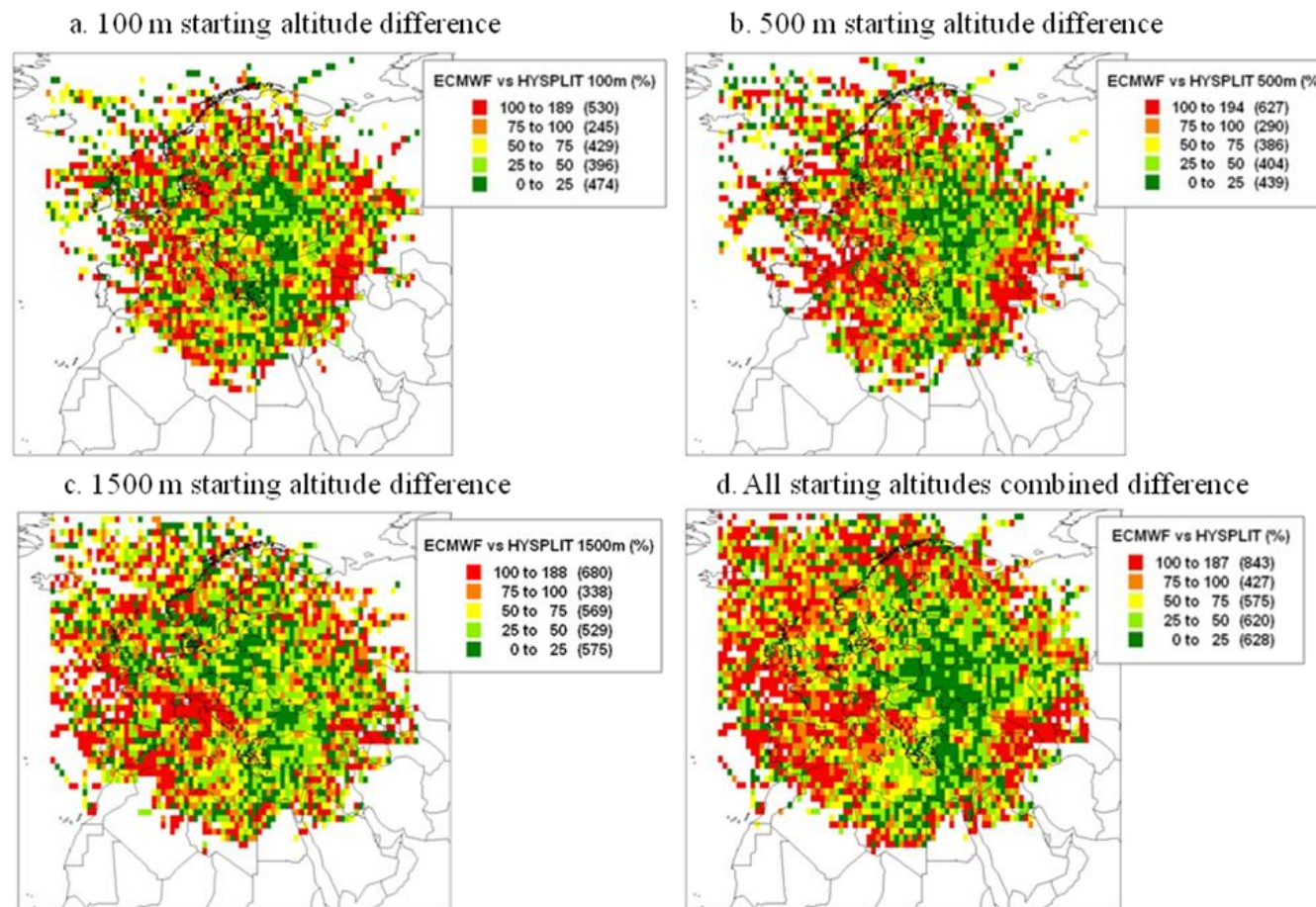


Figure 4.5 Grid-by-grid differences in air mass residence times calculated using ECMWF and HYSPLIT trajectories

The legends in the Figure 4.5 show the percent differences between numbers of segments generated by the two models. The darkest green color indicates < 25% difference and red color indicates > 100% difference. The numbers in parentheses indicate the number of grid cells in each category. Table 4.1, on the other hand shows the percentage of grids fulfilling each criterion.

Table 4.1 Fraction of grids (with data) in the domain indicating difference

Difference	100 m Starting altitude	500 m Starting altitude	1500 m Starting altitude	Combined
0% - 25%	22.9	20.5	21.4	20.3
25% - 50%	19.1	18.8	19.7	20.0
50% - 75%	20.7	18.0	21.1	18.6
75% - 100%	11.8	13.5	12.6	13.8
>100%	25.6	29.2	25.3	27.3
Total Number of grids	2074	2146	2691	3093

There is number of points worth noting in the Figure 4.5 and Table 4.1. First of all, numbers of grids are different for each starting altitude. It was pointed in the beginning of this discussion that, grids included in the Figure 4.5 are the ones that have segments from both trajectory models. This means if there is no segment from either one of the models the grid is not included in percent difference calculations and left blank. The number of grids increases from 100 m starting altitude to 1500 m starting altitude, indicating that as the starting altitude increases, backtrajectories get longer. Going from 100 m starting altitude to 500 m starting altitude adds 72 additional grids, whereas going from 500 m starting altitude to 1500 m starting altitude adds approximately 500 additional grids in the calculations. As trajectories get longer these additional grids are added to outer parts of the study area.

The second point to note is that although red shaded grids look fewer at trajectories starting from 100 m altitude, Table 4.1 demonstrates that there is no significant difference in the percentage of grids that has low and high percent difference values do not change significantly with starting altitudes. The number of grids with % difference < 25% is 474 for 100 m starting altitude, 439 at 500 m starting altitude and 575 at 1500 m starting altitude. Similarly, there are 580 grids with % difference > 100 at 100 m starting altitude, 627 grids at 500 starting altitude and 680 grids at 1500 m starting altitude. Although number of grids with < 25% and > 100% difference seem to increase with increasing starting altitude, it should be remembered that total number of grids also increase with increasing starting altitude. In relative terms (percentage), there is no substantial change between different starting altitudes. For example, grids having differences < 25% is 23% for 100 m starting altitude, 10% for 500 m starting altitude and 21% for 1500 m starting altitude. Similarly, grids having > 100% difference is 26% in trajectories starting at 100 m, 29% in trajectories starting from 500 m and 25% in trajectories starting at 1500 m. Consequently, smaller absolute number of red shaded grids in trajectories with 100 m starting altitude is due to smaller number of grids with data. The agreement between the air mass residence times calculated with ECMWF and HYSPLIT trajectory models is better than 50% in 40% of the grids and worse than 75% in another 40% of the grids.

The grids with large differences between residence times calculated by the two models are at the outer parts of the study area. The green shaded area, which indicates the geography where both models generate fairly similar segments in the grids, cover most part of the Europe, Ukraine and central parts of Russia, most of the Turkey and eastern part of the North Africa. It is not symmetric around the receptor point, but elongated along S – N axes. The orange and red shaded grids, where the two models generated fairly different number of segments, generally occur at the outer parts of the study area, France and Spain are two important source areas where uncertainty of the models are no very good. In addition to these to important countries (in terms of their potential for being source regions), Western part of the North Africa, Middle East and Eastern Russia are the other regions

where ECMWF and HYSPLIT models do not generate comparable number of trajectory segments.

It should be noted that at all starting altitudes the region, where the two models generate comparable number of segments (the region identified by green and yellow shaded grids), do not change significantly. However, new grids are occupied by segments with increasing starting altitude of trajectories and those grids, which take place at outer borders of the study area, are the ones with high percent differences.

4.1.3. Comparison of PSCF Results

Residence time analysis discussed in the previous sections provided information on how good the backtrajectories, which are calculated using ECMWF and HYSPLIT models, agree with each other. These discussions demonstrated that the agreement between trajectories generated with different models is good at the close proximity of the receptor and becomes poorer with increasing distance from the station. In the studies at METU-Environmental Engineering, these trajectory models have been used to calculate potential source areas in our study domain, which covers most of the Europe and parts of Africa and Asia, which influence measured concentrations of pollutants at different receptors (stations) in Turkey. Because of this, assessment of uncertainties in our source-region-apportionment is more important than recognition of differences between air mass residence times, which was discussed in previous sections.

Impact of trajectory model used on source-region-apportionment was explored by using the two trajectory models in the PSCF calculations using the same pollutant data set. Potential source contribution function (PSCF) is a statistical tool, which is very widely used in the field of trajectory statistics to determine source regions affecting a receptor. Since, principles and use of PSCF in air pollution studies is discussed lengthily in sections 2.2.3 and 3.3.2, only results of PSCF runs will be discussed in this section.

The PSCF exercise was performed using SO_4^{2-} data generated in Çubuk station in the years 1995 and 2000. Because daily SO_4^{2-} measurements in this station have been done since 1993, the trajectories of 1990 were excluded. The results are given in Figure 4.6. This Figure is prepared with the combined trajectories from all starting altitudes. This exercise was not extended to other stations, because, as pointed before in the manuscript, the objective is to compare the two trajectory models, and not to determine source regions affecting these stations.

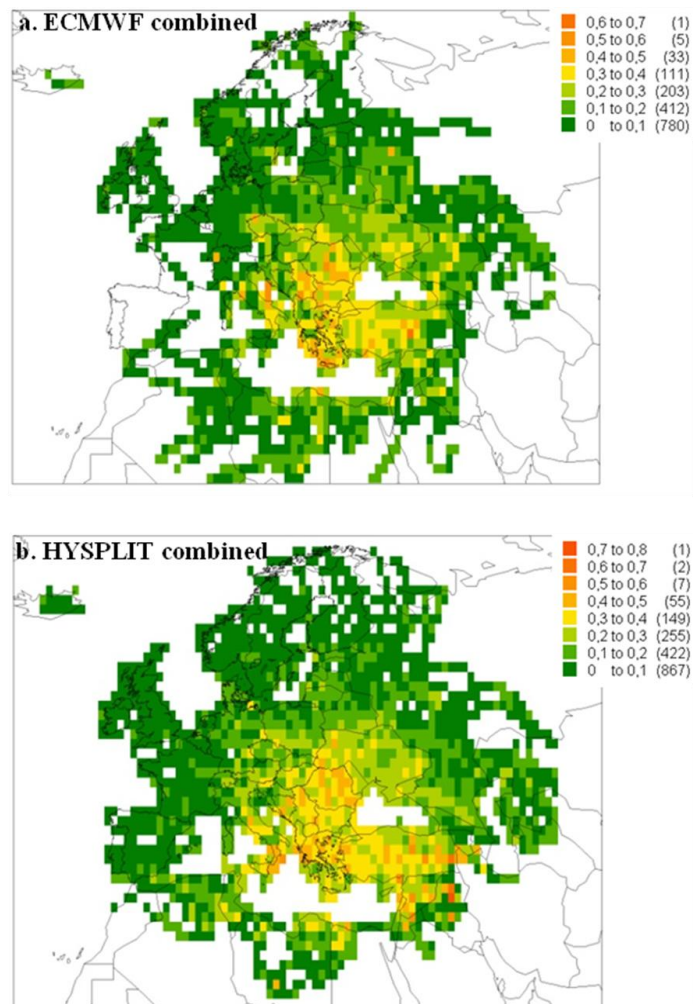


Figure 4.6 Comparison of potential source areas affecting SO_4^{2-} concentrations measured at Çubuk station, with PSCF using trajectories calculated with ECMWF and HYSPLIT trajectory models (Trajectories from all starting altitudes are combined)

As can be seen from the Figure 4.6, there is a general agreement between the source regions assigned by PSCF using trajectories generated by ECMWF and HYSPLIT models. In both cases the regions that strongly influence SO_4^{2-} concentration at the Çubuk station are located in the Balkan region, particularly at the western part of Turkey, Greece, Romania, Bulgaria, Italy and Ukraine. Both models also predicted small influence of the source areas in the western part of Europe, such as, sources in Germany, France and Spain. In addition to these regions that are common to both models, there are also differences between the results obtained from two models, For example, HYSPLIT model predicted stronger influence of the eastern Turkey and Middle East (Figure 4.6-b). These areas did not appear as strong source regions when ECMWF model was used to calculate trajectories (Figure 4.6-a).

The results from the two models can be compared more quantitatively using Figure 4.7, where grid based percent differences are plotted. Definition of percent differences was given earlier in the manuscript. As in the case of air mass residence time calculations, agreement between the distributions of PSCF distributions obtained using the two trajectory models is reasonably good in the vicinity of the station. The term “vicinity” in this case includes Turkey, Balkan countries (including Greece, Croatia, Serbia, Bosnia Herzegovina, Bulgaria, and Romania), Ukraine, Czech Republic, Southern parts of Russia. It is also interesting to note that the region, where agreement between the two models is good is not uniformly distributed around the receptor (Çubuk Station). Good agreement area is extended toward North and Northwest, but very short in the south. This is reasonable, because there is few trajectories arriving the station from south (please see the discussion on air mass residence times), resulting in a few segments to be used in PSCF calculations in the south sector. Small number of segments is the main source of uncertainty in PSCF calculations. Consequently, the lack of agreement between the PSCF values at the south is probably due to uncertainty arising from few trajectory segments computed for these grids. This distribution indicates that the agreement from the models are good all the way to Poland in Europe, but poorer agreement was found at western parts of the Europe, including Holland, Belgium, Germany, UK, France, Spain, Portugal.

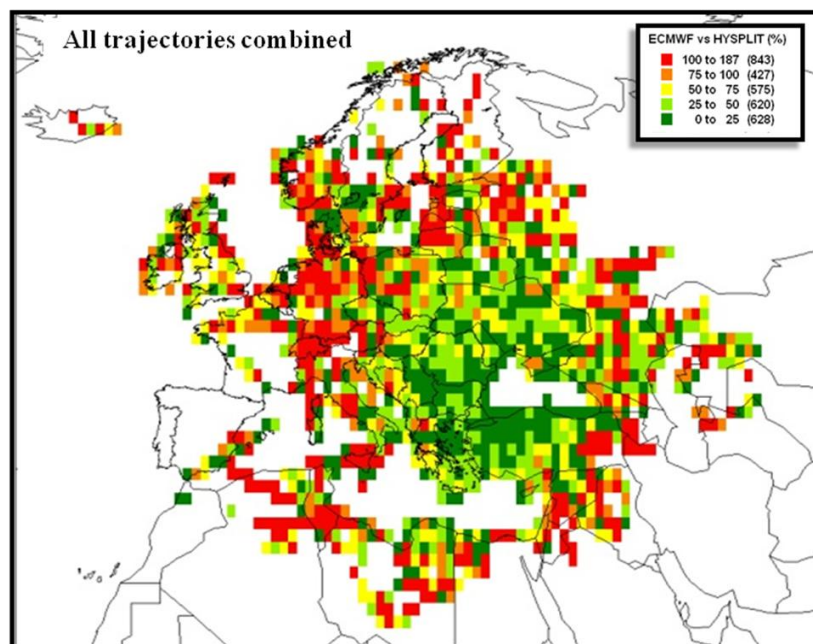


Figure 4.7 Distribution of percent difference, between the PSCF values for SO_4^{2-} obtained from ECMWF and HYSPLIT trajectories (Trajectories from all starting altitudes are combined)

The PSCF calculated from trajectories computed by ECMWF and HYSPLIT at three different starting altitudes are given in Figure 4.8 and percent differences at each grid are also depicted in Figure 4.9. The conclusions reached from combined trajectories in the previous paragraphs do not change significantly in these figures. Agreement between the source regions apportioned by the two models becomes worse with distance from the receptor. There is no obvious difference in the agreements in PSCF values with different trajectory starting altitude.

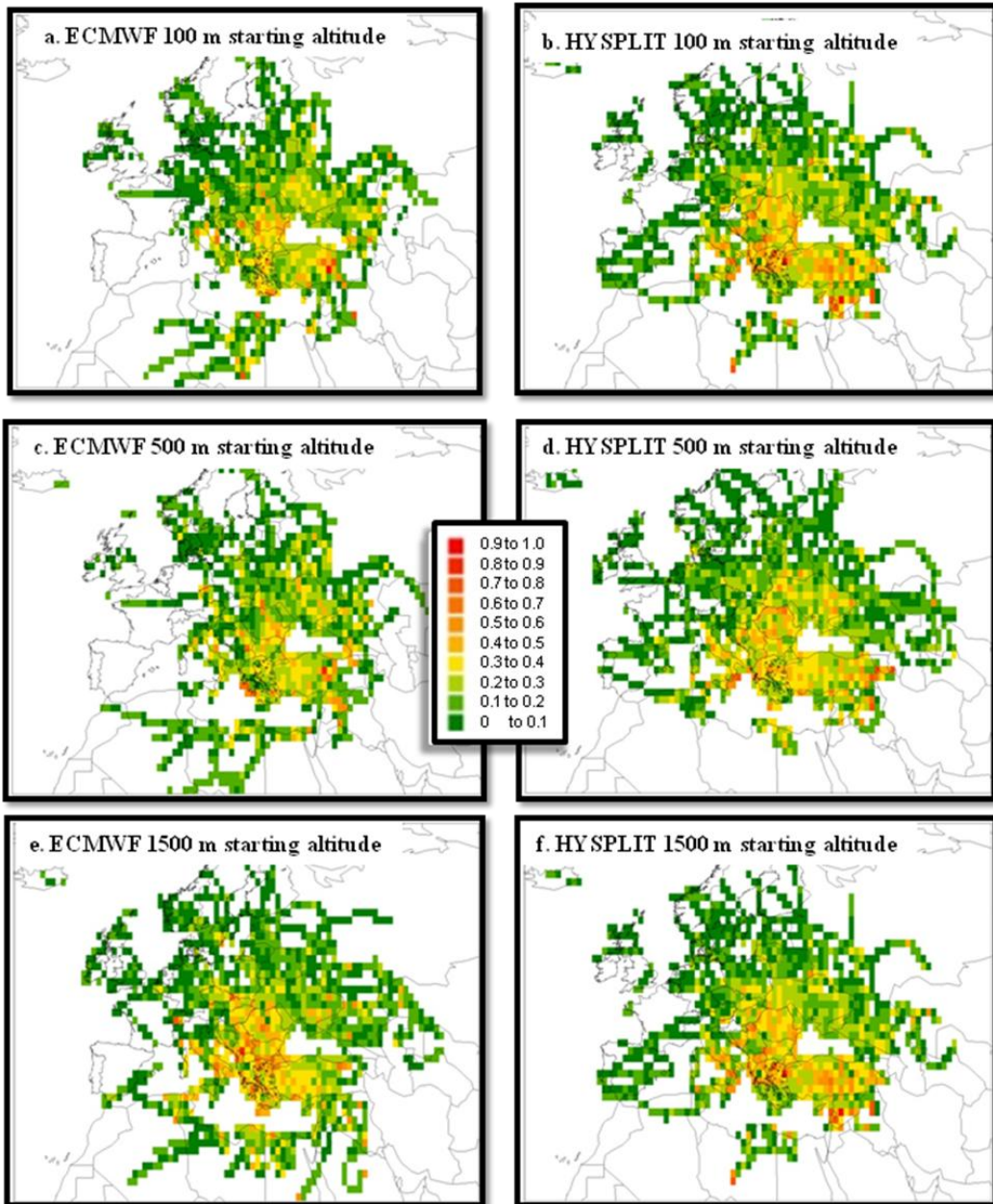


Figure 4.8 Distribution of PSCF values in the study domain at different trajectory starting altitudes

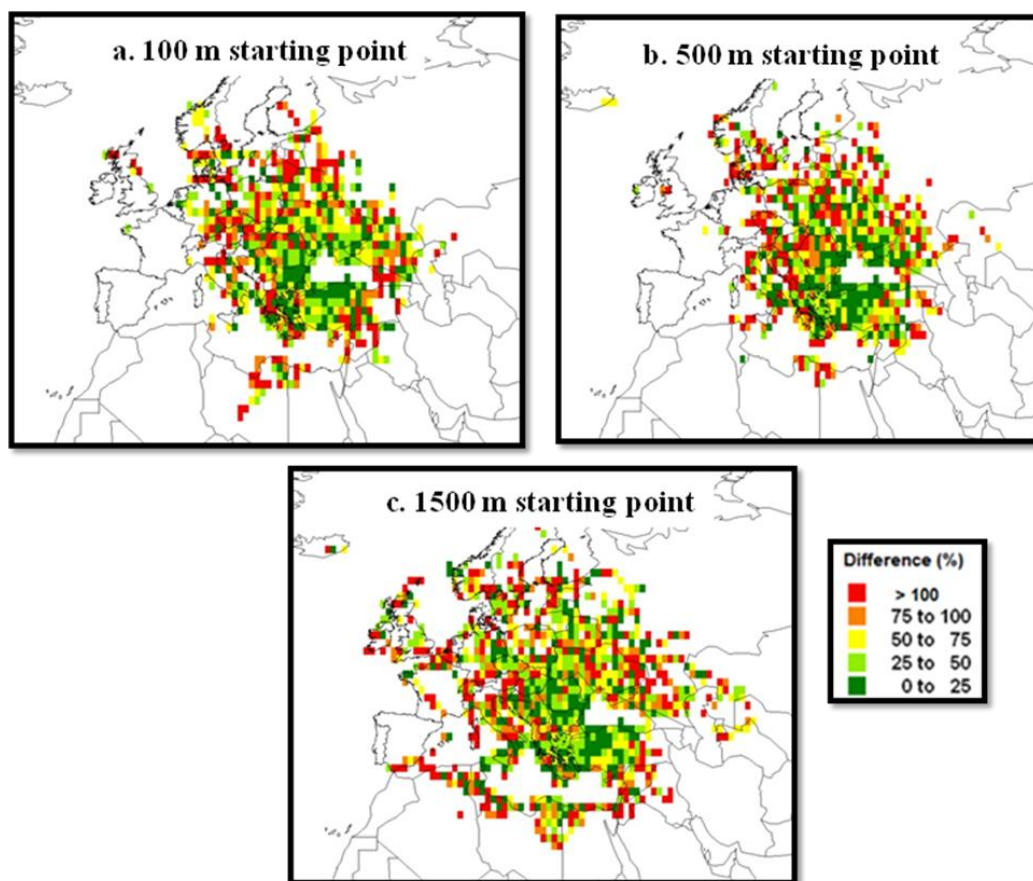


Figure 4.9 Distribution of percent difference, between the PSCF values for SO_4^{2-} obtained from ECMWF and HYSPLIT trajectories

The following points can be highlighted as a conclusion of the model comparison part of this study:

Both trajectory models have certain amount of uncertainty. It is well documented that these model-related uncertainties increase with distance from the receptor (Harris et al., 2005; Baumann and Stohl, 1997; Du et al., 1994; Kahl et al., 1989; Haagenson et al., 1987). Uncertainty associated with methods used in trajectory statistics largely arises from these model uncertainties. In these sections, the two models have been compared thoroughly to determine to what extent they can be used in trajectory statistics. The two model used in this comparison, namely ECMWF and HYSPLIT are very well tested and reliably used in many studies. The

objective was not to assess the deficiencies of these models, but to find the regions in our study domain, where trajectories produced by these two models agrees with each other, as these are the regions where sources can be apportioned with relatively low uncertainties. The areas where these two model products do not agree with each other are the areas where source apportionment (both with numerical modeling and receptor modeling) will have higher uncertainty.

The outcome of this comparison demonstrated that the trajectories calculated with these two models resulted in comparable air mass residence times around the station, but agreement degrades with distance from the receptor. This good-agreement-area includes Turkey, Balkan countries, Ukraine, part of Russia. In these regions the difference in number of trajectory segments generated by the two models are less than 50%. The agreement between the air mass residence times calculated by the two models were moderate (percent difference between number of segments from the two models is between 0%-100%) in countries at the central Europe, such as Czech Republic, Austria, Poland, Belarus and parts of Russia. The agreement was poor (the difference between the segments generated by two models is $> 100\%$ in countries at the peripherals of the European Continent, namely Germany, France, Spain, Portugal, UK, Scandinavian countries and large part of Russia and most of the countries located to the south of Turkey. This distribution agreement between the two model results is probably, at least partly, due to fewer segments generated at the outer parts of the study domain.

It is interesting to note that the so-called good-agreement-area is not uniformly distributed around the receptor. It is elongated in SE – NW direction and it can roughly be defined as ellipse, which is centered not at the receptor, but to the north of the Çubuk station.

Comparison of model products at different starting trajectory altitudes did not show large differences at different starting altitudes. Longer air mass residence times at longer distances are observed at 1500 m starting altitudes of trajectories, but the

difference was not dramatically different than results obtained from 500 and 100 m starting altitudes.

In the last step of comparison, distribution of PSCF values calculated using trajectories computed with both models were compared. As expected, the grid-based differences in PSCF values was very similar to the grid-based differences in residence times, indicating that the uncertainty in trajectory statistics is determined by the uncertainties in trajectory model outputs.

Since the starting altitude of trajectories did not show expected differences in good-, moderate- and poor-agreement regions in the study domain, the use of combined trajectories (trajectories at all starting altitudes) can be recommended in trajectory statistics. The reason is, combining trajectories results in larger number of segments in most of the grids and thus decreases the uncertainties arising from counting statistics. This would not be warranted if there were clear differences between the results of PSCF at different starting altitudes.

4.2. Assigning Potential Source Areas Based on Emission Inventories and Transport Patterns (Regions of Influence-RoI)

In this part of the study, results of source oriented approach which is developed for this study is discussed. The method developed and called as “Regions of Influence (RoI)” is a qualitative source oriented approach that generates information on potential source areas that affect concentrations of pollutants at a given receptor. The method developed here, is not an alternative to numerical models because, it does not produce quantitative information on pollutant concentrations at the receptor, but generate qualitative information on the potential source areas that can affect measured concentrations of pollutants at a receptor location, which is an information comparable to that generated with trajectory statistics.

The objective was to develop a source oriented method that can generate potential source areas using very few and simple input data, so that it can be used as a preliminary information in every laboratory, particularly in research groups where expertise for running sophisticated numerical transport and chemical models is not available.

The source regions affecting concentration of a pollutant at a receptor depends on five factors, including (1) emissions at the source region, (2) residence times of air masses, which are intercepted at the receptor, in the source region, (3) meteorology during transport of pollutants between source region and receptor, (4) topography between source and receptor and (5) chemistry during transport. If all these parameters are accurately known, one can calculate concentrations of pollutants, which are emitted from a given source at the receptor. However, such a computation requires sophisticated and expensive models. In RoI approach, only emissions and air mass residence times have been included in the model. The time resolution was taken as longer than 1 yr. Meteorology is indirectly included in computations (as the trajectory computations are based on meteorology). The output of the model is the relative significance of each $1^\circ \times 1^\circ$ grid in our study domain as a source area affecting our receptor.

In this study, RoI calculations were separately performed by using Antalya, Çubuk, Amasra and Corsica stations as receptors. Backtrajectories and SO₂ emissions for the years 1990, 1995, 2000, 2004, 2005, 2006 and with starting altitude of 100, 500, 1500 m were used. The RoI concept is discussed in four subsections, namely, (1) comparison of RoI results with distribution of PSCF values, (2) effect of trajectory starting altitudes on RoI distributions, (3) variation of RoI with time and (4) comparison of RoI distributions calculated for four different receptor locations.

4.2.1. Calculation of Potential Source Areas and Comparison with PSCF Distribution in the Study Domain

In this section RoI that were calculated for Çubuk station are compared with the distribution of PSCF values, again, calculated for the same location. Comparison of RoI results, with an established receptor oriented technique is one way of validating the RoI method. PSCF calculations is proper method to compare with the RoI results, because it is very frequently used in the literature for assessing potential source areas affecting pollutant concentrations at a given receptor (Karaca et al., 2009; Xu and Akhtar, 2009; Doğan et al., 2010; Uygur et al., 2010; Bahadur et al., 2010) and its weaknesses and strengths are well documented (Pekney et al., 2006; Begum et al., 2005)

Regions of Influence were calculated by multiplying emissions in each grid with the air-mass residence times at that particular grid. Emission data were obtained from EMEP website and air-mass residence times were computed by counting number of hourly trajectory segments in each grid in the study domain.

Since the objective in this section is to compare results obtained with distribution of PSCF's at different altitudes, and not to evaluate the RoI of different stations, which will be done later in the manuscript, the RoI, for this comparison, were computed only for the Çubuk station. HYSPLIT trajectories computed for the years 2004, 2005 and 2006 were used in calculations. PSCF calculations were also performed for the same station and for the same years by using these trajectories. Trajectories corresponding to days with the highest 40% of the SO_4^{2-} concentrations were formed the “polluted” trajectory group.

Distributions of RoI and PSCF for the Çubuk site are depicted in Figure 4.10. Trajectories starting at all altitudes are used to generate this Figure.

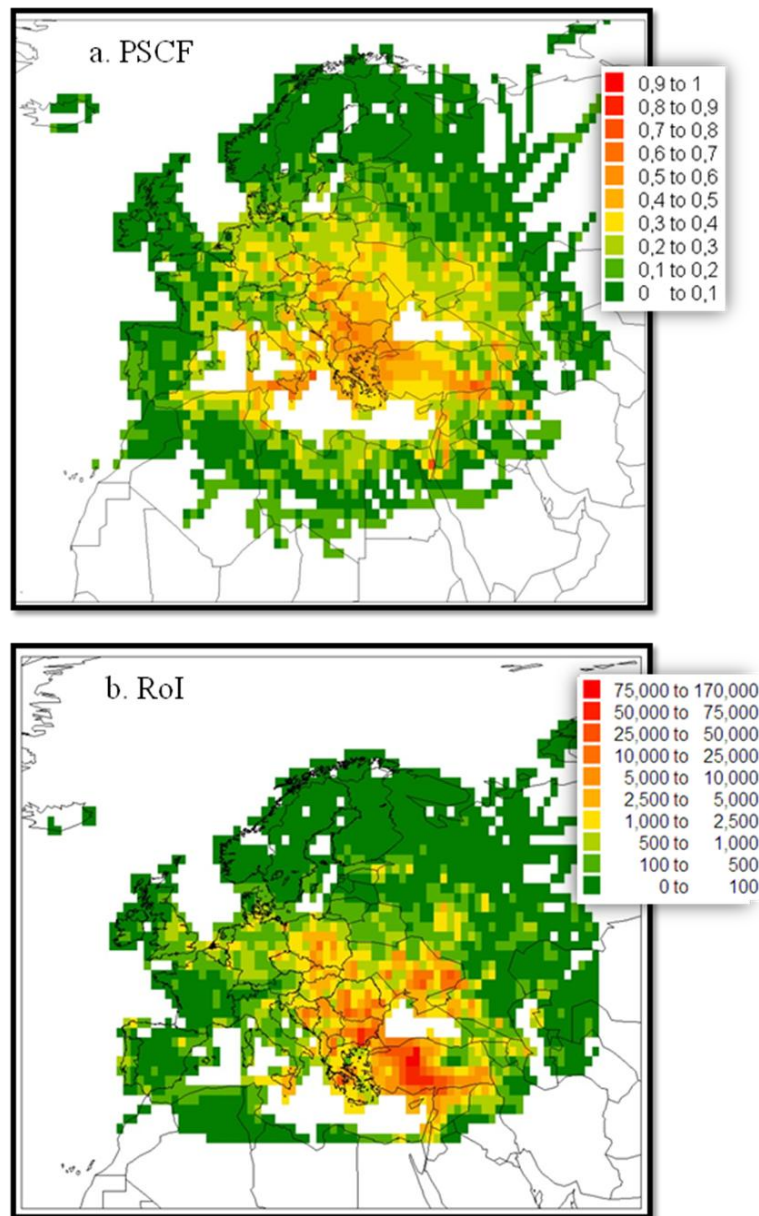


Figure 4.10 Comparison of PSCF and RoI results calculated using combined trajectories for the years 2004, 2005 and 2006 at Çubuk station

The main features in distribution of PSCF values are nicely imitated by the distribution of RoI. There are two important points that must be highlighted in the distribution of PSCF values. The first of these points is that most of the Turkey, Balkan countries and parts of Ukraine are the main source regions affecting SO_4^{2-}

concentrations at Çubuk (Figure 4.10-a). These are also the areas with high RoI index (Figure 4.10-b). The second point that needs to be highlighted in PSCF distributions is that the grids in distant areas, such as Scandinavia, UK, Spain, France and Germany generally have low PSCF values. This feature is also shared by the RoI values.

Another important performance check for both of these methods is to see if they can identify a well known emission source. There are two such well known SO₂ sources in our study domain. One of them is the Mt. Etna Volcano at Sicily, Italy and the second one is the Afşin Elbistan Power Plant at the Southeastern Turkey. Both of these sources are well identified in both PSCF and RoI results

Although the general agreement between the distributions of PSCF and RoI values is good, there are also some disagreements between the results of the two approaches. For example, Poland, which is a country with documented high SO₂ emissions (Kiuila, 2003; Klimont et al., 1994; Veldt, 1991), appears as a significant RoI, as expected. However, PSCF values in most of the grids in Poland are rather low, indicating that the SO₄²⁻ concentrations in samples corresponding to trajectories passing over Poland are not particularly high. A similar high RoI and low PSCF area also appears at the central Ukraine. Although both east and west parts of Ukraine are characterized by high PSCF and RoI values, PSCF values at the central Ukraine have low PSCF values.

These high RoI - low PSCF areas can be explained by the effect of wet particle scavenging. As pointed many times previously in the manuscript, PSCF technique is a receptor oriented technique and bases on measured SO₄²⁻ concentrations. If SO₄²⁻ particles are scavenged by rain on their way to Çubuk, then, naturally, SO₄²⁻ concentration in that sample is low, no matter from where the air mass comes from. And areas with frequent rain appear as low PSCF areas even if the SO₂ emissions are high. However, this rain scavenging is not taken into account in RoI approach.

On the contrary, high PSCF and low RoI values are observed at Southern Italy and North African coast in Figure 4.10. RoI values are low in these areas, because SO₂ emissions are low. These high-PSCF and low-RoI areas cannot be explained by scavenging. However, they are real, because in many studies, including studies performed in our group, high concentrations of anthropogenic species, such as SO₄²⁻, NO₃⁻ and trace elements were observed to be associated with backtrajectories that originate from North Africa (Celle-jeanton et al., 2009; Querol et al., 2009; Liu et al., 2009). This documented transport of anthropogenic species from North Africa is believed to be due to recirculation of air masses that originate from Europe between North Africa and the Mediterranean basin (Kallos et al., 1998; 2007). This recirculation of pollutants between North Africa and Mediterranean gives the impression that there are high-emission areas in the North Africa. These areas are identified as potential source areas in PSCF calculations. However, since concentrations are not taken into account in RoI calculations, the same areas have low RoI values.

4.2.2. Effect of Trajectory Starting Altitude on RoI Distribution

In the previous discussion, RoI (and also PSCF) were calculated using combined trajectories from all starting altitudes. In this section, on the other hand, the influence of starting altitudes of trajectories on RoI distribution is discussed. In this exercise, trajectories with starting altitudes 100 m, 500 m and 1500 m calculated in this case for the Antalya station, in the years 1990, 1995 and 2000 are used. Results of RoI calculations are depicted in Figure 4.11.

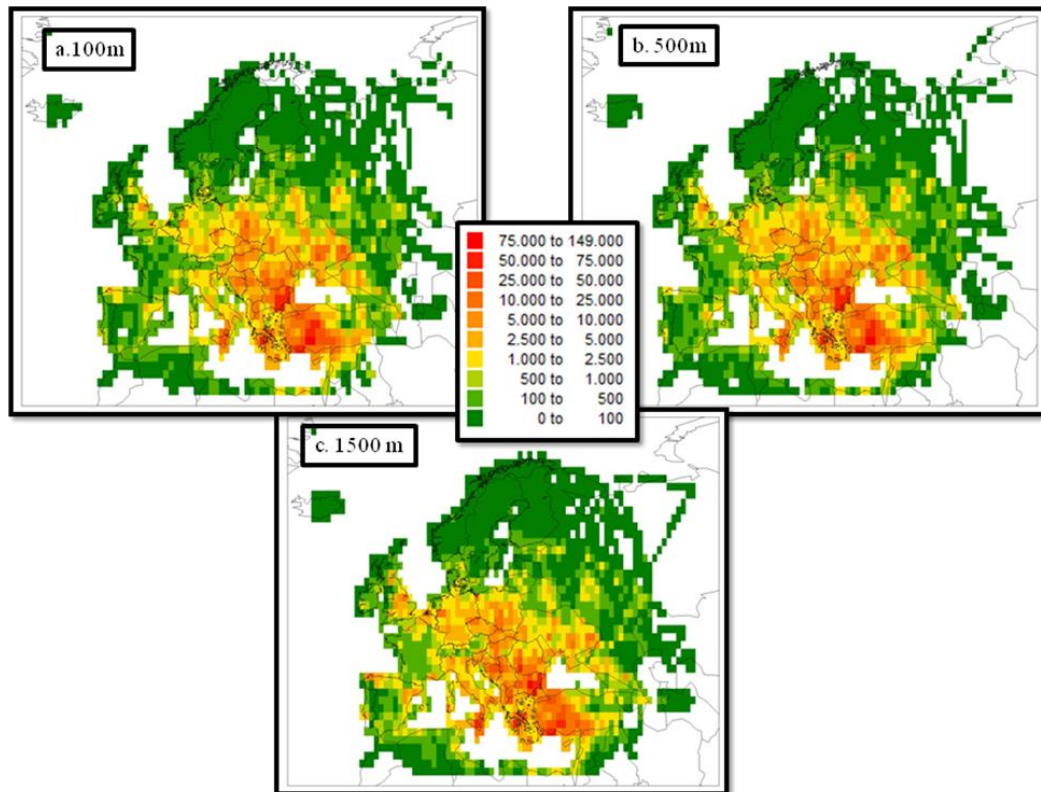


Figure 4.11 Regions of Influence calculated for Antalya station for each trajectory starting altitudes

Since gridded emissions do not change with starting altitude, differences between RoI distributions for different starting altitude is due to variations in air mass residence times as a function altitude. Figure 4.11 demonstrates that differences in RoI distributions between trajectories with different starting altitudes are not very much, particularly in the areas with closer distance to the receptor. However, there are slight differences in the outer parts of the study domain. For example, there are some additional high RoI grids in Spain, Tunisia and Morocco in when RoI calculations are based on 1500 m starting altitude (Figure 4.11-c). Grids in the Middle East, Turkey and most of the Europe have fairly similar distribution of RoI at all starting altitudes. This observation, suggests that the use of combined trajectories (trajectories starting at all altitudes) can be a proper approach in RoI

calculations, as combining all trajectories increases the number of segments in each grid, thus increasing statistical significance of results.

4.2.3. Variation of Regions of Influence with Time

The SO₂ emissions in Europe decreased steadily in last 20 years. Approximately 75 – 80% reductions in SO₂ emissions were reported in different parts of the Western Europe. Since the RoI calculations are based on SO₂ emissions and air mass residence times and since in previous sections it was demonstrated that air mass residence times did not change with time, then any change in RoI should be due to reductions in SO₂ emissions and should reflect the change in source regions affecting Turkey and Eastern Mediterranean regions. In other words, with changes in SO₂ emissions in Europe the areas that affect receptors are expected to change in time and source areas affecting SO₄²⁻ concentrations in 1990 is expected to be different from the source areas affecting SO₄²⁻ at the same site in the year 2000.

This variation of source areas in time is demonstrated for Antalya station in Figure 4.12. RoI calculations were performed for the years 1990, 1995 and 2000 using EMEP emission data for each of these years. Backtrajectories calculated for the years 1990, 1995 and 2000 are used in calculations and trajectories with all starting altitudes are included in computations.

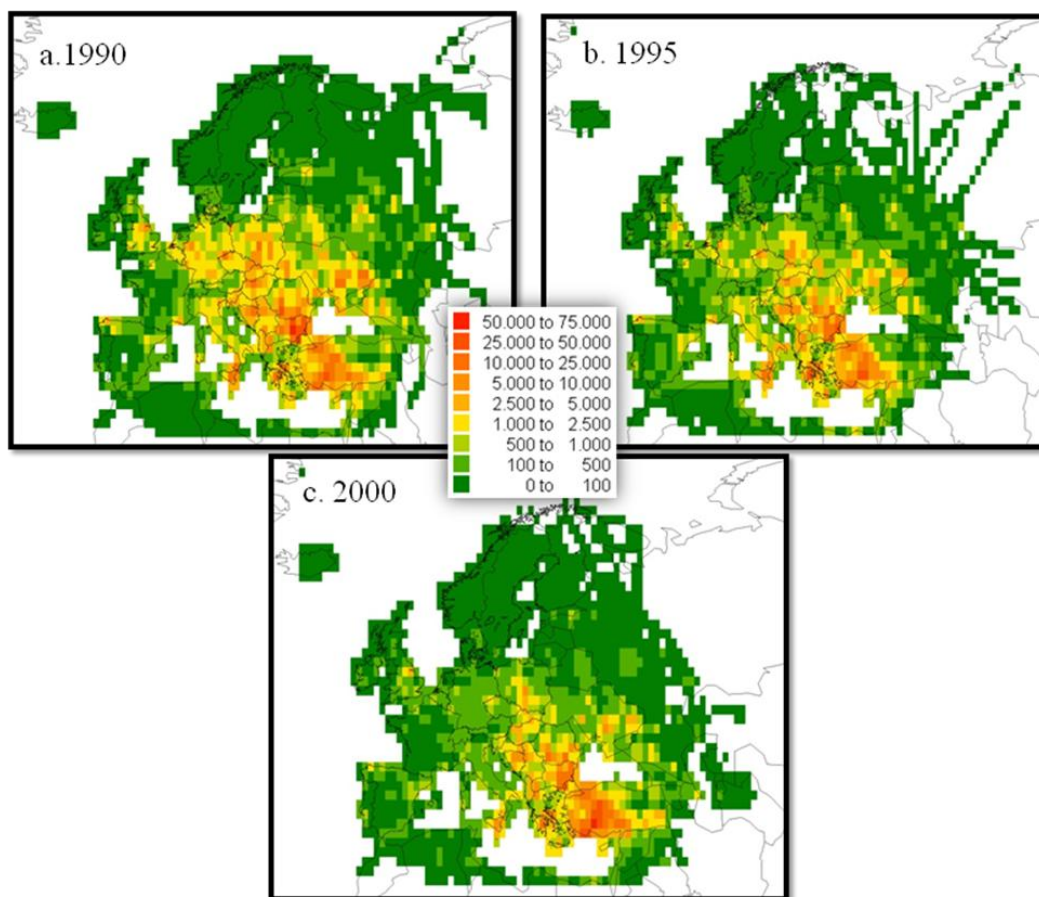


Figure 4.12 Variation in the distribution of regions of influence calculated for Antalya station between 1990 and 2000

Changes in potential source areas affecting SO₄²⁻ concentration Antalya station is very clear in the Figure 4.12. In the year 1990 (Figure 4.12-a), SO₄²⁻ concentrations in Antalya are affected from source areas in Turkey and Balkan countries, Italy, Central European countries such as Czech Republic, Slovakia, Belarus, Poland and Germany and Ukraine. Countries such as France Spain and northern parts of Russia are not expected to contribute significantly to measured SO₄²⁻ concentrations at Antalya.

In the year 1995 (Figure 4.12-b), Western part of Turkey, Balkan countries and Italy are still the most important source regions. But Germany and central European countries turned out to be less important sources of SO_4^{2-} concentrations at Antalya. Poland is still a source, but number of grids with high RoI values in Poland decreased. The same situation is also true for Ukraine. It is still a source, but not as important source as it was in 1990.

In the year 2000 (Figure 4.12-c), the significance of western European sources decreased observably, due to reductions in their emissions. The important source regions for observed SO_4^{2-} levels in at Antalya are confined to Western Turkey, Afşin Elbistan Thermal Plant, Balkan countries including Bulgaria, Romania Greece, Serbia and Montenegro and Croatia, Eastern Parts of Ukraine, Czech Republic and central parts of Poland, Regions which appeared as potential source areas in earlier years, such as Germany, UK, Italy, western parts of Ukraine and central parts of Russia are no longer important source areas for SO_4^{2-} concentrations at Antalya in the year 2000.

This discussion demonstrated that the source areas affecting pollutant concentrations in different parts of Mediterranean basin have changed significantly between 1990 and 2000. In general, the potential source areas in Turkey and Balkan countries remained the same, but the source regions in Western European countries, which were important in 1990, lost their strengths completely in the year 2000.

4.2.4. Comparison of the Potential Source Areas Affecting Eastern and Western Mediterranean Basins

Similarities and differences in potential source areas (high RoI areas) affecting SO_4^{2-} concentrations at Antalya, Çubuk, Amasra and Corsica stations are investigated. Because such a comparison can provide, not only, a general idea on the source region affecting different locations in Turkey, Eastern Mediterranean and Western Mediterranean, but also explain differences in chemical composition of particles at different locations in the Mediterranean basin.

Since it was demonstrated in previous sections for Antalya station, that RoI values changed in time and source regions that are effective in 1990 may not necessarily represent the situation in 2000, comparison was made separately for the years 1990, 1995 and 2000. Trajectories calculated by HYSPLIT were used and trajectories with different starting altitudes were combined to improve statistical significance of results. The distributions of RoI for Antalya, Amasra, Çubuk and Corsica stations in the year 1990 are depicted in Figure 4.13 – a, b, c, and d respectively.

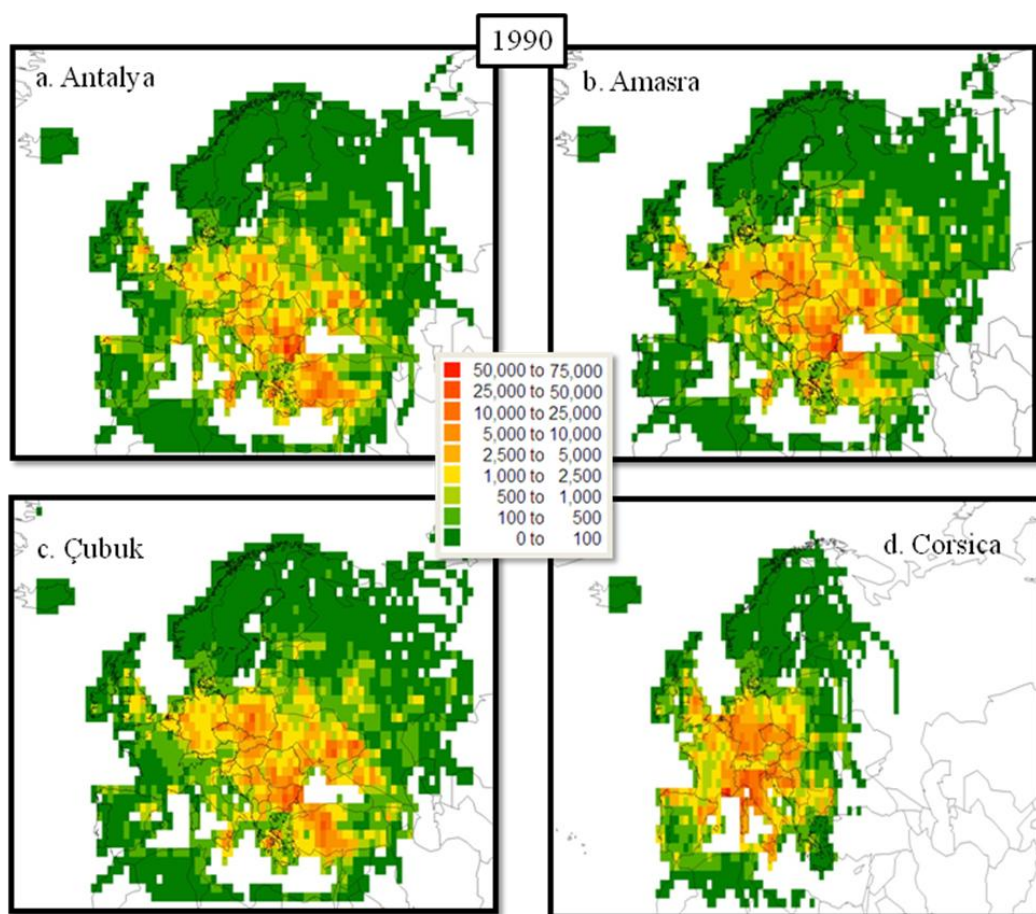


Figure 4.13 Variation in the distribution of regions of influence between different stations in the year 1990

For Antalya, Çubuk and Amasra, high RoI areas in the year 1990 resemble to each other with minor differences between them (Figure 4.13-a, b, c). However, distribution of high RoI areas for the Corsica Station is totally different (Figure 4.13-d). This explains different chemical compositions of particles at Eastern and Western Mediterranean basin, which was reported frequently in the literature.

For stations in the eastern Mediterranean basin (Antalya, Çubuk and Amasra), potential source areas in the year 1990 is distributed in whole Europe, except for France, Spain and Scandinavian countries. Since emissions were high throughout the Europe in 1990, this distribution is determined by distribution of air-mass residence time rather than lack of SO₂ emissions in France, Spain, Norway, Sweden and Finland.

Although general appearance of RoI distributions is similar for these three receptors, there are some differences in detail. For example, Antalya station is less influenced in sources in Ukraine and Central Russia, compared to Çubuk and Amasra stations. On the other hand, the effect of source regions in Italy and western Balkan countries on SO₄²⁻ data at the Amasra and Çubuk stations are not as much as their influence on Antalya station.

The differences in RoI affecting Amasra (Black Sea), Antalya (Eastern Mediterranean) and Çubuk (Central Anatolia) stations are not much and it can be concluded that these three stations are affected from the same anthropogenic source regions which are distributed throughout the Europe in the year 1990.

The RoI that affect SO₄²⁻ concentrations at western Mediterranean basin (Corsica) are substantially different. Corsica station is strongly influenced from SO₂ emissions in most of the Western Europe, but not influenced from emissions in Balkan Countries, Turkey, Ukraine and Russia.

This difference in RoI calculated for Eastern and Western Mediterranean Sea clearly suggests that chemical composition of atmospheric particles in these two basins is significantly different from each other. Like concentrations, the trends in pollutant concentrations are also expected to be different. Corsica station is affected much more strongly from emissions in Western Europe. Consequently measured concentrations of pollutants in this site are expected to demonstrate similar trends with the trends in pollutant emissions in Western part of Europe. However, emissions in Balkan countries, Ukraine, Turkey and Russia have stronger influence on measured pollutant concentrations in Eastern Mediterranean. Since decrease in pollutant emissions in these regions are not as significant as the emissions in Western Europe, then the decrease in concentrations of pollutants measured in Eastern Mediterranean basin are not expected to be as significant as the decrease in Western Mediterranean basin. There is not much data on the trends of pollutants in the western part of basin. Migon et al. (2008) demonstrated a rapid drop in Pb concentrations in the Western Mediterranean, which is correlated by phasing out of Pb from gasoline in Western European countries. On the contrary, SO_4^{2-} concentrations in the Eastern Mediterranean and Central Anatolia did not show a significant decrease between 1992 and 2000 (Işıkdemir, 2006; Tuncer et al., 2001; Yörük, 2004).

Distribution of calculated RoI values for Antalya, Amasra, Çubuk and Corsica for the years 1995 and 2000 are given in Figures 4.14 and 4.15 respectively. It is clear from these figures that the influence of distant sources, particularly those in the western part of Europe, SO_4^{2-} concentrations at three stations on the Eastern Mediterranean became less and less important in time due to continuous reduction in SO_2 emissions, particularly after the “Second Sulfur Protocol”, which became effective in 1994 (Vestreng et al., 2007b).

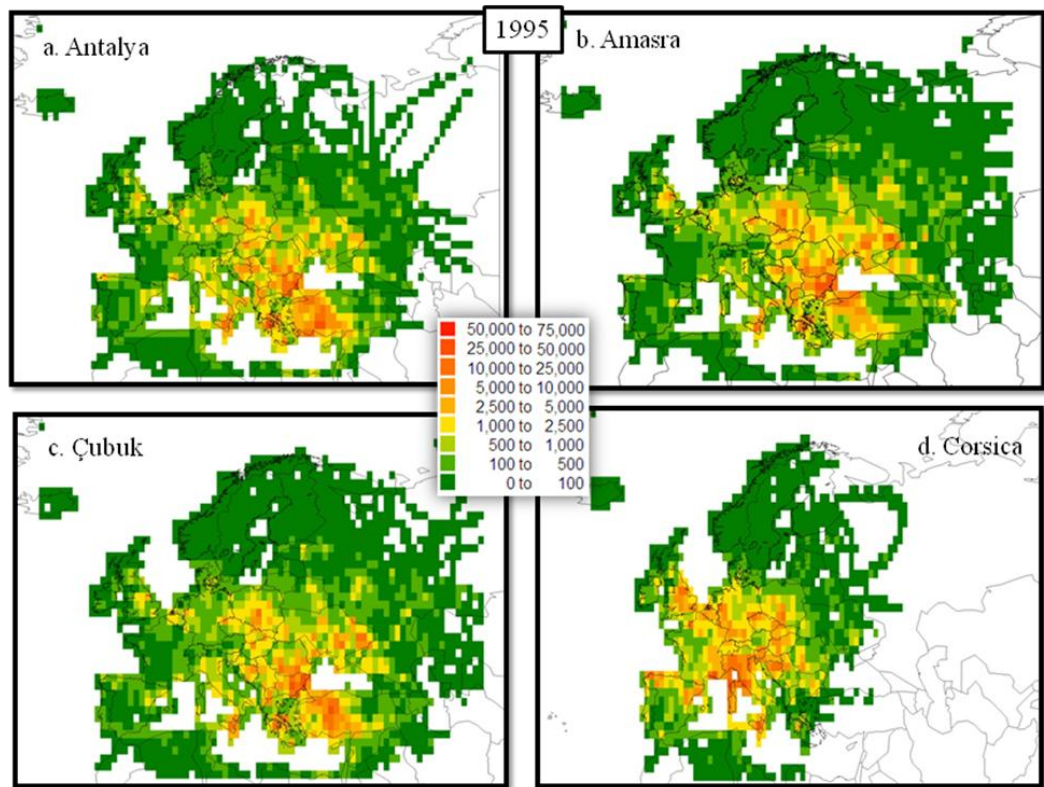


Figure 4.14 Variation in the distribution of regions of influence between different stations in the year 1995

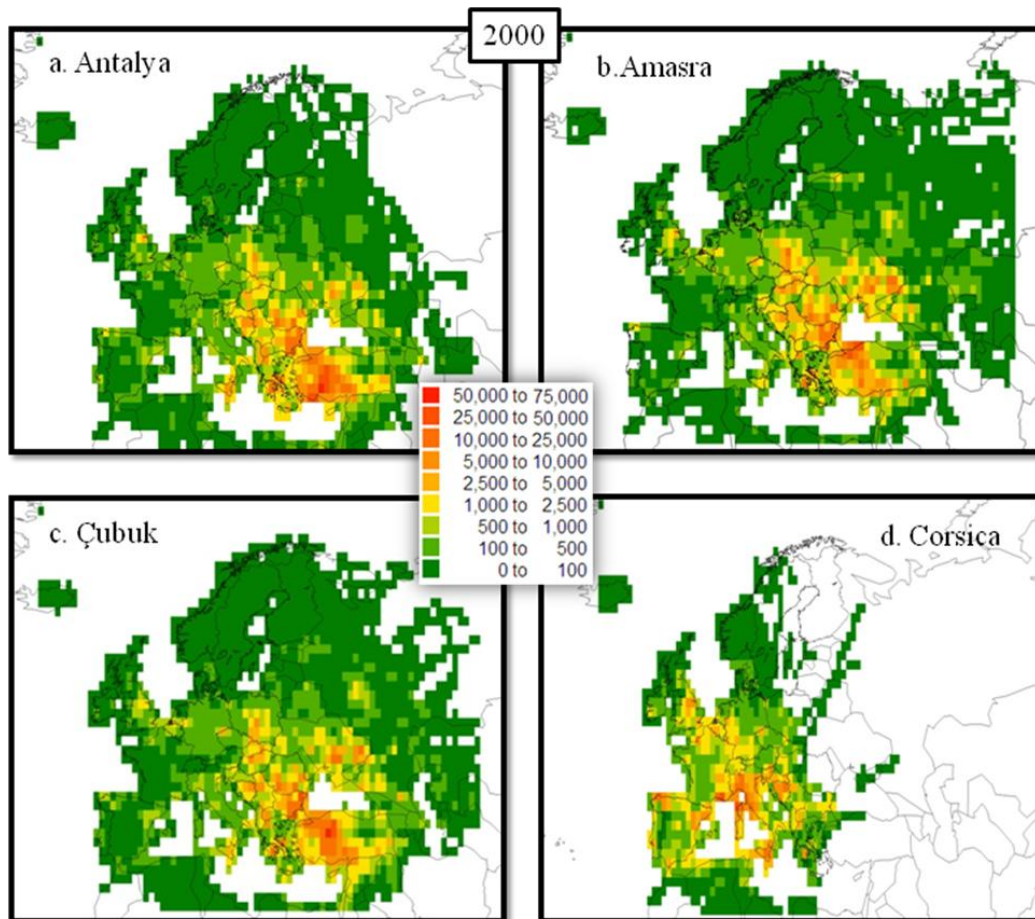


Figure 4.15 Variation in the distribution of regions of influence between different stations in the year 2000

The main source areas affecting these three stations in Turkey were western parts of Turkey, Balkan countries, including Bulgaria, Romania, Greece, Serbia, Bosnia Herzegovina, Slovakia, Poland, Ukraine and Russia. Germany and UK ceased to be important source areas for the Eastern Mediterranean in 1995 (Figure 4.14), Russia and Poland are still source areas, but they are not as important as they were in 1990 (Figure 4.13). In the year 2000, potential source areas affecting SO_4^{2-} concentration at the Eastern Mediterranean shrink even further (Figure 4.15). For example Italy, which is fairly close to receptors at the Eastern Mediterranean, is no longer an important source for any of the three receptors selected for this study. Basically

western parts of Turkey, Bulgaria, Romania, southern parts of Poland and Ukraine are the most important potential regions for the Eastern Mediterranean basin.

The differences in high RoI areas affecting Antalya, Çubuk and Amasra stations, which was previously discussed for the year 1990 (Figure 4.13-a, b, c) continued in the years 1995 (Figure 4.14-a, b, c) and 2000 (Figure 4.15-a, b, c). For example, Ukraine and Poland are less important source regions for Antalya than they are for Çubuk and Amasra in both 1995 and 2000. Italy and Greece, on the other hand, are less significant source regions for Amasra and Çubuk than they are for Antalya.

The variation in source regions was different for Corsica. In 1990 (Figure 4.13-d), areas that affected Corsica were in Western European countries, such as France and Germany, due to close proximity of the receptor to those emission areas. In 1995 (Figure 4.14-d), the influence of emission areas in France decreased significantly. Contributions of emissions in Germany also decreased compared to their contributions in 1990, but Germany continued to be an important RoI for Corsica station. Contributions of Central European countries and Poland did not change much in 1995 compared to their contributions in 1990. In the year 2000 (Figure 4.15-d), contributions of France, Germany and Poland on SO_4^{2-} concentrations measured in Corsica decreased further and they became insignificant source areas for the Western Mediterranean basin. The most important source region for the Western Mediterranean in 2000 is the Northern Italy, due to close proximity of emissions in Northern Italy to Corsica. In addition to Northern Italy, Serbia and some grids in Germany and Southern UK also contribute to SO_4^{2-} concentrations in Western Mediterranean basin.

4.3. Inclusion of Segment Height and Rain Amount in PSCF Calculations

PSCF is receptor-oriented method that uses chemical measurements of pollutants at the receptor site and meteorological information. Therefore, it combines flow frequency with the measured elemental composition of the region. As pointed out in previous sections, it is very widely used to assess source areas affecting pollutant

concentrations at a particular receptor. The concept of PSCF was introduced to identify geographical regions that may have a higher probability of being source areas of pollutants like sulfate in the study area. It is assumed that pollutants emitted within a grid cell are swept into the air parcel and transported to the receptor site without loss through diffusion, chemical transformation or atmospheric scavenging (Cheng et al., 1993; Lupu and Maenhaut, 2002). These assumptions make calculations easier but at the same time the reliability of the model will be loosened and uncertainties increased. In real situation, air parcels at different heights passing through a pollution source does not collect pollutants at the same amount i.e. air parcel close to the surface have higher probability of picking up of pollutants than air parcels that are far from surface. An occasional rain on the air parcel's trajectory could wash out the pollutant carried by the air parcel that will contribute inaccuracy of the PSCF results.

In this part of the study, it is tried to reduce the uncertainties in PSCF calculations, by weighting the segments based on their heights and on the presence or absence of precipitation at the coordinates of segments.

4.3.1. The Effect of Precipitation on PSCF Calculations

In PSCF calculations, rain or other forms of precipitation are not taken into account. It is assumed that pollutants that are picked up by air parcel at the emission point are transported to the receptor without dry or wet deposition. The “no-dry deposition” assumption does not pose a serious error, because dry deposition removes a certain fraction of pollutants and likelihood of dry deposition decreases substantially when pollutants gets away from the surface. Because of these factors, dry deposition cannot erase emission signatures from a trajectory. However, wet deposition is not like that. When an air parcel passes through a precipitation event, more than 90% of the pollutants are washed into the cloud or rain droplets, thus totally erasing emission information carried by that trajectory. If such a precipitation scavenging occurs, an air parcel, which passed through a very heavy emission area and loaded with pollutants can lose all its pollutants and may appear

as a clean trajectory at the receptor. It should also be noted that an air mass trajectory can pass through several precipitation events between the source and receptor. The precipitation scavenging does not render PSCF results totally meaningless, because PSCF calculations are based on information carried by hundreds of trajectories over a period of at least a year. In one year period, loss of source information from trajectories through precipitation scavenging occurs in some of the trajectories passing through a source grid, not in all them. The net result is decrease in PSCF values in grids. If this effect of scavenging would occur homogeneously in the study domain, the PSCF distribution would be flue but correct. However, effect of precipitation can be more pronounced in certain directions and increases with distance, which results in underweighting source areas in certain regions relative to others.

In this part of the study, rain information is attempted to be included into PSCF calculations. Assuming that backtrajectory information is included in the each segment endpoint of the backtrajectory, if the pollutants are washed out by sufficient amount of precipitation in some part of the trajectory, the assumption of transport of the pollutants without loss does not hold anymore and the probability of the locations before that point on the trajectory being a potential pollution source vanishes. Therefore it is logical to remove the trajectory segments before the point where rain occurs. This logic was applied to all the trajectories, which were used in PSCF calculations performed for Çubuk Station and for the years 2004, 2005 and 2006.

Rain information at the coordinates of each trajectory segment was requested within the HYSPLIT backtrajectory data. For each polluted trajectory, precipitation amounts were checked backwardly on time. Trajectory segments before the first existence of the “predefined amount of precipitation”, were excluded from the calculation of $m_{i,j}$ and $n_{i,j}$ values resulting a weighting of the PSCF values across rain occurrence.

The most difficult part of the study was to decide on the “predefined amount of precipitation”, which is actually weighting each trajectory segment based on the amount of precipitation associated with it. Since there is no scientifically sound quantitative relation between the rainfall and amount of pollutants scavenged, different weighting factors were applied. The results, which were weighted with 1 mm, 0.8 mm, 0.5 mm, 0.3 mm, 0.2 mm and 0.1 mm rain, are given in Figures 4.16 to 4.21. In each figure there are three distributions, including (a) distribution of PSCF values without any rain weighting. These figures (a) are the same in all figures between 4.16 and 4.21. It is repeatedly added to these figures to facilitate comparison with weighted distribution in the same figure. The second distributions (b) are the distributions of PSCF values when they are weighted with the certain mm of rain. The term “weighting” in this case refers to the threshold rainfall associated with each segment. For each trajectory in the polluted and unpolluted data sets used in PSCF calculations, this threshold rainfall is searched starting from the arrival time of the trajectory to the receptor. When this threshold rainfall is found (closest to the receptor), all the segments before that particular segment (all segments farther away, in time, from the receptor) are deleted from both polluted and unpolluted trajectory sets, because all the source information carried by the trajectory is lost when it passed through a rain. This is repeated for all the trajectories and after removal of segments influenced from rain, what is left behind (and what is used in PSCF calculations) is the trajectories that are not washed out by the rain events. The distributions (c) in each of these figures are the percent change between weighted and un-weighted PSCF values in each grid (Eq. 4.2).

$$\% \text{ change} = \frac{|x_2 - x_1|}{x_1} \times 100 \quad (4.2)$$

In Eq. (4.2), x_1 is the un-weighted PSCF value in the grid cell) and x_2 is rain weighted PSCF value. Different from percent difference formula used in previous sections, this formula was used in weighting part because the change from un-weighted values wanted to be observed or quantified. The percent change values were calculated for grid cells having un-weighted PSCF values only.

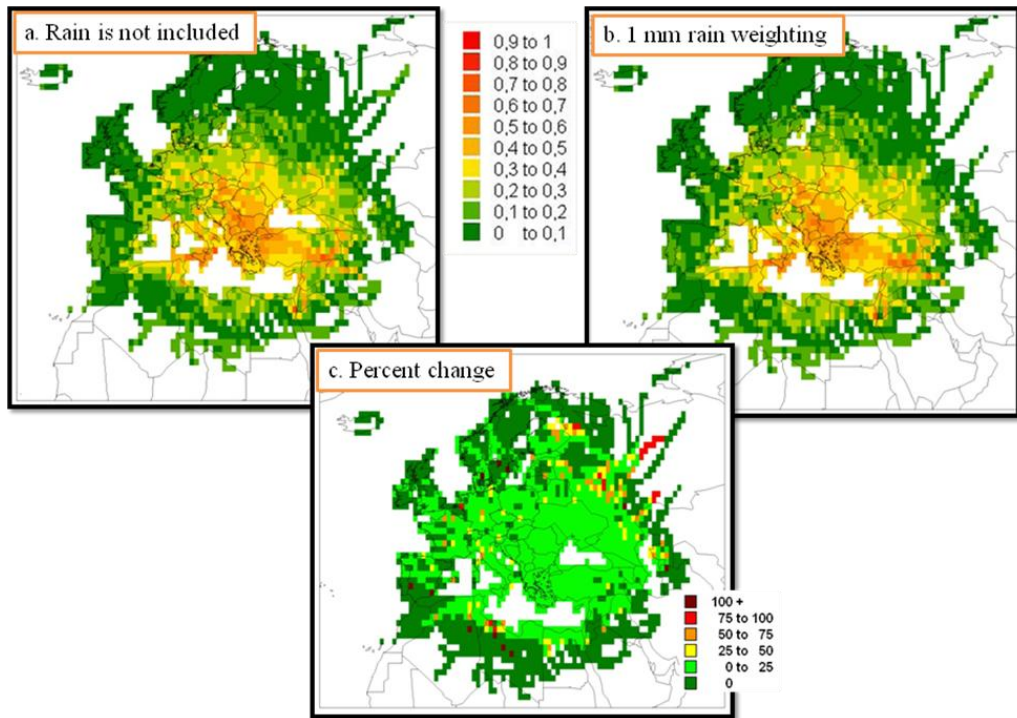


Figure 4.16 Distribution of PSCF values for %40 highest SO_4^{2-} calculated for Çubuk Station for the years 2004-2006 (Rain threshold is 1 mm)

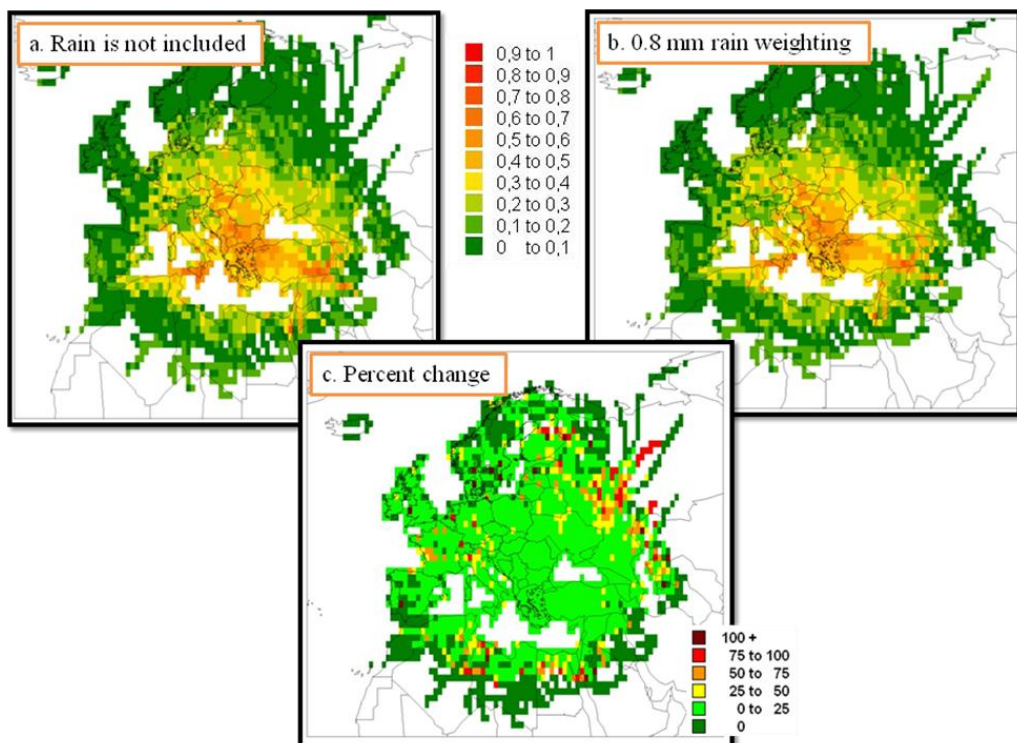


Figure 4.17 Distribution of PSCF values for %40 highest SO_4^{2-} calculated for Çubuk Station for the years 2004-2006 (Rain threshold is 0.8 mm)

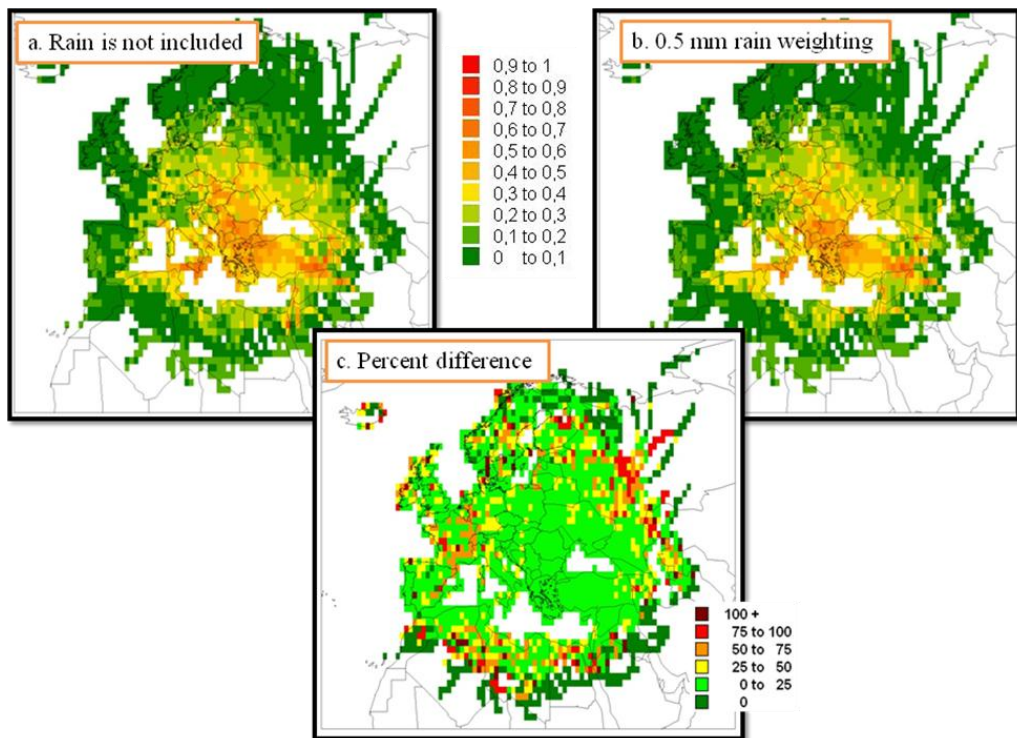


Figure 4.18 Distribution of PSCF values for 40% highest SO_4^{2-} calculated for Çubuk Station for the years 2004-2006 (Rain threshold is 0.5 mm)

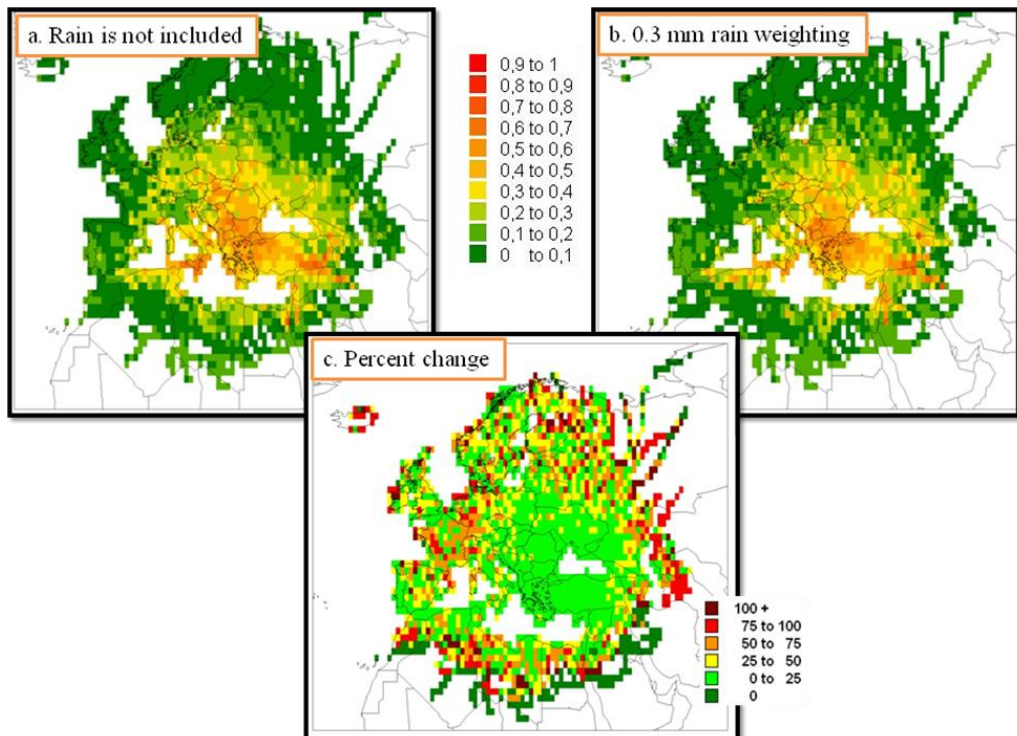


Figure 4.19 Distribution of PSCF values for %40 highest SO_4^{2-} calculated for Çubuk Station for the years 2004-2006 (Rain threshold is 0.3 mm)

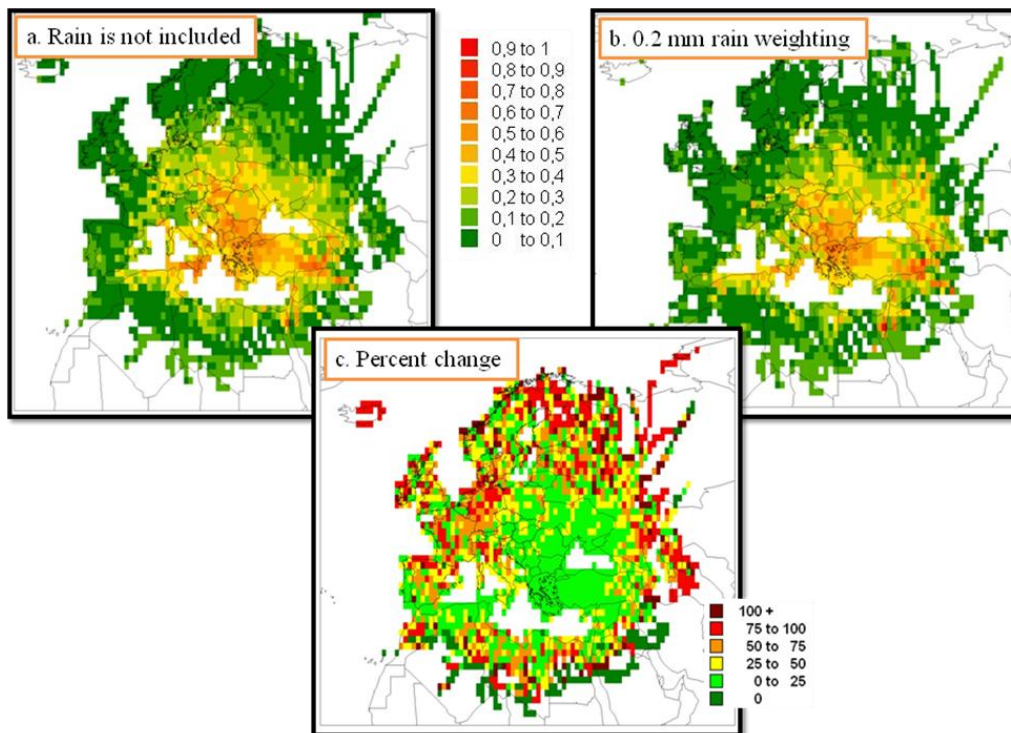


Figure 4.20 Distribution of PSCF values for %40 highest SO_4^{2-} calculated for Çubuk Station for the years 2004-2006 (Rain threshold is 0.2 mm)

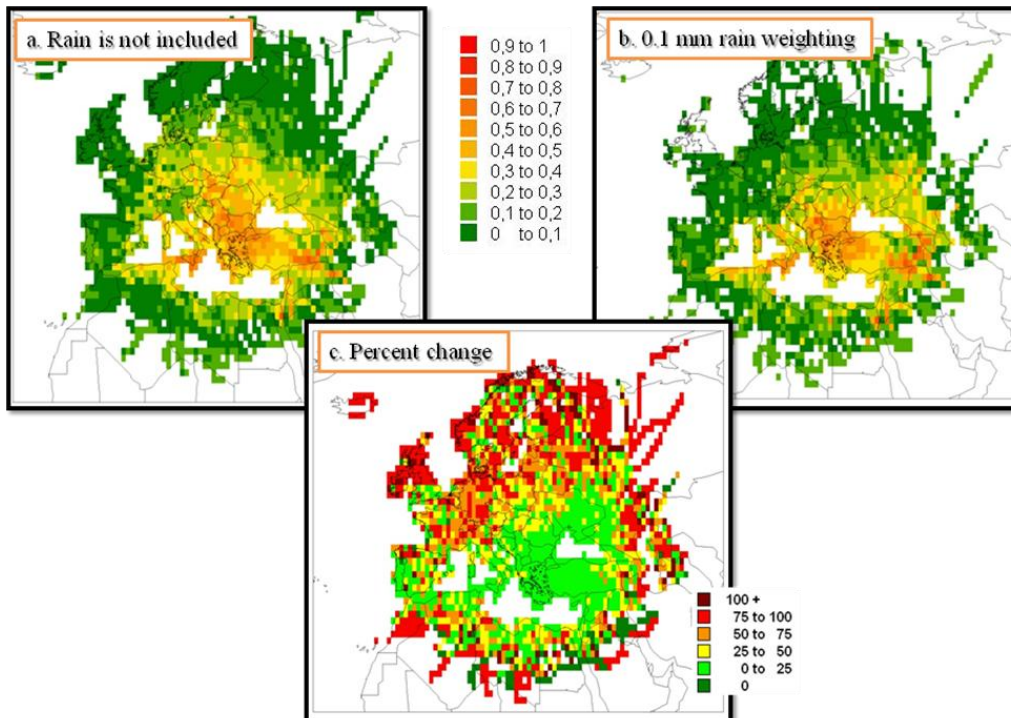


Figure 4.21 Distribution of PSCF values for %40 highest SO_4^{2-} calculated for Çubuk Station for the years 2004-2006 (Rain threshold is 0.1 mm)

The change between weighted and un-weighted PSCF distributions is not very different for threshold values of 1 mm and 0.8 mm rainfall (Figures 4.16 and 4.17). There are differences in some grids but these are very few to change the conclusions in the PSCF calculation. However, some visible changes can be observed starting with 0.5 mm threshold value (Figure 4.18). France and Spain are no longer strong potential source regions for SO_4^{2-} concentrations at Çubuk. The Figure 4.18-c demonstrate that most notable differences between weighted and un-weighted distributions occur at the north, and interestingly at the south ends of the study domain with 0.5 mm threshold.

The difference between weighted and un-weighted distributions of PSCF values became more pronounced when 0.3 mm, 0.2 and 0.1 mm thresholds are used (Figures 4.19, 4.20 and 4.21 respectively). With 0.3 mm rain threshold, countries such as Germany, France, and Poland are no longer important source regions for SO_4^{2-} concentrations at Central Anatolia. When 0.2 mm is used as threshold value, distribution is fairly similar to the distribution obtained when 0.3 mm was used as threshold, but larger differences between weighted and un-weighted distributions were observed, particularly in Scandinavian countries, Germany, Poland and at central parts of Russia. When 0.1 mm rain was used as threshold value, contribution of grids at the fringes of the study domain totally disappeared.

There are few interesting points that should be highlighted in this discussion of the influence of rain parcels on distribution PSCF values. The first point that should be noted is robustness of the source regions with different threshold rain values. Based on the PSCF calculations for Çubuk in the years between 2004 and 2006, the source regions affecting SO_4^{2-} concentrations are most of the Turkey, particularly İstanbul area and Afşin – Elbistan area, Greece, Bulgaria, Romania, Bosnia, Serbia, Italy, Croatia, parts of Ukraine and parts of Russia. It is interesting to note that these source areas did not change very much with changing threshold value for weighting. These areas were the potential source areas in un-weighted PSCF distribution; they were also potential source areas in all distributions after weighting with different threshold rainfall. What happened with decreasing rainfall threshold

values is; the part of the study domain, which is outside these countries, became less and less important potential source areas. For example, grids in France and Germany were moderate source areas in un-weighted distribution of PSCF values, they became insignificant source areas when threshold value of 0.5 mm was used and remained as that thereafter. It can be clearly seen, when percent differences were investigated that the difference between un-weighted and weighted PSCF distributions is <25% for most of the inner part of the study domain (Figures 4.16 to 4.21). This very stable part of the domain includes Turkey and extends to France, Germany and Poland on the northwest, to Central Russia to the North, includes Middle East, particularly Israel, but does not include North African Coast, except for the Moroccan coast, which appears to be a stable source region and survived rain weighting with all threshold values. It is not easy to explain the presence of such a strong source area in Morocco.

Obviously, rain has fairly strong contribution to PSCF values at the distant grids. This is not surprising, because air masses transported to Çubuk, or anywhere else in Turkey from Atlantic Ocean has higher chance of passing through rain events, than air masses originating from closer regions in Europe. This is why no matter what sort of filtering is applied, nearby source areas always turns out to be more important than distant ones.

4.3.2. The Effect Trajectory Segment Altitude on Calculated PSCF Values

Like rain, altitudes of backtrajectory segments used in the PSCF calculations are also expected to affect PSCF values. Normally altitudes of the segments are not included in PSCF calculations. This implicitly means that all trajectory segments, whatever their altitudes are, have the same chance of picking up pollutants when the trajectory passes over a source area. But, it is obvious that a segment with an altitude of 100 m have better chance of picking up pollutants than the segment at 3000 m altitude. Not taking this point into account in PSCF calculations increases the uncertainty in assignment of potential source regions.

In this part of the study, we attempted to weight the contributions of trajectory segments to m_{ij} and n_{ij} values in PSCF calculations. Like weighting with rainfall, there is no scientifically sound information on at which altitude the air parcels can pick up pollutants. Obviously, close to the surface, but it is not known that how close. In this study, PSCF calculations were performed for the Çubuk Station, combining the years 2004, 2005 and 2006, and using HYSPLIT trajectory model. The atmosphere have been divided into four slices between, 0-500 m, 500 – 1000 m, 1000 – 1500 m and > 1500 m and weighted each part separately. Weighting was achieved by multiplying segment counts with 1.0, 0.9, 0.8 and 0.5. The weighting factor 1.0 indicates that segment fully contribute to polluted population in the grid. It was used for segments that are close to the surface. Weighting factor 0.5 was used reduce the significance of that segment and was generally used for segments that are far from the surface. Four different weighting schemes were used in this part and presented in Table 4.2

Table 4.2 Weightings used in the inclusion of segment altitudes into PSCF calculations

	0 – 500 m	500 m – 1000 m	1000 m – 1500 m	>1500 m
Weighting scheme 1	1.0	1.0	0	0
Weighting scheme 2	1.0	0.5	0.5	0.5
Weighting scheme 3	1.0	0.8	0.5	0.5
Weighting scheme 4	1.0	1.0	0.5	0.5
Weighting scheme 5	1.0	0.8	0.8	0.5
Weighting scheme 6	1.0	0.9	0.8	0.5

Distributions of PSCF values for each of the cases given in Table 4.2 are given in the figures 4.22 to 4.27. In each figure there is a distribution of PSCF values without any weighting (figures a), distribution of PSCF values with weighting (figures b) and distribution of gridded percent differences between weighted and un-weighted PSCF values (figures c).

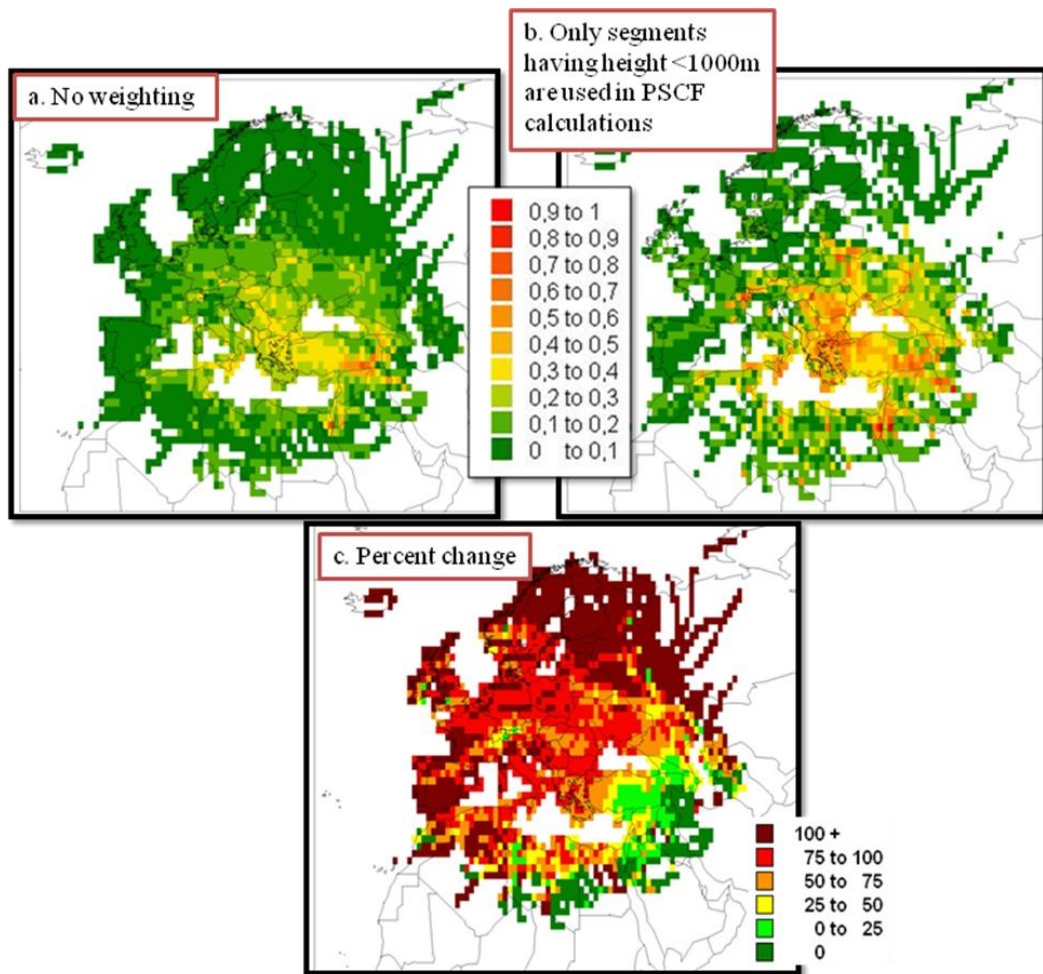


Figure 4.22 Distribution of PSCF values for %40 highest SO_4^{2-} calculated for Çubuk Station for the years 2004-2006 using only segments having height <1000 m in PSCF calculations

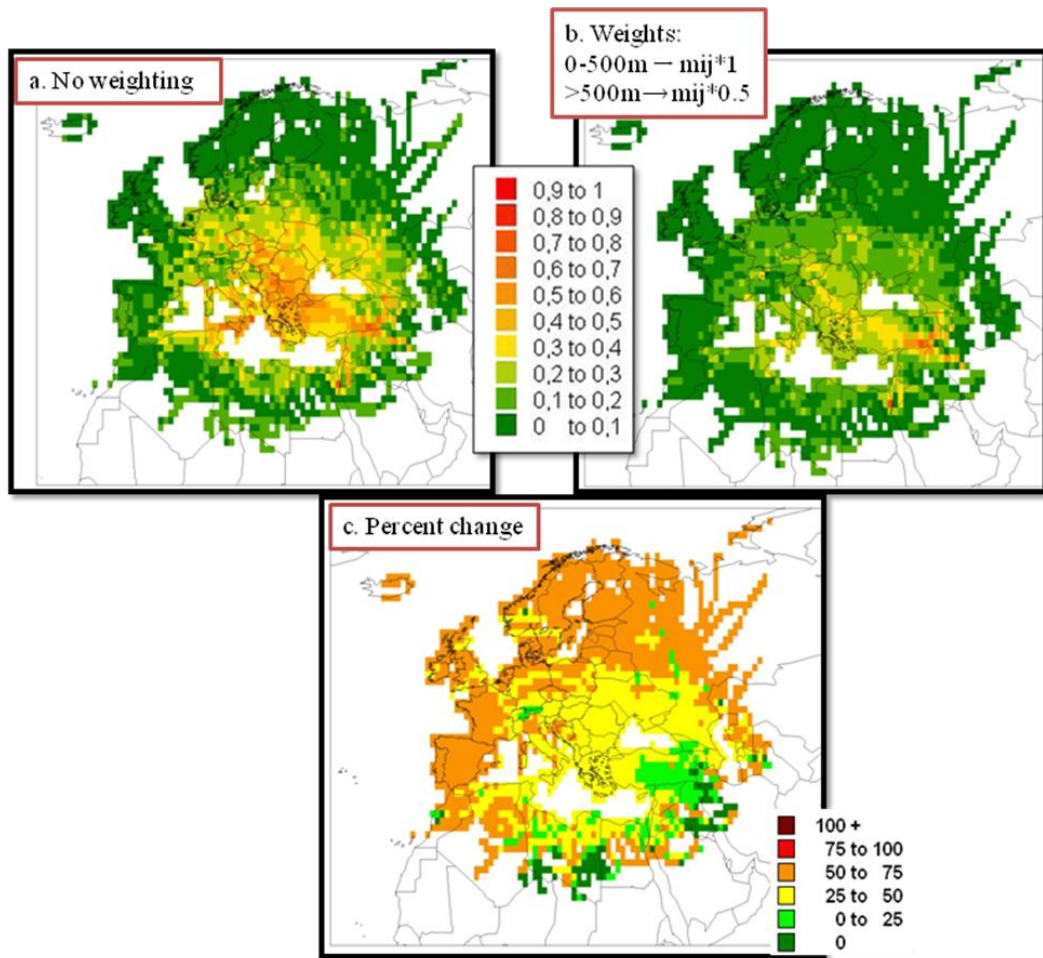


Figure 4.23 Distribution of PSCF values for %40 highest SO_4^{2-} calculated for Çubuk Station for the years 2004-2006, using the following weights: 0-500m \rightarrow $m_{ij} \cdot 1$, $>500m \rightarrow m_{ij} \cdot 0.5$

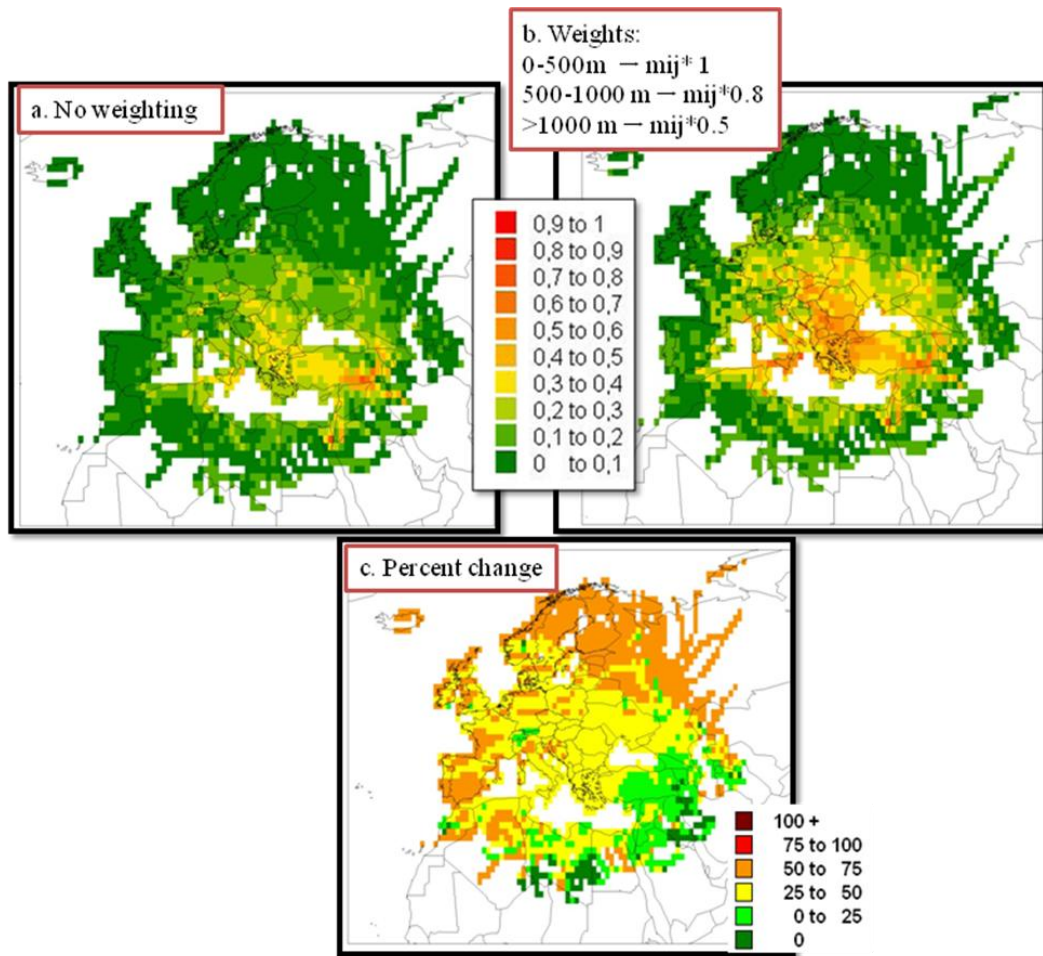


Figure 4.24 Distribution of PSCF values for %40 highest SO_4^{2-} calculated for Çubuk Station for the years 2004-2006 using the following weights 0-500m → mij* 1, 500-1000 m → mij* 0.8, >1000 m → mij*0.5

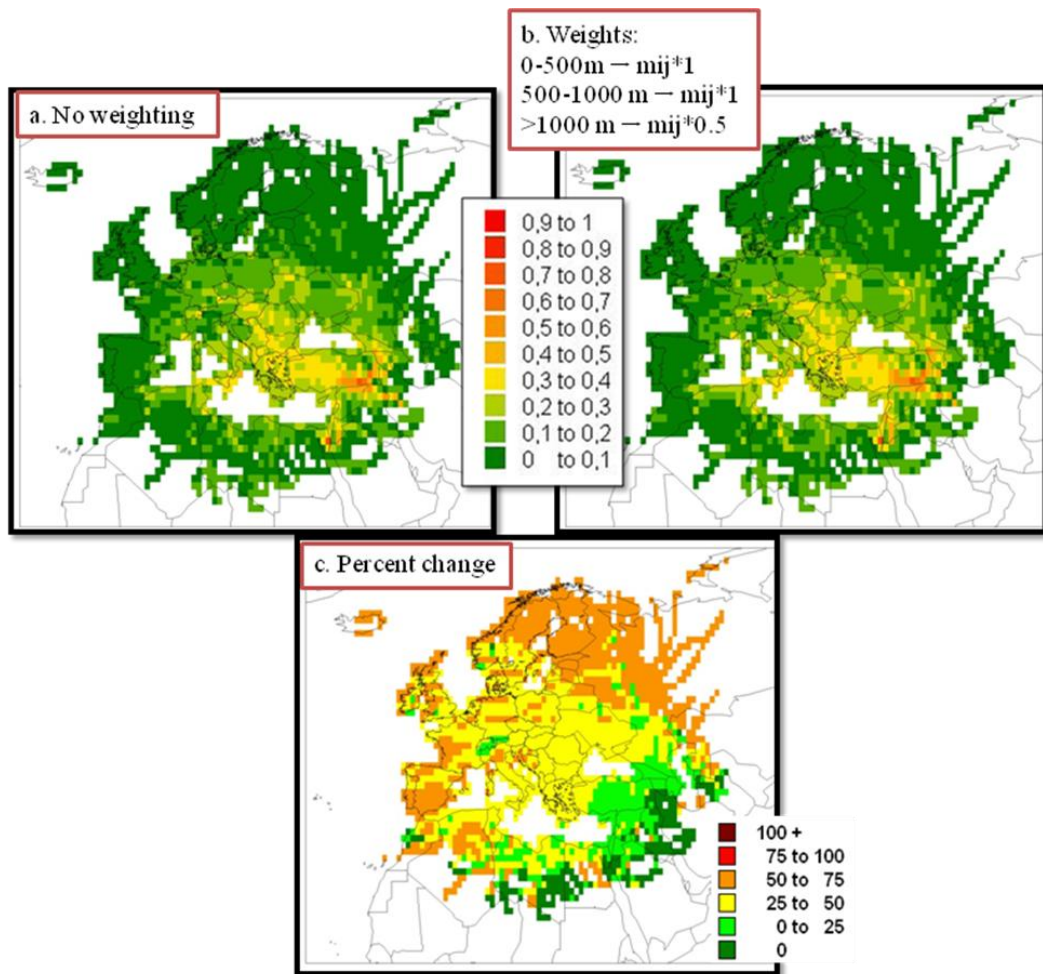


Figure 4.25 Distribution of PSCF values for %40 highest SO_4^{2-} calculated for Çubuk Station for the years 2004-2006 using the following weights 0-500m → mij* 1, 500-1000 m → mij* 1, >1000 m → mij*0.5

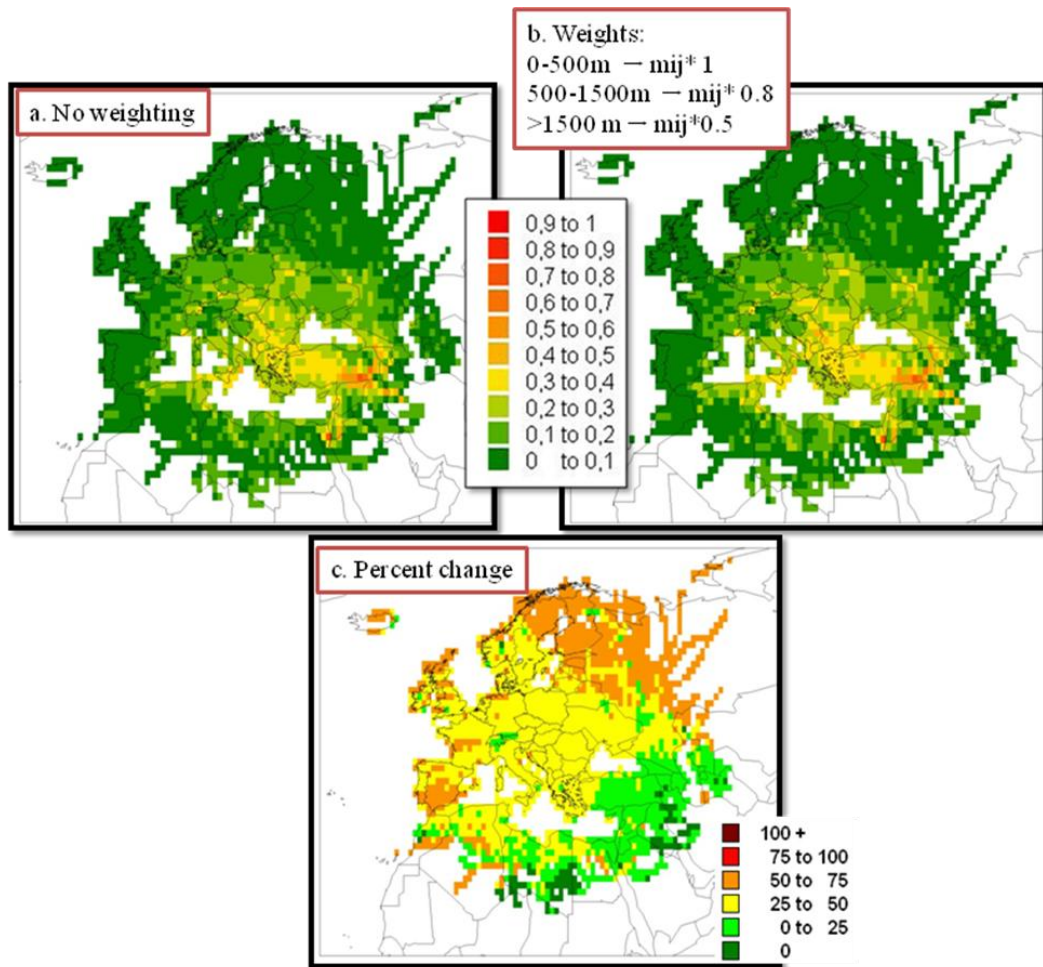


Figure 4.26 Distribution of PSCF values for %40 highest SO_4^{2-} calculated for Çubuk Station for the years 2004-2006 using the following weights 0-500m → mij* 1, 500-1500 m → mij* 0.8, >1500 m → mij*0.5

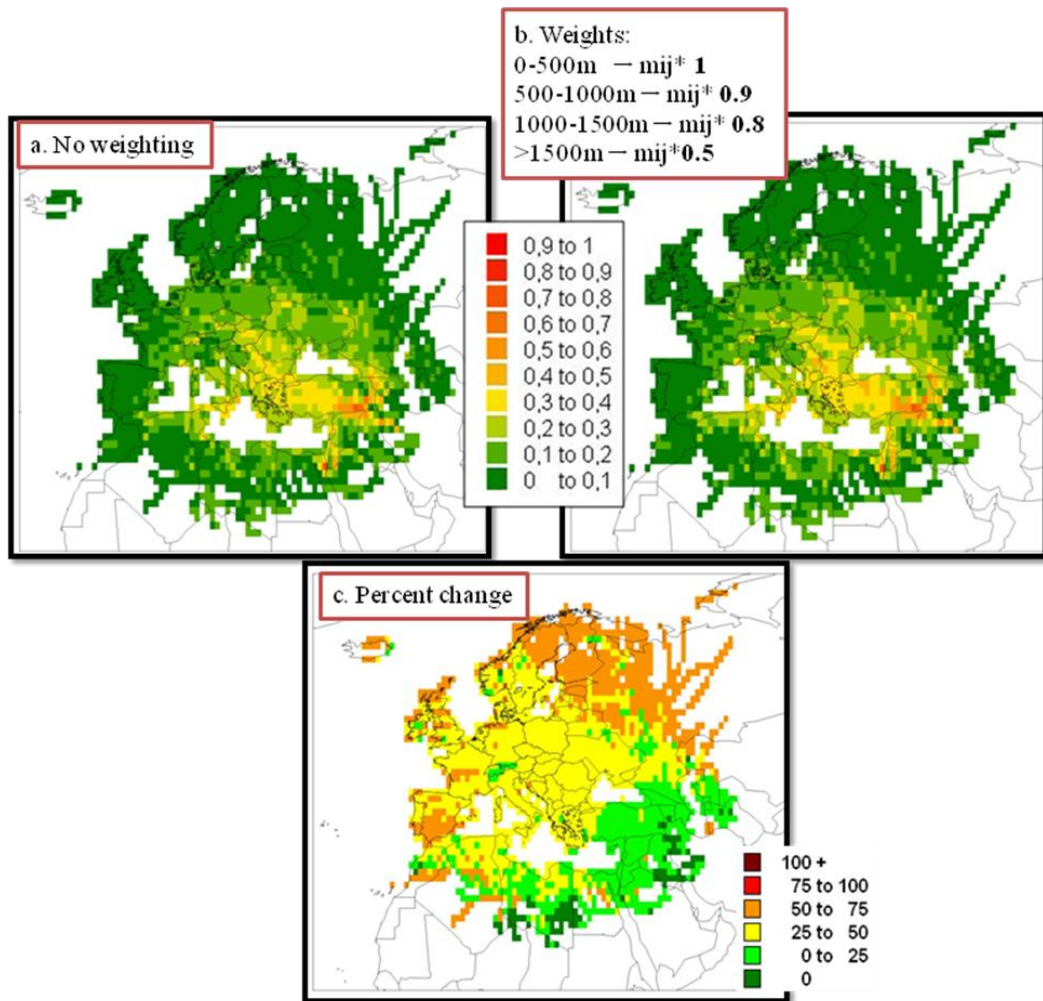


Figure 4.27 Distribution of PSCF values for %40 highest SO_4^{2-} calculated for Çubuk Station for the years 2004-2006 using the following weightings 0-500m \rightarrow $\text{mij}^* 1$, 500-1000m \rightarrow $\text{mij}^* 0.9$, 1000-1500m \rightarrow $\text{mij}^* 0.8$, >1500m \rightarrow $\text{mij}^* 0.5$

Figures 4.22 and 4.23 include extreme weighting cases. In Figure 4.22 (weighting scheme 1), Trajectory segments at altitudes > 1000 m are completely eliminated and not used in PSCF calculations. Weighting scheme 2 in the Table 4.2, which is shown in Figure 4.23 is also fairly radical weighting, because it is assumed that all segments with altitudes higher than 500 m are assumed to have half the contribution to PSCF values compared to segments associated with un-weighted case (all segments under 500 m is weighted by 1.0 and remaining segments have weighted by 0.5). This assumption also significantly reduced potential source areas that

determine measured SO_4^{2-} concentrations at Çubuk. In both of these cases resulting distributions of PSCF values appears unrealistically limited. Percent change figures clearly demonstrate that a large fraction of segments in the outer parts of the study domain is completely washed out, generating a large part of the study domain, starting immediately after Balkan countries having differences >75%. It should be noted that this observation indicates that segments at the outer parts of the study area have generally high altitudes and altitude weighting, like precipitation, will affect the significance of these areas as potential source regions for Çubuk station.

Other 4 cases of altitude weighting, which are given in Figures 4.24 – 27, were less radical and produced more reasonable distributions of PSCF values. In the case, which is given in Figure 4.24 and, which corresponds to weighting scheme 3 in Table 4.2, segments having altitudes <500 m were weighted by 1.0, the ones with altitudes between 500 m and 1000 m are weighted by 0.8 and segments with altitudes >1000 m is weighted by 0.5. In the case depicted in Figure 4.25 that corresponds to weighting scheme 4 in the table, all segments with altitudes below 1000 m are weighted by 1.0, those having altitudes above 1000 m are weighted by 0.5. In the case given in weighting scheme 5, which is also given in Figure 4.26, trajectory segments with altitudes <500 m are weighted by 1.0, those having altitudes between 500 m and 1500 m are weighted by 0.8 and those having altitudes >1500 m are weighted by 0.5. Finally, in the case shown in Figure 4.27 (weighting scheme 6 in the Table 4.2) segments with altitudes <500 m is weighted by 1.0, those between 500 m and 1000 m is weighted by 0.9 and segments having altitudes between 1000 m and 1500 m are weighted by 0.8 and those having altitudes >1500 m are weighted by 0.5.

Distributions of PSCF values resulting from all of these weighting schemes are given in Figure 4.28 for comparison. If one ignores the very extreme case where segments with altitudes >1000 m is totally ignored (Figure 4.22), distributions of PSCF values resulting from other weightings resemble each other. Generally the source areas affecting SO_4^{2-} a concentration at Çubuk is located in Turkey particularly in the South Eastern Turkey. This significance of South Eastern Turkey

as a source area affecting SO_4^{2-} concentrations at central Anatolia is due to presence of Afşin – Elbistan power plant, which is one of the highest SO_2 emitters in Europe. These grids appear as strong source region for central Anatolia regardless the filtering method used. Other source regions include Balkan countries (including Italy), Central European countries, Ukraine, central parts of Russia and Middle East region.

Comparison of percent differences between un-weighted and weighted distributions in figures 4.23 to 4.27 indicated that the difference in PSCF values between un-weighted and altitude weighted PSCF values are the same in Eastern and southern parts of the study domain. Gridded differences $>50\%$ were observed at the northern parts of the study area, including Northern parts of Russia and parts of the Scandinavian countries. In addition to these areas in the North, large differences between weighted and un-weighted distribution were also observed in Spain and at northern parts of UK. The gridded differences between un-weighted and weighted PSCF values were between 25 and 50% for most of the Europe. These conclusions did not change significantly between different weighting schemes.

The more conservative weighting scheme 6 which is shown in Figure 4.27, where all segments under 500 m is weighted with 1.0, segments between 500 m and 1000 m are weighted by 0.9, those between 1000 m and 1500 m are weighted by 0.8 and all the segments with altitudes >1500 are weighted by 0.5 is adopted to be used in our future PSCF applications.

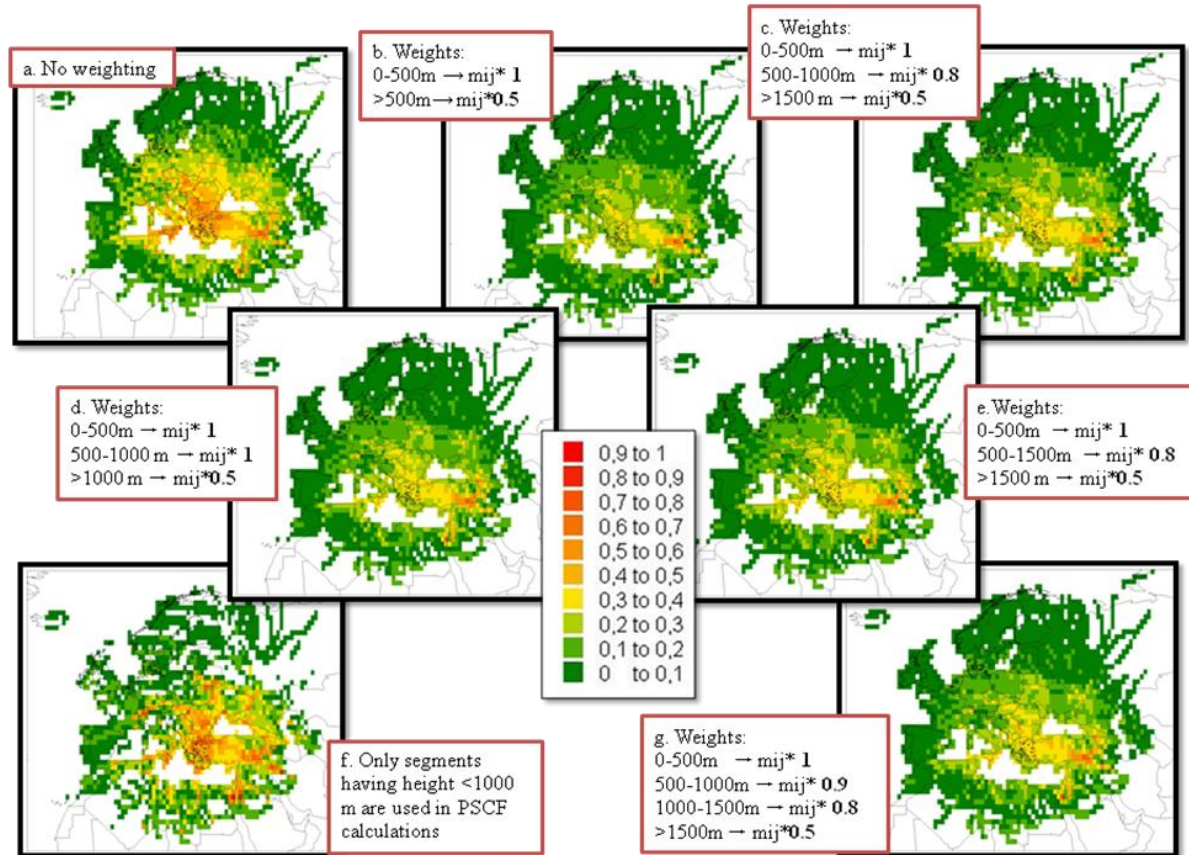


Figure 4.28 Distribution of PSCF values for %40 highest SO_4^{2-} calculated for Çubuk Station for the years 2004-2006 (All height weightings)

Finally the weighting by rain, which was discussed in previous sections, is combined with the weighting for altitude to see the results of combining the two filtering methods. Rain threshold value is taken as 0.2 mm in weighting segments for rain and weighting scheme 6 was used for altitude weighting. The results are given in Figure 4.29.

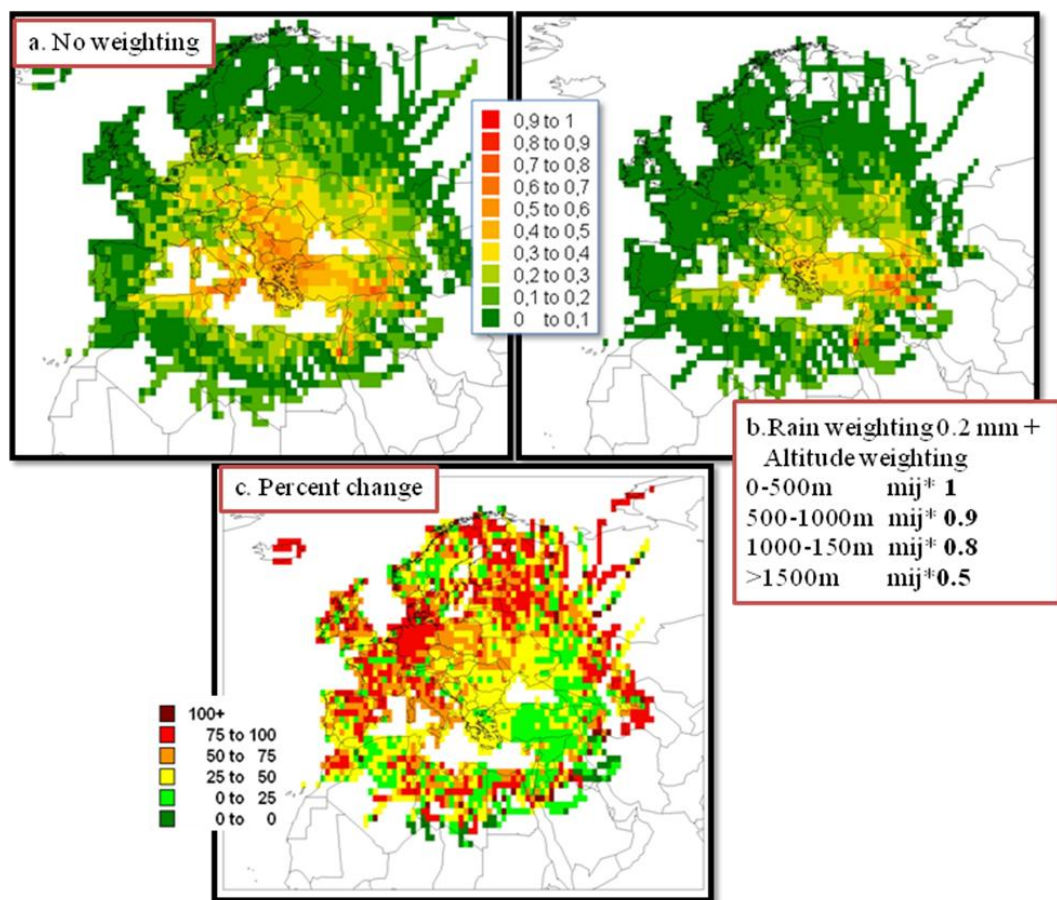


Figure 4.29 Distributions of PSCF after weighting for both rain and segment altitude

The filtering with rain and altitude significantly modified distributions of PSCF values in the study area. There are two interesting points about the Figure 4.29 that should be highlighted. The first one is the significant attenuation of potential source areas, particularly at the outer parts of the study area which can be clearly seen when un-weighted and weighted distributions are compared. This means that countries, such as Spain, Germany, France and Poland are not among the most important source regions affecting SO_4^{2-} concentrations at the Central Anatolia. This is not because their emissions are low, but due to more frequent rain air parcels encounter on their way to Central Anatolia and higher altitudes of the segments over those countries.

The second point is the different contributions of rain and altitude weighting to PSCF values at different parts of the study area. When percent difference figures in Figure 4.29 are compared with similar figures in previous discussions of rain and altitude filtering, it can be seen that rain weighting is more important on the PSCF values in the peripheral of the study area, whereas weighting by segment altitude is more effective on PSCF values Balkan and central European countries.

Another point that should be highlighted is that no matter what type of filtering is applied certain potential source regions did not change, indicating that these are robust source regions that has the highest influence on SO_4^{2-} concentrations at Central Anatolia. These source areas which can be seen an Figure 4.29 includes Turkey itself, Balkan countries, including Bulgaria, Romania, Greece, Central European countries, Hungary and Slovakia and countries at the north, namely Ukraine and Parts of Russia.

4.4. GIS Used and Developed in the Study

GIS are comprehensive tools that extensively used in this study. Integration of database operations such as query and statistical analysis with the visualization and geographical analysis of spatial data in GIS benefited in the pollution source identification studies. Although more detailed usage of GIS in this study explained

in the methodology section of the manuscript, it is worth to mention that GIS capabilities helped to reach the desired results timely and efficiently and understand the source-receptor relationship wisely and comprehensively. For example finding the differences between the resultant grids revealed much information that could not be attainable by comparing the grids visually. Thematic mapping features of GIS facilitated the differentiating several patterns in the distribution of the sources as could be seen from previous parts.

In addition to the use of MapInfo throughout the analyses, there are 5 MapBasic tools developed in this study. Two of them are developed to import the trajectory files in text file format into the MapInfo table files. These tools make the trajectory data import extremely easy when considering thousands of the trajectory files used in this study. One tool was developed for the drawing trajectory lines for the visual comparison in section 4.1.1. This tool can draw the trajectories of selected dates or all trajectories in one click. Manually drawing trajectories from the segment end points will not be feasible without this tool. To calculate PSCF values, a tool was developed in MapBasic that makes necessary calculations without much user effort. For inclusion of the rain and height information into the PSCF methodology, a MapBasic tool that is capable of filtering and weighting the trajectory end points according to either rain or height information. This tool can also calculate PSCF values by combining these two types of weightings.

All tools explained helped the automation of the processes in the source apportionment methods. Even without using the MapBasic tools, some part of the analyses such as randomly selecting trajectories, importing the trajectory files and then drawing the trajectories would not be achieved. One and the most important missing point in the developed tools is that these tools do not have graphical user interfaces for changing the parameters of analyses. All changes are applied by replacing the older parameters with new ones in the pseudo-codes via MapBasic.

Although the MapInfo and MapBasic software provided many benefits for the effective analyses, they have some deficiencies or drawbacks in the usage. Drawing features of the MapInfo sometimes seemed inadequate in some parts of the analyses such that drawing the wind rose shown in Figure 3.3 in section 3 was somehow challenging. Also publishing the maps should be improved. When turned to MapBasic, it worked well, but some feature such as making suggestions to automatic complete functions such as in java programming is missing. Finding the advanced column statistics as a variable in functions that is needed in the arbitrary weighting of PSCF calculations is also missing. These drawbacks, however, would be related to the used versions of the software. But as there is no chance to use the current versions of the software, the identified inadequacies should be taken as recommendations for the improvement of the commercial software.

CHAPTER 5

CONCLUSION AND RECOMMENDATIONS

5.1. Conclusion

This study aims mainly to improve the use of GIS in the air pollution researches develop an alternative source apportionment methodology as well as improving current methodology.

The backtrajectories obtained from 2 types of models, namely HYSPLIT and ECMWF were compared in different aspects. First they compared visually, and then using sector and grid based approach. The PSCF results using those two types of trajectories for Çubuk station were also compared. Two models produce good agreement around small distances from the receptor area but, in further distances trajectory models start to differentiate more. There is no obvious difference in the agreements in PSCF values with different trajectory starting altitude. The grid-based differences in PSCF values was very similar to the grid-based differences in residence times, indicating that the uncertainty in trajectory statistics is determined by the uncertainties in trajectory model outputs. These differences might be resulted from the uncertainties in both of the models (like methodology, spatial resolution and assumptions on vertical motion) and the meteorological data used in the trajectory calculations.

A source oriented method “Region of Influence” was developed and applied to 4 locations (Amasra, Ankara, Antalya in Turkey and Corsica in France) in order to test the method and find potential pollution sources in regional scale. The method developed here is a qualitative source oriented approach that generates information

on potential source areas that affect concentrations of pollutants at a given receptor. It is not an alternative to numerical models since they produce quantitative information on pollutant concentrations at the receptor, but the qualitative information generated on the potential source areas that can affect measured concentrations of pollutants at a receptor location, which is an information comparable to that generated with trajectory statistics. To validate the methodology, PSCF was applied with similar trajectory set. Similar changes on the source regions for each station were seen when they compared temporally. This method can generate potential source areas using very few and simple input data, so that it can be used as a preliminary information in every study, particularly in research groups where expertise for running sophisticated numerical transport and chemical models is not available. This brings important advantages to the researchers such as use of simple and solid approach, less time and money consuming (no need to do experiments at the source), the easy data acquisition from internet.

To overcome the current deficiencies and improve the PSCF methodology, rain and segment altitude information were included in this method. The results showed that the inclusion of rain and height produce more accurate findings for the potential pollution sources. Inclusion of this information helped on managing uncertainties.

GIS tools were developed for calculating PSCF values and inclusion of rain and height considerations into current method. Use of GIS in data preparation provided great advantages. GIS tools developed in this study make the analyses easier and time saving. For example, considering, MapBasic applications made preparation of the large volume of the data easier and faster, otherwise it might have taken very long time if these steps were done manually. Through this study, the use of GIS in the pollution source identification is expanded.

5.2. Recommendations for the Future Studies

In this study, PSCF analyses were done for only Çubuk station as a pilot study. The same analyses could be applied on other stations where the pollutant measurements are available.

In this study applications developed on MapBasic have not easily configurable with graphical user interfaces (GUI); they generally require some user modifications to use in other studies. Therefore, in future studies more user-friendly GUI could be developed. In addition to this, an application could be developed in MapBasic to implement the bootstrapping method, which provides better estimates of the probability values and their uncertainties in PSCF analysis. In addition, similar applications could be developed for the implementation of the other trajectory statistics to provide variety of the analyses.

Data inventory could be improved with recent measurements and obtaining recent trajectories. This would reveal recent changes in the pollution transport trends.

Inclusion of the other atmospheric removal mechanisms and chemistry of pollutant transport would be studied in future studies in order to integrate them into the current PSCF methodology. Inclusion of atmospheric removal mechanisms and height into RoI calculations could be studied to improve the methodology like in PSCF.

The grid size selected in this study was $1^{\circ} \times 1^{\circ}$. As the pollution influenced more from the areas surrounding the receptor, narrower grid size could be used for the areas near to receptor areas to assess the pollution sources more accurately.

REFERENCES

- Akata, N., Kawabata, H., Hasegawa, H., Kondo, K., Sato, T., Chikuchi, Y., et al., (2009). Air mass origins by back trajectory analysis for evaluating atmospheric ²¹⁰Pb concentrations at Rokkasho, Aomori, Japan. *Journal of Radioanalytical and Nuclear Chemistry*, 279(2): 493-498. Retrieved from www.scopus.com.
- Alagha, O. & Tuncel, G., (2003). Evaluation of air quality over the Black Sea Major ionic composition of rain water. *Water Air and Soil Pollution Focus*, 3 (5-6): 87-96.
- Alagha, O., Tuncel, G. & Tosun, S., (2001). Air Quality of the Black Sea Region: Local and Long Range Transported Pollutants. *Eurasian ChemTech Journal*, 3 (4): 273-279.
- Anwari, M., Tuncel, G. & Ataman, O. Y., (1992). Lead and Nickel Levels in the Black Sea Aerosols by ETA-AAS. *J. Environ. Anal. Chem.*, 47: 227-237.
- ARL, (2009). READY system for HYSPLIT Trajectory Model calculations, Air Resources Laboratory, ARL, "<http://www.ready.noaa.gov/ready/open/traj.html>", last accessed in 24 September 2009.
- ARL, (2010a). HYSPLIT Model Research, Air Resources Laboratory, ARL, "http://www.arl.noaa.gov/documents/Summaries/HYSPLIT_FINAL.pdf", last accessed in 05 March 2010.
- ARL, (2010b). HYSPLIT Frequently Asked Questions, Air Resources Laboratory, ARL, "http://www.arl.noaa.gov/faq_md4.php", last accessed in 06 March 2010.
- ARL, (2010c). HYSPLIT - Hybrid Single Particle Lagrangian Integrated Trajectory Model, Air Resources Laboratory, ARL, "http://www.arl.noaa.gov/HYSPLIT_info.php", last accessed in 06 March 2010.
- ARL, (2010d). HYSPLIT trajectory output file format, Air Resources Laboratory, ARL, "http://ready.arl.noaa.gov/HYSPLIT_trajinfo.php", last accessed in 12 January 2010.
- Aronoff, S. (1989). Geographic information systems: a management perspective. WDL Publ., Ottawa, Ont. 294pp.

- Ashbaugh, L. L., Malm, W. C. & Sadeh, W. Z., (1985). A residence time probability analysis of sulfur concentrations at Grand Canyon National Park. *Atmospheric Environment* 19: 1263-1270.
- Bahadur, R., Uplinger, T., Russell, L. M., Sive, B. C., Cliff, S. S., Millet, D. B., et al., (2010). Phenol groups in northeastern U.S. submicrometer aerosol particles produced from seawater sources. *Environmental Science and Technology*, 44(7): 2542-2548.
- Baker, J. (2010). A cluster analysis of long range air transport pathways and associated pollutant concentrations within the UK. *Atmospheric Environment*, 44(4): 563-571.
- Bashir, W., McGovern, F., O'Brien, P., Ryan, M., Burke, L. & Paull, B., (2008). Chemical trends in background air quality and the ionic composition of precipitation for the period 1980-2004 from samples collected at Valentia observatory, co. Kerry, Ireland. *Journal of Environmental Monitoring*, 10(6): 730-738. Retrieved from www.scopus.com.
- Baumann, K. & Stohl, A. (1997). Validation of a long-range trajectory model using gas balloon tracks from the Gordon Bennett Cup 95. *Journal of Applied Meteorology*, 36(6): 711-720. Retrieved from www.scopus.com.
- Begum, B.A., Kim, E., Jeong, C.-H., Lee, D.-W. & Hopke, P.K., (2005). Evaluation of the potential source contribution function using the 2002 Quebec forest fire episode. *Atmospheric Environment*, 39(20): 3719-3724.
- Bigg, E.K., Leck C. & Nilsson D., (1996). Sudden changes in arctic atmospheric aerosol concentrations during summer and autumn. *Tellus*, 48B:254-271.
- Birch, C.E., Brooks, I. M., Tjernström, M., Milton, S.F., Earnshaw, P., Söderberg, S., Persson P. & Ola G., (2009). The performance of a global and mesoscale model over the central Arctic Ocean during late summer. *Journal of Geophysical Research*, 114 (D13104):1-19.
- Borrego C., Tchepel, O., Costa, A.M., Amorim, J.H. & Miranda A.I., (2003). Emission and dispersion modelling of Lisbon air quality at local scale. *Atmospheric Environment*, 37:5197-5205.
- Briggs, D.J., Collins, S., Elliott, P., Fischer, P., Kingham, S., Lebet, E., Pryn, K., Van Reeuwijk, H., Smallbone, K. & Andvan Der Veen, A. (1997). Mapping urban air pollution using GIS: a regression-based approach. *International Journal of Geographical Information Science*, 11: 7, 699-718.

- Byers, H. R., (1974). *General Meteorology, 4th Edn.* McGraw-Hill, New York, U.S.A. in Stohl A., (2002). Chapter 21 Computation, accuracy and applications of trajectories-A review and bibliography. *Air Pollution Science for the 21st Century*, 615-654, Elsevier Science Ltd.
- Canepa E., D'Alberti F., D'Amati F. & Triacchini G., (2007). The GIS-based SafeAirView software for the concentration assessment of radioactive pollutants after an accidental release. *Science of the Total Environment* 373: 32–42
- CEIP, (2008). Centre on Emission Inventories and Projections, Emission data reported to Convention on Long-range Transboundary Air Pollution in 2008.
- CEIP, (2009). Emissions as used in EMEP models, Centre on Emission Inventories and Projections, CEIP, “<http://www.ceip.at/emission-data-webdab/emissions-used-in-emep-models/>”, last accessed in 17 September 2009.
- Celle-Jeanton, H., Travi, Y., Loÿe-Pilot, M., Huneau, F. & Bertrand, G. (2009). Rainwater chemistry at a Mediterranean inland station (Avignon, France): Local contribution versus long-range supply. *Atmospheric Research*, 91(1): 118-126.
- Challa, V. S., Indrcanti, J., Baham, J. M., Patrick, C., Rabarison, M. K., Young, J. H., et al., (2008). Sensitivity of atmospheric dispersion simulations by HYSPLIT to the meteorological predictions from a meso-scale model. *Environmental Fluid Mechanics*, 8(4): 367-387. Retrieved from www.scopus.com.
- Cheng, M.D., Hopke, P.K. & Zeng, Y., (1993). “A Receptor oriented methodology for determining source regions of particulate observed at Dorset, Ontario”, *Journal of Geophysical Research* 98, 16839-16849.
- Chiapello, I., Bergametti, G., Chatenet, B., Bousquet, P., Dulac, F. & Santos Soares, E., (1997). Origins of African dust transported over the northeastern tropical Atlantic. *Journal of Geophysical Research* 102: 13, 701-13,709 in Stohl A., (2002). Chapter 21 Computation, accuracy and applications of trajectories-A review and bibliography. *Air Pollution Science for the 21st Century*, 615-654, Elsevier Science Ltd.
- Clain, G., Baray, J.-L., Delmas, R., Keckhut, P. & Cammas, J.-P, (2010). A lagrangian approach to analyse the tropospheric ozone climatology in the tropics: Climatology of stratosphere-troposphere exchange at Reunion Island. *Atmospheric Environment*, 44(7): 968-975.

- COHA, (2010). Trajectory analysis, Causes of Haze Assessment COHA, “http://www.coha.dri.edu/web/general/tools_trajanaly.html”, last accessed in 11 April 2010.
- Crawford, J., Chambers, S., Cohen, D.D., Dyer, L., Wang, T. & Zahorowski, W., (2007). Receptor modelling using positive matrix factorisation, back trajectories and radon-222. *Atmospheric Environment*, 41(32): 6823-6837. Retrieved from www.scopus.com.
- Crawford, J., Zahorowski, W. & Cohen, D.D., (2009). A new metric space incorporating radon-222 for generation of back trajectory clusters in atmospheric pollution studies. *Atmospheric Environment*, 43(2): 371-381. Retrieved from www.scopus.com.
- CSU, (2010). Colorado State University, Back Trajectory Modeling, “<http://vista.cira.colostate.edu/docs/wrap/Modeling/BackTrajectoryModeling.doc>”, last accessed in 10 April 2010.
- D’Abreton, P.C. & Tyson, P.D., (1996). Three-dimensional kinematic trajectory modelling of water vapour transport over Southern Africa. *Water SA* 22: 297-306 in Stohl A., (2002). Chapter 21 Computation, accuracy and applications of trajectories-A review and bibliography. *Air Pollution Science for the 21st Century*, 615-654, Elsevier Science Ltd.
- Dabanlı, A. (2009). Personal communication with Ahmet DABANLI from Başarsoft, in December 2009, Ankara.
- Danielsen, E.F., (1961). Trajectories: isobaric, isentropic and actual. *Journal of Meteorology*, 18: 479-486. in Stohl A., (2002). Chapter 21 Computation, accuracy and applications of trajectories-A review and bibliography. *Air Pollution Science for the 21st Century*, 615-654, Elsevier Science Ltd.
- De Leeuw, F. A.A.M. (2002). A set of emission indicators for long-range transboundary air pollution, *Environmental Science & Policy* 5:135–145.
- Delcloo, A. W., & De Backer, H., (2008). Five day 3D back trajectory clusters and trends analysis of the Uccle ozone sounding time series in the lower troposphere (1969-2001). *Atmospheric Environment*, 42(19): 4419-4432. Retrieved from www.scopus.com.
- Dent, A.L., Fowler D.A., Kaplan B.M., Zarus G.M. & Henriques W.D., (2000). Using GIS to study the health impact of air emissions. *Drug Chem Toxicol.*, 23(1):161-78.
- Doğan G., (2005). Comparison of the rural atmosphere aerosol compositions at different parts of Turkey, *M.Sc. Thesis*, Department of Environmental Engineering, Middle East Technical University, Ankara, Turkey.

- Doğan, G., Güllü G. & Tuncel G., (2008). Sources and source regions effecting the aerosol composition of the Eastern Mediterranean, *Microchemical Journal* 88, 142–149.
- Doğan G., Güllü G., Karakas D. & Tuncel G., (2010). Comparison of Source Regions Affecting SO₂- and NO₃- concentrations at the Eastern Mediterranean and Black Sea Atmospheres. *Current Analytical Chemistry*, 6(1): 66-71.
- Draxler, R.R. & Hess G.D., (1997). Description of the HYSPLIT_4 Modeling System, *NOAA Technical Memorandum ERL, ARL-224*.
- Draxler, R.R., & Hess, G.D. (1998). An overview of the HYSPLIT_4 modelling system for trajectories, dispersion, and deposition, *Australian Meteorological Magazine*, 47(4): 295-308.
- Draxler, R.R. & Rolph, G.D., (2003). HYSPLIT (HYbrid Single-Particle Lagrangian Integrated Trajectory) Model access via NOAA ARL READY Website (<http://www.arl.noaa.gov/HYSPLIT.php>). NOAA Air Resources Laboratory, Silver Spring, MD.
- Du, S., Wilson, J.D. & Yee, E., (1994). Probability density functions for velocity in the convective boundary layer, and implied trajectory models. *Atmospheric Environment*, 28(6): 1211-1217. Retrieved from www.scopus.com.
- Dutton, S.J., Schauer, J.J., Vedal, S. & Hannigan, M.P., (2009). PM_{2.5} characterization for time series studies: Pointwise uncertainty estimation and bulk speciation methods applied in Denver. *Atmospheric Environment* 43:1136–1146.
- Dutton, J.A., (1986). The Ceaseless Wind. *An Introduction to the Theory of Atmospheric Motion*. Dover, New York. in Stohl A., (2002). Chapter 21 Computation, accuracy and applications of trajectories-A review and bibliography. *Air Pollution Science for the 21st Century*, 615-654, Elsevier Science Ltd.
- Dvorská, A., (2008). Methods to evaluate the distribution of organic pollutants in the environment. *Dissertation thesis*, Research Centre for Environmental Chemistry and Ecotoxicology (RECETOX), Masaryk University, Brno, Czech Republic.
- ECMWF, (2009). ECMWF EAccess login page, “<https://ecaccess.ecmwf.int/ecmwf/>”, last accessed in 22 December 2009.
- ECMWF, (2010a). MARS, the ECMWF archive, “<http://www.ecmwf.int/services/archive/>”, last accessed in 01 April 2010.

- Elbir, T. (2004). A GIS based decision support system for estimation, visualization and analysis of air pollution for large Turkish cities. *Atmospheric Environment* 38: 4509–4517.
- Elbir, T., Mangir, N., Kara, M., Simsir S., Eren T. & Ozdemir S, (2010). Development of a GIS-based decision support system for urban air quality management in the city of Istanbul. *Atmospheric Environment* 44: 441-454.
- EMEP, (2010a). Co-operative Programme for Monitoring and Evaluation of the Long-range Transmission of Air Pollutants in Europe, EMEP, “<http://www.emep.int>”, last accessed in 07 April 2010.
- EMEP, (2010b). EMEP Grid description, EMEP, “<http://emep.int/grid/griddescr.html>”, last accessed in 16 March 2010.
- Eneroth K., Kjellström E. & Holmén K., (2003). A trajectory climatology for Svalbard; investigating how atmospheric flow patterns influence observed tracer concentrations. *Physics and Chemistry of the Earth* 28:1191–1203.
- Erduran, M.S. & Tuncel, S.G., (2001). Sampling and analysis of gaseous pollutants and related particulate matter in a Mediterranean site: Antalya-Turkey. *Journal of Environmental Monitoring* 3(6): 661-665.
- Escudero, M., Stein, A., Draxler, R.R., Querol, X., Alastuey, A., Castillo, S. & Avila A., (2006). Determination of the contribution of northern Africa dust source areas to PM₁₀ concentrations over the central Iberian Peninsula using the Hybrid Single-Particle Lagrangian Integrated Trajectory model (HYSPPLIT) model, *J. Geophys. Res.*, 111 (D6), D06210-D06300.
- Fast J.D. & Berkowitz C.M., (1997). Evaluation of back trajectories associated with ozone transport during the 1993 North Atlantic Regional Experiment. *Atmospheric Environment*, 31(6): 825-837.
- Fink A.H. & Knippertz P., (2003). An extreme precipitation event in southern Morocco in spring 2002 and some hydrological implications. *Weather*, 58:377-392.
- Froude, L.S.R., (2009). Regional differences in the prediction of extratropical cyclones by the ECMWF ensemble prediction system. *Monthly Weather Review*, 137(3): 893-911. Retrieved from www.scopus.com.
- Gaga, E.O., Tuncel, G. & Tuncel S.G., (2009). Sources and Wet Deposition Fluxes of Polycyclic Aromatic Hydrocarbons (PAHs) in an Urban Site 1000 Meters High in Central Anatolia (Turkey). *Environmental Forensics*, 10: 339–351.

- Gao, N., Cheng, M.-D. & Hopke, P.K., (1993). Potential source contribution function analysis and source apportionment of sulfur species measured at Rubidoux, CA during the Southern California air quality study 1987. *Analytica Chimica Acta* 277: 369–380.
- Gao, N., Hopke, P.K. & Reid, N.W., (1996). Possible sources of some trace elements found in airborne particles and precipitation in Dorset, Ontario. *Journal of the Air and Waste Management Association* 46: 1035–1047.
- Güllü, G., Doğan, G. & Tuncel, G., (2005). Atmospheric trace element and major ion concentrations over the eastern Mediterranean Sea: Identification of anthropogenic source regions. *Atmospheric Environment* 39: 6376-6387.
- Haagenson, P. L., Ying-Hwa K., Skumanich, M. & Seaman, N. L., (1987). Tracer verification of trajectory models. *Journal of Climate & Applied Meteorology*, 26(3): 410-426. Retrieved from www.scopus.com.
- Hacısalıhoğlu, G., Balkaş, T.I., Ölmez, I., Arami, M. & Tuncel G., (1991-a). “Sampling and Analysis of Aerosols in the Black Sea Atmosphere” in *Black Sea Oceanography*, Izdar E., Murray J. Eds, pp 469-487, Kluwier Academic Publishers, Netherlands.
- Hacısalıhoğlu, G., Balkaş T.I., Tuncel, S.G., Herman, D.H., Ölmez, I. & Tuncel, G., (1991-b). Trace Element Composition of the Black Sea Aerosols. *Deep Sea Research*, 38: 1255-1266.
- Hacısalıhoğlu, G., Eliyakut, F., Balkaş T.I. & Tuncel, G., (1992). Chemical Composition of Particles in the Black Sea Aerosols. *Atmos. Environ.*, 26A: 3207-3218.
- Harris, J.M. & Kahl, J.D., (1990). A descriptive atmospheric transport climatology for the Mauna Loa Observatory, using clustered trajectories. *Journal of Geophysical Research* 95: 13651–13667. In Stohl A., (2002). Chapter 21 Computation, accuracy and applications of trajectories-A review and bibliography. *Air Pollution Science for the 21st Century*, 615-654, Elsevier Science Ltd.
- Harris, J. M., Draxler, R. R., & Oltmans, S. J., (2005). Trajectory model sensitivity to differences in input data and vertical transport method. *Journal of Geophysical Research D: Atmospheres*, 110(14): 1-8. Retrieved from www.scopus.com.
- Heintzenberg J. & Leck C., (1994). Seasonal Variation of the atmospheric aerosol near the top of the marine boundary layer over Spitsbergen related to Arctic sulphur cycle. *Tellus*, 46B:52-67.

- Hopke, P.K., Barrie, L.A., Li, S.-M., Cheng, M.-D., Li, C., & Xie, Y. (1995). Possible Sources and Preferred Pathways for Biogenic and Non-Seasalt Sulfur for the High Arctic, *J. Geophys. Res.* 100:16595–16603.
- Hsu, Y.-K., Holsen, T.M. & Hopke, P.K., (2003). Comparison of hybrid receptor models to locate PCB sources in Chicago. *Atmospheric Environment*, 37:545–562.
- Hwang, I. & Hopke, P.K, (2007). Estimation of source apportionment and potential source locations of PM_{2.5} at a west coastal IMPROVE site. *Atmospheric Environment* 41, 506-518.
- Işıkdemir, Ö., (2006). Investigation of 8-year-long composition record in the eastern Mediterranean precipitation, *M.S. Thesis*, Department of Environmental Engineering, Middle East Technical University, Ankara.
- Jensen S.S., (1998). Mapping human exposure to traffic air pollution using GIS. *Journal of Hazardous Materials*, 61 (1-3): 385-392.
- Jin T. & Fu L., (2005). Application of GIS to modified models of vehicle emission dispersion. *Atmospheric Environment*, 39: 6326–6333.
- Kahl, J. D., Harris, J. M., Herbert, G. A. & Olson, M. P., (1989). Intercomparison of three long-range trajectory models applied to arctic haze. *Tellus, Series B*, 41 B(5): 524-536. Retrieved from www.scopus.com.
- Kallos, G., Kotroni, V., Lagouvardos, K. & Papadopoulos, A. (1998). On the long-range transport of air pollutants from Europe to Africa. *Geophysical Research Letters*, 25(5): 619-622.
- Kallos, G., Astitha, M., Katsafados, P. & Spyrou, C. (2007). Long-range transport of anthropogenically and naturally produced particulate matter in the Mediterranean and north Atlantic: Current state of knowledge. *Journal of Applied Meteorology and Climatology*, 46(8): 1230-1251.
- Karaca, F., Anil, I. & Alagha, O., (2009). Long-range potential source contributions of episodic aerosol events to PM₁₀ profile of a megacity. *Atmospheric Environment*, 43(36): 5713-5722.
- Karakaş, D., Ölmez I., Tosun S. & Tuncel G., (2004). Trace element composition of Black Sea aerosols. *Journal of Radioanalytical and Nuclear Chemistry*, 159(2): 187-192.
- Katsoulis, B.D., (1999). The potential for long-range transport of air-pollutants into Greece: a climatological analysis. *Science of The Total Environment*, 231(2-3): 101-113.

- Kaya, G. & Tuncel, G., (1997). Trace element and major ion composition of wet and dry deposition in Ankara, Turkey. *Atmospheric Environment* 31: 3985-3998.
- Khosrawi, F., Ström, J., Minikin, A. & Krejci, R., (2010). Particle formation in the arctic free troposphere during the ASTAR 2004 campaign: A case study on the influence of vertical motion on the binary homogeneous nucleation of H₂SO₄/H₂O. *Atmospheric Chemistry and Physics*, 10(3): 1105-1120. Retrieved from www.scopus.com.
- Kiuila, O., (2003). Economic repercussions of sulfur regulations in Poland. *Journal of Policy Modeling*, 25(4): 327-333.
- Klimont, Z., Amann, M., Cofala, J., Gyórfás, F., Klaassen, G. & Schöpp, W., (1994). An emission inventory for the central European initiative 1988, *Atmospheric Environment*, 28(2): 235-246.
- Knippertz P., Fink, A.H., Reiner A. & Speth P., (2003). Three Late Summer/Early Autumn Cases of Tropical–Extratropical Interactions Causing Precipitation in Northwest Africa, *Monthly Weather Review*, 131: 116-135.
- Kuloğlu, E. & Tuncel G. (2005). Size distribution of trace elements and major ions in the Eastern Mediterranean atmosphere, *Water Air Soil Pollution*, 167 (1-4): 221-241.
- Lee, L.Y.L., Kwok, R.C.W., Cheung, Y.P. & Yu, K.N., (2004). Analyses of airborne ⁷Be concentrations in Hong Kong using back-trajectories. *Atmospheric Environment*, 38: 7033–7040.
- Lee, J. D., McFiggans, G., Allan, J. D., Baker, A. R., Ball, S. M., Benton, A. K., et al., (2010). Reactive halogens in the marine boundary layer (RHAMBLe): The tropical north Atlantic experiments. *Atmospheric Chemistry and Physics*, 10(3): 1031-1055. Retrieved from www.scopus.com.
- Lin, M-D & Lin Y-C, (2002). The application of GIS to air quality analysis in Taichung City, Taiwan, ROC. *Environmental Modelling & Software*, 17: 11-19.
- Liu D.H.F. & Lipták B.G. (Eds.), (2000). Air Pollution. Florida: CRC Press LLC.
- Liu, W., Hopke, P.K., Han, Y., Yi, S.-M., Holsen, T.M., Cybart, S., Kozłowski, K. & Milligan, M., (2003). Application of receptor modeling to atmospheric constituents at Potsdam and Stockton, NY. *Atmospheric Environment* 37: 4997-5007.

- Liu, J. J., Jones, D. B. A., Worden, J. R., Noone, D., Parrington, M. & Kar, J. (2009). Analysis of the summertime buildup of tropospheric ozone abundances over the middle east and north Africa as observed by the tropospheric emission spectrometer instrument. *Journal of Geophysical Research D: Atmospheres*, 114: D05304.
- Lupu, A. & Maenhaut, W., (2002). Application and comparison of two statistical trajectory techniques for identification of source regions of atmospheric aerosol species. *Atmospheric Environment* 36, 5607–5618.
- MapInfo Corp., (1999). MapBasic software version 5.5.
- MapInfo Corp., (2003). MapInfo software version 7.5 release, build 22.
- McGowan H. & Clark A., (2008). Identification of dust transport pathways from Lake Eyre, Australia using HYSPLIT, *Atmospheric Environment*, 42 (29): 6915-6925.
- McGrath, R. (1989). Trajectory models and their use in Irish Meteorological Service. Internal memorandum No:112/89, Irish Meteorological Service, Dublin, Ireland.
- Merrill, J.T., Bleck, R. & Boudra, D., (1986). Techniques of Lagrangian trajectory analysis in isentropic coordinates. *Monthly Weather Review* 114: 571-581. in Stohl A., (2002). Chapter 21 Computation, accuracy and applications of trajectories-A review and bibliography. *Air Pollution Science for the 21st Century*, 615-654, Elsevier Science Ltd.
- Microsoft Corp., (2007). Microsoft Office Suite, Excel version 2007.
- Migon, C., Robin, T., Dufour, A. & Gentili, B., (2008). Decrease of lead concentrations in the Western Mediterranean atmosphere during the last 20 years. *Atmospheric Environment* 42 (4):815-821.
- Miller J.M. & Harris J.M., (1985). The flow climatology to Bermuda and its implications for long-range transport, *Atmospheric Environment (1967)*, 19(3):409-414.
- MoEF, (2006). Ministry of Environment and Forestry, EU Integrated Environmental Approximation Strategy of Turkey (2007 - 2023), pp-26.
- MoEF, (2010). Ministry of Environment and Forestry of Turkey, National Air Quality Monitoring Network, “<http://www.havaizleme.gov.tr/Default.htm>”, last accessed in 04 April 2010.

- Moody, J.L. & Samson, P.J., (1989). The influence of atmospheric transport on precipitation chemistry at two sites in the Midwestern United States. *Atmospheric Environment*, 23: 2117-2132. in Stohl A., (2002). Chapter 21 Computation, accuracy and applications of trajectories-A review and bibliography. *Air Pollution Science for the 21st Century*, 615-654, Elsevier Science Ltd.
- Morcrette, J. -, Boucher, O., Jones, L., Salmond, D., Bechtold, P., Beljaars, A., et al., (2009). Aerosol analysis and forecast in the European Centre For Medium-Range Weather Forecasts integrated forecast system: Forward modeling. *Journal of Geophysical Research D: Atmospheres*, 114(6). Retrieved from www.scopus.com.
- Munzur B., (2008). Chemical composition of atmospheric particles in the Aegean Region, *M.S. Thesis*, Department of Environmental Engineering, Middle East Technical University, Ankara.
- NCAR, (2010). The National Center for Atmospheric Research, USA, NCEP/NCAR Global Reanalysis Products, 1948-continuing, “<http://dss.ucar.edu/datasets/ds090.0/>”, last accessed in 05 April 2010.
- NILU, (2010a). Norwegian Institute for Air Research, EMEP Measurement Network, “<http://tarantula.nilu.no/projects/ccc/network/index.html>”, last accessed in 05 April 2010.
- NILU, (2010b). Norwegian Institute for Air Research, EMEP Site Description of Çubuk “<http://tarantula.nilu.no/projects/ccc/sitedescriptions/tr/index.html>”, last accessed in 10 April 2010.
- Norman M., Leck, C. & Rodhe H., (2003). Differences across the ITCZ in the chemical characteristics of the Indian Ocean MBL aerosol during INDOEX. *Atmos. Chem. Phys.*, 3:563–579.
- Northwood Technologies Inc. and Marconi Mobile Limited, (2001). Vertical Mapper version 3.0.
- Paatero J., Hatakka J., Holmén K., Eneroth K. & Viisanen Y., (2003). Lead-210 concentration in the air at Mt. Zeppelin, Ny-Ålesund, Svalbard. *Physics and Chemistry of the Earth*, 28:1175–1180.
- Park S.K., O'Neill M.S., Stunder B.J., Vokonas P.S., Sparrow D., Koutrakis P. & Schwartz J., (2007). Source location of air pollution and cardiac autonomic function: trajectory cluster analysis for exposure assessment. *Journal of Exposure Science and Environmental Epidemiology*, 17(5): 488-97.
- Pekney, N., Davidson, C., Zhou, L., & Hopke, P. (2006). Application of PSCF and CPF to PMF-modeled sources of PM_{2.5} in Pittsburgh. *Aerosol Science and Technology*, 40(10): 952-961.

- , N., Pey, J., Castillo, S., Viana, M., Alastuey, A. & Querol, X., (2008). Interpretation of the variability of levels of regional background aerosols in the Western Mediterranean. *Science of the Total Environment* 407 (1): 527-540.
- Plaisance, H., Galloo, J.C. & Guillermo, R., (1997). Source identification and variation in the chemical composition of precipitation at two rural sites in France. *Science of the Total Environment* 206: 79-93.
- Polissar, A. V., Hopke, P. K. & Poirot, R. L. (2001). Atmospheric Aerosol over Vermont: Chemical Composition and Sources. *Environ. Sci. Technol.* 35:4604-4621.
- Querol, X., Pey, J., Pandolfi, M., Alastuey, A., Cusack, M., Pérez, N., et al. (2009). African dust contributions to mean ambient PM10 mass-levels across the Mediterranean basin. *Atmospheric Environment*, 43(28): 4266-4277.
- Reap, R.M., (1972). An operational three-dimensional trajectory model. *Journal of Applied Meteorology*, 11: 1193–1202.
- Ridame C., Guieu C. & Loÿe-Pilot M-D., (1999). Trend in total atmospheric deposition fluxes of aluminium, iron, and trace metals in the northwestern Mediterranean over the past decade (1985-1997) *J. of Geophys Res-Atmos* 104(D23): 30127-30138.
- Riddle, E. E., Voss, P. B., Stohl, A., Holcomb, D., Maczka, D., Washburn, K., et al., (2006). Trajectory model validation using newly developed altitude-controlled balloons during the international consortium for atmospheric research on transport and transformations 2004 campaign. *Journal of Geophysical Research D: Atmospheres*, 111(23). Retrieved from www.scopus.com.
- Rolph, G.D., (2003). Real-time Environmental Applications and Display sYstem (READY) Website (<http://www.arl.noaa.gov/ready.php>). NOAA Air Resources Laboratory, Silver Spring, MD.
- Rozwadowska, A., Zieliński, T., Petelski, T. & Sobolewski, P., (2010). Cluster analysis of the impact of air back-trajectories on aerosol optical properties at Hornsund, Spitsbergen. *Atmos. Chem. Phys.*, 10: 877-893.
- Russell, A., McGregor, G. R. & Marshall, G. J., (2008). Eastern Antarctic peninsula precipitation delivery mechanisms: Process studies and back trajectory evaluation. *Atmospheric Science Letters*, 9(4): 214-221. Retrieved from www.scopus.com.

- Salvador, P., Artíñano, B., Querol, X. & Alastuey, A., (2008). A combined analysis of backward trajectories and aerosol chemistry to characterize long-range transport episodes of particulate matter: The Madrid air basin, a case study. *Science of the Total Environment*, 390:495-506.
- Sandroni V. & Migon C., (1997). Significance of Trace-Metal Medium-Range Transport in the Western Mediterranean. *Science of The Total Environment*, 196 (1):83-89.
- Seibert, P., Kromp-Kolb, H., Baltensberger, U., Jost, D.T. & Schwikowski, M., (1994). Trajectory analysis of high-alpine air pollution data. In: Gryning, S.E., Millan, M.M. (Eds.), Air "Pollution Modelling and its Application X. Plenum Press, New York, pp. 595-596.
- Shad R., Mesgari M. S., Abkar A. & Shad A., (2009). Predicting air pollution using fuzzy genetic linear membership kriging in GIS. *Computers, Environment and Urban Systems*, 33: 472-481.
- Shadbolt, R. P., E. A. Waller, J. P. Messina, & J. A. Winkler (2006). Source regions of lower-tropospheric airflow trajectories for the lower peninsula of Michigan: A 40-year air mass climatology, *J. Geophys. Res.*, 111: D21117.
- Shan, W., Yin, Y., Lu, H., & Liang, S. (2009). A meteorological analysis of ozone episodes using HYSPLIT model and surface data. *Atmospheric Research*, 93(4): 767-776. Retrieved from www.scopus.com.
- Sharma, N., Bhandari, K., Rao, P., Shukla, A. (2010) GIS applications in air pollution modeling, GIS Development.net, "<http://www.gisdevelopment.net/application/environment/air/mi03220a.htm>", last accessed in 04 April 2010.
- SPO, (2007). State Planning Organization, Ninth Development Plan 2007-2013, Special Expertise Commission Report on Environment, pp. 20-22.
- Steinacker, R., (1984). Airmass and frontal movement around the Alps. *Rivista di Meteorologia Aeronautica*, 44:85-93 in Stohl A., (2002). Chapter 21 Computation, accuracy and applications of trajectories-A review and bibliography. *Air Pollution Science for the 21st Century*, 615-654, Elsevier Science Ltd.
- Stohl, A. (1996). Trajectory statistics - a new method to establish source-receptor relationships of air pollutants and its application to the transport of particulate sulfate in Europe. *Atmos. Environ.*, 30(4): 579-587.

- Stohl, A. & Seibert, P., (1997). Accuracy of trajectories as determined from the conservation of meteorological tracers. *Quarterly Journal of the Royal Meteorological Society*, in press. in Stohl A., (2002). Chapter 21 Computation, accuracy and applications of trajectories-A review and bibliography. *Air Pollution Science for the 21st Century*, 615-654, Elsevier Science Ltd.
- Stohl A., (1998). Computation, accuracy and applications of trajectories - a review and bibliography, *Atmospheric Environment*, 32: 947-966.
- Stohl A. & Koffi N.E., (1998). Evaluation of Trajectories Calculated from ECMWF Data Against Constant Volume Balloon Flights During ETEX. *Atmospheric Environment*, 32(24):4151-4156.
- Stohl, A., Haimberger, L., Scheele, M. P. & Wernli, H., (2001). An intercomparison of results from three trajectory models. *Meteorological Applications*, 8(2): 127-135. Retrieved from www.scopus.com.
- Stohl A., (2002). Chapter 21 Computation, accuracy and applications of trajectories-A review and bibliography. *Air Pollution Science for the 21st Century*, 615-654, Elsevier Science Ltd.
- Stohl, A., Eckhardt, S., Forster, C., James, P., Spichtinger, N. & Seibert, P., (2002). A replacement for simple back trajectory calculations in the interpretation of atmospheric trace substance measurements. *Atmospheric Environment*, 36(29): 4635-4648. Retrieved from www.scopus.com.
- Stohl, A., Forster, C., Frank, A., Seibert, P., & Wotawa, G., (2005). Technical note: The lagrangian particle dispersion model FLEXPART version 6.2. *Atmospheric Chemistry and Physics*, 5(9): 2461-2474. Retrieved from www.scopus.com.
- Thomas, E. R. & Bracegirdle, T. J., (2009). Improving ice core interpretation using in situ and reanalysis data. *Journal of Geophysical Research D: Atmospheres*, 114(20). Retrieved from www.scopus.com.
- Tuncel, S.G., Öztaş, N.B. & Erduran, M.S., (2008). Air and groundwater pollution in an agricultural region of the Turkish Mediterranean coast. *Journal of the Air and Waste Management Association* 58 (9): 1240-1249.
- Tuncer, B., Bayar, B., Yeşilyurt, C. & Tuncel, G., (2001). Ionic composition of precipitation at the central Anatolia (Turkey). *Atmospheric Environment*, 35: 5989-6002.
- UNECE, (1979). United Nations Economic Commission for Europe, Convention on Long-Range Transboundary Air Pollution.

- UNECE, (2004). United Nations Economic Commission for Europe, Handbook for the 1979 Convention on Long-Range Transboundary Air Pollution and Its Protocols.
- Uygun, N., Karaca, F. & Alagha, O., (2010). Prediction of sources of metal pollution in rainwater in Istanbul, Turkey using factor analysis and long-range transport models. *Atmospheric Research*, 95(1): 55-64.
- Veldt, C., (1991). Emissions of SO_x, NO_x, VOC and CO from East European countries *Atmospheric Environment*. Part A. General Topics, 25 (12): 2683-2700.
- Vestreng, V., Rigler, E., Adams, M., Kindbom, K., Pacyna, J. M., van der Gon, H. D.r, Reis, S. & Travnikov O., (2006). Inventory Review 2006; Emission Data Reported to the LRTAP Convention and NEC Directive.
- Vestreng, V., Mareckova, K., Kakareka, S., Malchykhina A. & Kukharchyk, T. (2007a). Inventory Report 2007; Emission Data Reported to LRTAP Convention and NEC Directive.
- Vestreng, V., Myhre, G., Fagerli, H., Reis, S. & Tarrasón, L., (2007b). Twenty-five years of continuous sulphur dioxide emission reduction in Europe. *Atmospheric Chemistry and Physics*, 7(13): 3663-3681.
- Vienneau, D., de Hoogh, K. & Briggs D., (2009). A GIS-based method for modelling air pollution exposures across Europe. *Science of the Total Environment*, 408:255–266.
- Wain, A. G., Lee, S., Mills, G. A., Hess, G. D., Cope, M. E., & Tindale, N., (2006). Meteorological overview and verification of HYSPLIT and AAQFS dust forecasts for the dust storm of 22-24 October 2002. *Australian Meteorological Magazine*, 55(1): 35-46. Retrieved from www.scopus.com.
- Walmsley, J.L. & Mailhot, J., (1983). On the numerical accuracy of trajectory models for long-range transport of atmospheric pollutants. *Atmos.-Ocean*, 21: 14-39 in Stohl A., (2002). Chapter 21 Computation, accuracy and applications of trajectories-A review and bibliography. *Air Pollution Science for the 21st Century*, 615-654, Elsevier Science Ltd.
- Wang Y.Q., Zhang X.Y. & Draxler, R.R. (2009). TrajStat: GIS-based software that uses various trajectory statistical analysis methods to identify potential sources from long-term air pollution measurement data. *Environmental Modelling & Software*, 24: 938-939.
- Wehrens, R., Putter, H. & Buydens, L.M.C., (2000). “The bootstrap: a tutorial”. *Chemometrics And Intelligent Laboratory Systems*, 54: 35-52.

- Woodfine, D., MacLeod, M. & Mackay, D., (2002). A regionally segmented national scale multimedia contaminant fate model for Canada with GIS data input and display. *Environmental Pollution*, 119:341–355.
- Wotawa, G. & Kröger H., (1999). Testing the ability of trajectory statistics to reproduce emission inventories of air pollutants in cases of negligible measurement and transport errors. *Atmospheric Environment*, 33: 3037-3043.
- Xie Y. & Berkowitz C.M., (2007). The use of conditional probability functions and potential source contribution functions to identify source regions and advection pathways of hydrocarbon emissions in Houston, Texas. *Atmospheric Environment*, 41: 5831–5847.
- Xu, X. & Akhtar, U.S., (2009). Identification of potential regional sources of atmospheric total gaseous mercury in Windsor, Ontario, Canada using hybrid receptor modeling, *Atmos. Chem. Phys. Discuss.*, 9: 24847–24874.
- Yörük, E., (2004). Composition of atmosphere at the Central Anatolia. *M.Sc. Thesis*, Department of Environmental Engineering, Middle East Technical University, Ankara, Turkey.
- Žabkar R., Rakovec J. & Gaberšek S., (2008). A trajectory analysis of summertime ozone pollution in Slovenia. *Geofizika Vol. 25 No. 2*: 179-202.
- Zeng, Y. & Hopke, P.K., (1989). A study of the sources of acid precipitation in Ontario, Canada. *Atmospheric Environment* 23: 1499-1509.
- Zhao, W. & Hopke, P. K., (2006). Source Investigation for Ambient PM_{2.5} in Indianapolis, IN, *Aerosol Science and Technology*, 40: 898–909.
- Zhou L., Hopke, P.K. & Liu W., (2004) Comparison of two trajectory based models for locating particle sources for two rural New York sites. *Atmospheric Environment* 38: 1955–1963.

APPENDIX A

SAMPLE RAW DATA OF A HYSPLIT BACKTRAJECTORY

```

3 1
CDC1 90 7 1 0 0
CDC1 90 8 1 0 0
CDC1 90 9 1 0 0
3 BACKWARD THETA
90 8 1 14 40.169 33.180 100.0
90 8 1 14 40.169 33.180 500.0
90 8 1 14 40.169 33.180 1500.0
3 PRESSURE THETA RAINFALL
1 1 90 8 1 14 0 0 0.0 40.169 33.180 100.0 881.9 305.1 0.0
2 1 90 8 1 14 0 0 0.0 40.169 33.180 500.0 840.6 305.6 0.0
3 1 90 8 1 14 0 0 0.0 40.169 33.180 1500.0 746.5 309.8 0.0
1 1 90 8 1 13 0 0 -1.0 40.355 33.328 114.2 889.1 304.8 0.0
2 1 90 8 1 13 0 0 -1.0 40.340 33.332 651.1 824.1 306.1 0.0
3 1 90 8 1 13 0 0 -1.0 40.323 33.251 1582.1 744.8 309.6 0.0
1 1 90 8 1 12 0 0 -2.0 40.524 33.438 135.8 893.6 304.6 0.0
2 1 90 8 1 12 0 0 -2.0 40.494 33.453 705.7 833.7 305.6 0.0
3 1 90 8 1 12 0 0 -2.0 40.467 33.306 1660.5 743.2 309.4 0.0
1 1 90 8 1 11 0 0 -3.0 40.682 33.542 168.3 897.6 302.8 0.0
2 1 90 8 1 11 0 0 -3.0 40.644 33.575 773.2 834.6 304.6 0.0
3 1 90 8 1 11 0 0 -3.0 40.612 33.365 1738.1 741.3 309.1 0.0
1 1 90 8 1 10 0 0 -4.0 40.833 33.670 225.8 899.6 301.3 0.0
2 1 90 8 1 10 0 0 -4.0 40.798 33.728 871.2 831.6 303.8 0.0
3 1 90 8 1 10 0 0 -4.0 40.764 33.446 1817.3 739.4 308.8 0.0
1 1 90 8 1 9 0 0 -5.0 40.983 33.838 360.9 893.9 300.2 0.0
2 1 90 8 1 9 0 0 -5.0 40.959 33.904 995.7 825.3 303.2 0.0
3 1 90 8 1 9 0 0 -5.0 40.926 33.544 1898.2 737.8 308.5 0.0
1 1 90 8 1 8 0 0 -6.0 41.140 34.049 550.8 876.2 300.0 0.0
2 1 90 8 1 8 0 0 -6.0 41.127 34.098 1135.3 817.9 302.6 0.0
3 1 90 8 1 8 0 0 -6.0 41.097 33.656 1980.5 736.4 308.2 0.0
1 1 90 8 1 7 0 0 -7.0 41.304 34.274 751.9 864.6 299.6 0.0
2 1 90 8 1 7 0 0 -7.0 41.304 34.307 1279.9 811.0 302.1 0.0
3 1 90 8 1 7 0 0 -7.0 41.278 33.776 2063.8 735.4 307.9 0.0
1 1 90 8 1 6 0 0 -8.0 41.479 34.506 975.6 848.9 299.4 0.0
2 1 90 8 1 6 0 0 -8.0 41.491 34.522 1424.9 804.0 301.9 0.0
3 1 90 8 1 6 0 0 -8.0 41.471 33.902 2147.5 734.8 307.6 0.0
1 1 90 8 1 5 0 0 -9.0 41.663 34.724 1170.9 832.4 299.9 0.0
2 1 90 8 1 5 0 0 -9.0 41.683 34.715 1555.7 797.4 302.2 0.0
3 1 90 8 1 5 0 0 -9.0 41.673 34.015 2231.3 734.0 307.4 0.0
1 1 90 8 1 4 0 0 -10.0 41.849 34.910 1316.9 826.7 300.1 0.0
2 1 90 8 1 4 0 0 -10.0 41.876 34.871 1665.0 794.8 302.3 0.0
3 1 90 8 1 4 0 0 -10.0 41.884 34.098 2317.5 733.2 307.3 0.0
1 1 90 8 1 3 0 0 -11.0 42.035 35.064 1429.0 823.3 300.2 0.0

```

2	1	90	8	1	3	0	0	-11.0	42.070	34.995	1758.3	793.2	302.2	0.0
3	1	90	8	1	3	0	0	-11.0	42.103	34.155	2406.2	732.4	307.1	0.0
1	1	90	8	1	2	0	0	-12.0	42.217	35.186	1517.0	821.7	300.2	0.0
2	1	90	8	1	2	0	0	-12.0	42.264	35.090	1840.0	792.3	302.2	0.0
3	1	90	8	1	2	0	0	-12.0	42.331	34.186	2498.9	731.5	306.9	0.0
1	1	90	8	1	1	0	0	-13.0	42.397	35.282	1584.9	821.8	300.1	0.0
2	1	90	8	1	1	0	0	-13.0	42.457	35.160	1912.2	792.2	302.1	0.0
3	1	90	8	1	1	0	0	-13.0	42.569	34.191	2595.2	728.9	306.8	0.0
1	1	90	8	1	0	0	0	-14.0	42.572	35.355	1632.8	821.5	300.1	0.0
2	1	90	8	1	0	0	0	-14.0	42.650	35.203	1970.9	789.0	302.2	0.0
3	1	90	8	1	0	0	0	-14.0	42.816	34.164	2691.0	722.3	307.0	0.0
1	1	90	7	31	23	0	0	-15.0	42.749	35.408	1671.1	820.5	300.2	0.0
2	1	90	7	31	23	0	0	-15.0	42.848	35.222	2024.7	786.2	302.3	0.0
3	1	90	7	31	23	0	0	-15.0	43.074	34.103	2787.6	715.7	307.2	0.0
1	1	90	7	31	22	0	0	-16.0	42.936	35.444	1712.6	818.2	300.3	0.0
2	1	90	7	31	22	0	0	-16.0	43.054	35.217	2080.6	782.6	302.5	0.0
3	1	90	7	31	22	0	0	-16.0	43.343	34.006	2879.5	709.5	307.4	0.0
1	1	90	7	31	21	0	0	-17.0	43.130	35.460	1757.6	815.2	300.4	0.0
2	1	90	7	31	21	0	0	-17.0	43.270	35.188	2138.3	778.9	302.6	0.0
3	1	90	7	31	21	0	0	-17.0	43.625	33.872	2965.5	704.1	307.6	0.0
1	1	90	7	31	20	0	0	-18.0	43.331	35.455	1805.9	812.0	300.6	0.0
2	1	90	7	31	20	0	0	-18.0	43.494	35.133	2197.1	775.1	302.7	0.0
3	1	90	7	31	20	0	0	-18.0	43.922	33.699	3044.4	699.5	307.7	0.0
1	1	90	7	31	19	0	0	-19.0	43.537	35.427	1857.2	808.5	300.7	0.0
2	1	90	7	31	19	0	0	-19.0	43.726	35.051	2256.2	771.2	302.8	0.0
3	1	90	7	31	19	0	0	-19.0	44.236	33.485	3114.8	695.8	307.7	0.0
1	1	90	7	31	18	0	0	-20.0	43.748	35.375	1911.1	804.7	300.8	0.0
2	1	90	7	31	18	0	0	-20.0	43.968	34.938	2314.8	767.3	302.9	0.0
3	1	90	7	31	18	0	0	-20.0	44.570	33.226	3175.4	693.3	307.7	0.0
1	1	90	7	31	17	0	0	-21.0	43.955	35.290	1964.6	800.9	300.8	0.0
2	1	90	7	31	17	0	0	-21.0	44.209	34.789	2370.3	763.6	302.8	0.0
3	1	90	7	31	17	0	0	-21.0	44.916	32.920	3226.8	692.0	307.5	0.0
1	1	90	7	31	16	0	0	-22.0	44.152	35.167	2013.3	797.6	300.8	0.0
2	1	90	7	31	16	0	0	-22.0	44.442	34.602	2420.0	760.6	302.8	0.0
3	1	90	7	31	16	0	0	-22.0	45.264	32.574	3267.6	688.4	307.4	0.0
1	1	90	7	31	15	0	0	-23.0	44.341	35.010	2057.9	794.7	300.7	0.0
2	1	90	7	31	15	0	0	-23.0	44.670	34.378	2464.4	758.2	302.7	0.0
3	1	90	7	31	15	0	0	-23.0	45.608	32.196	3301.7	684.2	307.4	0.0
1	1	90	7	31	14	0	0	-24.0	44.522	34.819	2098.3	792.1	300.7	0.0
2	1	90	7	31	14	0	0	-24.0	44.893	34.118	2503.8	756.2	302.6	0.0
3	1	90	7	31	14	0	0	-24.0	45.942	31.790	3326.4	680.8	307.4	0.0
1	1	90	7	31	13	0	0	-25.0	44.696	34.598	2135.0	789.9	300.6	0.0
2	1	90	7	31	13	0	0	-25.0	45.112	33.825	2537.7	753.4	302.6	0.0
3	1	90	7	31	13	0	0	-25.0	46.265	31.355	3340.1	678.3	307.5	0.0
1	1	90	7	31	12	0	0	-26.0	44.864	34.348	2168.4	787.9	300.6	0.0
2	1	90	7	31	12	0	0	-26.0	45.329	33.502	2568.6	749.6	302.6	0.0
3	1	90	7	31	12	0	0	-26.0	46.580	30.890	3342.4	676.4	307.5	0.0
1	1	90	7	31	11	0	0	-27.0	45.033	34.075	2198.9	786.0	300.4	0.0
2	1	90	7	31	11	0	0	-27.0	45.553	33.158	2600.8	745.7	302.6	0.0
3	1	90	7	31	11	0	0	-27.0	46.897	30.407	3335.4	675.2	307.3	0.0
1	1	90	7	31	10	0	0	-28.0	45.211	33.788	2225.8	782.4	300.5	0.0
2	1	90	7	31	10	0	0	-28.0	45.792	32.797	2635.9	741.4	302.6	0.0
3	1	90	7	31	10	0	0	-28.0	47.229	29.915	3320.1	673.6	307.2	0.0
1	1	90	7	31	9	0	0	-29.0	45.401	33.487	2253.2	778.6	300.5	0.0
2	1	90	7	31	9	0	0	-29.0	46.045	32.418	2673.4	737.0	302.6	0.0
3	1	90	7	31	9	0	0	-29.0	47.574	29.417	3295.2	670.6	307.2	0.0
1	1	90	7	31	8	0	0	-30.0	45.602	33.170	2281.1	774.8	300.6	0.0
2	1	90	7	31	8	0	0	-30.0	46.312	32.021	2709.8	732.4	302.6	0.0

3	1	90	7	31	8	0	0	-30.0	47.927	28.930	3273.9	669.5	307.2	0.0
1	1	90	7	31	7	0	0	-31.0	45.817	32.835	2309.3	771.0	300.6	0.0
2	1	90	7	31	7	0	0	-31.0	46.589	31.608	2741.5	728.1	302.7	0.0
3	1	90	7	31	7	0	0	-31.0	48.290	28.461	3255.7	668.7	307.2	0.0
1	1	90	7	31	6	0	0	-32.0	46.044	32.483	2337.8	767.3	300.6	0.0
2	1	90	7	31	6	0	0	-32.0	46.879	31.175	2766.6	724.1	302.7	0.0
3	1	90	7	31	6	0	0	-32.0	48.662	28.003	3239.7	668.5	307.3	0.0
1	1	90	7	31	5	0	0	-33.0	46.279	32.117	2359.5	763.8	300.9	0.0
2	1	90	7	31	5	0	0	-33.0	47.175	30.724	2775.9	720.8	302.9	0.0
3	1	90	7	31	5	0	0	-33.0	49.038	27.552	3223.0	668.8	307.3	0.0
1	1	90	7	31	4	0	0	-34.0	46.512	31.745	2362.1	762.4	301.1	0.0
2	1	90	7	31	4	0	0	-34.0	47.470	30.259	2761.9	719.9	303.0	0.0
3	1	90	7	31	4	0	0	-34.0	49.405	27.100	3209.5	669.6	307.4	0.0
1	1	90	7	31	3	0	0	-35.0	46.742	31.367	2343.1	762.7	301.3	0.0
2	1	90	7	31	3	0	0	-35.0	47.758	29.791	2729.9	721.1	303.0	0.0
3	1	90	7	31	3	0	0	-35.0	49.761	26.642	3199.7	670.0	307.4	0.0
1	1	90	7	31	2	0	0	-36.0	46.963	30.982	2261.7	768.9	301.2	0.0
2	1	90	7	31	2	0	0	-36.0	48.036	29.335	2664.2	724.2	303.1	0.0
3	1	90	7	31	2	0	0	-36.0	50.106	26.174	3195.8	669.8	307.4	0.0
1	1	90	7	31	1	0	0	-37.0	47.171	30.593	2155.8	777.2	301.2	0.0
2	1	90	7	31	1	0	0	-37.0	48.300	28.889	2597.8	727.3	303.2	0.0
3	1	90	7	31	1	0	0	-37.0	50.438	25.698	3197.2	669.7	307.4	0.0
1	1	90	7	31	0	0	0	-38.0	47.364	30.198	2023.2	787.7	301.2	0.0
2	1	90	7	31	0	0	0	-38.0	48.550	28.448	2530.4	730.9	303.2	0.0
3	1	90	7	31	0	0	0	-38.0	50.757	25.218	3203.5	669.5	307.4	0.0
1	1	90	7	30	23	0	0	-39.0	47.540	29.802	1877.3	800.7	300.9	0.0
2	1	90	7	30	23	0	0	-39.0	48.794	28.013	2467.5	735.4	303.2	0.0
3	1	90	7	30	23	0	0	-39.0	51.068	24.742	3216.0	670.2	307.4	0.0
1	1	90	7	30	22	0	0	-40.0	47.705	29.413	1738.8	812.6	300.6	0.0
2	1	90	7	30	22	0	0	-40.0	49.040	27.587	2412.8	739.3	303.1	0.0
3	1	90	7	30	22	0	0	-40.0	51.375	24.278	3233.2	671.2	307.4	0.0
1	1	90	7	30	21	0	0	-41.0	47.860	29.038	1618.8	821.5	300.4	0.0
2	1	90	7	30	21	0	0	-41.0	49.288	27.171	2370.9	742.6	303.0	0.0
3	1	90	7	30	21	0	0	-41.0	51.676	23.824	3252.9	672.0	307.3	0.0
1	1	90	7	30	20	0	0	-42.0	48.007	28.678	1516.4	829.3	300.2	0.0
2	1	90	7	30	20	0	0	-42.0	49.537	26.766	2344.0	744.5	303.0	0.0
3	1	90	7	30	20	0	0	-42.0	51.974	23.375	3274.7	672.6	307.3	0.0
1	1	90	7	30	19	0	0	-43.0	48.149	28.332	1432.5	835.8	300.0	0.0
2	1	90	7	30	19	0	0	-43.0	49.786	26.371	2331.7	745.1	303.0	0.0
3	1	90	7	30	19	0	0	-43.0	52.270	22.929	3297.7	673.1	307.3	0.0
1	1	90	7	30	18	0	0	-44.0	48.288	28.001	1369.3	840.7	299.9	0.0
2	1	90	7	30	18	0	0	-44.0	50.037	25.985	2331.9	744.6	303.0	0.0
3	1	90	7	30	18	0	0	-44.0	52.565	22.486	3320.6	673.1	307.3	0.0
1	1	90	7	30	17	0	0	-45.0	48.421	27.681	1318.2	843.2	299.7	0.1
2	1	90	7	30	17	0	0	-45.0	50.283	25.595	2335.2	743.0	303.0	0.2
3	1	90	7	30	17	0	0	-45.0	52.860	22.030	3369.0	669.8	307.3	0.0
1	1	90	7	30	16	0	0	-46.0	48.539	27.371	1242.8	849.0	299.7	0.1
2	1	90	7	30	16	0	0	-46.0	50.522	25.188	2344.0	741.9	303.0	0.2
3	1	90	7	30	16	0	0	-46.0	53.154	21.552	3415.9	666.9	307.2	0.0
1	1	90	7	30	15	0	0	-47.0	48.640	27.073	1167.5	855.2	299.7	0.1
2	1	90	7	30	15	0	0	-47.0	50.751	24.762	2351.5	742.0	303.0	0.2
3	1	90	7	30	15	0	0	-47.0	53.446	21.053	3459.6	664.3	307.2	0.0
1	1	90	7	30	14	0	0	-48.0	48.724	26.785	1093.0	860.9	299.7	0.1
2	1	90	7	30	14	0	0	-48.0	50.970	24.317	2357.4	743.1	302.9	0.1
3	1	90	7	30	14	0	0	-48.0	53.739	20.535	3500.1	662.0	307.2	0.0
1	1	90	7	30	13	0	0	-49.0	48.789	26.504	1014.4	867.3	299.8	0.1
2	1	90	7	30	13	0	0	-49.0	51.180	23.853	2361.3	744.3	302.8	0.1
3	1	90	7	30	13	0	0	-49.0	54.033	19.999	3537.2	659.9	307.2	0.0

1	1	90	7	30	12	0	0	-50.0	48.832	26.228	926.7	874.7	299.8	0.1
2	1	90	7	30	12	0	0	-50.0	51.380	23.368	2364.0	745.6	302.7	0.1
3	1	90	7	30	12	0	0	-50.0	54.325	19.448	3568.6	657.2	307.2	0.0
1	1	90	7	30	11	0	0	-51.0	48.867	25.962	859.0	882.8	299.5	0.0
2	1	90	7	30	11	0	0	-51.0	51.577	22.877	2370.5	747.3	302.7	0.2
3	1	90	7	30	11	0	0	-51.0	54.613	18.890	3596.7	655.0	307.2	0.0
1	1	90	7	30	10	0	0	-52.0	48.912	25.702	825.8	883.7	299.4	0.0
2	1	90	7	30	10	0	0	-52.0	51.773	22.394	2379.4	748.5	302.7	0.3
3	1	90	7	30	10	0	0	-52.0	54.901	18.325	3620.2	652.9	307.2	0.0
1	1	90	7	30	9	0	0	-53.0	48.966	25.446	818.4	882.6	299.3	0.0
2	1	90	7	30	9	0	0	-53.0	51.966	21.919	2391.5	750.0	302.7	0.2
3	1	90	7	30	9	0	0	-53.0	55.188	17.757	3643.0	650.9	307.2	0.0
1	1	90	7	30	8	0	0	-54.0	49.032	25.189	834.6	879.7	299.2	0.0
2	1	90	7	30	8	0	0	-54.0	52.155	21.450	2405.4	751.1	302.6	0.2
3	1	90	7	30	8	0	0	-54.0	55.474	17.188	3667.9	648.9	307.2	0.0
1	1	90	7	30	7	0	0	-55.0	49.111	24.933	875.3	875.2	299.1	0.0
2	1	90	7	30	7	0	0	-55.0	52.341	20.983	2420.9	751.9	302.6	0.2
3	1	90	7	30	7	0	0	-55.0	55.752	16.625	3697.1	646.9	307.2	0.0
1	1	90	7	30	6	0	0	-56.0	49.209	24.677	955.8	866.8	299.1	0.0
2	1	90	7	30	6	0	0	-56.0	52.522	20.514	2437.1	752.3	302.5	0.1
3	1	90	7	30	6	0	0	-56.0	56.025	16.070	3728.4	644.9	307.2	0.0
1	1	90	7	30	5	0	0	-57.0	49.315	24.427	1019.5	859.4	299.4	0.0
2	1	90	7	30	5	0	0	-57.0	52.697	20.040	2449.5	751.6	302.6	0.0
3	1	90	7	30	5	0	0	-57.0	56.281	15.524	3757.1	642.9	307.2	0.0
1	1	90	7	30	4	0	0	-58.0	49.415	24.187	1051.5	857.2	299.6	0.0
2	1	90	7	30	4	0	0	-58.0	52.859	19.563	2458.0	751.2	302.7	0.0
3	1	90	7	30	4	0	0	-58.0	56.510	14.984	3785.5	641.0	307.2	0.0
1	1	90	7	30	3	0	0	-59.0	49.502	23.955	1053.2	857.8	299.8	0.0
2	1	90	7	30	3	0	0	-59.0	53.009	19.085	2462.8	751.1	302.7	0.0
3	1	90	7	30	3	0	0	-59.0	56.710	14.445	3811.1	639.0	307.1	0.0
1	1	90	7	30	2	0	0	-60.0	49.571	23.733	1022.3	861.3	300.0	0.0
2	1	90	7	30	2	0	0	-60.0	53.144	18.604	2465.4	751.2	302.7	0.0
3	1	90	7	30	2	0	0	-60.0	56.882	13.902	3831.6	637.5	307.1	0.0
1	1	90	7	30	1	0	0	-61.0	49.618	23.525	952.3	868.5	300.0	0.0
2	1	90	7	30	1	0	0	-61.0	53.265	18.119	2467.3	751.3	302.8	0.0
3	1	90	7	30	1	0	0	-61.0	57.029	13.349	3846.1	636.4	307.1	0.0
1	1	90	7	30	0	0	0	-62.0	49.637	23.343	841.4	880.3	300.1	0.0
2	1	90	7	30	0	0	0	-62.0	53.371	17.629	2470.0	751.5	302.8	0.0
3	1	90	7	30	0	0	0	-62.0	57.156	12.781	3853.8	635.9	307.0	0.0
1	1	90	7	29	23	0	0	-63.0	49.645	23.201	732.2	895.1	300.1	0.0
2	1	90	7	29	23	0	0	-63.0	53.462	17.141	2472.3	751.3	302.8	0.0
3	1	90	7	29	23	0	0	-63.0	57.259	12.192	3854.2	635.7	307.0	0.0
1	1	90	7	29	22	0	0	-64.0	49.664	23.092	640.5	903.9	300.2	0.0
2	1	90	7	29	22	0	0	-64.0	53.535	16.665	2471.7	751.2	302.9	0.0
3	1	90	7	29	22	0	0	-64.0	57.337	11.581	3856.5	635.5	307.0	0.0
1	1	90	7	29	21	0	0	-65.0	49.685	23.029	346.3	944.4	298.4	0.0
2	1	90	7	29	21	0	0	-65.0	53.591	16.198	2467.8	751.6	302.9	0.0
3	1	90	7	29	21	0	0	-65.0	57.395	10.949	3861.0	634.8	307.1	0.0
1	1	90	7	29	20	0	0	-66.0	49.717	22.998	140.8	953.7	298.3	0.0
2	1	90	7	29	20	0	0	-66.0	53.628	15.737	2464.6	751.6	302.9	0.0
3	1	90	7	29	20	0	0	-66.0	57.440	10.297	3868.1	633.9	307.1	0.0
1	1	90	7	29	19	0	0	-67.0	49.759	22.982	0.0	973.0	298.1	0.0
2	1	90	7	29	19	0	0	-67.0	53.645	15.279	2461.9	751.6	302.9	0.0
3	1	90	7	29	19	0	0	-67.0	57.478	9.629	3878.1	633.2	307.1	0.0
1	1	90	7	29	18	0	0	-68.0	49.826	22.970	0.0	973.1	299.2	0.0
2	1	90	7	29	18	0	0	-68.0	53.645	14.823	2459.9	751.7	302.9	0.0
3	1	90	7	29	18	0	0	-68.0	57.515	8.949	3889.3	632.4	307.1	0.0
1	1	90	7	29	17	0	0	-69.0	49.905	22.942	0.0	973.3	299.3	0.0

2	1	90	7	29	17	0	0	-69.0	53.631	14.373	2455.6	752.4	303.1	0.0
3	1	90	7	29	17	0	0	-69.0	57.537	8.264	3904.2	631.8	307.1	0.0
1	1	90	7	29	16	0	0	-70.0	49.973	22.879	0.0	973.4	299.4	0.0
2	1	90	7	29	16	0	0	-70.0	53.608	13.932	2442.7	754.0	303.3	0.0
3	1	90	7	29	16	0	0	-70.0	57.532	7.583	3927.2	630.5	307.0	0.0
1	1	90	7	29	15	0	0	-71.0	50.031	22.783	0.0	973.9	299.5	0.0
2	1	90	7	29	15	0	0	-71.0	53.572	13.498	2421.9	756.3	303.4	0.0
3	1	90	7	29	15	0	0	-71.0	57.500	6.904	3959.4	628.8	307.0	0.0
1	1	90	7	29	14	0	0	-72.0	50.077	22.656	0.0	974.5	299.7	0.0
2	1	90	7	29	14	0	0	-72.0	53.520	13.070	2392.7	759.3	303.5	0.0
3	1	90	7	29	14	0	0	-72.0	57.443	6.226	4015.7	624.6	307.1	0.0
1	1	90	7	29	13	0	0	-73.0	50.112	22.501	61.9	967.8	299.8	0.0
2	1	90	7	29	13	0	0	-73.0	53.451	12.648	2341.5	764.7	303.5	0.0
3	1	90	7	29	13	0	0	-73.0	57.372	5.546	4072.4	620.5	307.1	0.0
1	1	90	7	29	12	0	0	-74.0	50.134	22.325	107.3	963.0	299.8	0.0
2	1	90	7	29	12	0	0	-74.0	53.365	12.230	2291.6	769.7	303.5	0.0
3	1	90	7	29	12	0	0	-74.0	57.294	4.859	4128.0	616.3	307.1	0.0
1	1	90	7	29	11	0	0	-75.0	50.150	22.149	146.8	960.1	298.8	0.0
2	1	90	7	29	11	0	0	-75.0	53.271	11.824	2244.3	774.3	303.4	0.0
3	1	90	7	29	11	0	0	-75.0	57.203	4.173	4181.1	611.4	307.1	0.0
1	1	90	7	29	10	0	0	-76.0	50.170	21.990	189.4	956.7	297.8	0.0
2	1	90	7	29	10	0	0	-76.0	53.176	11.437	2198.0	778.5	303.3	0.0
3	1	90	7	29	10	0	0	-76.0	57.091	3.493	4238.0	606.2	307.1	0.0
1	1	90	7	29	9	0	0	-77.0	50.198	21.850	236.3	951.6	296.9	0.0
2	1	90	7	29	9	0	0	-77.0	53.077	11.066	2151.0	782.5	303.3	0.0
3	1	90	7	29	9	0	0	-77.0	56.962	2.817	4296.7	600.8	307.0	0.0
1	1	90	7	29	8	0	0	-78.0	50.241	21.726	291.4	946.4	296.3	0.0
2	1	90	7	29	8	0	0	-78.0	52.971	10.706	2100.9	786.6	303.3	0.0
3	1	90	7	29	8	0	0	-78.0	56.817	2.143	4356.8	594.9	307.0	0.0
1	1	90	7	29	7	0	0	-79.0	50.303	21.620	363.2	940.2	295.8	0.0
2	1	90	7	29	7	0	0	-79.0	52.858	10.356	2045.1	791.2	303.3	0.0
3	1	90	7	29	7	0	0	-79.0	56.658	1.470	4420.1	588.4	307.0	0.0
1	1	90	7	29	6	0	0	-80.0	50.391	21.527	469.6	930.7	295.6	0.0
2	1	90	7	29	6	0	0	-80.0	52.736	10.015	1980.2	796.5	303.4	0.0
3	1	90	7	29	6	0	0	-80.0	56.491	0.792	4487.8	581.4	307.1	0.0
1	1	90	7	29	5	0	0	-81.0	50.500	21.436	600.7	914.8	296.5	0.0
2	1	90	7	29	5	0	0	-81.0	52.613	9.685	1912.3	803.5	303.2	0.0
3	1	90	7	29	5	0	0	-81.0	56.314	0.116	4554.0	574.8	307.4	0.0
1	1	90	7	29	4	0	0	-82.0	50.617	21.336	705.7	903.0	296.9	0.0
2	1	90	7	29	4	0	0	-82.0	52.499	9.369	1847.3	809.5	303.1	0.0
3	1	90	7	29	4	0	0	-82.0	56.110	-0.546	4603.9	568.9	307.7	0.0
1	1	90	7	29	3	0	0	-83.0	50.735	21.230	770.9	897.3	297.2	0.0
2	1	90	7	29	3	0	0	-83.0	52.391	9.072	1783.9	814.9	303.0	0.0
3	1	90	7	29	3	0	0	-83.0	55.875	-1.195	4629.5	565.8	307.8	0.0
1	1	90	7	29	2	0	0	-84.0	50.853	21.120	796.3	896.3	297.4	0.0
2	1	90	7	29	2	0	0	-84.0	52.290	8.795	1720.7	820.4	302.9	0.0
3	1	90	7	29	2	0	0	-84.0	55.612	-1.829	4635.8	564.2	307.8	0.0
1	1	90	7	29	1	0	0	-85.0	50.969	21.006	786.0	899.1	297.5	0.0
2	1	90	7	29	1	0	0	-85.0	52.193	8.540	1655.4	825.8	302.9	0.0
3	1	90	7	29	1	0	0	-85.0	55.328	-2.453	4629.6	563.4	307.7	0.0
1	1	90	7	29	0	0	0	-86.0	51.080	20.889	746.4	905.1	297.5	0.0
2	1	90	7	29	0	0	0	-86.0	52.099	8.308	1585.9	831.8	302.9	0.0
3	1	90	7	29	0	0	0	-86.0	55.022	-3.068	4623.8	563.7	307.5	0.0
1	1	90	7	28	23	0	0	-87.0	51.185	20.772	703.4	913.7	297.3	0.0
2	1	90	7	28	23	0	0	-87.0	52.007	8.103	1513.3	838.8	302.7	0.0
3	1	90	7	28	23	0	0	-87.0	54.703	-3.671	4627.7	563.3	307.8	0.0
1	1	90	7	28	22	0	0	-88.0	51.285	20.660	673.5	918.1	297.2	0.0
2	1	90	7	28	22	0	0	-88.0	51.916	7.929	1436.4	846.0	302.5	0.0

3	1	90	7	28	22	0	0	-88.0	54.380	-4.261	4647.3	561.7	307.9	0.0
1	1	90	7	28	21	0	0	-89.0	51.380	20.553	651.9	921.7	297.2	0.0
2	1	90	7	28	21	0	0	-89.0	51.827	7.786	1351.1	854.2	302.4	0.0
3	1	90	7	28	21	0	0	-89.0	54.057	-4.839	4682.5	559.0	307.9	0.0
1	1	90	7	28	20	0	0	-90.0	51.472	20.452	634.6	924.7	297.1	0.0
2	1	90	7	28	20	0	0	-90.0	51.741	7.678	1248.1	863.8	302.3	0.1
3	1	90	7	28	20	0	0	-90.0	53.734	-5.402	4734.6	555.5	307.9	0.0
1	1	90	7	28	19	0	0	-91.0	51.561	20.356	616.9	927.5	297.1	0.0
2	1	90	7	28	19	0	0	-91.0	51.662	7.608	1100.4	876.3	302.2	0.1
3	1	90	7	28	19	0	0	-91.0	53.414	-5.950	4801.3	551.4	307.9	0.0
1	1	90	7	28	18	0	0	-92.0	51.648	20.266	588.5	930.9	297.1	0.0
2	1	90	7	28	18	0	0	-92.0	51.597	7.583	851.0	899.0	302.1	0.1
3	1	90	7	28	18	0	0	-92.0	53.102	-6.483	4882.1	546.4	307.9	0.0
1	1	90	7	28	17	0	0	-93.0	51.727	20.179	535.2	936.9	296.7	0.0
2	1	90	7	28	17	0	0	-93.0	51.558	7.607	531.4	938.8	301.2	0.0
3	1	90	7	28	17	0	0	-93.0	52.795	-6.997	4963.6	540.7	308.3	0.3
1	1	90	7	28	16	0	0	-94.0	51.794	20.093	420.8	947.2	296.2	0.0
2	1	90	7	28	16	0	0	-94.0	51.541	7.660	181.7	973.9	300.4	0.0
3	1	90	7	28	16	0	0	-94.0	52.485	-7.490	5033.9	536.9	308.5	0.4
1	1	90	7	28	15	0	0	-95.0	51.847	20.019	159.4	974.9	295.9	0.0
2	1	90	7	28	15	0	0	-95.0	51.541	7.710	0.0	997.5	301.0	0.0
3	1	90	7	28	15	0	0	-95.0	52.172	-7.965	5093.2	533.4	308.8	0.4
1	1	90	7	28	14	0	0	-96.0	51.899	19.975	0.0	1000.1	295.4	0.0
2	1	90	7	28	14	0	0	-96.0	51.535	7.736	0.0	997.6	301.0	0.0
3	1	90	7	28	14	0	0	-96.0	51.857	-8.427	5144.1	530.5	309.0	0.3
1	1	90	7	28	13	0	0	-97.0	51.964	19.942	0.0	1000.8	295.3	0.0
2	1	90	7	28	13	0	0	-97.0	51.512	7.758	0.0	997.6	301.2	0.0
3	1	90	7	28	13	0	0	-97.0	51.545	-8.882	5188.6	528.0	309.1	0.3
1	1	90	7	28	12	0	0	-98.0	52.037	19.896	0.0	1001.7	295.2	0.0
2	1	90	7	28	12	0	0	-98.0	51.473	7.776	0.0	997.5	301.3	0.0
3	1	90	7	28	12	0	0	-98.0	51.241	-9.332	5228.6	525.8	309.1	0.2
1	1	90	7	28	11	0	0	-99.0	52.106	19.843	0.0	1001.8	293.9	0.0
2	1	90	7	28	11	0	0	-99.0	51.420	7.804	50.8	994.1	299.4	0.0
3	1	90	7	28	11	0	0	-99.0	50.953	-9.790	5262.2	523.5	309.2	0.1
1	1	90	7	28	10	0	0	-100.0	52.160	19.796	0.0	1003.1	292.5	0.0
2	1	90	7	28	10	0	0	-100.0	51.351	7.860	105.1	984.3	297.9	0.0
3	1	90	7	28	10	0	0	-100.0	50.683	-10.270	5288.0	521.4	309.2	0.1
1	1	90	7	28	9	0	0	-101.0	52.201	19.752	0.0	1003.6	291.2	0.0
2	1	90	7	28	9	0	0	-101.0	51.268	7.917	155.6	978.7	296.9	0.0
3	1	90	7	28	9	0	0	-101.0	50.429	-10.773	5303.1	519.9	309.4	0.0
1	1	90	7	28	8	0	0	-102.0	52.230	19.712	0.0	1003.9	289.9	0.0
2	1	90	7	28	8	0	0	-102.0	51.172	7.969	208.1	972.9	296.2	0.0
3	1	90	7	28	8	0	0	-102.0	50.193	-11.298	5307.2	519.1	309.5	0.0
1	1	90	7	28	7	0	0	-103.0	52.246	19.676	0.0	1004.1	288.6	0.0
2	1	90	7	28	7	0	0	-103.0	51.062	8.013	266.4	965.0	295.8	0.0
3	1	90	7	28	7	0	0	-103.0	49.978	-11.845	5302.7	518.9	309.5	0.0
1	1	90	7	28	6	0	0	-104.0	52.251	19.644	0.0	1004.2	287.4	0.0
2	1	90	7	28	6	0	0	-104.0	50.938	8.046	328.4	957.0	295.7	0.0
3	1	90	7	28	6	0	0	-104.0	49.791	-12.410	5294.6	519.0	309.5	0.0
1	1	90	7	28	5	0	0	-105.0	52.255	19.622	0.0	1004.4	287.2	0.0
2	1	90	7	28	5	0	0	-105.0	50.805	8.076	380.2	949.5	296.8	0.0
3	1	90	7	28	5	0	0	-105.0	49.632	-12.978	5290.4	519.9	309.6	0.1
1	1	90	7	28	4	0	0	-106.0	52.272	19.618	0.0	1004.7	286.9	0.0
2	1	90	7	28	4	0	0	-106.0	50.670	8.111	414.1	944.7	297.5	0.0
3	1	90	7	28	4	0	0	-106.0	49.497	-13.535	5287.3	520.5	309.7	0.1
1	1	90	7	28	3	0	0	-107.0	52.301	19.632	0.0	1005.1	286.7	0.0
2	1	90	7	28	3	0	0	-107.0	50.535	8.152	432.4	941.6	298.1	0.0
3	1	90	7	28	3	0	0	-107.0	49.390	-14.079	5288.9	520.6	309.7	0.0

1	1	90	7	28	2	0	0	-108.0	52.343	19.663	0.0	1005.7	286.4	0.0
2	1	90	7	28	2	0	0	-108.0	50.401	8.198	435.9	940.2	298.4	0.0
3	1	90	7	28	2	0	0	-108.0	49.313	-14.604	5296.6	520.2	309.7	0.0
1	1	90	7	28	1	0	0	-109.0	52.396	19.711	0.0	1006.4	286.2	0.0
2	1	90	7	28	1	0	0	-109.0	50.270	8.252	425.2	940.3	298.6	0.0
3	1	90	7	28	1	0	0	-109.0	49.270	-15.108	5311.5	519.2	309.7	0.0
1	1	90	7	28	0	0	0	-110.0	52.461	19.776	0.0	1007.3	285.9	0.0
2	1	90	7	28	0	0	0	-110.0	50.143	8.318	400.8	942.0	298.7	0.0
3	1	90	7	28	0	0	0	-110.0	49.259	-15.589	5333.6	517.6	309.7	0.0
1	1	90	7	27	23	0	0	-111.0	52.541	19.846	11.0	1005.5	286.7	0.0
2	1	90	7	27	23	0	0	-111.0	50.025	8.394	342.3	945.0	299.1	0.0
3	1	90	7	27	23	0	0	-111.0	49.272	-16.069	5365.7	515.5	309.6	0.0
1	1	90	7	27	22	0	0	-112.0	52.632	19.910	6.9	1006.1	287.2	0.0
2	1	90	7	27	22	0	0	-112.0	49.927	8.486	222.7	954.2	298.7	0.0
3	1	90	7	27	22	0	0	-112.0	49.304	-16.571	5402.9	512.7	309.5	0.0
1	1	90	7	27	21	0	0	-113.0	52.732	19.967	0.0	1007.1	287.8	0.0
2	1	90	7	27	21	0	0	-113.0	49.855	8.608	11.4	972.6	297.9	0.0
3	1	90	7	27	21	0	0	-113.0	49.363	-17.096	5448.3	509.3	309.4	0.0
1	1	90	7	27	20	0	0	-114.0	52.844	20.019	0.0	1007.0	288.4	0.0
2	1	90	7	27	20	0	0	-114.0	49.808	8.747	0.0	976.9	298.8	0.0
3	1	90	7	27	20	0	0	-114.0	49.456	-17.643	5501.0	505.2	309.2	0.0
1	1	90	7	27	19	0	0	-115.0	52.970	20.065	0.0	1007.1	289.0	0.0
2	1	90	7	27	19	0	0	-115.0	49.778	8.870	0.0	975.1	300.2	0.0
3	1	90	7	27	19	0	0	-115.0	49.588	-18.217	5556.8	500.6	309.2	0.0
1	1	90	7	27	18	0	0	-116.0	53.110	20.108	0.0	1007.2	289.6	0.0
2	1	90	7	27	18	0	0	-116.0	49.765	8.975	0.0	973.9	301.6	0.0
3	1	90	7	27	18	0	0	-116.0	49.768	-18.820	5613.1	495.9	309.2	0.0
1	1	90	7	27	17	0	0	-117.0	53.260	20.145	0.0	1007.8	289.8	0.3
2	1	90	7	27	17	0	0	-117.0	49.761	9.073	0.0	973.4	301.4	0.0
3	1	90	7	27	17	0	0	-117.0	49.984	-19.436	5660.6	491.4	309.6	0.0
1	1	90	7	27	16	0	0	-118.0	53.415	20.175	0.0	1008.4	290.0	0.3
2	1	90	7	27	16	0	0	-118.0	49.746	9.165	0.0	947.3	301.7	0.0
3	1	90	7	27	16	0	0	-118.0	50.214	-20.038	5692.2	489.4	309.8	0.0
1	1	90	7	27	15	0	0	-119.0	53.574	20.201	0.0	1009.0	290.1	0.3
2	1	90	7	27	15	0	0	-119.0	49.706	9.218	473.2	856.1	301.9	0.0
3	1	90	7	27	15	0	0	-119.0	50.446	-20.607	5713.2	488.5	310.0	0.0
1	1	90	7	27	14	0	0	-120.0	53.735	20.226	0.0	1009.6	290.2	0.2
2	1	90	7	27	14	0	0	-120.0	49.680	9.305	1449.1	969.8	300.9	0.0
3	1	90	7	27	14	0	0	-120.0	50.679	-21.141	5729.3	488.0	310.1	0.0

APPENDIX B

SOURCE CODE OF HYSPLIT TRAJECTORY DATA IMPORT TOOL

```
dim k ,m,i as integer
dim yil,pth,ay ,gun as string
pth = Applicationdirectory$(0)
if right$(pth,1) <> "\" then
    pth = pth + "\"
end if

Create Table "p100" (h_id Char(4),_COL2 Char(8),year Char(5),month Char(8),day Float,hour
Float,_COL7 Float,_COL8 Smallint,t_counter Float,lat Float,long Float,h Float,_COL13
Float,_COL14 Float, rain Float,tarih Char(8)) file pth + "p100.tab" TYPE NATIVE Charset
"WindowsTurkish"
Create Map For p100 CoordSys Earth Projection 1, 0
Create Table "p500" (h_id Char(4),_COL2 Char(8),year Char(5),month Char(8),day Float,hour
Float,_COL7 Float,_COL8 Smallint,t_counter Float,lat Float,long Float,h Float,_COL13
Float,_COL14 Float, rain Float,tarih Char(8)) file pth + "p500.tab" TYPE NATIVE Charset
"WindowsTurkish"
Create Map For p500 CoordSys Earth Projection 1, 0
Create Table "p1500" (h_id Char(4),_COL2 Char(8),year Char(5),month Char(8),day Float,hour
Float,_COL7 Float,_COL8 Smallint,t_counter Float,lat Float,long Float,h Float,_COL13
Float,_COL14 Float, rain Float,tarih Char(8)) file pth + "p1500.tab" TYPE NATIVE Charset
"WindowsTurkish"
Create Map For p1500 CoordSys Earth Projection 1, 0

Open Table pth + "p100.tab" Interactive
Open Table pth + "p500.tab" Interactive
Open Table pth + "p1500.tab" Interactive

for k = 1990 to 2006
for m = 1 to 12
for i = 1 to 31
do case m
case 1
ay = "ocak"
case 2
ay = "ubat"
case 3
ay = "mart"
case 4
ay = "nisan"
case 5
ay = "mayis"
case 6
ay = "haziran"
```

```

case 7
ay = "temmuz"
case 8
ay = "agustos"
case 9
ay = "eylul"
case 10
ay = "ekim"
case 11
ay = "kasim"
case 12
ay = "aralik"
end case
yil = k
if i < 10 then
    gun = "0" + i
else
    gun = i
end if
if m < 10 then
    gun = gun + "0"+m
else
    gun = gun + m
end if
gun = gun + right$(Str$(k),2)

if not fileexists(pth + yil + "\" + ay + "\" + gun + ".txt") then
goto gec1
end if

Register Table pth + yil + "\" + ay + "\" + gun + ".txt" TYPE ASCII Delimiter 32 Charset
"WindowsTurkish" Into pth + yil + "\" + ay + "\" + gun + ".TAB"
Open Table pth + yil + "\" + ay + "\" + gun + ".TAB" as data2 Interactive
commit table data2 as pth + yil + "\" + ay + "\" + data1.tab"
Open Table pth + yil + "\" + ay + "\" + data1.TAB" as data1 Interactive
Alter Table data1 ( add tarih Char(8) ) Interactive
update data1 set tarih = gun

Select * from data1 where rowid >= 10 and col1 = any("1","2","3") order by col9 desc ,col1 into sel1
select * from sel1 where col1 = "1" into sel2
insert into p100 select * from sel2
select * from sel1 where col1 = "2" into sel2
insert into p500 select * from sel2
select * from sel1 where col1 = "3" into sel2
insert into p1500 select * from sel2
close table data1
close table data2

gec1:
next
next
next

```

APPENDIX C

SAMPLE RAW DATA OF A ECMWF BACKTRAJECTORY

TRAJECTORY NUMBER 1

START: LAT 40.2 DEG N PRESSURE LEVEL 1000 HPA
 LON 33.2 DEG E TIME 14 UTC ON 1. 8.90

END: TIME 0 UTC ON 27. 7.90

ANALYSIS FIELDS FROM TIME 14 UTC ON 1. 8.90

HOURS LAT LON LEVEL U-WIND V-WIND W-WIND PS

0	40.17 N	33.18 E	1000.0	9.0	1.8	-0.25	874.2
1	40.10 N	32.79 E	873.3	-2.6	-2.8	-0.19	874.2
2	40.19 N	32.88 E	873.3	-2.3	-2.6	-0.22	874.2
3	40.26 N	32.95 E	873.3	-2.1	-2.5	-0.19	874.2
4	40.34 N	33.02 E	873.4	-1.8	-2.3	-0.16	874.4
5	40.40 N	33.07 E	873.7	-1.6	-2.0	-0.12	874.7
6	40.45 N	33.12 E	874.1	-1.3	-1.7	-0.09	875.2
7	40.50 N	33.17 E	874.6	-1.1	-1.3	-0.05	875.7
8	40.53 N	33.20 E	875.6	-0.7	-0.8	-0.01	876.2
9	40.56 N	33.23 E	875.7	-0.9	-1.1	0.01	876.6
10	40.60 N	33.28 E	875.2	-1.2	-1.4	0.02	877.3
11	40.66 N	33.33 E	874.1	-1.6	-1.8	0.04	878.3
12	40.72 N	33.42 E	871.9	-2.3	-2.2	0.08	879.9
13	40.80 N	33.53 E	868.2	-3.2	-2.7	0.13	882.2
14	40.89 N	33.69 E	862.1	-3.6	-3.1	0.19	885.9
15	41.00 N	33.84 E	855.7	-3.7	-3.9	0.17	890.9
16	41.14 N	34.00 E	850.3	-3.4	-4.5	0.13	898.0
17	41.29 N	34.14 E	846.1	-2.8	-4.8	0.10	906.9
18	41.45 N	34.25 E	842.9	-2.1	-5.0	0.08	917.4
19	41.61 N	34.32 E	840.1	-1.3	-5.0	0.07	928.9
20	41.78 N	34.36 E	837.7	-0.7	-5.1	0.06	941.2
21	41.94 N	34.38 E	834.7	-0.2	-5.0	0.11	953.7
22	42.10 N	34.38 E	829.7	0.1	-4.9	0.17	966.0
23	42.26 N	34.37 E	822.4	0.3	-5.0	0.24	978.0
24	42.43 N	34.35 E	812.7	0.5	-5.0	0.31	989.2
25	42.59 N	34.33 E	800.4	0.8	-5.3	0.38	999.8
26	42.78 N	34.29 E	785.6	1.1	-6.0	0.45	1009.6
27	42.99 N	34.23 E	770.8	1.7	-6.8	0.37	1018.1
28	43.22 N	34.14 E	758.7	2.5	-7.4	0.30	1024.2
29	43.47 N	34.01 E	748.8	3.1	-7.8	0.25	1027.1
30	43.73 N	33.86 E	740.7	3.6	-8.2	0.20	1026.6
31	44.00 N	33.70 E	733.9	3.9	-8.6	0.18	1023.2

32	44.28 N	33.51 E	727.6	4.2	-8.9	0.17	1017.7
33	44.57 N	33.30 E	721.7	4.9	-9.0	0.15	1012.1
34	44.87 N	33.07 E	716.6	5.4	-9.3	0.13	1007.9
35	45.17 N	32.81 E	712.3	5.9	-9.7	0.11	1006.4
36	45.49 N	32.53 E	708.7	6.4	-10.0	0.09	1008.0
37	45.82 N	32.21 E	705.4	7.2	-10.2	0.08	1012.0
38	46.15 N	31.85 E	702.8	8.4	-10.2	0.06	1016.4
39	46.48 N	31.42 E	700.8	9.7	-10.2	0.05	1018.3
40	46.81 N	30.94 E	699.1	10.8	-10.1	0.04	1016.2
41	47.13 N	30.41 E	697.8	11.5	-9.7	0.03	1010.3
42	47.43 N	29.85 E	697.3	11.9	-8.8	0.00	1002.7
43	47.70 N	29.27 E	698.5	12.0	-7.5	-0.06	995.3
44	47.92 N	28.69 E	701.9	12.0	-6.1	-0.12	988.3
45	48.11 N	28.13 E	705.9	11.3	-5.8	-0.10	981.1
46	48.30 N	27.59 E	709.1	10.9	-5.9	-0.07	974.0
47	48.49 N	27.06 E	712.0	10.8	-6.1	-0.08	967.4
48	48.69 N	26.53 E	716.3	10.8	-6.3	-0.15	961.8
49	48.90 N	25.99 E	724.0	11.0	-6.5	-0.28	957.8
50	49.11 N	25.43 E	736.3	11.4	-6.7	-0.41	955.6
51	49.33 N	24.87 E	749.4	11.3	-6.4	-0.31	955.7
52	49.54 N	24.31 E	758.3	10.9	-6.3	-0.19	957.2
53	49.74 N	23.78 E	763.5	10.4	-6.2	-0.10	959.7
54	49.94 N	23.27 E	765.5	9.8	-6.1	-0.02	962.8
55	50.13 N	22.79 E	765.3	9.3	-5.8	0.03	966.2
56	50.31 N	22.32 E	763.7	9.0	-5.3	0.06	969.7
57	50.48 N	21.87 E	762.0	8.8	-5.1	0.04	973.5
58	50.64 N	21.42 E	760.9	8.5	-4.9	0.02	977.4
59	50.80 N	21.00 E	760.2	8.1	-4.9	0.02	981.5
60	50.96 N	20.59 E	759.3	7.8	-5.0	0.03	985.5
61	51.12 N	20.19 E	758.0	7.6	-4.9	0.05	989.2
62	51.27 N	19.80 E	755.7	7.7	-4.6	0.08	992.1
63	51.41 N	19.38 E	752.9	8.3	-3.9	0.08	994.0
64	51.53 N	18.94 E	749.9	8.6	-3.5	0.09	994.7
65	51.64 N	18.49 E	746.5	8.8	-3.3	0.10	994.7
66	51.74 N	18.03 E	742.5	8.7	-3.0	0.12	994.2
67	51.84 N	17.58 E	738.0	8.5	-2.6	0.13	993.2
68	51.91 N	17.14 E	733.7	8.2	-2.0	0.11	992.1
69	51.96 N	16.71 E	730.1	8.1	-1.1	0.08	991.5
70	51.99 N	16.29 E	727.4	7.8	-0.5	0.06	991.0
71	52.00 N	15.89 E	725.5	7.4	-0.2	0.05	990.7
72	52.00 N	15.52 E	724.1	6.9	0.0	0.04	990.6
73	52.00 N	15.17 E	722.6	6.3	0.1	0.04	990.5
74	51.99 N	14.86 E	720.9	5.7	0.3	0.06	990.5
75	51.98 N	14.56 E	719.2	5.5	0.4	0.04	990.5
76	51.96 N	14.27 E	718.2	5.4	0.5	0.02	990.4
77	51.95 N	13.99 E	717.6	5.3	0.4	0.01	990.1
78	51.94 N	13.71 E	717.4	5.3	0.3	0.00	989.5
79	51.93 N	13.43 E	717.2	5.2	0.1	0.01	988.9
80	51.93 N	13.16 E	716.7	5.3	-0.1	0.02	988.1
81	51.94 N	12.88 E	716.3	5.3	-0.1	0.01	987.2
82	51.94 N	12.61 E	715.9	5.2	0.0	0.01	986.2
83	51.94 N	12.33 E	715.4	5.2	-0.1	0.02	984.9
84	51.94 N	12.06 E	714.4	5.1	-0.1	0.04	983.6
85	51.94 N	11.79 E	712.7	5.1	-0.1	0.06	982.1
86	51.94 N	11.53 E	710.4	5.0	0.0	0.08	980.6
87	51.93 N	11.26 E	708.0	5.0	0.7	0.05	978.6
88	51.90 N	11.00 E	706.5	5.0	1.3	0.03	976.1
89	51.85 N	10.74 E	705.8	4.9	1.8	0.01	973.3

90	51.78 N	10.49 E	705.9	4.6	2.2	-0.01	970.5
91	51.71 N	10.26 E	706.6	4.4	2.4	-0.03	967.8
92	51.63 N	10.04 E	707.7	4.1	2.5	-0.04	965.5
93	51.54 N	9.83 E	708.2	3.9	2.7	0.01	963.9
94	51.45 N	9.63 E	707.2	3.8	2.8	0.04	962.8
95	51.36 N	9.44 E	705.1	3.7	2.9	0.07	962.0
96	51.26 N	9.25 E	702.0	3.6	3.0	0.10	961.6
97	51.16 N	9.06 E	698.2	3.5	3.1	0.12	961.4
98	51.06 N	8.88 E	693.6	3.4	3.2	0.14	961.6
99	50.96 N	8.69 E	689.0	3.8	3.1	0.12	961.9
100	50.86 N	8.48 E	684.6	4.3	3.1	0.12	962.6
101	50.76 N	8.25 E	680.6	4.9	3.2	0.11	963.4
102	50.66 N	7.99 E	676.9	5.4	3.3	0.10	964.4
103	50.55 N	7.70 E	673.6	6.0	3.4	0.09	965.3
104	50.44 N	7.38 E	670.9	6.6	3.5	0.07	966.2
105	50.32 N	7.04 E	668.2	6.7	4.0	0.08	966.7
106	50.18 N	6.70 E	665.1	6.8	4.5	0.09	967.0
107	50.03 N	6.35 E	661.9	7.1	5.2	0.09	967.5
108	49.85 N	5.98 E	659.1	7.4	5.9	0.07	968.7
109	49.65 N	5.60 E	657.3	7.8	6.6	0.03	971.4
110	49.42 N	5.20 E	657.2	8.3	7.3	-0.03	975.8
111	49.18 N	4.80 E	658.8	7.9	7.4	-0.06	981.4
112	48.94 N	4.42 E	661.1	7.3	7.4	-0.07	987.2
113	48.70 N	4.08 E	663.2	6.7	7.4	-0.05	992.3
114	48.46 N	3.76 E	664.0	6.3	7.3	0.00	995.7
115	48.23 N	3.45 E	662.7	6.2	7.2	0.07	996.9
116	48.00 N	3.15 E	658.6	6.5	7.2	0.16	995.6
117	47.75 N	2.83 E	655.7	6.8	7.9	0.01	991.0
118	47.49 N	2.49 E	659.1	7.0	8.5	-0.19	984.0
119	47.21 N	2.16 E	670.1	7.0	8.9	-0.41	976.5
120	46.91 N	1.82 E	687.5	7.3	9.1	-0.55	971.2
121	46.62 N	1.46 E	708.0	7.8	9.1	-0.59	970.3
122	46.32 N	1.08 E	727.8	8.5	9.1	-0.51	974.7
123	46.04 N	0.70 E	742.0	8.0	8.4	-0.28	981.9
124	45.78 N	0.35 E	749.5	7.2	7.7	-0.14	990.5
125	45.54 N	0.04 E	753.2	6.3	7.0	-0.07	998.4
126	45.32 N	0.24 W	755.7	5.5	6.5	-0.07	1004.6
127	45.12 N	0.48 W	758.9	4.9	6.0	-0.10	1008.5
128	44.93 N	0.69 W	763.6	4.5	5.6	-0.16	1009.9
129	44.76 N	0.88 W	769.3	4.0	4.8	-0.15	1009.5
130	44.62 N	1.06 W	774.4	3.7	3.9	-0.13	1007.8
131	44.51 N	1.23 W	778.5	3.6	2.9	-0.10	1005.6
132	44.43 N	1.39 W	781.1	3.5	2.0	-0.05	1003.7
133	44.38 N	1.55 W	782.1	3.6	1.2	0.00	1002.5
134	44.35 N	1.71 W	781.0	3.6	0.8	0.03	1002.0

TRAJECTORY NUMBER 2

START: LAT 40.2 DEG N PRESSURE LEVEL 955 HPA
 LON 33.2 DEG E TIME 14 UTC ON 1. 8.90

END: TIME 0 UTC ON 27. 7.90

ANALYSIS FIELDS FROM TIME 14 UTC ON 1. 8.90

HOURS LAT LON LEVEL U-WIND V-WIND W-WIND PS

0	40.17 N	33.18 E	955.0	5.0	-0.1	-0.23	874.2
1	40.16 N	32.96 E	873.3	-2.5	-3.1	-0.20	874.1
2	40.26 N	33.04 E	873.3	-2.2	-3.0	-0.23	874.3
3	40.35 N	33.12 E	873.6	-2.0	-2.9	-0.20	874.5
4	40.43 N	33.18 E	874.0	-1.7	-2.6	-0.17	875.1
5	40.50 N	33.23 E	874.7	-1.5	-2.4	-0.14	875.8
6	40.57 N	33.28 E	875.5	-1.2	-2.0	-0.10	876.8
7	40.62 N	33.31 E	876.4	-0.9	-1.5	-0.06	877.7
8	40.66 N	33.34 E	878.0	-0.4	-0.9	-0.02	878.4
9	40.69 N	33.36 E	878.4	-0.6	-1.1	0.00	879.1
10	40.73 N	33.39 E	878.2	-0.9	-1.3	0.02	880.0
11	40.78 N	33.43 E	877.1	-1.3	-1.6	0.04	881.2
12	40.83 N	33.50 E	875.0	-1.9	-2.0	0.08	883.0
13	40.90 N	33.60 E	871.1	-2.9	-2.4	0.14	885.7
14	40.98 N	33.75 E	864.7	-3.2	-2.8	0.20	889.5
15	41.09 N	33.89 E	858.1	-3.3	-3.7	0.17	894.8
16	41.22 N	34.03 E	852.9	-3.1	-4.3	0.13	902.3
17	41.37 N	34.15 E	848.9	-2.5	-4.7	0.09	911.5
18	41.52 N	34.25 E	845.8	-1.8	-4.9	0.08	922.1
19	41.68 N	34.30 E	843.1	-1.1	-4.9	0.07	933.6
20	41.84 N	34.34 E	840.9	-0.5	-5.0	0.06	945.6
21	42.00 N	34.35 E	837.9	0.0	-4.9	0.11	958.0
22	42.16 N	34.35 E	832.9	0.3	-4.9	0.17	969.9
23	42.32 N	34.33 E	825.5	0.5	-4.9	0.24	981.6
24	42.48 N	34.30 E	815.7	0.7	-5.0	0.31	992.4
25	42.64 N	34.27 E	803.3	0.9	-5.3	0.38	1002.5
26	42.82 N	34.22 E	788.3	1.3	-6.0	0.45	1011.9
27	43.04 N	34.16 E	773.4	1.9	-6.8	0.38	1019.9
28	43.27 N	34.06 E	761.2	2.6	-7.4	0.31	1025.5
29	43.51 N	33.93 E	751.2	3.2	-7.9	0.25	1027.8
30	43.78 N	33.77 E	743.1	3.7	-8.3	0.20	1026.8
31	44.05 N	33.60 E	736.2	4.0	-8.7	0.18	1022.9
32	44.34 N	33.41 E	729.9	4.4	-9.0	0.17	1017.2
33	44.63 N	33.19 E	724.1	5.1	-9.1	0.15	1011.7
34	44.93 N	32.95 E	719.2	5.6	-9.4	0.12	1007.9
35	45.24 N	32.68 E	715.1	6.1	-9.7	0.10	1007.1
36	45.56 N	32.38 E	711.6	6.7	-10.0	0.09	1009.3
37	45.88 N	32.05 E	708.7	7.6	-10.1	0.07	1013.5
38	46.21 N	31.67 E	706.5	8.9	-10.0	0.05	1017.4
39	46.53 N	31.22 E	705.1	10.1	-10.0	0.03	1018.5
40	46.85 N	30.72 E	704.0	11.0	-9.8	0.02	1015.5
41	47.16 N	30.19 E	703.4	11.5	-9.3	0.01	1009.2
42	47.45 N	29.63 E	704.0	11.7	-8.3	-0.04	1001.4
43	47.69 N	29.07 E	706.3	11.7	-6.9	-0.09	993.7
44	47.90 N	28.50 E	710.5	11.6	-5.5	-0.14	986.1
45	48.07 N	27.96 E	714.9	11.0	-5.4	-0.11	978.3
46	48.25 N	27.43 E	718.1	10.6	-5.6	-0.07	970.8
47	48.44 N	26.92 E	720.8	10.5	-5.9	-0.08	964.3
48	48.63 N	26.40 E	724.8	10.5	-6.1	-0.14	959.2
49	48.83 N	25.88 E	732.0	10.7	-6.2	-0.26	955.8
50	49.04 N	25.34 E	743.6	11.1	-6.2	-0.37	954.4
51	49.23 N	24.79 E	755.2	10.9	-6.0	-0.28	954.7
52	49.42 N	24.26 E	763.4	10.6	-5.9	-0.18	956.1
53	49.61 N	23.74 E	768.2	10.2	-5.9	-0.09	958.0
54	49.80 N	23.24 E	770.2	9.6	-5.8	-0.02	960.2
55	49.98 N	22.77 E	770.1	9.1	-5.6	0.02	962.4
56	50.16 N	22.32 E	768.7	8.7	-5.1	0.05	965.0

57	50.32 N	21.89 E	767.1	8.5	-5.0	0.03	967.9
58	50.48 N	21.46 E	766.2	8.2	-4.8	0.02	971.5
59	50.63 N	21.05 E	765.6	7.8	-4.8	0.02	975.4
60	50.79 N	20.66 E	764.9	7.4	-4.9	0.02	979.7
61	50.95 N	20.29 E	763.7	7.1	-4.9	0.04	984.0
62	51.11 N	19.93 E	761.8	7.0	-4.9	0.07	988.0
63	51.26 N	19.56 E	759.3	7.5	-4.3	0.07	991.0
64	51.39 N	19.16 E	756.6	7.8	-3.9	0.08	992.7
65	51.51 N	18.75 E	753.4	8.0	-3.6	0.09	993.5
66	51.62 N	18.33 E	749.7	8.0	-3.5	0.11	993.7
67	51.74 N	17.92 E	745.5	7.8	-3.4	0.12	993.5
68	51.84 N	17.51 E	741.0	7.5	-3.0	0.13	992.9
69	51.92 N	17.12 E	736.9	7.5	-2.1	0.10	992.4
70	51.98 N	16.73 E	733.5	7.3	-1.5	0.08	992.0
71	52.02 N	16.35 E	730.7	7.0	-1.1	0.07	991.8
72	52.05 N	15.99 E	728.2	6.6	-0.8	0.07	991.9
73	52.08 N	15.66 E	725.9	6.1	-0.7	0.07	992.4
74	52.10 N	15.35 E	723.3	5.5	-0.7	0.07	993.0
75	52.12 N	15.06 E	721.0	5.4	-0.5	0.06	994.0
76	52.13 N	14.78 E	719.3	5.3	-0.4	0.04	995.0
77	52.15 N	14.50 E	718.2	5.2	-0.4	0.03	996.1
78	52.16 N	14.23 E	717.4	5.1	-0.5	0.02	997.3
79	52.18 N	13.96 E	716.8	5.0	-0.7	0.02	998.4
80	52.20 N	13.70 E	716.0	5.0	-0.8	0.02	999.4
81	52.23 N	13.43 E	715.4	5.1	-0.8	0.01	1000.1
82	52.25 N	13.16 E	715.3	5.2	-0.8	0.00	1000.7
83	52.28 N	12.89 E	715.3	5.2	-0.8	0.00	1001.0
84	52.31 N	12.61 E	715.3	5.2	-0.8	0.00	1001.2
85	52.33 N	12.33 E	715.0	5.2	-0.9	0.01	1001.1
86	52.37 N	12.06 E	714.3	5.2	-1.0	0.03	1000.9
87	52.39 N	11.77 E	713.5	5.4	-0.2	0.01	999.8
88	52.38 N	11.49 E	713.5	5.4	0.5	-0.01	997.8
89	52.35 N	11.20 E	714.2	5.3	1.2	-0.03	995.0
90	52.30 N	10.93 E	715.8	5.2	1.8	-0.06	991.7
91	52.23 N	10.66 E	718.2	4.9	2.3	-0.08	988.0
92	52.15 N	10.41 E	721.2	4.6	2.7	-0.09	984.2
93	52.06 N	10.18 E	723.6	4.3	2.8	-0.04	980.9
94	51.97 N	9.96 E	724.2	4.1	3.0	0.01	977.9
95	51.87 N	9.75 E	723.2	3.9	3.1	0.05	975.2
96	51.77 N	9.55 E	721.0	3.7	3.2	0.08	972.9
97	51.67 N	9.36 E	717.8	3.5	3.2	0.10	970.9
98	51.56 N	9.18 E	713.9	3.4	3.2	0.12	969.4
99	51.46 N	9.00 E	710.1	3.5	3.1	0.09	968.1
100	51.36 N	8.81 E	706.9	3.8	3.0	0.08	967.5
101	51.27 N	8.60 E	704.3	4.1	2.9	0.07	967.3
102	51.17 N	8.38 E	702.0	4.6	2.9	0.06	967.5
103	51.08 N	8.13 E	699.9	5.1	2.9	0.05	968.2
104	50.98 N	7.85 E	698.2	5.7	3.0	0.04	969.1
105	50.88 N	7.55 E	696.2	5.9	3.4	0.07	970.0
106	50.76 N	7.24 E	693.3	6.1	3.8	0.09	970.4
107	50.63 N	6.92 E	689.8	6.4	4.3	0.11	970.3
108	50.48 N	6.59 E	685.9	6.6	4.9	0.11	969.9
109	50.31 N	6.24 E	682.0	7.0	5.7	0.10	969.4
110	50.11 N	5.88 E	678.7	7.5	6.6	0.08	969.5
111	49.89 N	5.51 E	677.0	7.4	6.8	0.01	970.7
112	49.67 N	5.14 E	677.3	7.1	6.9	-0.03	973.1
113	49.45 N	4.80 E	678.8	6.5	6.9	-0.06	976.8
114	49.23 N	4.49 E	680.8	5.9	6.7	-0.05	981.3

115	49.01 N	4.22 E	682.0	5.2	6.5	-0.02	985.8
116	48.81 N	3.98 E	681.6	4.7	6.2	0.04	989.9
117	48.60 N	3.75 E	679.6	4.6	6.5	0.06	993.4
118	48.39 N	3.53 E	678.3	4.6	6.8	0.01	995.4
119	48.16 N	3.30 E	680.5	4.7	7.2	-0.13	995.3
120	47.92 N	3.07 E	688.6	4.7	7.7	-0.32	992.7
121	47.66 N	2.84 E	704.0	4.7	8.1	-0.52	987.7
122	47.39 N	2.62 E	726.0	4.5	8.6	-0.68	980.9
123	47.12 N	2.40 E	747.3	4.7	8.3	-0.52	974.1
124	46.85 N	2.17 E	763.1	5.1	7.8	-0.35	968.5
125	46.61 N	1.93 E	773.6	5.3	7.2	-0.23	965.6
126	46.39 N	1.68 E	780.6	5.2	6.6	-0.16	965.6
127	46.18 N	1.45 E	785.3	4.8	6.0	-0.11	967.9
128	46.00 N	1.24 E	788.8	4.2	5.4	-0.08	971.5
129	45.84 N	1.07 E	793.0	3.3	4.6	-0.15	974.8
130	45.70 N	0.94 E	799.3	2.4	3.7	-0.20	977.6
131	45.59 N	0.85 E	807.4	1.5	2.8	-0.25	979.4
132	45.52 N	0.80 E	817.3	0.7	1.7	-0.30	980.3
133	45.48 N	0.79 E	829.3	-0.1	0.6	-0.37	980.3
134	45.48 N	0.81 E	843.7	-0.4	0.0	-0.40	980.0

TRAJECTORY NUMBER 3

START: LAT 40.2 DEG N PRESSURE LEVEL 850 HPA
 LON 33.2 DEG E TIME 14 UTC ON 1. 8.90

END: TIME 0 UTC ON 27. 7.90

ANALYSIS FIELDS FROM TIME 14 UTC ON 1. 8.90

HOURS LAT LON LEVEL U-WIND V-WIND W-WIND PS

0	40.17 N	33.18 E	850.0	-4.4	-4.5	-0.15	874.2
1	40.32 N	33.35 E	856.3	-3.8	-4.6	-0.20	874.9
2	40.47 N	33.50 E	864.1	-2.8	-4.7	-0.24	876.5
3	40.62 N	33.60 E	872.6	-2.0	-4.4	-0.23	878.8
4	40.75 N	33.67 E	879.6	-1.3	-3.9	-0.21	881.9
5	40.86 N	33.71 E	882.9	-1.0	-3.4	-0.19	885.2
6	40.96 N	33.74 E	886.4	-0.5	-2.8	-0.16	888.7
7	41.04 N	33.75 E	889.7	-0.1	-2.1	-0.13	891.7
8	41.09 N	33.74 E	892.3	0.3	-1.3	-0.10	893.9
9	41.13 N	33.72 E	894.0	0.3	-1.1	-0.06	895.5
10	41.16 N	33.71 E	895.4	0.2	-0.9	-0.02	896.9
11	41.19 N	33.71 E	895.5	0.0	-0.8	0.02	898.1
12	41.21 N	33.71 E	894.0	-0.4	-0.7	0.07	899.3
13	41.24 N	33.74 E	890.6	-0.9	-0.8	0.12	900.7
14	41.26 N	33.80 E	884.9	-1.6	-0.9	0.19	902.4
15	41.31 N	33.88 E	878.7	-2.1	-2.0	0.15	905.6
16	41.39 N	33.98 E	874.2	-2.4	-2.9	0.10	911.1
17	41.50 N	34.08 E	871.2	-2.3	-3.5	0.06	918.7
18	41.62 N	34.18 E	869.3	-2.0	-3.9	0.04	927.7
19	41.74 N	34.25 E	868.1	-1.4	-4.1	0.03	937.6
20	41.88 N	34.29 E	867.1	-0.6	-4.2	0.03	947.9
21	42.01 N	34.30 E	864.8	0.1	-3.9	0.09	958.0
22	42.13 N	34.29 E	860.5	0.5	-3.8	0.15	967.5
23	42.25 N	34.26 E	853.7	0.7	-3.7	0.22	976.6

24	42.38 N	34.23 E	844.2	0.8	-3.9	0.30	985.4
25	42.51 N	34.19 E	831.9	0.9	-4.2	0.38	994.6
26	42.65 N	34.14 E	816.8	1.2	-4.7	0.46	1003.4
27	42.82 N	34.09 E	801.5	1.3	-5.6	0.39	1012.1
28	43.02 N	34.03 E	788.8	1.4	-6.7	0.32	1020.1
29	43.25 N	33.97 E	778.6	1.8	-7.5	0.25	1026.0
30	43.51 N	33.88 E	770.6	2.2	-8.1	0.20	1028.4
31	43.78 N	33.77 E	764.1	2.5	-8.6	0.16	1026.9
32	44.06 N	33.65 E	758.5	2.8	-9.1	0.15	1022.1
33	44.36 N	33.51 E	753.1	3.7	-9.2	0.14	1015.7
34	44.66 N	33.33 E	748.2	4.3	-9.3	0.13	1009.9
35	44.96 N	33.12 E	743.9	4.8	-9.4	0.11	1006.2
36	45.26 N	32.89 E	740.2	5.2	-9.5	0.10	1005.4
37	45.57 N	32.64 E	736.7	5.7	-9.5	0.09	1007.6
38	45.88 N	32.36 E	733.3	6.5	-9.5	0.09	1011.6
39	46.18 N	32.03 E	730.3	7.6	-9.3	0.08	1015.7
40	46.48 N	31.65 E	727.7	8.6	-9.2	0.07	1017.8
41	46.78 N	31.22 E	725.2	9.5	-9.1	0.07	1016.6
42	47.06 N	30.75 E	722.8	10.1	-8.6	0.07	1012.2
43	47.33 N	30.26 E	721.0	10.6	-7.7	0.04	1006.2
44	47.55 N	29.74 E	720.7	10.9	-6.3	-0.02	1000.1
45	47.74 N	29.22 E	722.5	10.6	-5.5	-0.08	994.6
46	47.91 N	28.71 E	725.3	10.2	-5.1	-0.08	988.9
47	48.08 N	28.23 E	727.8	9.9	-5.0	-0.06	982.9
48	48.24 N	27.75 E	729.8	9.6	-5.1	-0.06	976.6
49	48.41 N	27.28 E	732.7	9.6	-5.1	-0.10	970.4
50	48.57 N	26.81 E	738.5	9.6	-5.0	-0.22	964.6
51	48.73 N	26.35 E	746.9	9.4	-5.1	-0.25	960.2
52	48.90 N	25.89 E	755.4	9.2	-4.9	-0.22	957.3
53	49.05 N	25.44 E	762.5	9.0	-4.7	-0.17	955.8
54	49.20 N	25.00 E	767.2	8.8	-4.6	-0.10	955.5
55	49.35 N	24.58 E	769.4	8.4	-4.5	-0.02	956.0
56	49.49 N	24.17 E	769.1	7.9	-4.5	0.04	957.2
57	49.64 N	23.78 E	767.8	7.7	-4.7	0.03	958.6
58	49.79 N	23.40 E	767.0	7.5	-4.7	0.02	960.4
59	49.94 N	23.03 E	766.5	7.2	-4.6	0.01	962.4
60	50.09 N	22.67 E	766.1	6.8	-4.5	0.01	964.8
61	50.23 N	22.34 E	765.5	6.3	-4.4	0.02	967.6
62	50.37 N	22.04 E	764.3	5.6	-4.5	0.04	971.1
63	50.52 N	21.76 E	762.4	5.5	-4.3	0.07	974.9
64	50.65 N	21.48 E	759.6	5.5	-4.1	0.08	978.6
65	50.78 N	21.20 E	756.7	5.5	-3.8	0.08	982.1
66	50.90 N	20.92 E	753.8	5.5	-3.6	0.08	985.2
67	51.02 N	20.64 E	751.2	5.4	-3.4	0.07	988.0
68	51.13 N	20.36 E	748.9	5.2	-3.5	0.06	990.5
69	51.25 N	20.10 E	747.9	4.9	-3.9	-0.01	992.9
70	51.38 N	19.85 E	749.2	4.6	-4.0	-0.06	995.2
71	51.51 N	19.62 E	752.4	4.2	-4.0	-0.11	997.1
72	51.63 N	19.41 E	757.2	3.8	-3.7	-0.15	998.6
73	51.75 N	19.22 E	763.3	3.4	-3.4	-0.19	999.7
74	51.85 N	19.06 E	770.5	2.8	-3.0	-0.22	1000.4
75	51.94 N	18.91 E	777.0	3.0	-2.7	-0.14	1000.9
76	52.03 N	18.75 E	780.7	3.1	-2.6	-0.07	1001.2
77	52.11 N	18.58 E	782.3	3.2	-2.6	-0.02	1001.4
78	52.19 N	18.41 E	782.2	3.3	-2.6	0.02	1001.6
79	52.27 N	18.23 E	780.9	3.4	-2.6	0.05	1001.7
80	52.36 N	18.05 E	778.8	3.5	-2.7	0.07	1002.0
81	52.45 N	17.87 E	776.7	3.3	-2.7	0.05	1002.3

82	52.54 N	17.70 E	775.0	3.1	-2.7	0.04	1002.6
83	52.63 N	17.54 E	773.4	2.9	-2.8	0.04	1003.1
84	52.72 N	17.39 E	771.7	2.7	-2.8	0.05	1003.6
85	52.81 N	17.25 E	769.6	2.6	-2.9	0.06	1004.2
86	52.91 N	17.11 E	767.1	2.6	-3.0	0.08	1004.8
87	53.00 N	16.96 E	764.3	3.0	-2.8	0.07	1005.5
88	53.08 N	16.79 E	761.9	3.5	-2.5	0.06	1006.2
89	53.16 N	16.59 E	760.0	3.9	-2.2	0.04	1006.8
90	53.22 N	16.37 E	758.9	4.2	-1.8	0.02	1007.6
91	53.28 N	16.13 E	758.9	4.6	-1.4	-0.01	1008.4
92	53.31 N	15.87 E	760.0	4.9	-1.0	-0.05	1009.4
93	53.34 N	15.61 E	762.0	4.5	-0.6	-0.06	1010.8
94	53.35 N	15.39 E	764.0	4.0	-0.1	-0.06	1012.2
95	53.35 N	15.18 E	766.1	3.5	0.4	-0.06	1013.6
96	53.33 N	15.00 E	768.0	3.1	0.9	-0.05	1014.8
97	53.29 N	14.85 E	769.6	2.6	1.3	-0.04	1015.9
98	53.24 N	14.72 E	770.8	2.2	1.8	-0.02	1016.9
99	53.19 N	14.61 E	771.8	1.8	1.3	-0.03	1017.5
100	53.16 N	14.52 E	773.1	1.4	0.9	-0.04	1018.1
101	53.13 N	14.46 E	774.8	1.0	0.5	-0.05	1018.6
102	53.12 N	14.42 E	776.9	0.5	0.1	-0.06	1019.0
103	53.13 N	14.40 E	779.4	0.0	-0.3	-0.07	1019.3
104	53.14 N	14.41 E	782.3	-0.5	-0.7	-0.08	1019.5
105	53.17 N	14.45 E	784.8	-0.7	-1.0	-0.06	1019.5
106	53.21 N	14.49 E	786.6	-0.9	-1.4	-0.04	1019.4
107	53.26 N	14.54 E	787.5	-1.1	-1.8	-0.02	1019.2
108	53.32 N	14.61 E	787.7	-1.4	-2.2	0.00	1018.9
109	53.40 N	14.70 E	787.2	-1.8	-2.5	0.02	1018.4
110	53.49 N	14.81 E	786.2	-2.4	-2.9	0.04	1017.6
111	53.59 N	14.95 E	784.9	-2.7	-3.2	0.04	1016.4
112	53.69 N	15.10 E	783.4	-2.9	-3.5	0.04	1015.1
113	53.82 N	15.27 E	781.5	-3.2	-4.0	0.06	1013.7
114	53.96 N	15.45 E	779.1	-3.4	-4.6	0.08	1012.5
115	54.12 N	15.64 E	775.7	-3.6	-5.4	0.11	1011.4
116	54.31 N	15.85 E	771.2	-3.8	-6.3	0.14	1010.9
117	54.52 N	16.07 E	766.3	-4.1	-6.7	0.13	1011.1
118	54.74 N	16.31 E	762.1	-4.6	-7.0	0.11	1012.0
119	54.97 N	16.58 E	758.4	-5.1	-7.1	0.10	1013.6
120	55.20 N	16.88 E	755.0	-5.6	-7.1	0.09	1015.5
121	55.43 N	17.21 E	751.7	-6.0	-7.0	0.09	1017.3
122	55.65 N	17.57 E	748.4	-6.4	-7.0	0.09	1018.9
123	55.89 N	17.93 E	744.8	-6.2	-7.4	0.11	1019.6
124	56.13 N	18.29 E	740.7	-6.1	-7.9	0.12	1019.9
125	56.40 N	18.65 E	736.0	-6.2	-8.4	0.14	1019.8
126	56.68 N	19.02 E	730.3	-6.4	-8.9	0.17	1019.8
127	56.97 N	19.40 E	723.5	-6.5	-9.4	0.21	1020.1
128	57.29 N	19.79 E	715.5	-6.5	-10.0	0.24	1021.0
129	57.62 N	20.18 E	708.0	-6.3	-10.6	0.18	1022.3
130	57.97 N	20.56 E	702.3	-6.2	-11.0	0.13	1023.6
131	58.33 N	20.94 E	698.1	-6.3	-11.2	0.10	1024.4
132	58.69 N	21.33 E	694.6	-6.2	-11.2	0.09	1024.1
133	59.05 N	21.71 E	691.5	-5.9	-10.9	0.08	1022.9
134	59.40 N	22.07 E	689.0	-5.6	-10.8	0.07	1021.9

NOTES: IMS MODEL

1) LATITUDES AND LONGITUDES ARE IN DEGREES.

2) PRESSURE LEVELS ARE IN HECTOPASCALS (HPA).

3) THE FOLLOWING ABBREVIATIONS ARE USED:

U-WIND - U-COMPONENT OF WIND (METRES PER SECOND)

V-WIND - V-COMPONENT OF WIND (METRES PER SECOND)

W-WIND - VERTICAL WIND COMPONENT (PASCALS PER SECOND)

PS - SURFACE PRESSURE (HPA)

APPENDIX D

SOURCE CODE OF ECMWF TRAJECTORY DATA IMPORT TOOL

```
set progressbars off
dim k ,m,i as integer
dim yil, pth, ay, gun as string

pth = Applicationdirectory$( )
if right$(pth,1) <> "\" then
    pth = pth + "\"
end if

Create Table "p100_ecmwf" (hours Char(10),lat Float,latn Char(4),long Float,longe Char(6),level
Float,uwind Float,vwind Float,wwind Float,ps Float,tarih Char(10)) file pth + "p100_ecmwf.tab"
TYPE NATIVE Charset "WindowsTurkish"
Create Map For p100_ecmwf CoordSys Earth Projection 1, 0
Create Table "p500_ecmwf" (hours Char(10),lat Float,latn Char(4),long Float,longe Char(6),level
Float,uwind Float,vwind Float,wwind Float,ps Float,tarih Char(10)) file pth + "p500_ecmwf.tab"
TYPE NATIVE Charset "WindowsTurkish"
Create Map For p500_ecmwf CoordSys Earth Projection 1, 0
Create Table "p1500_ecmwf" (hours Char(10),lat Float,latn Char(4),long Float,longe Char(6),level
Float,uwind Float,vwind Float,wwind Float,ps Float,tarih Char(10)) file pth + "p1500_ecmwf.tab"
TYPE NATIVE Charset "WindowsTurkish"
Create Map For p1500_ecmwf CoordSys Earth Projection 1, 0

Open Table pth + "p100_ecmwf.tab" Interactive
Open Table pth + "p500_ecmwf.tab" Interactive
Open Table pth + "p1500_ecmwf.tab" Interactive

for k = 1990 to 2000
for m = 1 to 12
for i = 1 to 31
do case m
case 1
ay = "ocak"
case 2
ay = "ubat"
case 3
ay = "mart"
case 4
ay = "nisan"
case 5
ay = "mayis"
case 6
ay = "haziran"
case 7
```

```

ay = "temmuz"
case 8
ay = "agustos"
case 9
ay = "eylul"
case 10
ay = "ekim"
case 11
ay = "kasim"
case 12
ay = "aralik"
end case
yil = k
if i < 10 then
    gun = "0" + i
else
    gun = i
end if
if m < 10 then
    gun = gun + "0"+m
else
    gun = gun + m
end if
gun = gun + right$(Str$(k),2)

if not fileexists(pth + yil + "\" + ay + "\"+gun+".txt") then
goto gec1
end if

Register Table pth + yil + "\" + ay + "\"+gun+".txt" TYPE ASCII Delimiter 32 Charset
"WindowsTurkish" Into pth + yil + "\"+ay+ "\"+gun+".TAB"
Open Table pth + yil + "\"+ay+ "\"+gun+".TAB" as data2 Interactive

commit table data2 as pth +yil + "\" + ay + "\"data1.tab"
Open Table pth + yil+ "\"+ay+ "\"data1.TAB" as data1 Interactive
Alter Table data1 ( add tarih Char(8) ) Interactive
Alter Table "data1" ( modify _COL1 Integer ) Interactive
update data1 set tarih = gun

Select _COL1, _COL2, _COL3, _COL4, _COL5, _COL6, _COL7, _COL8, _COL9, _COL10, tarih
from data1 where col3 = any("N","S") and col5 = any("E","W") order by col1 into sel1
select * from sel1 where rowid mod 3 = 0 and rowid <= 363 into sel2
insert into p100_ecmwf select * from sel2
select * from sel1 where rowid mod 3 = 1 and rowid <= 363 into sel2
insert into p500_ecmwf select * from sel2
select * from sel1 where rowid mod 3 = 2 and rowid <= 363 into sel2
insert into p1500_ecmwf select * from sel2

close table data1
close table data2

gec1:
next
next
next
next

select * from p100_ecmwf where longe = "W" into sel1 noselect
update sel1 set long = -1*long

```

```

select * from p100_ecmwf where latn = "S" into sel1 noselect
update sel1 set lat = -1*lat
select * from p1500_ecmwf where longe = "W" into sel1 noselect
update sel1 set long = -1*long
select * from p1500_ecmwf where latn = "S" into sel1 noselect
update sel1 set lat = -1*lat
select * from p500_ecmwf where longe = "W" into sel1 noselect
update sel1 set long = -1*long
select * from p500_ecmwf where latn = "S" into sel1 noselect
update sel1 set lat = -1*lat

```

```

commit table p100_ecmwf
commit table p1500_ecmwf
commit table p500_ecmwf

```

```

Select * from p100_ecmwf into Sel3
Commit Table Sel3 As pth +"pbir_ecmwf.tab" TYPE NATIVE Charset "WindowsTurkish"
Open Table pth +"pbir_ecmwf.TAB" Interactive
Insert Into pbir_ecmwf ( COL1, COL2, COL3, COL4, COL5, COL6, COL7, COL8, COL9, COL10,
COL11) Select COL1, COL2, COL3, COL4, COL5, COL6, COL7, COL8, COL9, COL10, COL11
From p500_ecmwf
Insert Into pbir_ecmwf ( COL1, COL2, COL3, COL4, COL5, COL6, COL7, COL8, COL9, COL10,
COL11) Select COL1, COL2, COL3, COL4, COL5, COL6, COL7, COL8, COL9, COL10, COL11
From p1500_ecmwf
Commit Table pbir_ecmwf Interactive

```

```

Update p100_ecmwf
  Set obj = CreatePoint(long, lat)
Update p500_ecmwf
  Set obj = CreatePoint(long, lat)
Update p1500_ecmwf
  Set obj = CreatePoint(long, lat)
Update pbir_ecmwf
  Set obj = CreatePoint(long, lat)

```

```

Browse * From p100_ecmwf
Browse * From p500_ecmwf
Browse * From p1500_ecmwf
Browse * From pbir_ecmwf

```

```

Commit Table p100_ecmwf Interactive
Commit Table p500_ecmwf Interactive
Commit Table p1500_ecmwf Interactive
Commit Table pbir_ecmwf Interactive

```

APPENDIX E

SOURCE CODE OF CREATE LINE TOOL

```
include "mapbasic.def"

declare sub main
declare sub Create_LineAll
declare sub Create_Line
declare sub Create_Linehys
declare sub Create_Lineecm
declare sub Create_30rndLine
declare sub kapat

dim XCoor(1) as float
dim YCoor(1) as float
dim count as integer

sub main
create menu "PointToLine" as
    "Create Line" calling Create_Line,
    "Secili Tarihlere Gore Cizgi hysplit Ciz" calling Create_Linehys,
    "Secili Tarihlere Gore Cizgi ecmwf Ciz" calling Create_Lineecm,
    "rasgele 30 gun ciz" calling Create_30rndLine,
    "Tablodaki tum tarihlerer gore Tum cizgileri ciz" calling Create_LineAll,
    "(-",
    "Kapat..." calling kapat
Alter Menu Bar Add "PointToLine"

print "In the Browser table, the name of the"
print "latitude column must be B"
print "longitude column must be C"
end sub

sub Create_Line
dim i as integer
dim Table_Name as string
dialog title "Enter Table_Name"
    control EditText into Table_Name
    control OKButton
    control CancelButton
if not commandinfo(1) then exit sub end if
if numwindows() = 0 then print "a??k pencere yok" exit sub end if
if windowinfo(frontwindow(),3) <> 1 then print "?ndeki pencere harita de?il" exit sub end if
set map layer 0 editable on selectable on
set map redraw on
```

```

note tableinfo(Table_Name,TAB_INFO_NROWS)
redim XCoor(tableinfo(Table_Name,TAB_INFO_NROWS))
redim YCoor(tableinfo(Table_Name,TAB_INFO_NROWS))
select * from Table_Name into sel
fetch first from sel
for i = 1 to tableinfo(Table_Name,TAB_INFO_NROWS)
XCoor(i) = sel.long
YCoor(i) = sel.lat
fetch next from sel
next
select * from sel where B = -1
for i = 1 to count-1
Create Line into window frontwindow()(XCoor(i),YCoor(i))(XCoor(i + 1),YCoor(i + 1))
next
print "Line Created. You can save Cosmetic Layer menu MAP>Save Cosmetic Objects..."
print "Erdinc TASEL production for Oznur Oguz :)"
end sub

```

```

sub Create_Linehys
' Ahmet DABANLI

dim i as integer
dim Table_Name as string
if not selectioninfo(3) then exit sub end if
select * from selection into sel_secilen
select tarih,_col12 from sel_secilen group by tarih into seciliTarih
dim k as integer
dim h as float
dim o as object
dim s,t as string
for k = 1 to tableinfo(seciliTarih,8)
fetch rec k from seciliTarih
s = seciliTarih.col1
h = seciliTarih.col2
select * from sel_secilen where tarih = s into sel
count = tableinfo(sel,TAB_INFO_NROWS)
redim XCoor( count)
redim YCoor(count)
fetch first from sel
t = sel.tarih
print k + "/" + tableinfo(seciliTarih,8) + " " + t
for i = 1 to count
XCoor(i) = sel.c
YCoor(i) = sel.b
fetch next from sel
next
Create pLine into variable o 0
for i = 1 to count
alter object o node add (XCoor(i), YCoor(i))
next
insert into cizgihys(obj, tarih, height) values(o, t, h)
next
end sub

```

```

sub Create_Lineecm
' Ahmet Dabanlı
' basarsoft

dim i as integer
dim Table_Name as string
if not selectioninfo(3) then exit sub end if
select * from selection into sel_secilen
select tarih,level from sel_secilen group by tarih into seciliTarih
dim k as integer
dim h1,h2 as float
dim o as object
dim s,t as string
for k = 1 to tableinfo(seciliTarih,8)
    fetch rec k from seciliTarih
    s = seciliTarih.col1
    h1=seciliTarih.col2
if h1=1000 then h2=100
elseif h1=955 then h2=500
elseif h1=850 then h2=1500
else h2=0
end if
select * from sel_secilen where tarih = s into sel
count = tableinfo(sel,TAB_INFO_NROWS)
redim XCoor( count)
redim YCoor(count)
fetch first from sel
t = sel.tarih
print k + "/" + tableinfo(seciliTarih,8) + " " + t
for i = 1 to count
    XCoor(i) = sel.long
    YCoor(i) = sel.lat
    fetch next from sel
next
Create pLine into variable o 0
for i = 1 to count
    alter object o node add (XCoor(i), YCoor(i))
next
insert into cizgiecm(obj, tarih, height) values(o, t, h2)
next
end sub
sub kapat
    end program
end sub

```

```

sub Create_LineAll
' Ahmet Dabanlı
' basarsoft

dim i as integer
dim Table_Name as string
dialog title "Tablo Adi "
    control edittext value "p1500" into table_name
    control okbutton
    control cancelbutton
if not commandinfo(1) then
exit sub

```

```

end if
select * from table_name into sel_secilen
select tarih from sel_secilen group by tarih into seciliTarih
dim k as integer
dim o as object
dim s,t as string
for k = 1 to tableinfo(seciliTarih,8)
    fetch rec k from seciliTarih
    s = seciliTarih.col1
select * from sel_secilen where tarih = s into sel
count = tableinfo(sel,TAB_INFO_NROWS)
redim XCoor( count)
redim YCoor(count)
fetch first from sel
t = sel.tarih
print k + "/" + tableinfo(seciliTarih,8) + " " + t
for i = 1 to count
    XCoor(i) = sel.C
    YCoor(i) = sel.B
    fetch next from sel
next
Create pLine into variable o 0
for i = 1 to count
    alter object o node add (XCoor(i), YCoor(i))
next
insert into cizgi(obj, tarih) values(o, t)
commit table cizgi
next
end sub

sub Create_30rndLine
' Ahmet Dabanlı
' basarsoft

dim i,j,g as integer
dim Table_Name as string
dim k,m,r as integer
dim t1,t2 as string
dim h1,h2 as float
dim o as object
dim s,t as string
select tarih from p100_ecmwf group by tarih into sel1 noselect
insert into tarihler select * from sel1
for i = 1 to 15
select * from tarihler into sel1 noselect
set progressbars off
r = tableinfo(sel1,8)-1
randomize
k = rnd(1)*r +1
fetch rec k from sel1
t1 = sel1.tarih
'note k + " " + t1
tekrar:
k = rnd(1)*r +1
fetch rec k from sel1
t2 = sel1.tarih
'note k + " " + t2
if t1 = t2 then goto tekrar end if

```

```

for g=1 to 6
if g=1 then Table_Name= "p100_ecmwf"
elseif g=2 then Table_Name="p500_ecmwf"
elseif g=3 then Table_Name="p1500_ecmwf"
elseif g=4 then Table_Name="p100h"
elseif g=5 then Table_Name="p500h"
elseif g=6 then Table_Name="p1500h"
end if
select * from Table_Name where tarih = any(t1,t2) into sel_secilen
if g=any(1,2,3) then select tarih,level from sel_secilen group by tarih into seciliTarih
else select tarih,_col12 from sel_secilen group by tarih into seciliTarih
end if
for m = 1 to tableinfo(seciliTarih,8)
    fetch rec m from seciliTarih
    s = seciliTarih.col1
    h1=seciliTarih.col2
if h1=1000 then h2=100
elseif h1=955 then h2=500
elseif h1=850 then h2=1500
else h2=h1
end if
select * from sel_secilen where tarih = s into sel
count = tableinfo(sel,TAB_INFO_NROWS)
redim XCoor( count)
redim YCoor(count)
fetch first from sel
t = sel.tarih
print m + "/" + tableinfo(seciliTarih,8) + " " + t
for j = 1 to count
if g=any(1,2,3)then XCoor(j) = sel.long
                    YCoor(j) = sel.lat
    else XCoor(j) = sel.c
        YCoor(j) = sel.b
end if
fetch next from sel
next
Create pLine into variable o 0
for j = 1 to count
alter object o node add (XCoor(j), YCoor(j))
next
if g=any(1,2,3) then insert into cizgiecm(obj, tarih, height) values(o, t, h2)
else insert into cizgihys(obj, tarih, height) values(o, t, h2)
end if
next
next
select * from tarihler where tarih = any(t1,t2) into sel2
delete from sel2
next
rollback table tarihler
end sub

```

APPENDIX F

SOURCE CODE OF PSCF TOOL

```
declare sub kirlilikdatahazirla
declare sub kirlilikdatahazirla1
declare sub PscfBul
declare sub trajbirlestir
declare sub pscfhopke

dim pth, griddosyasi, trajdosya, excel1, excel as string

create buttonpad "PSCF tool" as
    pushbutton icon 102 calling kirlilikdatahazirla1 helpmsg "\nkirlilik excel ac "
    pushbutton icon 102 calling kirlilikdatahazirla helpmsg "\nkirlilik tarih data hazirla"
    pushbutton icon 117 calling trajbirlestir helpmsg "\ntrajjectoryleri birlestir "
separator
    pushbutton icon 113 calling PscfBul helpmsg "\npscf hesapla"
    pushbutton icon 105 calling pscfhopke helpmsg "\nhopke methoduyla pscf hesapla"

griddosyasi = "Cubuk_Grid"
trajdosya = "pbir040506"
excel1="cubuk20042006mi"
excel="cubuk20042006"

pth = Applicationdirectory$( )
if right$(pth,1) <> "\" then
    pth = pth + "\"
end if

sub kirlilikdatahazirla1
Register Table pth+excel+".xls" TYPE XLS Titles Range "Sayfa1!A4:E1099" Into
pth+excel+".TAB"
Open Table pth+excel+".TAB" Interactive
Browse * From excel
Commit Table excel As pth+excel1+".tab" TYPE NATIVE Charset "WindowsTurkish"
Close Table excel Interactive
Open Table pth+excel1+".tab" Interactive
Browse * From excel1
end sub
```

```

sub kirlilikdatahazirla
Alter Table excel1 ( add tarih Char(10) ) Interactive
Update excel1 Set tarih = day
select * from excel1 where day < 10 into sel1
Update sel1 Set tarih = "0"+day
select * from excel1 where month < 10 into sel1
Update sel1 Set tarih = tarih + "0"+month
select * from excel1 where month >= 10 into sel1
Update sel1 Set tarih = tarih+month
Update excel1 Set tarih = tarih + right$(str$(year),2)
Commit Table excel1 Interactive
end sub

```

```

sub trajbirlestir
Select * from p100 where right$(tarih,2) = any("06","04","05") into sel1
Browse * From sel1
Commit Table sel1 As pth+trajdosya+".tab" TYPE NATIVE Charset "WindowsTurkish"
Open Table pth+trajdosya+".tab" Interactive
Browse * From trajdosya
Browse * From p500
Select * from p500 where right$(tarih,2) = any("06","04","05") into sel1
Insert Into trajdosya ( COL1, COL2, COL3, COL4, COL5, COL6, COL7, COL8, COL9, COL10,
COL11, COL12, COL13, COL14, COL15, COL16) Select COL1, COL2, COL3, COL4, COL5,
COL6, COL7, COL8, COL9, COL10, COL11, COL12, COL13, COL14, COL15, COL16 From sel1
Select * from p1500 where right$(tarih,2) = any("06","04","05") into sel1
Insert Into trajdosya ( COL1, COL2, COL3, COL4, COL5, COL6, COL7, COL8, COL9, COL10,
COL11, COL12, COL13, COL14, COL15, COL16) Select COL1, COL2, COL3, COL4, COL5,
COL6, COL7, COL8, COL9, COL10, COL11, COL12, COL13, COL14, COL15, COL16 From sel1
Commit Table trajdosya Interactive
end sub

```

```

sub PscfBul
Add Column griddosyasi (Nij)From trajdosya Set To Count(*) Where within
select * from excel1 order by SO4 where so4 into sel1
browse * from Selection
dim r as integer
r = tableinfo(sel1,8) * 0.6
print r
fetch rec r from sel1
dim fs as float
fs = sel1.so4
note fs
select * from excel1 where so4 >= fs into sel1
Alter Table trajdosya ( add kirli Smallint ) Interactive 'Sadece ilk basta bir kere yapiliyor'
Add Column trajdosya (kirli )From sel1 Set To 1 Where tarih= tarih
Browse * From trajdosya
Commit Table trajdosya Interactive
select * from trajdosya where kirli into sel2
browse * from sel2
Add Column griddosyasi (Mij )From sel2 Set To Count(*) Where within
Browse * From griddosyasi
select * from griddosyasi where nij into sel2
Update sel2 Set PSCF = Mij / Nij
Commit Table griddosyasi Interactive
end sub

```

```

sub pscfhopke
dim a as integer
select avg (Nij) from Table griddosyasi into sel
a=sel.col1
select * from griddosyasi where Nij > (2*a) into sel41
update sel41 set wpscf_hopke = PSCF
select * from griddosyasi where (Nij <= (2*a)and Nij > a) into sel41
update sel41 set wpscf_hopke = PSCF*0.75
select * from griddosyasi where (Nij <= a and Nij > (a/2)) into sel41
update sel41 set wpscf_hopke = PSCF*0.5
select * from griddosyasi where Nij <= (a/2) into sel41
update sel41 set wpscf_hopke = PSCF*0.15
commit table griddosyasi
end sub

```

APPENDIX G

SOURCE CODE OF TOOL FOR RAIN & HEIGHT INTEGRATION TO PSCF CALCULATIONS

```
declare sub HPscfBul
declare sub RPscfBul
declare sub rainheight

create buttonpad "WeigtedPSCF" as
    pushbutton icon 113 calling HPscfBul helpmsg "\npscf yukseklik agirlikli hesapla"
    pushbutton icon 115 calling RPscfBul helpmsg "\npscf yagmur agirlikli hesapla"
    pushbutton icon 116 calling rainheight helpmsg "\npscf yagmur ve yukseklik birarada agirlikli
hesapla"

sub rainheight
dim b as float

b=0.2
Select * From pbir040506 where _COL1= "1" into sel1
Select tarih, Max(_COL9),_COL1 from sel1 where _COL15 >=b group by tarih into yagmurlular100
Browse * From yagmurlular100
Add Column "sel1" (yagmur )From yagmurlular100 Set To COL2 Where COL16 = COL1
Select* From sel1 where yagmur< 0 into sel2
Select * from sel2 where yagmur >= _COL9 into Sel3
delete from Sel3
Select * From pbir040506 where _COL1= "2" into sel4
Select tarih, Max(_COL9),_COL1 from sel4 where _COL15 >=b group by tarih into yagmurlular500
Browse * From yagmurlular500
Add Column "sel4" (yagmur )From yagmurlular500 Set To COL2 Where COL16 = COL1
Select* From sel4 where yagmur< 0 into sel5
Select * from sel5 where yagmur >= _COL9 into Sel6
delete from Sel6
Select * From pbir040506 where _COL1= "3" into sel7
Select tarih, Max(_COL9),_COL1 from sel7 where _COL15 >=b group by tarih into
yagmurlular1500
Browse * From yagmurlular1500
Add Column "sel7" (yagmur )From yagmurlular1500 Set To COL2 Where COL16 = COL1
Select* From sel7 where yagmur< 0 into sel8
Select * from sel8 where yagmur >= _COL9 into Sel9
delete from Sel9
Add Column Cubuk_Grid (RH_nij)From pbir040506 Set To Count(*) Where within
select * from pbir040506 where _COL12 <= 500 and kirli=1 into sel10
Browse * From sel10
update sel10 set wn = 1
select * from pbir040506 where _COL12 <= 1000 and _COL12 > 500 and kirli=1 into sel10
```

```

update sel10 set wn = 0.9
select * from pbir040506 where _COL12 <= 1500 and _COL12 > 1000 and kirli=1 into sel10
update sel10 set wn = 0.8
select * from pbir040506 where _COL12 > 1500 and kirli=1 into sel10
update sel10 set wn = 0.5
select * from pbir040506 where kirli into sel11
browse * from sel11
Add Column Cubuk_Grid (RH_mij) From sel11 Set To proportion sum(wn) Where within Dynamic
Browse * From Cubuk_Grid
select * from Cubuk_Grid where RH_nij into sel12
Browse * From sel12
Update sel12 Set RH_pscf = RH_mij / RH_nij
Commit Table Cubuk_Grid Interactive
Rollback Table pbir040506
end sub

sub RPscfBul
'Rain weighting

'1mm/h
Select * From pbir040506 where _COL1= "1" into sel1
Select tarih, Max(_COL9),_COL1 from sel1 where _COL15 >=b group by tarih into yagmurlular100
Browse * From yagmurlular100
Add Column "sel1" (yagmur )From yagmurlular100 Set To COL2 Where COL16 = COL1
Select* From sel1 where yagmur < 0 into sel2
Select * from sel2 where yagmur >= _COL9 into Sel3
delete from Sel3
Select * From pbir040506 where _COL1= "2" into sel4
Select tarih, Max(_COL9),_COL1 from sel4 where _COL15 >=1 group by tarih into yagmurlular500
Browse * From yagmurlular500
Add Column "sel4" (yagmur )From yagmurlular500 Set To COL2 Where COL16 = COL1
Select* From sel4 where yagmur < 0 into sel5
Select * from sel5 where yagmur >= _COL9 into Sel6
delete from Sel6
Select * From pbir040506 where _COL1= "3" into sel7
Select tarih, Max(_COL9),_COL1 from sel7 where _COL15 >=1 group by tarih into
yagmurlular1500
Browse * From yagmurlular1500
Add Column "sel7" (yagmur )From yagmurlular1500 Set To COL2 Where COL16 = COL1
Select* From sel7 where yagmur < 0 into sel8
Select * from sel8 where yagmur >= _COL9 into Sel9
delete from Sel9
Add Column Cubuk_Grid (wr_nij1)From pbir040506 Set To Count(*) Where within
select * from pbir040506 where kirli into sel10
Add Column Cubuk_Grid (wr_mij1 )From sel10 Set To Count(*) Where within
Browse * From Cubuk_Grid
select * from Cubuk_Grid where wr_nij1 into sel11
Browse * From sel11
Update sel11 Set Rpscf1 = wr_mij1 / wr_nij1
Rollback Table pbir040506
dim a as integer
select avg (wr_nij1) from Cubuk_Grid into sel
a=sel.col1
select * from Cubuk_Grid where wr_nij1 > (2*a) into sel13
update sel13 set RWpscf1 = Rpscf1
select * from Cubuk_Grid where (wr_nij1 <= (2*a) and wr_nij1 > a) into sel13
update sel13 set RWpscf1 = Rpscf1 *0.75
select * from Cubuk_Grid where (wr_nij1 <= a and wr_nij1 > (a/2)) into sel13

```

```

update sel13 set RWpscfl = Rpscfl *0.5
select * from Cubuk_Grid where wr_nij1 <= (a/2) into sel13
update sel13 set RWpscfl = Rpscfl *0.15

'0.8 mm/h
Select * From pbir040506 where _COL1= "1" into sel1
Select tarih, Max(_COL9),_COL1 from sel1 where _COL15 >=0.8 group by tarih into
yagmurlular100
Browse * From yagmurlular100
Add Column "sel1" (yagmur )From yagmurlular100 Set To COL2 Where COL16 = COL1
Select* From sel1 where yagmur< 0 into sel2
Select * from sel2 where yagmur >= _COL9 into Sel3
delete from Sel3
Select * From pbir040506 where _COL1= "2" into sel4
Select tarih, Max(_COL9),_COL1 from sel4 where _COL15 >=0.8 group by tarih into
yagmurlular500
Browse * From yagmurlular500
Add Column "sel4" (yagmur )From yagmurlular500 Set To COL2 Where COL16 = COL1
Select* From sel4 where yagmur< 0 into sel5
Select * from sel5 where yagmur >= _COL9 into Sel6
delete from Sel6
Select * From pbir040506 where _COL1= "3" into sel7
Select tarih, Max(_COL9),_COL1 from sel7 where _COL15 >=0.8 group by tarih into
yagmurlular1500
Browse * From yagmurlular1500
Add Column "sel7" (yagmur )From yagmurlular1500 Set To COL2 Where COL16 = COL1
Select* From sel7 where yagmur< 0 into sel8
Select * from sel8 where yagmur >= _COL9 into Sel9
delete from Sel9
Add Column Cubuk_Grid (wr_nij08)From pbir040506 Set To Count(*) Where within
select * from pbir040506 where kirli into sel10
Add Column Cubuk_Grid (wr_mij08 )From sel10 Set To Count(*) Where within
Browse * From Cubuk_Grid
select * from Cubuk_Grid where wr_nij08 into sel11
Browse * From sel11
Update sel11 Set Rpscfl08 = wr_mij08 / wr_nij08
Rollback Table pbir040506
select avg (wr_nij08) from Cubuk_Grid into sel
a=sel.col1
select * from Cubuk_Grid where wr_nij08 > (2*a) into sel13
update sel13 set RWpscfl08 = Rpscfl08
select * from Cubuk_Grid where (wr_nij08 <= (2*a) and wr_nij08 > a) into sel13
update sel13 set RWpscfl08 = Rpscfl08 *0.75
select * from Cubuk_Grid where (wr_nij08 <= a and wr_nij08 > (a/2)) into sel13
update sel13 set RWpscfl08 = Rpscfl08 *0.5
select * from Cubuk_Grid where wr_nij08 <= (a/2) into sel13
update sel13 set RWpscfl08 = Rpscfl08 *0.15

```

```

'0.5 mm/h
Select * From pbir040506 where _COL1= "1" into sel1
Select tarih, Max(_COL9),_COL1 from sel1 where _COL15 >=0.5 group by tarih into
yagmurlular100
Browse * From yagmurlular100
Add Column "sel1" (yagmur )From yagmurlular100 Set To COL2 Where COL16 = COL1
Select* From sel1 where yagmur< 0 into sel2
Select * from sel2 where yagmur >= _COL9 into Sel3
delete from Sel3
Select * From pbir040506 where _COL1= "2" into sel4

```

```

Select tarih, Max(_COL9),_COL1 from sel4 where _COL15 >=0.5 group by tarih into
yagmurlular500
Browse * From yagmurlular500
Add Column "sel4" (yagmur )From yagmurlular500 Set To COL2 Where COL16 = COL1
Select* From sel4 where yagmur< 0 into sel5
Select * from sel5 where yagmur >= _COL9 into Sel6
delete from Sel6
Select * From pbir040506 where _COL1= "3" into sel7
Select tarih, Max(_COL9),_COL1 from sel7 where _COL15 >=0.5 group by tarih into
yagmurlular1500
Browse * From yagmurlular1500
Add Column "sel7" (yagmur )From yagmurlular1500 Set To COL2 Where COL16 = COL1
Select* From sel7 where yagmur< 0 into sel8
Select * from sel8 where yagmur >= _COL9 into Sel9
delete from Sel9
Add Column Cubuk_Grid (wr_nij05)From pbir040506 Set To Count(*) Where within
select * from pbir040506 where kirli into sel10
Add Column Cubuk_Grid (wr_mij05 )From sel10 Set To Count(*) Where within
Browse * From Cubuk_Grid
select * from Cubuk_Grid where wr_nij05 into sel11
Browse * From sel11
Update sel11 Set Rpscf05 = wr_mij05 / wr_nij05
Rollback Table pbir040506
select avg (wr_nij05) from Cubuk_Grid into sel
a=sel.col1
select * from Cubuk_Grid where wr_nij05 > (2*a) into sel13
update sel13 set RWpscf05 = Rpscf05
select * from Cubuk_Grid where (wr_nij05 <= (2*a) and wr_nij05 > a) into sel13
update sel13 set RWpscf05 = Rpscf05 *0.75
select * from Cubuk_Grid where (wr_nij05 <= a and wr_nij05 > (a/2)) into sel13
update sel13 set RWpscf05 = Rpscf05 *0.5
select * from Cubuk_Grid where wr_nij05 <= (a/2) into sel13
update sel13 set RWpscf05 = Rpscf05 *0.15

'0.3 mm/h
Select * From pbir040506 where _COL1= "1" into sel1
Select tarih, Max(_COL9),_COL1 from sel1 where _COL15 >=0.3 group by tarih into
yagmurlular100
Browse * From yagmurlular100
Add Column "sel1" (yagmur )From yagmurlular100 Set To COL2 Where COL16 = COL1
Select* From sel1 where yagmur< 0 into sel2
Select * from sel2 where yagmur >= _COL9 into Sel3
delete from Sel3
Select * From pbir040506 where _COL1= "2" into sel4
Select tarih, Max(_COL9),_COL1 from sel4 where _COL15 >=0.3 group by tarih into
yagmurlular500
Browse * From yagmurlular500
Add Column "sel4" (yagmur )From yagmurlular500 Set To COL2 Where COL16 = COL1
Select* From sel4 where yagmur< 0 into sel5
Select * from sel5 where yagmur >= _COL9 into Sel6
delete from Sel6
Select * From pbir040506 where _COL1= "3" into sel7
Select tarih, Max(_COL9),_COL1 from sel7 where _COL15 >=0.3 group by tarih into
yagmurlular1500
Browse * From yagmurlular1500
Add Column "sel7" (yagmur )From yagmurlular1500 Set To COL2 Where COL16 = COL1
Select* From sel7 where yagmur< 0 into sel8
Select * from sel8 where yagmur >= _COL9 into Sel9

```

```

delete from Sel9
Add Column Cubuk_Grid (wr_nij03)From pbir040506 Set To Count(*) Where within
select * from pbir040506 where kirli into sel10
Add Column Cubuk_Grid (wr_mij03 )From sel10 Set To Count(*) Where within
Browse * From Cubuk_Grid
select * from Cubuk_Grid where wr_nij03 into sel11
Browse * From sel11
Update sel11 Set Rpsc03 = wr_mij03 / wr_nij03
Rollback Table pbir040506
select avg (wr_nij03) from Cubuk_Grid into sel
a=sel.col1
select * from Cubuk_Grid where wr_nij03 > (2*a) into sel13
update sel13 set RWpsc03 = Rpsc03
select * from Cubuk_Grid where (wr_nij03 <= (2*a) and wr_nij03 > a) into sel13
update sel13 set RWpsc03 = Rpsc03 *0.75
select * from Cubuk_Grid where (wr_nij03 <= a and wr_nij03 > (a/2)) into sel13
update sel13 set RWpsc03 = Rpsc03 *0.5
select * from Cubuk_Grid where wr_nij03 <= (a/2) into sel13
update sel13 set RWpsc03 = Rpsc03 *0.15

'0.2 mm/h
Select * From pbir040506 where _COL1= "1" into sel1
Select tarih, Max(_COL9),_COL1 from sel1 where _COL15 >=0.2 group by tarih into
yagmurlular100
Browse * From yagmurlular100
Add Column "sel1" (yagmur )From yagmurlular100 Set To COL2 Where COL16 = COL1
Select* From sel1 where yagmur< 0 into sel2
Select * from sel2 where yagmur >= _COL9 into Sel3
delete from Sel3
Select * From pbir040506 where _COL1= "2" into sel4
Select tarih, Max(_COL9),_COL1 from sel4 where _COL15 >=0.2 group by tarih into
yagmurlular500
Browse * From yagmurlular500
Add Column "sel4" (yagmur )From yagmurlular500 Set To COL2 Where COL16 = COL1
Select* From sel4 where yagmur< 0 into sel5
Select * from sel5 where yagmur >= _COL9 into Sel6
delete from Sel6
Select * From pbir040506 where _COL1= "3" into sel7
Select tarih, Max(_COL9),_COL1 from sel7 where _COL15 >=0.2 group by tarih into
yagmurlular1500
Browse * From yagmurlular1500
Add Column "sel7" (yagmur )From yagmurlular1500 Set To COL2 Where COL16 = COL1
Select* From sel7 where yagmur< 0 into sel8
Select * from sel8 where yagmur >= _COL9 into Sel9
delete from Sel9
Add Column Cubuk_Grid (wr_nij02)From pbir040506 Set To Count(*) Where within
select * from pbir040506 where kirli into sel10
Add Column Cubuk_Grid (wr_mij02 )From sel10 Set To Count(*) Where within
Browse * From Cubuk_Grid
select * from Cubuk_Grid where wr_nij02 into sel11
Browse * From sel11
Update sel11 Set Rpsc02 = wr_mij02 / wr_nij02
Rollback Table pbir040506
select avg (wr_nij02) from Cubuk_Grid into sel
a=sel.col1
select * from Cubuk_Grid where wr_nij02 > (2*a) into sel13
update sel13 set RWpsc02 = Rpsc02
select * from Cubuk_Grid where (wr_nij02 <= (2*a) and wr_nij02 > a) into sel13

```

```

update sel13 set RWpscf02 = Rpsc02 *0.75
select * from Cubuk_Grid where (wr_nij02 <= a and wr_nij02 > (a/2)) into sel13
update sel13 set RWpscf02 = Rpsc02 *0.5
select * from Cubuk_Grid where wr_nij02 <= (a/2) into sel13
update sel13 set RWpscf02 = Rpsc02 *0.15

'0.1 mm/h
Select * From pbir040506 where _COL1= "1" into sel1
Select tarih, Max(_COL9),_COL1 from sel1 where _COL15 >=0.1 group by tarih into
yagmurlular100
Browse * From yagmurlular100
Add Column "sel1" (yagmur )From yagmurlular100 Set To COL2 Where COL16 = COL1
Select* From sel1 where yagmur< 0 into sel2
Select * from sel2 where yagmur >= _COL9 into Sel3
delete from Sel3
Select * From pbir040506 where _COL1= "2" into sel4
Select tarih, Max(_COL9),_COL1 from sel4 where _COL15 >=0.1 group by tarih into
yagmurlular500
Browse * From yagmurlular500
Add Column "sel4" (yagmur )From yagmurlular500 Set To COL2 Where COL16 = COL1
Select* From sel4 where yagmur< 0 into sel5
Select * from sel5 where yagmur >= _COL9 into Sel6
delete from Sel6
Select * From pbir040506 where _COL1= "3" into sel7
Select tarih, Max(_COL9),_COL1 from sel7 where _COL15 >=0.1 group by tarih into
yagmurlular1500
Browse * From yagmurlular1500
Add Column "sel7" (yagmur )From yagmurlular1500 Set To COL2 Where COL16 = COL1
Select* From sel7 where yagmur< 0 into sel8
Select * from sel8 where yagmur >= _COL9 into Sel9
delete from Sel9
Add Column Cubuk_Grid (wr_nij01)From pbir040506 Set To Count(*) Where within
select * from pbir040506 where kirli into sel10
Add Column Cubuk_Grid (wr_mij01 )From sel10 Set To Count(*) Where within
Browse * From Cubuk_Grid
select * from Cubuk_Grid where wr_nij01 into sel11
Browse * From sel11
Update sel11 Set Rpsc01 = wr_mij01 / wr_nij01
Rollback Table pbir040506
select avg (wr_nij01) from Cubuk_Grid into sel
a=sel.col1
select * from Cubuk_Grid where wr_nij01 > (2*a) into sel13
update sel13 set RWpscf01 = Rpsc01
select * from Cubuk_Grid where (wr_nij01 <= (2*a) and wr_nij01 > a) into sel13
update sel13 set RWpscf01 = Rpsc01 *0.75
select * from Cubuk_Grid where (wr_nij01 <= a and wr_nij01 > (a/2)) into sel13
update sel13 set RWpscf01 = Rpsc01 *0.5
select * from Cubuk_Grid where wr_nij01 <= (a/2) into sel13
update sel13 set RWpscf01 = Rpsc01 *0.15
end sub

sub HPscfBul
'heigh weighting

Add Column Cubuk_Grid (Nij)From pbir040506 Set To Count(*) Where within

```

```
'scheme 1
select * from pbir040506 where _COL12 <= 1000 and kirli=1 into sel10
Browse * From sel10
update sel10 set wn = 1
select * from pbir040506 where _COL12 > 1000 and kirli=1 into sel10
update sel10 set wn = 0
select * from pbir040506 where kirli into sel11
browse * from sel11
Add Column Cubuk_Grid (Hmij_f) From sel11 Set To proportion sum(wn) Where within Dynamic
select * from Cubuk_Grid where Nij into sel12
Browse * From sel12
Update sel12 Set Hpsc_f = Hmij_f / Nij
select * from Cubuk_Grid where Nij > 160 into sel13
update sel13 set HWpsc_f = Hpsc_f
select * from Cubuk_Grid where (Nij <= 160 and Nij > 80) into sel13
update sel13 set HWpsc_f = Hpsc_f * 0.75
select * from Cubuk_Grid where (Nij <= 80 and Nij > 40) into sel13
update sel13 set HWpsc_f = Hpsc_f * 0.5
select * from Cubuk_Grid where Nij <= 40 into sel13
update sel13 set HWpsc_f = Hpsc_f * 0.15
select * from Cubuk_Grid where wpsc_hopke into sel14
update sel14 set fark_f = (wpsc_hopke - HWpsc_f) / wpsc_hopke * 100
Rollback Table pbir040506
```

```
'scheme 2
select * from pbir040506 where _COL12 <= 500 and kirli=1 into sel10
Browse * From sel10
update sel10 set wn = 1
select * from pbir040506 where _COL12 > 500 and kirli=1 into sel10
update sel10 set wn = 0.5
select * from pbir040506 where kirli into sel11
browse * from sel11
Add Column Cubuk_Grid (Hmij_b) From sel11 Set To proportion sum(wn) Where within Dynamic
select * from Cubuk_Grid where Nij into sel12
Browse * From sel12
Update sel12 Set Hpsc_b = Hmij_b / Nij
select * from Cubuk_Grid where Nij > 160 into sel13
update sel13 set HWpsc_b = Hpsc_b
select * from Cubuk_Grid where (Nij <= 160 and Nij > 80) into sel13
update sel13 set HWpsc_b = Hpsc_b * 0.75
select * from Cubuk_Grid where (Nij <= 80 and Nij > 40) into sel13
update sel13 set HWpsc_b = Hpsc_b * 0.5
select * from Cubuk_Grid where Nij <= 40 into sel13
update sel13 set HWpsc_b = Hpsc_b * 0.15
select * from Cubuk_Grid where wpsc_hopke into sel14
update sel14 set fark_b = (wpsc_hopke - HWpsc_b) / wpsc_hopke * 100
Rollback Table pbir040506
```

```
'scheme 3
select * from pbir040506 where _COL12 <= 500 and kirli=1 into sel10
Browse * From sel10
update sel10 set wn = 1
select * from pbir040506 where _COL12 <= 1000 and _COL12 > 500 and kirli=1 into sel10
update sel10 set wn = 0.8
select * from pbir040506 where _COL12 > 1000 and kirli=1 into sel10
update sel10 set wn = 0.5
select * from pbir040506 where kirli into sel11
```

```

browse * from sel11
Add Column Cubuk_Grid (Hmij_c) From sel11 Set To proportion sum(wn) Where within Dynamic
select * from Cubuk_Grid where Nij into sel12
Browse * From sel12
Update sel12 Set Hpscfc_c = Hmij_c / Nij
select * from Cubuk_Grid where Nij > 160 into sel13
update sel13 set HWpscfc_c = Hpscfc_c
select * from Cubuk_Grid where (Nij <= 160 and Nij > 80) into sel13
update sel13 set HWpscfc_c = Hpscfc_c *0.75
select * from Cubuk_Grid where (Nij <= 80 and Nij > 40) into sel13
update sel13 set HWpscfc_c = Hpscfc_c *0.5
select * from Cubuk_Grid where Nij <= 40 into sel13
update sel13 set HWpscfc_c = Hpscfc_c *0.15
select * from Cubuk_Grid where wpscfc_hopke into sel14
update sel14 set fark_c= (wpscfc_hopke-HWpscfc_c)/wpscfc_hopke*100
Rollback Table pbir040506

```

'scheme 4

```

select * from pbir040506 where _COL12 <= 1000 and kirli=1 into sel10
Browse * From sel10
update sel10 set wn = 1
select * from pbir040506 where _COL12 > 1000 and kirli=1 into sel10
update sel10 set wn = 0.5
select * from pbir040506 where kirli into sel11

```

browse * from sel11

```

Add Column Cubuk_Grid (Hmij_d) From sel11 Set To proportion sum(wn) Where within Dynamic
select * from Cubuk_Grid where Nij into sel12
Browse * From sel12
Update sel12 Set Hpscfd_d = Hmij_d / Nij
select * from Cubuk_Grid where Nij > 160 into sel13
update sel13 set HWpscfd_d = Hpscfd_d
select * from Cubuk_Grid where (Nij <= 160 and Nij > 80) into sel13
update sel13 set HWpscfd_d = Hpscfd_d *0.75
select * from Cubuk_Grid where (Nij <= 80 and Nij > 40) into sel13
update sel13 set HWpscfd_d = Hpscfd_d *0.5
select * from Cubuk_Grid where Nij <= 40 into sel13
update sel13 set HWpscfd_d = Hpscfd_d *0.15
select * from Cubuk_Grid where wpscfd_hopke into sel14
update sel14 set fark_d= (wpscfd_hopke-HWpscfd_d)/wpscfd_hopke*100
Rollback Table pbir040506

```

'scheme 5

```

select * from pbir040506 where _COL12 <= 500 and kirli=1 into sel10
Browse * From sel10
update sel10 set wn = 1
select * from pbir040506 where _COL12 <= 1500 and _COL12 > 500 and kirli=1 into sel10
update sel10 set wn = 0.8
select * from pbir040506 where _COL12 > 1500 and kirli=1 into sel10
update sel10 set wn = 0.5
select * from pbir040506 where kirli into sel11

```

browse * from sel11

```

Add Column Cubuk_Grid (Hmij_e) From sel11 Set To proportion sum(wn) Where within Dynamic
select * from Cubuk_Grid where Nij into sel12
Browse * From sel12
Update sel12 Set Hpscfe_e = Hmij_e / Nij
select * from Cubuk_Grid where Nij > 160 into sel13
update sel13 set HWpscfe_e = Hpscfe_e
select * from Cubuk_Grid where (Nij <= 160 and Nij > 80) into sel13

```

```

update sel13 set HWpscfe = Hpscfe *0.75
select * from Cubuk_Grid where (Nij <= 80 and Nij > 40) into sel13
update sel13 set HWpscfe = Hpscfe *0.5
select * from Cubuk_Grid where Nij <= 40 into sel13
update sel13 set HWpscfe = Hpscfe *0.15
select * from Cubuk_Grid where wpscfe_hopke into sel14
update sel14 set fark_e= (wpscfe_hopke-HWpscfe)/wpscfe_hopke*100
Rollback Table pbir040506

'scheme 6
select * from pbir040506 where _COL12 <= 500 and kirli=1 into sel10
Browse * From sel10
update sel10 set wn = 1
select * from pbir040506 where _COL12 <= 1000 and _COL12 > 500 and kirli=1 into sel10
update sel10 set wn = 0.9
select * from pbir040506 where _COL12 <= 1500 and _COL12 > 1000 and kirli=1 into sel10
update sel10 set wn = 0.8
select * from pbir040506 where _COL12 > 1500 and kirli=1 into sel10
update sel10 set wn = 0.5
select * from pbir040506 where kirli into sel11
browse * from sel11
Add Column Cubuk_Grid (Hmij_g) From sel11 Set To proportion sum(wn) Where within Dynamic
select * from Cubuk_Grid where Nij into sel12
Browse * From sel12
Update sel12 Set Hpscfe_g = Hmij_g / Nij
select * from Cubuk_Grid where Nij > 160 into sel13
update sel13 set HWpscfe_g = Hpscfe_g
select * from Cubuk_Grid where (Nij <= 160 and Nij > 80) into sel13
update sel13 set HWpscfe_g = Hpscfe_g *0.75
select * from Cubuk_Grid where (Nij <= 80 and Nij > 40) into sel13
update sel13 set HWpscfe_g = Hpscfe_g *0.5
select * from Cubuk_Grid where Nij <= 40 into sel13
update sel13 set HWpscfe_g = Hpscfe_g *0.15
select * from Cubuk_Grid where wpscfe_hopke into sel14
update sel14 set fark_g= (wpscfe_hopke-HWpscfe_g)/wpscfe_hopke*100
Rollback Table pbir040506
Commit Table Cubuk_Grid Interactive
end sub

```